

ธรรมนูญโบราณคดีของการตั้งถิ่นฐานชุมชนโบราณในพื้นที่ทุ่งกุลาร้องไห้ด้านตะวันออก  
บริเวณจังหวัดศรีสะเกษและยโสธร ภาคตะวันออกเฉียงเหนือของประเทศไทย



บทคัดย่อและแฟ้มข้อมูลฉบับเต็มของวิทยานิพนธ์ตั้งแต่ปีการศึกษา 2554 ที่ให้บริการในคลังปัญญาจุฬาฯ (CUIR)  
เป็นแฟ้มข้อมูลของนิสิตเจ้าของวิทยานิพนธ์ ที่ส่งผ่านทางบัณฑิตวิทยาลัย

The abstract and full text of theses from the academic year 2011 in Chulalongkorn University Intellectual Repository (CUIR)  
are the thesis authors' files submitted through the University Graduate School.

วิทยานิพนธ์นี้เป็นส่วนหนึ่งของการศึกษาตามหลักสูตรปริญญาวิทยาศาสตรมหาบัณฑิต  
สาขาวิชาโลกศาสตร์ ภาควิชาธรณีวิทยา  
คณะวิทยาศาสตร์ จุฬาลงกรณ์มหาวิทยาลัย  
ปีการศึกษา 2560  
ลิขสิทธิ์ของจุฬาลงกรณ์มหาวิทยาลัย

GEOARCHAEOLOGY OF ANCIENT SITE SETTLEMENT AT EASTERN THUNGKULA RONGHAI,  
SRISAKET AND YASOTHON PROVINCES IN NORTHEAST THAILAND



A Thesis Submitted in Partial Fulfillment of the Requirements  
for the Degree of Master of Science Program in Earth Sciences

Department of Geology

Faculty of Science

Chulalongkorn University

Academic Year 2017

Copyright of Chulalongkorn University

Thesis Title	GEOARCHAEOLOGY OF ANCIENT SITE SETTLEMENT AT EASTERN THUNGKULA RONGHAI, SRISAKET AND YASOTHON PROVINCES IN NORTHEAST THAILAND
By	Miss Patcharaporn Ngerkerd
Field of Study	Earth Sciences
Thesis Advisor	Professor Montri Choowong, Ph.D.

---

Accepted by the Faculty of Science, Chulalongkorn University in Partial  
Fulfillment of the Requirements for the Master's Degree

.....Dean of the Faculty of Science  
(Associate Professor Polkit Sangvanich, Ph.D.)

THESIS COMMITTEE

.....Chairman  
(Associate Professor Srilert Chotpantararat, Ph.D.)

.....Thesis Advisor  
(Professor Montri Choowong, Ph.D.)

.....Examiner  
(Akkaneewut Chabangborn, Ph.D.)

.....External Examiner  
(Assistant Professor Chawalit Khaokheiw)

พัชรพร เงินเกิด : ธรณีโบราณคดีของการตั้งถิ่นฐานชุมชนโบราณในพื้นที่ทุ่งกุลาร้องไห้ด้านตะวันออก บริเวณจังหวัดศรีสะเกษและยโสธร ภาคตะวันออกเฉียงเหนือของประเทศไทย (GEOARCHAEOLOGY OF ANCIENT SITE SETTLEMENT AT EASTERN THUNGKULA RONGHAI, SRISAKET AND YASOTHON PROVINCES IN NORTHEAST THAILAND) อ. ที่ปรึกษาวิทยานิพนธ์หลัก: ศ. ดร. มนตรี ชูวงศ์, หน้า.

การศึกษางานโบราณคดีในประเทศไทยปัจจุบัน มักมีความเกี่ยวข้องกับงานด้านธรณีวิทยา ในแง่ของการนำทฤษฎี เทคนิค และเครื่องมือมาประยุกต์ใช้ สำหรับงานวิจัยนี้มีวัตถุประสงค์ในการศึกษาความสัมพันธ์ระหว่างการตั้งถิ่นฐานของชุมชนโบราณกับรูปแบบธรณีสัณฐานภายใต้แนวคิด "ธรณีโบราณคดี" บริเวณพื้นที่ทุ่งกุลาร้องไห้ด้านตะวันออก ในเขตจังหวัดศรีสะเกษและยโสธร ภาคตะวันออกเฉียงเหนือของประเทศไทย โดยจากการรวบรวมข้อมูลเบื้องต้นได้พบชุมชนโบราณตั้งอยู่ในพื้นที่ศึกษาทั้งหมด 54 แห่ง มีอายุสมัยตั้งแต่ยุคก่อนประวัติศาสตร์ตอนปลาย (2,500 - 1,500 ปีมาแล้ว) จนถึงยุคประวัติศาสตร์สมัยทวารวดีและเขมร (ราวพุทธศตวรรษที่ 13-18) ซึ่งผู้วิจัยได้นำวิธีการศึกษาทางด้านธรณีสัณฐานมาประยุกต์ใช้ในการศึกษา อันได้แก่ ข้อมูลโทรมสัมผัส เครื่องมือธรณีฟิสิกส์ และการสำรวจทางธรณีวิทยา จากการศึกษาพบว่า ในพื้นที่ทุ่งกุลาร้องไห้ด้านตะวันออก ระหว่างแม่น้ำมูลและแม่น้ำชี มีลักษณะรูปทางธรณีสัณฐานที่สำคัญทั้งหมด 3 รูปแบบ ได้แก่ ร่องรอยทางน้ำโบราณ โดมเกลือระดับตื้น หรือ แอ่งยุบภูมิลักษณะวงแหวน และเนินลมพาททรายแผ่ ซึ่งชุมชนโบราณในพื้นที่ศึกษาส่วนใหญ่มักนิยมเลือกตั้งอยู่บนเนินดินของแอ่งยุบภูมิลักษณะวงแหวนใกล้กับทางน้ำโบราณ อย่างไรก็ตาม พบชุมชนโบราณบางแห่ง ที่เลือกตั้งถิ่นฐานอยู่บนส่วนปลายของเนินลมพาททรายแผ่ เนื่องจากพื้นที่ดังกล่าวมีแหล่งน้ำจืดที่อยู่ใต้ดินในระดับตื้น และใกล้กับลำน้ำ รวมถึงบริเวณเนินทรายนั้นมีระดับความสูงกว่าพื้นที่โดยรอบ สามารถป้องกันน้ำท่วม และใช้ประโยชน์ของที่ราบน้ำท่วมถึงในการทำเกษตรกรรมได้ นอกจากนี้ ได้พบแหล่งศาสนสถานที่มีอายุอยู่ในสมัยทวารวดี (ราวพุทธศตวรรษที่ 13-15) มักนิยมเลือกตั้งอยู่บนเนินลมพาททรายแผ่ สันนิษฐานว่าน่าจะมีความเกี่ยวข้องกับศาสนาและความเชื่อ ณ พื้นที่ดังกล่าว โดยสรุปจะพบว่า การเลือกตั้งถิ่นฐานของชุมชนโบราณทั้ง 2 ยุค แสดงให้เห็นว่า มนุษย์ในอดีตที่อาศัยอยู่ในพื้นที่ทุ่งกุลาร้องไห้ด้านตะวันออกได้คำนึงถึงปัจจัยทางธรรมชาติในการเลือกตั้งถิ่นฐานเป็นหลัก คือ ระดับความสูง และแหล่งน้ำธรรมชาติ ซึ่งบางชุมชนมีการปรับสภาพพื้นที่ธรรมชาติโดยการสร้างคูน้ำและคันดินเพื่อใช้ในการจัดการน้ำสำหรับ อุปโภค บริโภคและเกษตรกรรมเพาะปลูกข้าว

ภาควิชา ธรณีวิทยา ลายมือชื่อนิสิต .....

สาขาวิชา โลกศาสตร์ ลายมือชื่อ อ.ที่ปรึกษาหลัก .....

ปีการศึกษา 2560

# # 5871999823 : MAJOR EARTH SCIENCES

KEYWORDS: SETTLEMENT / THUNGKULA / GROUND-PENETRATING RADAR /  
PALEOCHANNEL / ANNULAR LANDFORM DEPRESSION / AEOLIAN SAND / NORTHEAST /  
PHEHISTORY / DVARAVATI / ARCHAEOLOGY / GEOARCHAEOLOGY

PATCHARAPORN NGERNKERD: GEOARCHAEOLOGY OF ANCIENT SITE  
SETTLEMENT AT EASTERN THUNGKULA RONGHAI, SRISAKET AND YASOTHON  
PROVINCES IN NORTHEAST THAILAND. ADVISOR: PROF. MONTRI CHOOWONG,  
Ph.D., pp.

Archaeology in Thailand is generally associated with geological application. In this work, the relationship between ancient site settlement and geomorphology is carried out under geoarchaeological approach. Study area is located on the eastern Thungkula Ronghai (TKR) bordered between Mun and Chi Rivers in Srisaket and Yasothon where many archaeological sites have been found. The research focuses on aerial photograph and satellite imaginary interpretation, application of ground penetrating radar (GPR) on sand splays morphology and GIS software to analyze ancient site location on geomorphology for reconstructing the relationship of human past with their landscapes. Results indicate the interesting landforms of the study area including paleochannels, annular depression landform (ADL) and aeolian sand splays. 54 archaeological sites are almost placed close to paleochannel with ADL, in contrast to a few moated sites located on distal sand splay due to shallow groundwater level and short distance from streams. In addition, the historical settlement associated with the sand splays, especially the temples. They can be explained under approach of landscape archaeology that the religion or the faith is realized. Finally, the spatial analysis suggests that “water resources” with higher elevation are the major factor for considering to be occupied. The moats and earthworks are implied to an adaptation of water management for using in living and agriculture.

Department: Geology Student's Signature .....

Field of Study: Earth Sciences Advisor's Signature .....

Academic Year: 2017

## ACKNOWLEDGEMENTS

This thesis was mainly supported financial by Morphology of Earth Surface and Advanced Geohazards Research Unit (MESA RU), Department of Geology, Faculty of Science, Chulalongkorn University, Thailand and 90 years of Chulalongkorn University Scholarship, thus, author would like to thank and recognize.

Great acknowledgement goes to Professor Dr. Montri Choowong, my thesis advisor, Department of Geology, Faculty of Science, Chulalongkorn University for his valuable encouragement and inspiration on scientific thinking. Thanks also to Assistant Professor Chawalit Khaokhiew, Department of Archaeology, Faculty of Archaeology, Silpakorn University for inspiration on geoarchaeological study and precious encouragement and suggestion in everything for me as his student. Moreover, Assistant Professor Dr. Sombat Youmuang, Dr. Akkaneewut Chabangborn, Associate Professor Dr. Santi Phailoplee, Associate Professor Dr. Srilert Chotpantararat, Dr. Piyaphong Chenrai is thanked for their valuable advises, helpful, and comments in this research.

I would like to extent the thankful acknowledgement to Dr. Krit Won-in of Department of Earth Science, Kasetsart University for advises about GPR interpretation. For the encouragement, I thanks to Dr. Prasit Auetrakulvit and Ms. Praon Silapanth, Department of Archaeology, Faculty of Archaeology, Silpakorn University. During field survey, I derived the suggestion and helpful form these persons as followed; Mr. Stapana Kongsan, Ms. Prapawadee Srisunthon, Mr. Aritach Nokngarm and Mr. Sutinan Trakulkasemsuk, so I also thanks.

Finally, I always have to thanks my parents for encouragement and supporting that I feel appreciate and respect. In addition to Ms. Wipada Onwimol, Ms. Alisa Saisavetvaree, Ms. Jitthada Reuksuk, Ms. Pimploy Piyathunmaporn and other friends in both Earth Science and Archaeology major that give me the direct and indirect encouragement.

## CONTENTS

	Page
THAI ABSTRACT .....	iv
ENGLISH ABSTRACT .....	v
ACKNOWLEDGEMENTS .....	vi
CONTENTS .....	vii
LIST OF FIGURES.....	1
LIST OF TABLES .....	6
Chapter 1 Introduction.....	7
1.1 Background .....	7
1.2 Objectives .....	8
1.3 Study area.....	8
1.4 Methodology .....	10
1.5 Benefits.....	11
This research is expected to provide the benefit as follows: .....	11
Chapter 2 Literature Review.....	12
2.1 Concepts of Geoarchaeology.....	12
2.2 Previous study of geoarchaeology in Northeast Thailand .....	16
2.3 Background of archaeology at Thungkula Ronghai in Northeast Thailand.....	18
2.4 Geology and Geomorphology of Thungkula Ronghai Area .....	23
2.5 Ground-penetrating radar (techniques and methods).....	59
Chapter 3 Methodology .....	65
3.1 Study Plan.....	65
3.2 Aerial photograph and satellite imagery interpretation.....	67

	Page
3.3 Ground Penetrating Radar survey with coring .....	70
3.4 Archaeological Survey .....	78
Chapter 4 Results .....	80
4.1 Geomorphology from aerial photo interpretation .....	80
4.1.1 Paleo-channel features.....	81
4.1.2 Annular landform depression (ADL).....	81
4.2.1 Radar facies and radar stratigraphy .....	97
4.2.2 GPR data interpretation based on radar facies and radar stratigraphy....	101
4.3.1 Grain size distribution.....	112
4.4 Dating of sand splays.....	125
Chapter 5 Discussion.....	128
5.1 Formation of aeolian sand splays with remarkably archaeological significances from GPR profiles and grain-size distributions.....	129
5.2 Implication of GPR profile and grain size distribution at Wat Don Kleua .....	143
5.3 Relationship between ancient site settlement and geomorphology at the eastern TKR.....	150
5.3.1 Prehistoric settlements of Iron Age (2,500-1,500 BP) .....	151
5.3.2 Historical settlements of Dvaravati and Pre-Angkor to Angkor periods in Thailand (9 <sup>th</sup> -12 <sup>th</sup> century A.D.).....	153
Chapter 6 Conclusion .....	161
.....	163
REFERENCES .....	163
VITA.....	176



## LIST OF FIGURES

	Page
<b>Figure 1</b> Study area located in Srisaket and Yasothon provinces.....	9
<b>Figure 2</b> Concept of geoarchaeology.....	13
<b>Figure 3</b> Examples of Roi-et ware.....	20
<b>Figure 4</b> Stratigraphic Profile across lower Mun River basin.....	25
<b>Figure 5</b> Quaternary stratigraphic sections of the Khorat Plateau.....	26
<b>Figure 6</b> Maha Sarakham Formation.....	27
<b>Figure 7</b> Alignment of Sand splay in the study area.....	28
<b>Figure 8</b> Section view of sand dune and Dune migration.....	29
<b>Figure 9</b> Model of mechanism of sand shadow dunes formation.....	31
<b>Figure 10</b> Formation of dune types.....	33
<b>Figure 11</b> Sorting and definitions in sand dune deposits.....	36
<b>Figure 12</b> Main internal stratification features in an ideal simple barchan dune.....	36
<b>Figure 13</b> Depositional model of internal structures in shadow dunes.....	37
<b>Figure 14</b> Formation of adhesion lamination in each water content level.....	38
<b>Figure 15</b> Examples of ADL found in Roi-et and Surin.....	40
<b>Figure 16</b> Salt diapir instrusion which push up overburden.....	41
<b>Figure 17</b> Diagram showing schematic shapes of salt structures.....	42
<b>Figure 18</b> Modes of diapir piercement shown in schematic cross sections.....	43
<b>Figure 19</b> Cross sections from physical models of salt dome.....	45
<b>Figure 20</b> Relationship of downstream changes.....	48
<b>Figure 21</b> Classification of channel types.....	50

<b>Figure 22</b> Sinoucity Index Theory (SI) in river morphology.....	51
<b>Figure 23</b> Morphological features of meandering river .....	53
<b>Figure 24</b> Transformation modes following expansion, translation and rotation .....	54
<b>Figure 25</b> Level of terraces originated from vertical erosion of stream .....	55
<b>Figure 26</b> Relationship between grain size and fluvial channel patterns .....	56
<b>Figure 27</b> Meandering river system .....	57
<b>Figure 28</b> Characteristics of channel fills of bed-load, mixed-load, and suspended-load rivers based on Galloway (1985).....	57
<b>Figure 29</b> Dune structures from GPR Profiles of linear sand dunes .....	61
<b>Figure 30</b> Five different aeolian radar facies within a parabolic dune.....	63
<b>Figure 31</b> Radar facies on GPR Profiles of paraglacial barrier systems.....	64
<b>Figure 32</b> Flow chart of methodology in this research.....	66
<b>Figure 33</b> Process of aerial photo interpretation by the mirror stereoscope.....	68
<b>Figure 34</b> Process of data analysis by GIS software.....	69
<b>Figure 35</b> Data sources as satellite imagery of LANDSAT 8 and GDEM 30 m.....	69
<b>Figure 36</b> Block diagram depicting main components of GPR system .....	71
<b>Figure 37</b> Instruments of GPR.....	71
<b>Figure 38</b> Examples of GPR data derived from GPR survey .....	72
<b>Figure 39</b> GPR lines tracked on sand splays at 3 sites .....	72
<b>Figure 40</b> A GPR line was tracked on Wat Don Kleua .....	73
<b>Figure 41</b> Table of Udden-Wenworth size classes.....	75
<b>Figure 42</b> Sieving methods.....	76
<b>Figure 43</b> Collecting the data by various methods in this research.....	77
<b>Figure 44</b> Archaeological survey map.....	78

<b>Figure 45</b> Archaeological survey in study area .....	79
<b>Figure 46</b> Geomorphic map .....	83
<b>Figure 47</b> The 3 groups of paleo-drainage founded in the Lower Mun and Chi River of eastern TKR basin .....	84
<b>Figure 48</b> The 16 ADLs with type orders founded on the Lower Mun and Chi valley or eastern TKR basin .....	84
<b>Figure 49</b> Aeolian sand splays discovered in study area .....	86
<b>Figure 50</b> The 54 archaeological sites of prehistory and history located in the study area .....	95
<b>Figure 51</b> Area of GPR survey run on 3 sites of sand splays.....	96
<b>Figure 52</b> Area of GPR survey tracked on Site 4 (a moated site).....	96
<b>Figure 53</b> Characteristics and depositional sub-environments of radar facies.....	100
<b>Figure 54</b> GPR interpretation of Line 1 at Site 1 .....	105
<b>Figure 55</b> GPR interpretation of Line 1 at Site 2.....	106
<b>Figure 56</b> GPR interpretation of Line 1 at Site 2.....	107
<b>Figure 57</b> GPR interpretation of Line 2 at Site 2.....	108
<b>Figure 58</b> GPR interpretation of Line 2 at Site 2.....	109
<b>Figure 59</b> GPR interpretation of Line 1 and 2 at Site 3.....	110
<b>Figure 60</b> GPR interpretation with elevation of Site 4.....	111
<b>Figure 61</b> Grain size distribution of S2C1 identified as aeolian sand splays.....	115
<b>Figure 62</b> Grain size distribution of S3C1 identified as aeolian sand splays.....	116
<b>Figure 63</b> Cumulative probability and frequency curves of aeolian sediments at S2C1 and S3C1 .....	117
<b>Figure 64</b> Grain size distribution of S4C1 identified as a mound .....	118
<b>Figure 65</b> Grain size distribution of S4C2 .....	119

<b>Figure 66</b> Cumulative probability and frequency curves of floodplain sediments at S4C1 and S4C2 .....	120
<b>Figure 67</b> Scatter plots of S2C1 that OSL samples.....	122
<b>Figure 68</b> Scatter plots of S3C1 that OSL samples.....	123
<b>Figure 69</b> Scatter plots of S4C1 and S4C2.....	124
<b>Figure 70</b> Stratigraphy of the 2 sections in this study along with OSL dating and grain size.....	126
<b>Figure 71</b> Soil profiles of Site 2 and Site 3 on the distal part of sand splays.....	127
<b>Figure 72</b> The Friedman response diagram modified by Besler (1983).....	130
<b>Figure 73</b> GPR profiles with internal structure from stratigraphic section.....	135
<b>Figure 74</b> Model of wind direction at sand splays from Site 2 .....	138
<b>Figure 75</b> Stages of sand splays formation at the study area .....	140
<b>Figure 76</b> Archaeological evidences were founded in the distal part of sand splays at Site 2.....	142
<b>Figure 77</b> Stratigraphic sections of Phor Kham Chan site with the characteristics of both soil deposits.....	143
<b>Figure 78</b> Grain size distribution with four parameters of S4C1.....	145
<b>Figure 79</b> Bivariate plot between mean size and sorting of S4C1 (mound) and S4C2 (moats) at Site 4 Wat Don Kleau.....	145
<b>Figure 80</b> Interpretation from mean size analysis and archaeological records founded in stratigraphy .....	146
<b>Figure 81</b> Electrical Conductivity was analyzed in the sediments of Site 4 related to salt percentage .....	148
<b>Figure 82</b> Frequency and cumulative curves of S4C1 and S4C2.....	149
<b>Figure 83</b> Water routes as a small canal from main paleochannels to moats of prehistoric sites .....	153

<b>Figure 84</b> Flow chart concluded the influencing factors of ancient settlement during 2,500 BP to 750 BP.....	157
<b>Figure 85</b> Archaeological evidences founded at historical sites .....	158
<b>Figure 86</b> Density of prehistoric sites associated with location of ADL and paleochannels.....	159
<b>Figure 87</b> Density of historical sites associated with ADL and Sand splays .....	160



## LIST OF TABLES

	Page
<b>Table 1</b> Lithofacies classification of fluvial deposits .....	58
<b>Table 2</b> List of 85 aerial photos in WWS projects from RTSD.....	68
<b>Table 3</b> Archaeological sites located in the study area .....	88
<b>Table 4</b> OSL dating results.....	126



## Chapter 1

### Introduction

#### 1.1 Background

Many archaeological sites have been found at Northeast Thailand. Especially, at Thungkula Ronghai area in the Khorat basin, the archaeological features on the aerial photography and satellite imagery such as an encircling mound site and a moated site in circle, oval and square shape were found. Moreover, the artifacts and ancient monuments can be found in these areas. They indicate the development of human settlements during prehistoric period (about 4,000-1,500 yr BP) to Angkor period (950-650 yr BP) (Baoneod, 2010: 37-38). Recently, O'Reilly (2015) has studied the relationship between sites and their locations from remote-sensing technique applied to survey for searching the archaeological sites at region of Mun and Chi River. The results illustrate that most of human past settlements occupied in close water resource (O'Reilly and Scott, 2015).

The study area of this research is located at the eastern Thungkula Ronghai where many people recently realize that there is the negative settlement area because of drought, in contrast to discovering many archaeological evidences described the human past had chosen this area for settlements and built the great civilization. They are organized to form the cultural group by Valibhotama (1992) known as "Thungkula Ronghai Culture". As mentioned above, not only the cultural factors (i.e. religion, economics, politics and society) effect to the development of community, but the natural factors may play a role too.

The results of interpretation from aerial photography show the cultural and natural features illustrating various geomorphologies. They include aeolian sand splay (as one type of sand dune), salt dome, annular depression landform (ADL) and fluvial landform. However, the only aerial photograph interpretation cannot provide the entire detail of evolution and internal structure of these geomorphologies, geophysics instrument, thus, is applied in this research. For this research, Ground Penetrating Radar (GPR) is used to study internal structure of sand splay found at old

terrace of Chi River in Yasothon and Srisaket provinces. Finally, these results are analyzed in order to explain the possible reasons of choosing for human past settlements in the study area. The advantage and disadvantage of these geomorphologies leads to utilize from these landforms influencing shape, size and function of archaeological sites. Overall, the site location is plotted in geomorphologic map and the relationship between archaeological site settlements with geomorphology at eastern Thungkula Ronghai area is discussed beneath the approach of geoarchaeology.

## 1.2 Objectives

1.2.1 To interpret geomorphology in eastern Thungkula Ronghai area by using the remote-sensing data (i.e. aerial photography and satellite imagery).

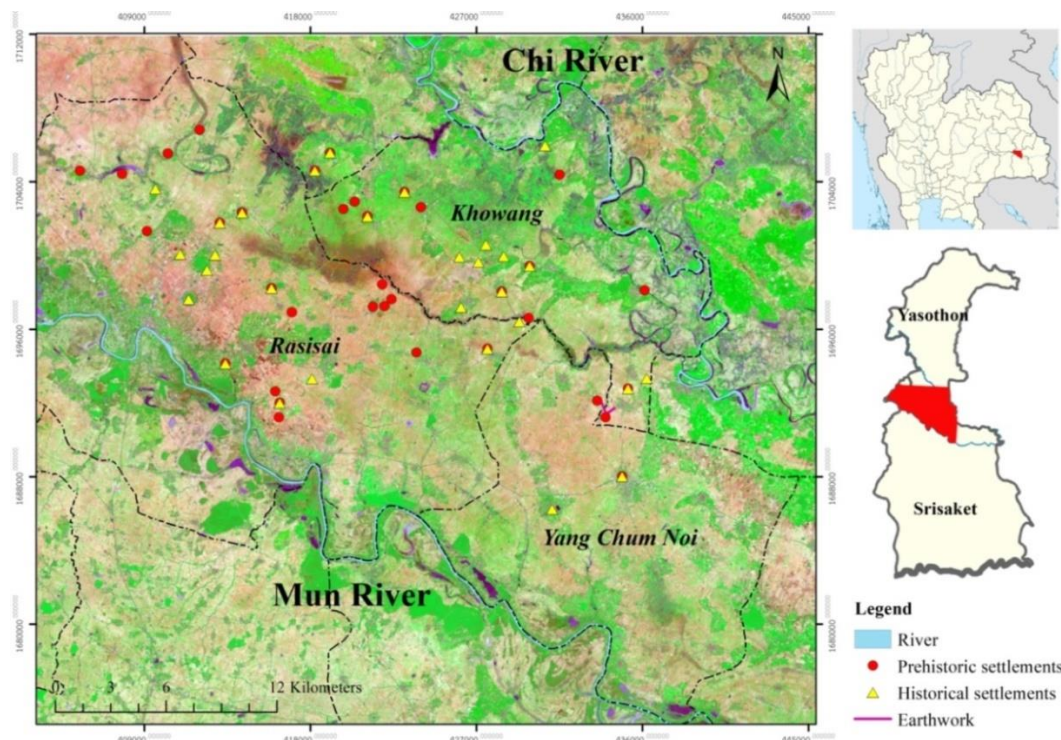
1.2.2 To study the internal structure of aeolian sand splay in study area by application of geophysics method (using the ground penetrating radar instrument).

1.2.3 To study the influences of geomorphology that effect to the human settlement during prehistoric period (4,000-1,500 yr BP) to historical period of Angkor (the 8<sup>th</sup> – 13<sup>th</sup> century AD).

## 1.3 Study area

The study area is located in the north of Srisaket and the south of Yasothon provinces that it is called “the eastern part of Thungkula Ronghai”. It is situated between Mun and Chi Rivers or the Lower Mun and Chi Valley (Figure 1).

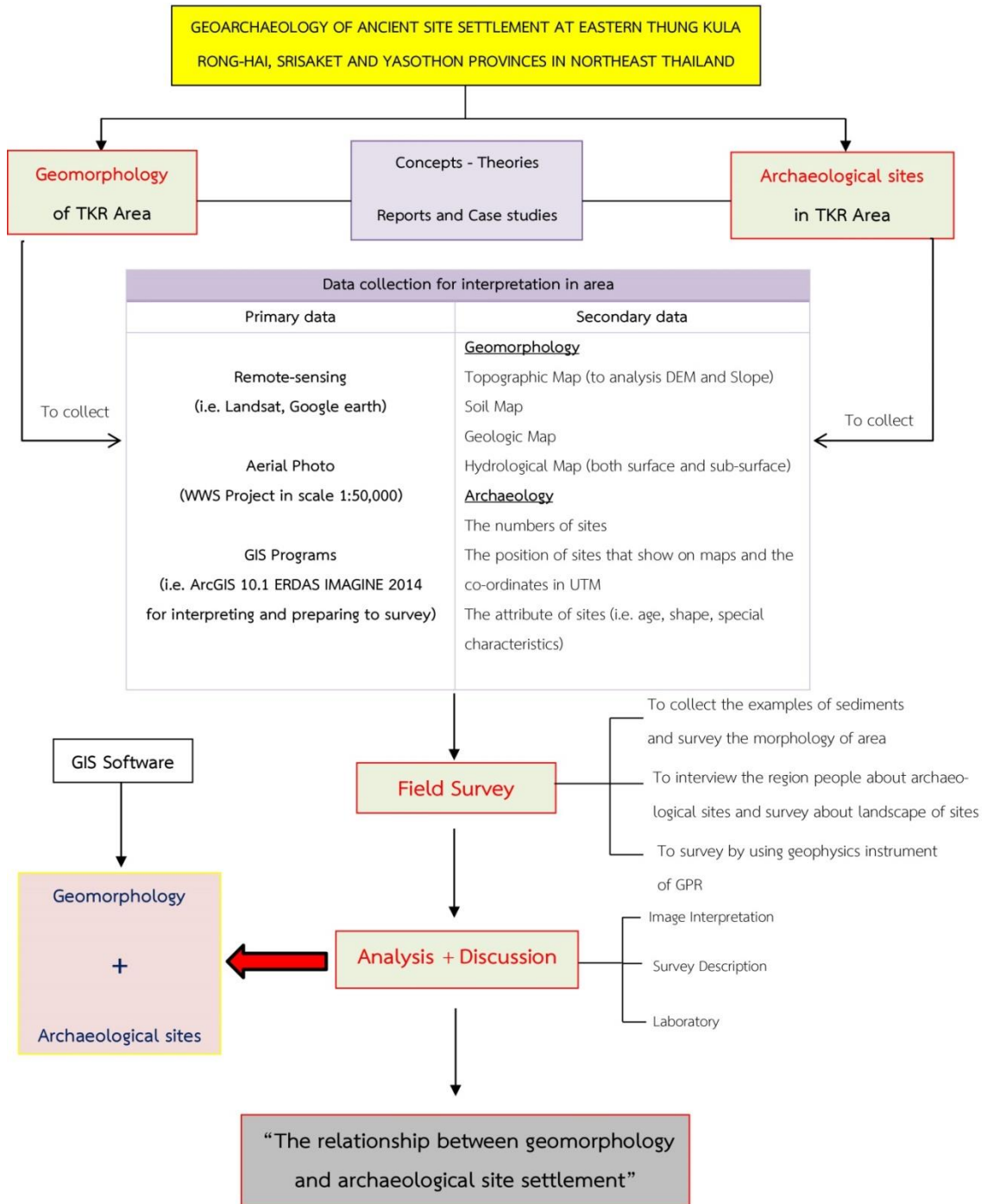




**Figure 1** Map showing the study area located in part of Srisaket and Yasothon provinces.



### 1.4 Methodology



### 1.5 Benefits

This research is expected to provide the benefit as follows:

1.5.1 This work will improve the understanding in the effects of natural factor which scope and control the human past settlements in eastern Thungkula Ronghai area due to advantages or disadvantages of geomorphology.

1.5.2 This research will improve the relationship between types of archaeological sites (i.e. habitat sites, burial sites, regional sites, and industrial sites) and their location.



## Chapter 2

### Literature Review

#### 2.1 Concepts of Geoarchaeology (or *geo-archaeology*)

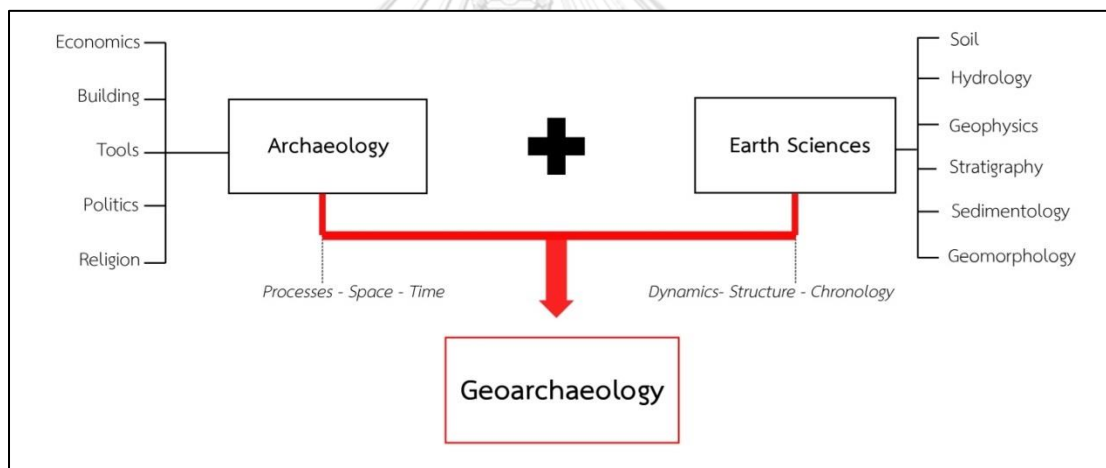
Archaeology is the study of human past that can be called “culture” as everything is built by human. The key of this subject is a reconstruction the cultures in the past on a region by understanding the behaviors and ideas of human. In 1960s, Lewis R. Binford, an American archaeologist, introduced his revolutionary idea for changing archaeological perspective to “New Archaeology or Processual Archaeology” and then the science was applied. In 1970s, the geoarchaeology approach was developed from the archaeologist who is interested in environment and process of stratigraphy in an archaeological pit. As a result, it was the first that apply the theories, principles, methods and techniques of geology to archaeology.

##### 2.1.1 Approach of geoarchaeology

The term of *geoarchaeology* using techniques and methods of earth science (or geoscience) has been used with increasing frequency since the 1970s. There are many definitions; for example, Reid Ferring (1994) defined geoarchaeology as a “grossly empirical approach to archaeological problems” or the “new empiricism”. The term “geoarchaeology” refers to the application of any earth-science concept, technique, or knowledge for study the time frame of human history which base to the study of artifacts and the processes involved in the creation of the archaeological record (Ferring, 1994). Indeed, its widest scope includes the application of these earth-science disciplines and subfields to the study of the archaeological records.

Thus, geoarchaeology should be defined as a branch of archaeology which is the study to understand the human past as its fundamental goal. It represents a specific focus of archaeology that may be considered, including hydrology, climatology, lithology, geomorphology and ecology, as a subdivision of earth science in the broadest sense (Figure 2). Geoarchaeological aspects, in contrast, can be considered from the viewpoints of *dynamics*, *structure*, and *chronology* while

it is compared between archaeology and earth sciences. Firstly, dynamics (or processes) relate to the effects of physical and chemical forces. Secondly, structures relate to composition and arrangement of materials or landscapes. Finally, chronology and history are concerned with time, origins, and development (Rapp and Hill, 2006: 1-3; Butzer, 1982). The relation of these principles can be created to a model that will be linked with information on biota, demography, and material culture to generate a higher order model of prehistoric settlement and subsistence pattern. Most of geoarchaeological reports, however, have failed to focus on cultural factors in site formation, on physical disturbance and modification of cultural residues in addition to the unique potential of this work mode in archaeological survey (Butzer, 1982: 35-39). As a result, this research will emphasize and strongly focus on the influences of physical factors that effect to the culture of human past.



**Figure 2** Concept of geoarchaeology which applies the earth sciences methods and techniques to study culture of human past.

### 2.1.2 The study components of geoarchaeology

Butzer (1982) has considered the primary study components in geoarchaeology that could be divided to various contexts for different scale and scope of study area following landscape context, stratigraphic context, site formation, site modification, and landscape modification.

**1) Landscape context** is analyzed to three scales including *site micro-environment*, defined in terms of the local environmental elements that influenced original site selection and the period of its use, *site meso-environment*, primarily the topographic setting and landforms of the area utilized directly for subsistence that helps reconstruct the paleoenvironment, and *site macro-environment*, necessarily the regional environment analyzed the process of regional ecosystem.

**2) Stratigraphic context** can be considered the reconstruction of sequential natural events receiving from geologic and geomorphic records (i.e. soils, sediments and etc.)

**3) Landscape modification** means that human is an intervenor the landscape such as roadways, irrigation networks, ditches and etc. that these features was constructed for adaptation.

As mentioned previously, the study components of geoarchaeology indicate that the archaeological reconstruction can be filled perfectly with studying in landscape and environment by an approach of geoarchaeology in order to analyze the relationship between human past and their environment or resource. For this research, the landscape and stratigraphic contexts are used and discussed as well as the components of landscape modification.

### 2.1.3 Landscape archaeological perspective

Significantly, the geoarchaeological concepts are similar to *Landscape Archaeology* principles. It is a term generally used to characterize the spatially archaeological research that considered the landscape being the relationship between sites and physical spaces. There are two principles. The first is “landscape analysis” approach that is the identification of clues within the present landscapes such as analysis of field morphology and cartographic evidence and combination the archaeological methods for environmental aspect interpretation. The second is the scientific reconstruction concentrated on the physical remains of the past or the examination of botanical remains is the interpretation of environment and landscape

in those areas. (Chapman, 2006: 11-12). As well as these principles, the study of landscape archaeology has brought post-processual theory, a concept of thoughts in type of sensual perception, to interpret the landscape since 1990s (Tilley, 1994; Tuan, 1977). It is believed that the archaeological landscape is an interaction between places and spaces that divided the perspective of landscape to practical and theoretical approaches. For the practical approach that derives from processual perspective, it is essential focusing on techniques and methods. The distribution of sites on maps and the interpretation of sequencing and phasing within the landscape are important. The same geoarchaeology has been considered the application of earth science techniques and methods to investigate the paleoenvironment commonly. Typically, the attributes of physical sites on the ground or through aerial photography is usually investigated by landscape archaeologists and geoarchaeologists to make consideration the environmental factors being the influences to human behavior, along with building a picture of environment in the past. The theoretical approach is an interpretation of space considered to be a cultural construct. The post-processual perspective clearly influences to this approach. In order words, it makes the distinction of spaces and places; the space becomes a meaningful term in which an area is created a meaning or a symbol of activities, in contrast to a place, as an element of space, it is a location or point of activity. Besides, Tilley (1994) argues that the role of the individual as a vehicle for experiencing the landscape. He has been attempted to classification the particular kinds of spaces in the literature to generalize. The following forms of space might be identified: 1. Somatic space, 2. Perceptual space, 3. Existential space, 4. Architectural space, and 5. Cognitive space (Tilley, 1994: 14-15).

Finally, the study of relationship between human and their environment would effect to the principle of “settlement” that be defined as the interrelationship of human and their environment such as culture, space, and time. The definition of settlement mentioned above, was included to archaeology, then, *settlement archaeology* was developed by Trigger (1976). The settlement archaeology is different from settlement in the present, because it emphasizes the relation of

human and environment in the past by investigation or interpretation from archaeological records (i.e. artifacts, ecofacts, site locations, and etc.) (Trigger, 1967).

## 2.2 Previous study of ge archaeology in Northeast Thailand

The approach of ge archaeology as mentioned previously is the application of earth sciences concepts, techniques, and methods for interpretation the culture of human past. Recently, O'Reilly et al. (2015) discovered new many archaeological sites or about 146 newly sites identified the Iron Age moated sites in the Mun and Chi valleys of Khorat plateau by using Google Earth satellite imagery. However, the context of ge archaeology study in Northeast Thailand might be occurred since 1997s or the Origins of Angkor Archaeological Project (OAAP) was taken which is a corporation between Otago University, Southern Cross University, New South Wales and the Thai Fine Arts Department. Their study area is the upper Mun river valley located in Noen U-Loke, Non Muang Kao and Ban Lum Khao, Nakorn Ratchasima province, the southwest of Khorat plateau (Higham and Thosarat, 1998).

In 1997-1998, the archaeological project was taken place by the excavation of 7 moated sites: Noen U-Loke, Non Muang Khao, Ban Non Khrua Chut, Ban Non Ngiu, Ban Makham Thae, and Ban Non Wat. The aims focus on the moat as a significant structure that has tended to obscure the relationships between site and landscape. When the excavation was succeeded, the results of examination in stratigraphy and cross sectional morphology were analyzed. The excavated trenches represent the first excavations of any significance within the moats themselves. They revealed the presence of buried channels beneath the actual archaeological mound features which is resemble small low-flow channels set in wide shallow flood-flow style channels. Furthermore, the aerial photographs interpretation indicated that the geomorphology of their location is floodplain showing much of paleochannel features distinctively that the moated sites are discovered. As a result, these features such as the buried channels beneath the archaeological mound and their geomorphology that they are located were referred to the relationship between the nature represented by geomorphology and sediment analysis and the culture in a moated site. In conclusion, the archaeological sites appear to be at least spatially



linked with bands of river channels that have a longer history than the moats. It is possible that their moated construction was an adaptation for protecting floodwater on the land surface and may have been managed as controlled flow or supply into the constructed moats (Boyd et al., 1999a; Boyd et al., 1999b; McGrath et al., 2008).

In the present day, the technology of remote-sensing is developed, especially the satellite imaginary resolution and Geographic Information System (GIS) software (i.e. ArcGIS, and QGIS). It is convenient for geoarchaeology and landscape archaeology analysis until Scott and O'Reilly (2015) studied the rainfall average and circular moated sites in northeast Thailand discovered by using Google Earth, as mentioned above, with GIS software. They have studied the site density determined by a kernel density model in ArcGIS and used K-means analysis as the basis to divide the moated sites into 8 distinct groups. Finally, they were analyzed along with rainfall data in type of a rainfall distribution map and site size showing the most of moated sites in Mun and Chi valley are located in regions with the lowest precipitation, those receiving c. 1000-1200 mm and 1200-1400 mm annually (Scott and O'Reilly, 2015). On the other hand, the relationship between rainfall and site size was assumed that arid areas would not be able to support large populations and so the size of sites in relation to the amount of rainfall was also examine. The predicted mean size of sites indicated that the smallest in this area is receiving the least annual rainfall. In addition, Scott et al. (2015) have studied the number of moats at a site together with rainfall data. The results are sites in the driest areas would have multiple moats to collect much of water as possible in case of an assumption that moats were constructed around these sites to collect and store water in contrast to McGrath et al. (2008) who have suggested that the moats served to protect sites from flooding.

Moreover, the study of paleoclimate in Northeast Thailand related to human adaptation has been proven by Boyd et al. (2001) that they used pollen analysis from the infill of Iron Age features to indicate the paleoclimate in regions where moated sites occupied. His notice is why low density settlement of Bronze Age was shift to high density of Iron Age. The pollen record represents a period in which the floodplain was initially dominated by forest as wet phase and its replacement by grassland as dry phase took place later or in the Late Holocene period. Boyd et al.

(2001) introduced that human had adapted to cultivation in dry phase because of surviving in severe condition that climate influenced to human activity (Boyd and McGrath, 2001). These results are similar to Wohlfarth et al. (2016) who studied mid-to late-Holocene climate changes in Northeast Thailand. They analyzed paleoclimate from the records of Lake Kumphawapi and Lake Pa Kho by sedimentary coring. The analysis and interpretation from these records reflects to lake level in the past indicated that the late Holocene period had climate fluctuation that related to summer monsoon in Southeast Asia. Finally, they attempts to reconstruct paleoclimate and links them to the moats construction of Iron Age human that the function of these construction was a represent water storage facilities and reservoirs due to adaptation for agriculture in climate conditions (Wohlfarth et al., 2016).

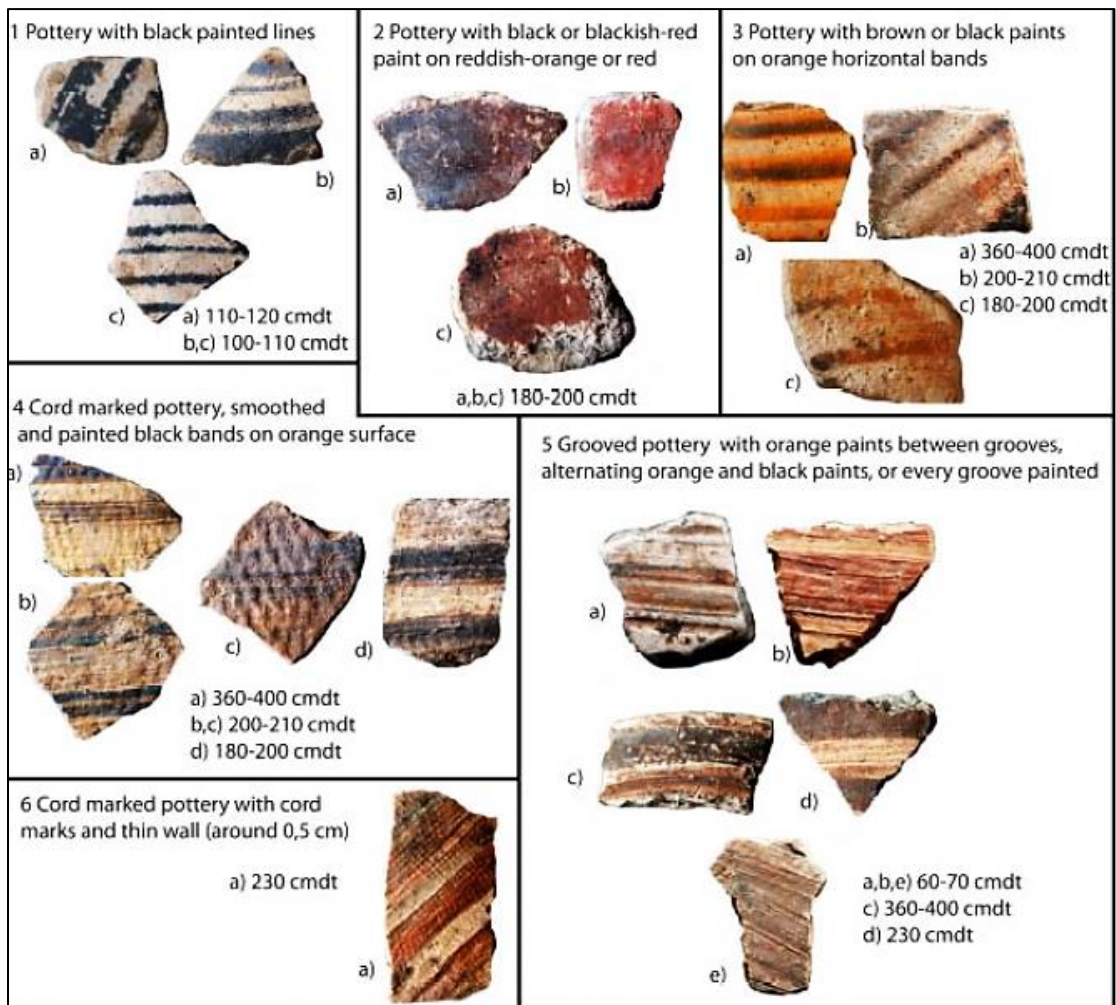
### **2.3 Background of archaeology at Thungkula Ronghai in Northeast Thailand**

The study of archaeology at Thungkula Ronghai (TKR) had been started up since 1996 under “The archaeological survey at Thungkula Ronghai Project” along with the excavation was taken place at Ban Muang Bua being a moated site in prehistoric period by 11<sup>th</sup> regional office of Fine Arts Department (Ubon Ratchathani). This excavation uncovered the important archaeological records such as sherds (pottery’s fragments), human remains, tools and ornaments, especially the burial culture indicating the various in ceremony of this tradition. It can be dated to about 3,200-1,300 yr BP or the late prehistoric period. These results, therefore, tend to establish a research project of burial tradition in late prehistoric period of Thungkula Ronghai culture in 2000. The burial tradition of Thungkula Ronghai culture is different from others since it is a ceremony. The human remains were brought to bury within a pottery in the second time or called “Secondary burial” in contrast to “Primary burial” that is the first buried in a grave (Baoneod, 2010: 50-51). In addition, the archaeological survey reveals 408 sites locating in region of TKR where is the boundary in Roi-et, Maha Sarakham, Surin, Srisaket and Yasothon provinces. Most of archaeological sites are the late prehistoric sites or Iron Age that Valibhotama (1990) argued that the TKR area could be divided to two cultures basis on evidences found in archaeological excavation and survey: 1) Thungkula Ronghai culture, in Roi-et,

Maha Sarakham and Surin provinces and 2) Thung Rasisai culture, in Rasisai, Srisaket province as well as some area of Yasothon province. These sites are located in the lower Mun and Chi River of the northeast Thailand.

### 2.3.1 Thungkula Ronghai and Thung Rasisai culture

As mentioned previously, the difference of these cultures is the style of pottery decoration. For the TKR culture, the technique of mixture ivory color is remarkable. It is from burning Kaolin clay by burning. When the burning is succeeded, the burnt pottery appears to grey color. The ivory colored potsherds are quite thin decorated by slipping, painting and polishing known as “Roi-et ware” that was discovered in the excavation at Ban Non Deau, Don Ta Phan, Bo Phan Khan at Suwanabhum district, Roi-et province by Charles Higham (1977). Its characteristic is cord marks impressed, then smoothed and painted red bands and is dated about ca 1,895±53 B.P. (Higham, 1977: 103-142) which is a wide range of time. Thung Rasisai culture, on the other hand, has the distinct characteristics as toned-white painted on the black pottery or various slipping colors in orange or red (Valibhotama, 1990: 457-458) (Figure 3). This characteristic of pottery decoration is generally founded in archaeological sites that located on bordering eastern part of Thungkula Ronghai.



**Figure 3** Examples of Roi-et ware which is generally found in the excavation at Wat Pa Sai Ngam belonging to Thungkula Ronghai culture (Auetrakulvit and Winayalai, 2012).

### 2.3.2 Dating of Thungkula Ronghai culture from archaeological records

In archaeological approach can be divided into two methods of dating as following 1) Absolute dating and 2) Relative dating like the geology and earth science dating methods. However, absolute dating is more believable for geologist and archaeologist because of using scientific methods. The archaeological excavation is a method for the study of human past culture that the evidences buried in subsurface are not changed or moved by modern human activity called as *in-situ*. As a result, these evidences can be dated accurately by scientific methods, but it should be carefully collected.

The 1969 excavation of Non Dua in Roi-et province examining the pattern of Iron Age settlement revealed features of salt pan and archaeological mound including cultural deposits reach down 4.85 m from the mound's surface. It has been divided into three ceramics phases. The first phase is represented by red-slipped pottery vessels dated from about 500-1 BC. The second layer has a characteristic pottery style called Roi-et ware dated to 1-700 AD. The final phase has a thin white pottery which can be dated about 700-1,000 A.D. However, no burials were found due to limited excavation area in contrast to iron slag discovered at the bottom of the site (Higham and Thosarat, 2012: 207-209). The Roi-et materials, in addition, were investigated by radiocarbon dating that illustrates to 228-597 A.D. and 250 BC-AD 341.

The 1981 excavation of Non Yang in Surin province can be dated about  $3,000 \pm 250$  yr BP by radiocarbon dating from a charcoal founded in 2.2 m depth. Pornchai Sujit, a professor of Silpakorn University, assumed that these regions might be occupied since 4,000 yr BP at least.

The 1997-1999 excavation of Ban Muang Bua in Roi-et province revealed archaeological records that can be dated about 3,200-1,300 B.P. by relative dating. Three years after this excavation was completed, the Fine Arts Department officers (FAD) had excavated nearby last excavation area. The excavation reached the natural substrate at the depth 4.0 meters that the cultural layers were divided into two phases: The first phase illustrated to the burial tradition and residence activity that these evidences were dated about  $4,000 \pm 250$  yr BP to  $2,620 \pm 240$  yr BP by radiocarbon dating and the final phase was interpreted to burial activities or graves function that received dating about  $2,440 \pm 210$  yr BP to  $1,280 \pm 210$  yr BP (FAD, 2010: 98, 113-117). The both of them are considered belonging to TKR culture. Meanwhile, the excavation was taken at Ban Pone Thong nearby Ban Muang Bua mentioned above. It shows only phase of culture being a burial site. The radiocarbon dating indicates to  $2,360 \pm 220$  yr BP and  $1,460 \pm 200$  yr BP (FAD, 2010: 117-118).

Recently, the excavation of Ban Pone Bang is completed. It discovers much of evidences that a charcoal from the bottom of layer 12 can be dated to  $1,808 \pm 25$  yr BP by radiocarbon dating. The pottery decorated styles relate to Roi-et

ware which was found in Ban Non Dua dated to 2,000-1,300 yr BP apart from being found the pottery of Thung Rasisai style (Auetrakulvit and Winayalai, 2012). Thus, the age of this site should be concluded that the culture occurred since 1,900-1,800 yr BP and started to group under TKR culture in 2,000-1,300 BP.

In conclusion, the development of settlements in TKR culture should be grow up since 3,000-2,500 BP and developed to the TKR culture group or organization about 2,000-1,800 BP until 1,500-1,300 BP that progressed to proto-history.

The archaeological site study at the lower Mun and Chi River in study area of this research might be started up when Vallibhotama (2003), an archaeological professor of Silpakorn University, had surveyed in Thungkula Ronghai area since in 1981. He argued that the sites located in terrace and floodplain between Mun and Chi River that was called Thung Rasisai (the most are moated sites) was older than sites located in the southern Mun River. As a result, many evidences indicated the cultural development of these settlements was grown up from proto-historic to historic period. It appeared remarkably in Khmer period at the south of Mun River. Thus, it is possible that the human past who occupied in the between Mun and Chi River of Thung Rasisai since prehistoric or proto-historic period migrated to the upper land in southern Mun River later due to influences of Khmer culture in those time (Valibhotama, 2003).

Many categories and functions of archaeological sites such as salt making sites, metal smelting sites, burial sites and habitation sites were found in this study area which are considered by activity records of human past. It is possible that these sites are dated about 2,000-1,500 BP or the late prehistoric to proto-historical period (Late Iron Age) i.e. Ban Non Sung, Ban Don Kluea, Ban Khu Song, Ban Pone Bok, Ban Lub Moke, Ban Pone Bang and etc. After that, the prehistoric culture of these peoples developed to the power and commercial basis on adaptation in using natural resources. Moreover, Vallibhotama (2003) believed that the sedentary settlement in Khorat basin had developed the culture in floodplain of the middle

Mun River on the mounds before moving to the lower Mun River that developed to moated sites that the appearance of chiefdom in proto-history.

## **2.4 Geology and Geomorphology of Thungkula Ronghai Area**

Northeastern Thailand occupies an area approximately 168,800 km<sup>2</sup>. In the south is bounded by the San Khampang and Phanom Dong Ruk Ranges and the boundary on the west is the Phetchabun and Dong Phraya Yen Ranges. The general geography of this region is mostly undulating high plateau interspersed with low hills and ridges with board crests and gentle sloping 20 to 30 m relief (Udomchoke, 1988: 69-71; Loffler et al., 1984). Geologically, an extensive outcrop of Mesozoic rocks occurs on the Khorat Plateau which is similar to distorted square with high boundaries at the northern, western and southern margins. This plateau is rimmed by an escarpment of mostly and steeply dipping sediments forming cuestas rising from 600-1,000 m above sea level on its western and southern margins in addition to being a sauce-pan morphology called “Khorat Basin” (Piyasin, 1995). Moreover, in the north of Khorat plateau is the smaller Sakon Nakhon basin that is divided by the Phu Phan Range.

The previous geological study in the Khorat plateau demonstrated the formation of this geological area that was detached from the western landmass by rifting of the continental Southeast Asia and by the opening of the Gulf of Thailand during Late Cretaceous to Tertiary Periods (Bunopas and Vella, 1983). Later, the Phu Phan Range had uplifted along with downwarping of the Khorat and Sakon Nakhon Basins during the Himalayan epeirogeny. During Mio-Pliocene to Middle Pleistocene epochs, volcanic eruptions produced basaltic hills along the southern part of the Khorat Basin. Thus, the sedimentary sequence in this area consists of an initial rift sequence of Carboniferous to Triassic, and a “sag” sequence of Late Triassic to Cretaceous (Wannakomol, 2014).

### **2.4.1 Previous study of geomorphology at TKR**

In 1964, the first major attempt to conceptualize the development of landforms or geomorphologies in the Northeastern Thailand taken place when

Moorman et al. (1964) divided the Quaternary deposits on the Khorat Plateau into four units based on landform development (Loffler et al., 1984: 322-323). In 1977, Boonsener (1977) reported that a stratigraphic section of the Quaternary sediments in Khon Kaen province consists of nine sedimentary units of aeolian and fluvial deposits overlying the weathered Khok Kruat clay.

The geomorphological study of TKR occurred at the first since 1980s when Loffler et al. (1984) had reported “Quaternary geomorphological development of the Lower Mun River Basin, North East Thailand” that his work excellently illustrated the stratigraphic information of TKR located on the Lower Mun River. The results of Loffler et al. (1984) showed that the structure of the lower Mun River basin represents a basin within the larger Khorat basin being some TKR depression. Furthermore, the factors influencing to geomorphological development of the Mun River basin are the tectonically control on river base levels and climate changes within Quaternary derived from sediment records accumulated up to 150 m thick (Figure 4), in contrast to the terrace model of Moorman et al. (1964).

Tuckson et al. (1983) indicated the evolution of TKR landscape in six phases described as below.

**1) Erosional Landscape** is relatively low relief developed over the near horizontal to slightly warped Maha Sarakham Formation.

**2) Incision and Valley Deepening Phase** follows the previous erosional landform of Maha Sarakham Formation.

**3) Non-organic Sand Deposits** was filled up gradually with alluvial sands in an environment which was drier than the present because of the lack of organic matter.

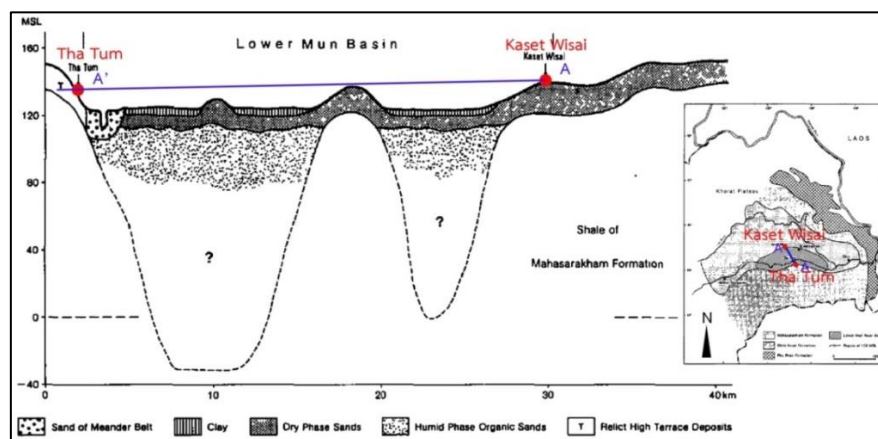
**4) Organic Sand Deposits** are accumulation of organic sand during 34,000 to 20,000 years BP of humid phase earlier to the last glacial maximum that was dated by radiocarbon dating. These deposits are found in the depression area of TKR. The grain size of sands widely varied from very fine to medium sand in the northern part of TKR to fine sand and fine gravel in the southern part, closer to the recent Mun River (Loffler et al., 1984: 125).



**5) Non-organic Aeolian Sand Deposits** (i.e. red or yellow loess and windblown sand) is the aeolian activity for short distance transportation from the bed of braided river during the cold and dry phase of the last glacial maximum 20,000 years BP. These non-organic sands are probably continuous over the entire of TKR as well as appearing in the thick sand sheets covering all the hills and rises within the TKR (Loffler et al., 1984: 125).

**6) Alluvium** is the final phase of deposition during the end of the last glacial maximum to present that is accumulated to clayey sand and silty sand. The alluvium is always found in the floodplain area of present streams.

In addition, Loffler et al. (1984) incorporated with Soil Survey Division Land Development Department of Thailand had studied geomorphology of Thungkula Ronghai for development. In fact, the landform of TKR is a broad depression formed by an extensive alluvial plain and bordered to the south and north by gently undulating to low hilly uplands. Structurally, the TKR basin acts a saucer shaped basin similar to the Khorat Basin along with uplifted margins to the south and north. The bedrock forms to the formation known as Maha Sarakham Formation. It consists of interbedded shales, siltstones and sandstones containing salt bodies ranging in size from small salt veins to large salt domes (Loffler et al., 1984) (Figure 6). However, the concept of TKR's evolution is similar to Tuckson et al. (1983) as mentioned above.



**Figure 4** Stratigraphic Profile across lower Mun River basin between Kaset Wisai and Tha Tum (modified from Loffler et al., 1984).

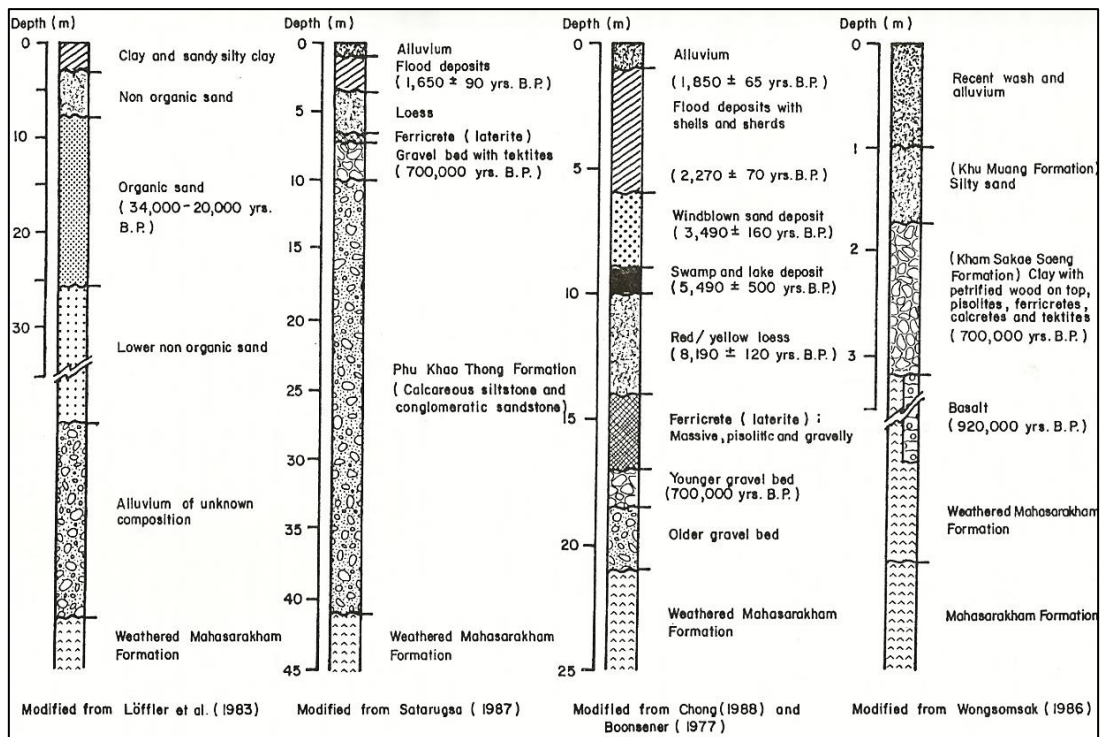


Figure 5 Comparison of the Quaternary stratigraphic sections of the Khorat Plateau (Udomchoke, 1988: 69-115).

Formation	Unit	Symbol	Range of thickness (m)
	Top Soil Alluvial and Loesslike deposits		1-168
PHUKHAOTHONG	Sandstone, Conglomerate, Siltstone		0-31
PHUTOK	Upper Clastic		0-1000
<b>Maha Sarakham</b>	Anhydrite Upper Salt		0-6
	Upper Salt		0-65
	Middle Clastic		0-84
	Anhydrite Middle Salt		0-12
	Middle Salt		0-171
	Lower Clastic		0-95
	Anhydrite Color Salt		0-2
	Color Salt		0-45
	Potash Zone		0-244
	Lower Salt		0-392
	Basal Anhydrite		0-6
KHOKKRAUT	Siltstone, Sandstone, Conglomerate		-

**Figure 6** Maha Sarakham Formation including three layers of salt related to salt tectonics in the Khorat Plateau (modified from Youngmee, 2004).

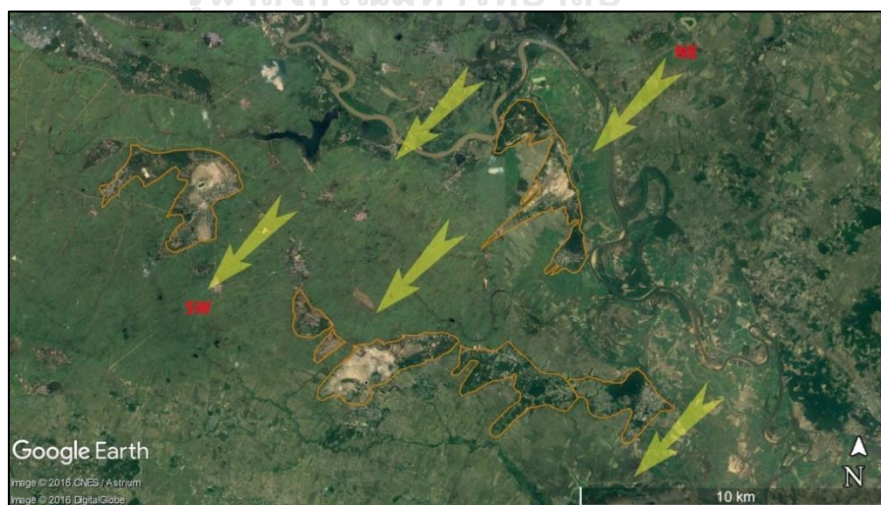
#### 2.4.2 Specific landforms of TKR

Recently, the analysis and interpretation from aerial photography or satellite imagery illustrates the various landforms in TKR broad depression. The sand dune and salt dome morphologies are interesting for this study, as well as fluvial system.

### 1) Sand splay (as sand dune)

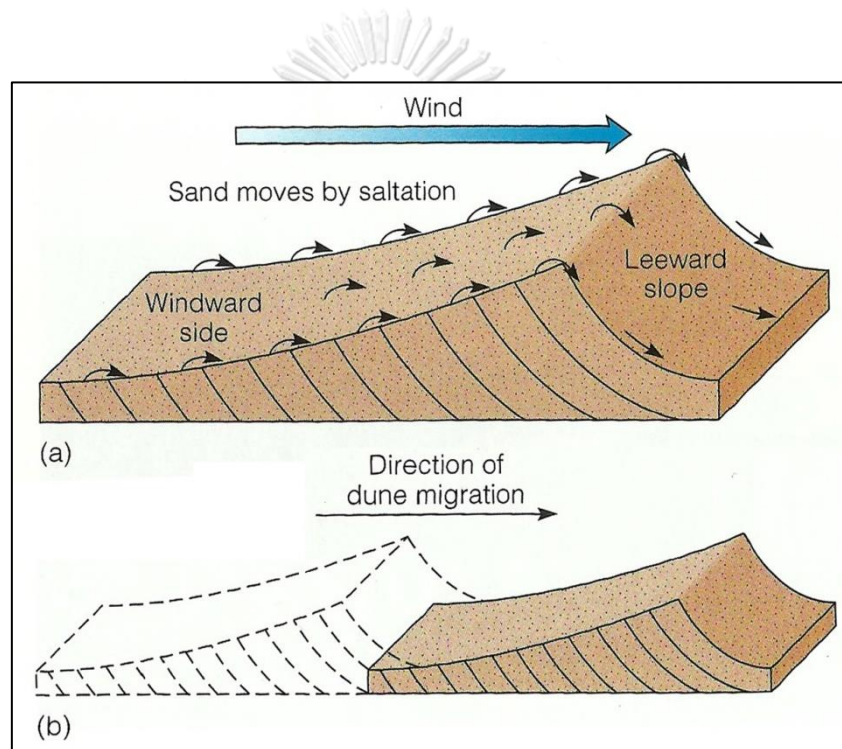
Sand splay is defined as sand dune forming from aeolian activity when wind flows over and around an obstruction. They are found in Yasothon, Srisaket and some parts of Rot-et, Surin and Ubon Ratchathani (Hokjareon, 1989). They are mounds or ridges of wind-deposited sand that stand a few meters above surrounding paddy field and be surrounded by natural forest (Figure 7). The sand cover is various thick and overlies the partly weathered regolith of the Maha Sarakham Formation. In addition, the sand is between 1 to 3 meters in thickness (Pramojanee et al., 1985) and the color is from pale brown to yellow- occasionally light grey. The texture is fine to medium sand that these are proved by grain size analysis of 20 samples resulting to being fine grained (0.16-0.22 mm).

Hokjareon (1989) examined on Landsat Images which appear the features of sand splay more than 200 points illustrating that they are aligned within a narrow range of azimuth angles approximately NE-SW and side slope are usually very gentle. Moreover, the study of grain size analysis of 20 samples as mentioned above showed that the sand are the product of short term aeolian mobilization of fluvial materials during changes of avulsion in the Khorat basin. They are believed that the formation was caused by obstacles in the path of sand drift and originated during the last glacial episode or continued to postglacial period.



**Figure 7** Alignment of Sand splay (orange lines) in the study area (base map is modified from Google Earth Pro taken in 2016).

Fundamentally, most dunes have an asymmetric profile (ripple) including a gentle windward slope and a steeper downwind slope (or leeward) that is inclined in the direction of the prevailing wind (Wicander and Monroe, 1998: 319-320) (Figure 8). The ripple geometry can also help to identify aeolian paleoenvironments and directions of sediment transport in ancient sandstones (McKee, 1945). Generally, the maximum linear dimension of individual dunes ranges from less than 1 m to several tens of kilometers while the height ranges from a few tens of centimeters to more than 150 m. Dunes may also be linked together to form dune chains or dune networks.



**Figure 8** (a) Section view of sand dune and (b) Dune migrates when sand moves up the windward side and slides down the leeward slope (Wicander and Monroe, 1998).

### ***1.1 Classification of sand dunes***

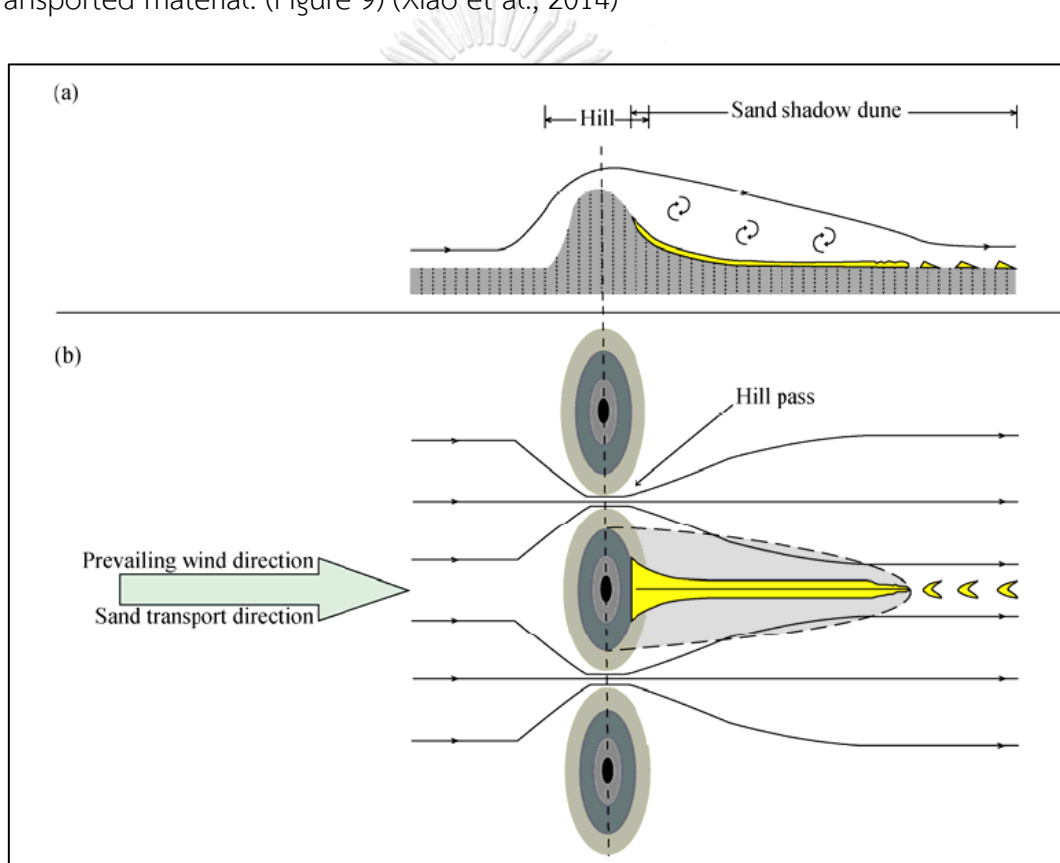
McKee (1979) classified sand dunes based on a combination of shape, number and orientation of slip-faces close to the prevailing wind or sand drift direction, and degree of form mobility same as others (e.g. Bryan, 1932; Melton, 1940; Hunter et al., 1983). This classification of sand dune as follows; the simple dunes consist of individual dune forms which are spatially separate from their

neighbors. This type is followed by three subtype based on formation. First, their development is related to topographic obstacle such as lee dunes, cliff-top dunes and echo dunes. Second, the self-accumulated dunes are developed by themselves such as barchans dunes, transverse dunes, linear dunes and dome dune. Third, dunes develop under influences of vegetation such as parabolic dunes and vegetated linear dunes. As mentioned above indicates that the Sand splay may be related to this dune type, especially the first dune formation which is developed by topographic obstacle. Compound dunes consist of two or more dunes of the same type which have coalesced or are superimposed. Lastly, complex dunes consist of two or more types of simple dunes which have coalesced or are superimposed.

#### *1.1.1 Shadow Dunes: the dune influenced by topographic obstacles*

This formation is developed by topographic obstacles such as escarpments, boulders and hills induce zones of airflow acceleration, deceleration and enhanced turbulence (Gaylord and Dawson, 1987). The resulting dunes are static that they do not elongate once they have reached a steady. Some geologist used the term of this dune that “sand shadow” or “lee dune” to describe a tapering accumulation of sand formed in the lee of an obstacle where the wind velocity is locally reduced (Bagnold, 1941: 189-190). For this research uses a term “**Shadow dunes**” for explanation of this formation. They are developed under a nearly unidirectional wind regime. Accordingly, they break up downwind at a distance where topographic obstacle is not effective and may develop to individual barchan dunes which are the preferred form in open areas of unidirectional wind (Bagnold, 1941: 194; H. T. U. Smith, 1954; Howard, 1985). Furthermore, the sand accumulation can occur in the lee of gap between two obstacles that sand flow is speeded up and funneled through the gap but fans out and slowed down on the lee side leading to sand deposition. These are important factors for the formation of sand shadow dunes. Sometimes, sand accumulations are also found in the lee of cliffs that elongated lee dunes form leading to formation of Echo dunes (Tsoar, 1983) and Cliff-Top dunes (Jackson, 1976).

However, the research of Xiao et al. (2014) who had studied morphology and formation mechanism of sand shadow dunes on the Qinghai-Tibet Plateau indicated that the sand shadow dunes can form in areas where there are strong wind as well as sufficient sand supply and dry climate, especially the suitable obstacles that one or both sides of them must have a hill pass effecting to “narrow-pipe effect” and the windward side of the obstacle should to have a wide and flat area for providing the spaces for wind flow and transport of material whereas the leeward side must have a sufficiently broad and flat area to allow the release of transported material. (Figure 9) (Xiao et al., 2014)



**Figure 9** Model of mechanism of sand shadow dunes formation; (A) section view and (B) plan view (Xiao et al., 2014).

### 1.1.2 Barchan Dunes

Barchan dunes are crescent-shaped dunes whose horns point downwind. The windward slope is typically convex with an average maximum slope of  $12^\circ$  while the leeward slope is characterized by a slip face at  $33\text{-}34^\circ$  apart from a

separate crest and brink in some barchan dunes (Pye and Tsoar, 2009). They form in areas having a generally flat, dry surface with little vegetation, a limited supply of sand and a nearly constant wind direction (Wicander and Monroe, 1998: 320) or it depends on changing in wind and sand supply conditions. The barchan dunes form a crescentic plan before they are high enough to develop a slip face since sand is transported more rapidly across and around the sides of the sand patch than across its center.

### 1.1.3 Transverse Dunes

Transverse dunes form long ridges perpendicular to the prevailing wind direction in areas where abundant sand is available and little or no vegetation exists. The crests of transverse dunes can be as high as 200 m and the width can be more 3 km. In fact, increasing in sand supply of individual barchan dunes, it may link to form the ridges oriented perpendicular to the strongest wind or resultant sand drift direction that displays on alternating barchanoid (downwind-facing) and linguoid (upwind-facing) and is called transverse ridges that consists of many ridges leading to transverse dunes.

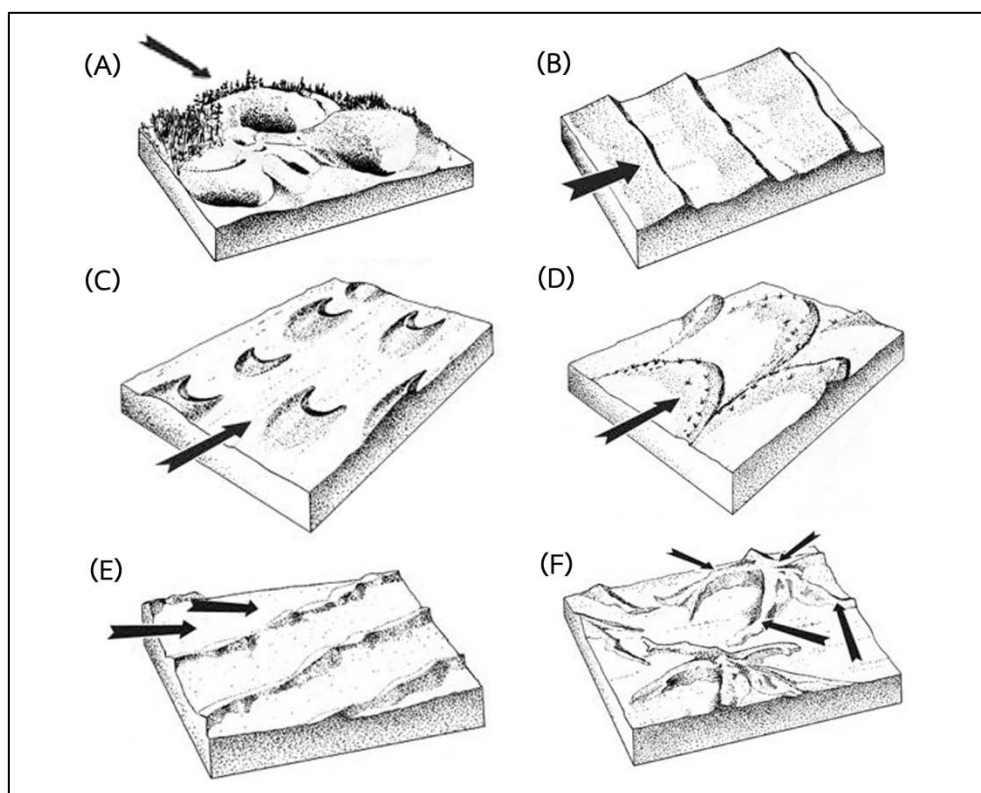
### 1.1.4 Linear Dunes

Linear dunes are characterized by their length, relative straightness, parallelism, regular spacing, and low ratio of dune to inter-dune areas (Lancaster, 1982b). Its ridge is parallel to the direction of the prevailing winds that forms in where the sand supply is limited. They range in size from about 3 m to more than 100 m high and some stretch for more than 100 km (Wicander and Monroe, 1998: 320). The linear dunes can be divided into two major types; 1) unvegetated dune and 2) vegetated dune (Tsoar, 1989). Sometimes, they are called “Seif dune” because the former has a sharp crest due to the lack of vegetation while the vegetated dune type has a more rounded crest. Many geologists support the theory that linear dunes develop thanks to the presence of parallel helical vortices in unidirectional wind regimes (Hanna, 1969; Cooke and Warren, 1973). This dune type is related to the sand shadow dune which can develop to linear dune due to the factors of wind velocity and gap in the area (Xiao et al., 2014: 23-24).



### 1.1.5 Parabolic dunes as reversing dunes

Generally, most parabolic dunes are found in coastal areas with abundant sand, strong onshore winds and a partial cover of vegetation. Its form is similar to the barchan dunes, but the slip face alternates from one side of the dune to the other or changes orientation in this way. The parabolic dunes can be formed in the area where vegetation cover is broken and deflation produces a deflation hollow or blowout.



**Figure 10** Formation of dune types; (A) shadow dune, (B) transverse dune, (C) barchan dune, (D) parabolic dune, (E) linear dune and (F) star dune.

### **1.2 Internal sedimentary structure of aeolian sand deposits**

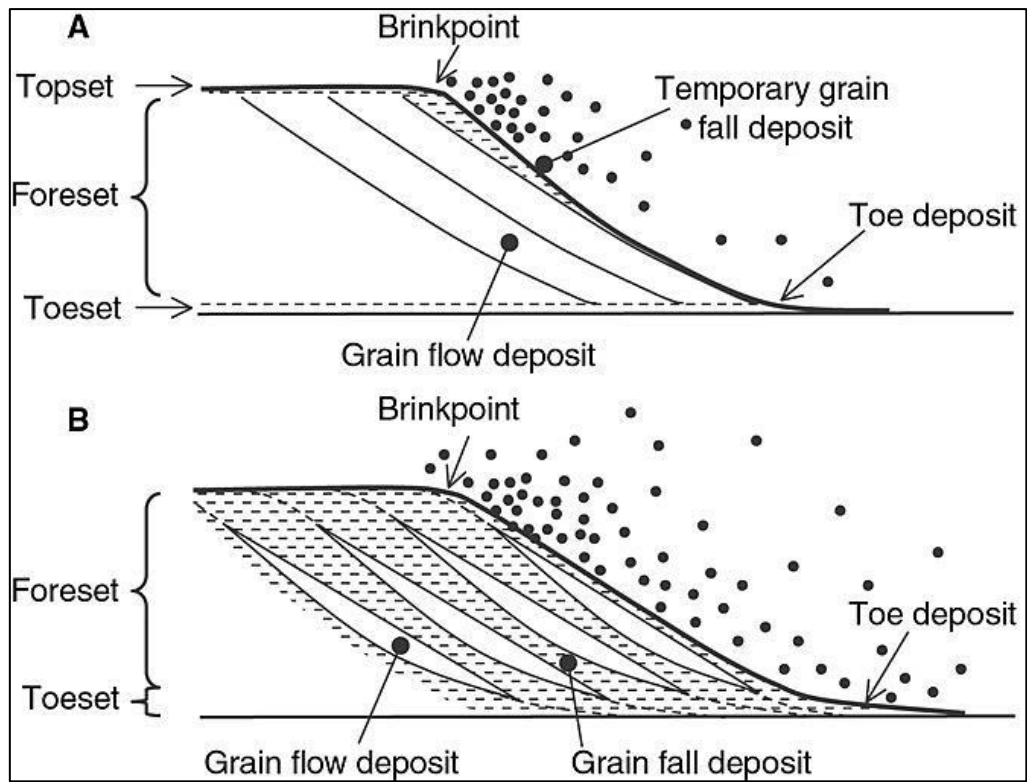
The study of internal sedimentary structures of Aeolian sand deposits is necessary for this research owing to four main reasons. First, they introduce to the growth and dynamics of modern dunes and compare with sand drift directions calculated using present-day wind data. Second, they can be used to identify bed form types represented by ancient aeolian deposits (e.g. Kocurek and

Dott, 1981; Glennie, 1972; Rubin and Hunter, 1983; Rubin and Hunter, 1985). Third, internal structures in ancient dunes provide the reconstructing palaeo-wind directions. Finally, sedimentary structures of sand dunes indicate the permeability characteristics of hydrocarbon reservoirs and aquifers in those areas. (e.g. Lupe and Ahlbrandt, 1979; Harari, 1996).

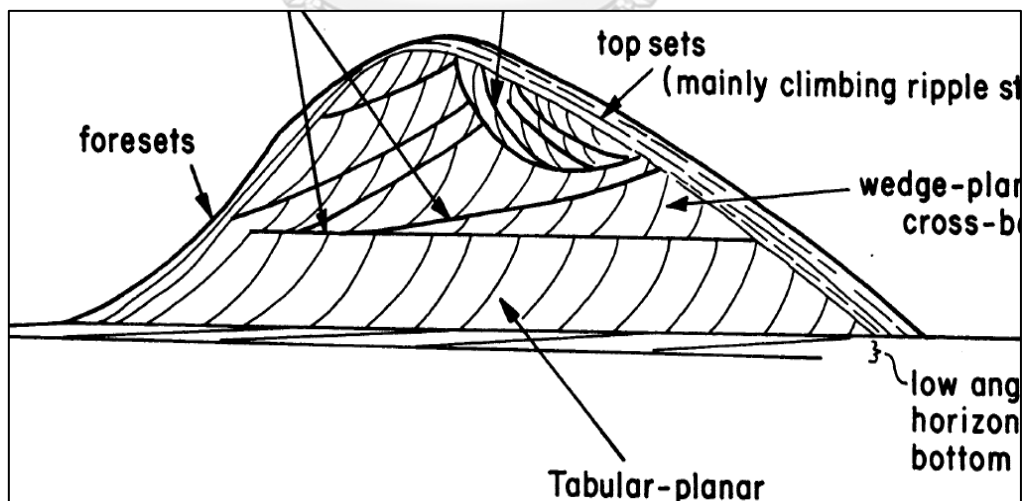
Hunter (1977) introduced the internal structures of aeolian sand deposits into two broad groups: primary structures and secondary structures. The primary structures illustrate the processes of transportation and initial deposition of the sand, whereas the secondary structures form syn- or post- deposition because of disturbance of the primary depositional fabric. Three groups of processes are listed to the formation of sand dune respectively (Figure 11) following 1) grain flow deposition (or *sand flow cross-stratification*), 2) grain fall deposition (or *grain-fall lamination*) and 3) tractional deposition. For the last process, Hunter (1977) suggested that tractional deposition may produce five possible stratification type as follows; subcritically climbing translent stratification, supercritically climb stratification, ripple foreset cross-lamination, ripple-form lamination and plane-bed lamination (Hunter, 1977) (Figure 12). In detailed, the rolling and saltation of sand along the surface creates wind ripples and the migration of ripples forms laminae which are commonly fine grained and form inverse graded laminae less than 1 cm. thickness that are inclined from horizontal up to the angle of repose around 32-34°. Fine-grained sand particles are transported in suspension by turbulence and deposited in form the air-fall laminae. Lee-side of dunes results in avalanching where sand grains flow down the dune slipface in a grainflow (Hunter, 1977). Secondary sedimentary structures are the post deposition due to disturbance of primary sedimentary structures such as slumping, flowage of wet sand as a result of tectonic disturbance, bioturbation, cryogenic processes and erosional episodes including wind or water (McKee et al., 1971; Horowitz, 1982). In case of wet surface, the saltation of dry sand had blown across a wet or damp surface affected to the some grains become trapped by surface tension. This case had been described by Van Straaten (1953) that the results of this phenomenon originated to “anti-ripplets structure”. Reineck (1955) recognized two distinct forms as following; adhesion ripples and

adhesion warts (Reineck, 1955) that Hunter (1980) proposed the adhesion plane bed forms as an additional adhesion structure. It is similar to the structure termed by Kocurek and Fielder (1982).

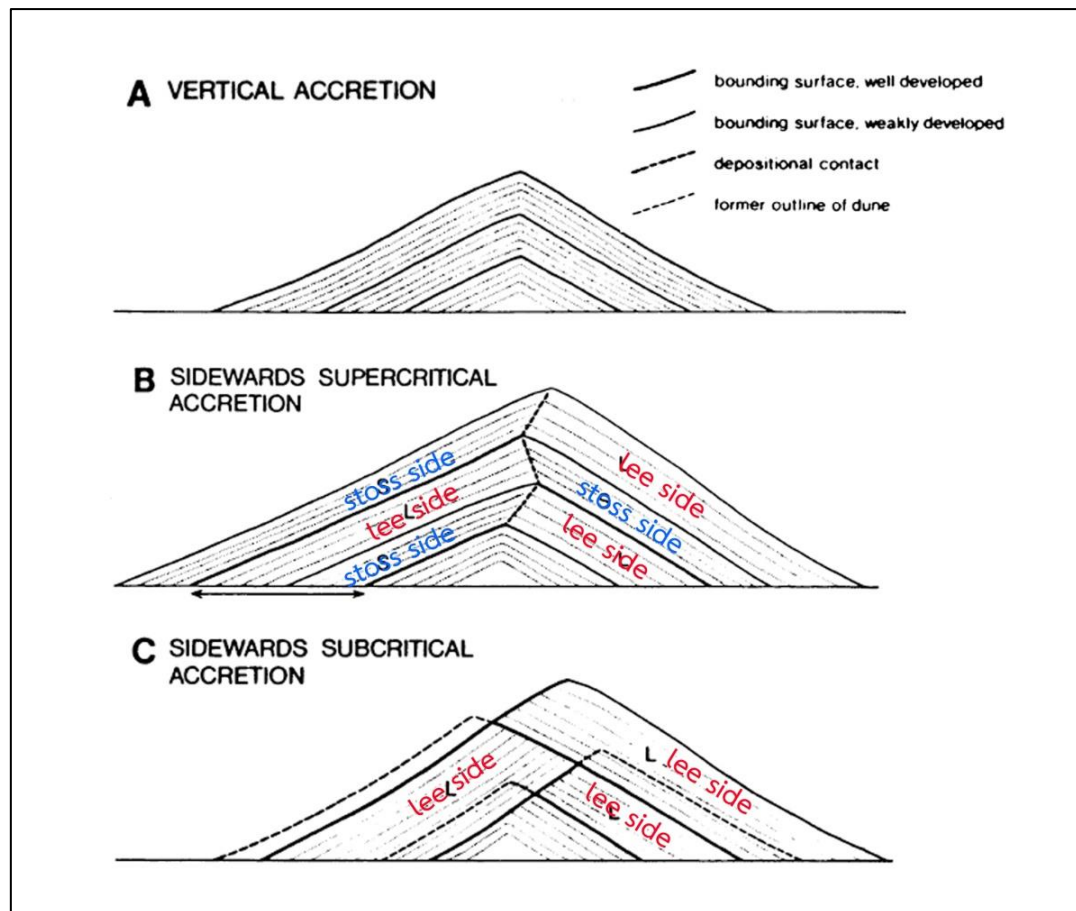
First, adhesion ripples are small, sub-parallel ridges perpendicular to the wind. They have wavelength of less than 1 cm and heights of 0.3-3 mm. The ripple crests are slightly convex in the upwind direction that it is different from the cross section of internal structure of dune in large scale which the downwind slopes are commonly steeper than the upwind slopes. These indicate that the features grow slowly upwind by accretion of saltating sand (Hunter, 1973). Moisture content is the main factor for control over adhesion structure morphology that the adhesion ripple growth stopped at lower water content and the ripples forms began to be eroded by saltating sand grains. Therefore, these adhesion ripples could extend farther downwind from their dry sand source than adhesion ripples formed at higher water contents. Second, adhesion warts, it shows the distinctive shape which is irregular and open-arched nature. They are essentially small domes or oval bumps which tend to have a random distribution rather than adhesion ripples. Their formation exhibits to be favored by a shifting wind direction rapidly which supports vertical rather than lateral growth. Third, adhesion plane bed is generally smooth, with irregularities not much larger than grain roughness. Their characteristics are faint, crinkly and only a single-grain to a few millimeters thick that they are distinct from other parallel-laminated deposits due to the extreme thinness, faintness and crinkly appearance of the laminae. This lamination type is mostly formed in low-water content (Figure 14) (Kocurek and Fielder, 1982).



**Figure 11** (A) Sorting and definitions in sand dune deposits and (B) Sorting in sand-gravel dune deposits, where only grainflow deposits are preserved on the lee slope (Kleinhaus, 2005).



**Figure 12** Schematic diagram showing the main internal stratification features in an ideal simple barchan dune (Pye and Tsoar, 2009).



**Figure 13** Depositional model of internal structures in shadow dunes. (Pye and Tsoar, 2009).

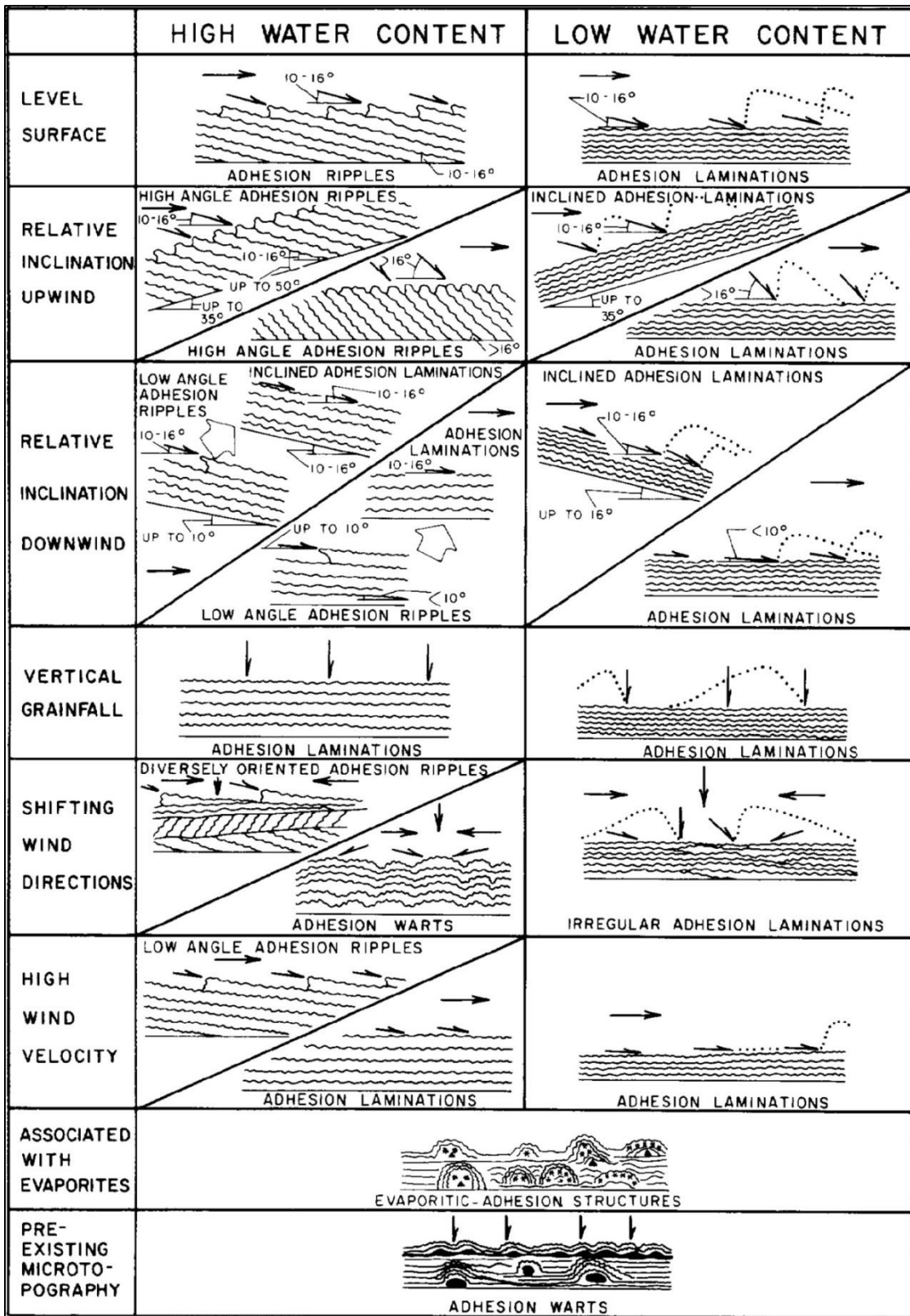
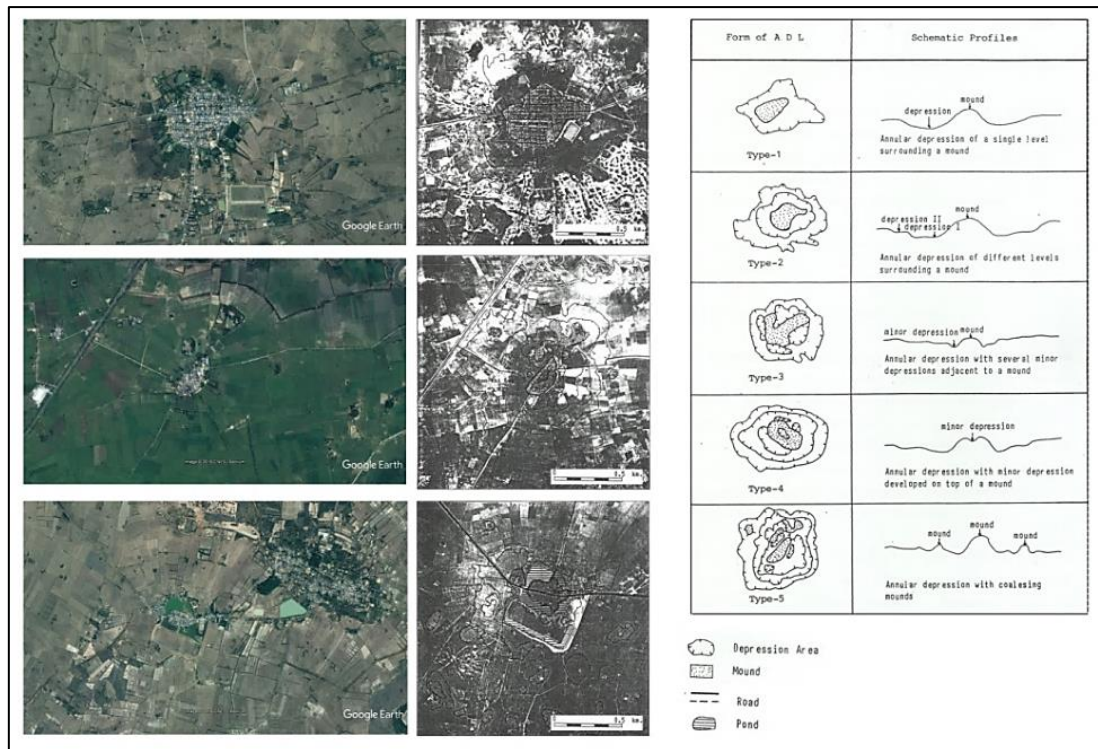


Figure 14 Formation of adhesion lamination in each water content level.

## 2) Salt dome as Annular Depression Landform (ADL)

In northeast of Thailand, the salt dome is generally found because their terrain known as Khorat Basin is underlain by sedimentary strata interbedded with thick salt layers of Maha Sarakham formation. While the unique natural landforms of somewhat circular feature including ring shape depression area enclosing mound of higher elevation has been recognized on aerial photograph along with them. Vichapan (1992) had studied this unique landform. Gravity survey method was applied in study of structure of salt dome and related landforms which he introduced the specific term of this particular feature manifested on aerial photograph; Annular Depression Landform (ADL). The landforms of this type were reported to be related to moated ancient settlement and were believed to be underlain by salt dome (Supajanya, 1980; Rau and Supajanya, 1985) (Figure 15).

Annular Depression landform was proved by gravity survey. The results demonstrated that ADL is related to stages of development of salt dome which could be classified to five types based on their characteristics in plan-view. In addition, Vichapan (1992) concluded that the ADL locations are found only in some areas underlain by Maha Sarakham Formation, but they are not found in younger deposit areas. To circular features, the ADL locations are found on the rim of the circular features (Vichapan, 1992: 97-98). Specifically, this research reviews in structures and processes of salt dome formation are related to form the ADL in study area.



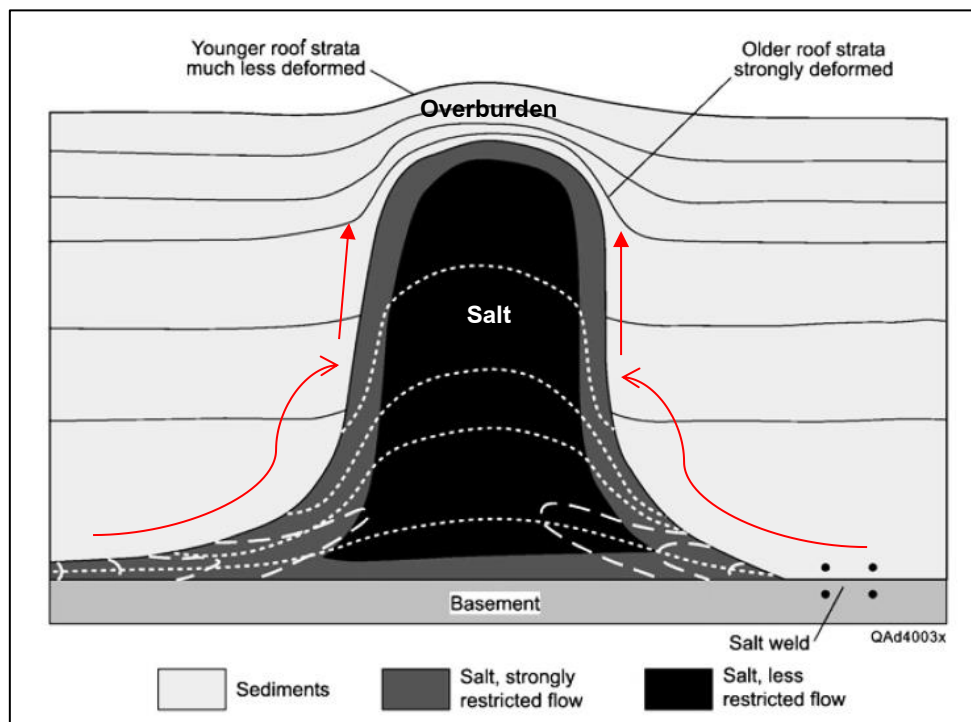
**Figure 15** Examples of ADL found in Roi-et and Surin and classification of ADL types. (middle and right diagrams were modified from Vichapan, 1992; whereas left pictures were taken from Google Earth Pro in 2016).

## 2.1 Salt structures

Salt dome can be grouped to dome and basin structure. The terms of dome and basin are used loosely for plunging anticlines and synclines with slightly more elongate closed outcrop patterns (Zulauf et al., 2016). The word “diapir” was coined by L. Marzic in 1902 to describe salt features of the Romanian Alps. Warren (1999) defined salt diapirs as salt structures having inconsistent contacts with the encasing sedimentary strata known as overburden rather than to surround notions of active piercement or shouldering aside of thick piles of adjacent sediments (Figure 16). Diapirs are not just composed of salt and other evaporate salts, but can be composed of shale, serpentinite and any other material which acts a lower relative density than its overburden. For explaining the salt structure, the term of *allochthonous salt* is necessary. Allochthonous salt or salt glacier is the salt layer overlying parts of its overburden as flowing salt beds which are typically no



longer connected with the original salt bed, but they can spread in hundreds of square kilometers area and up to several kilometers in thickness. In contrast, a salt structure that extends several kilometers in depth to the primary source layer is defined as *autochthonous salt* (Warren, 1999: 166-167).

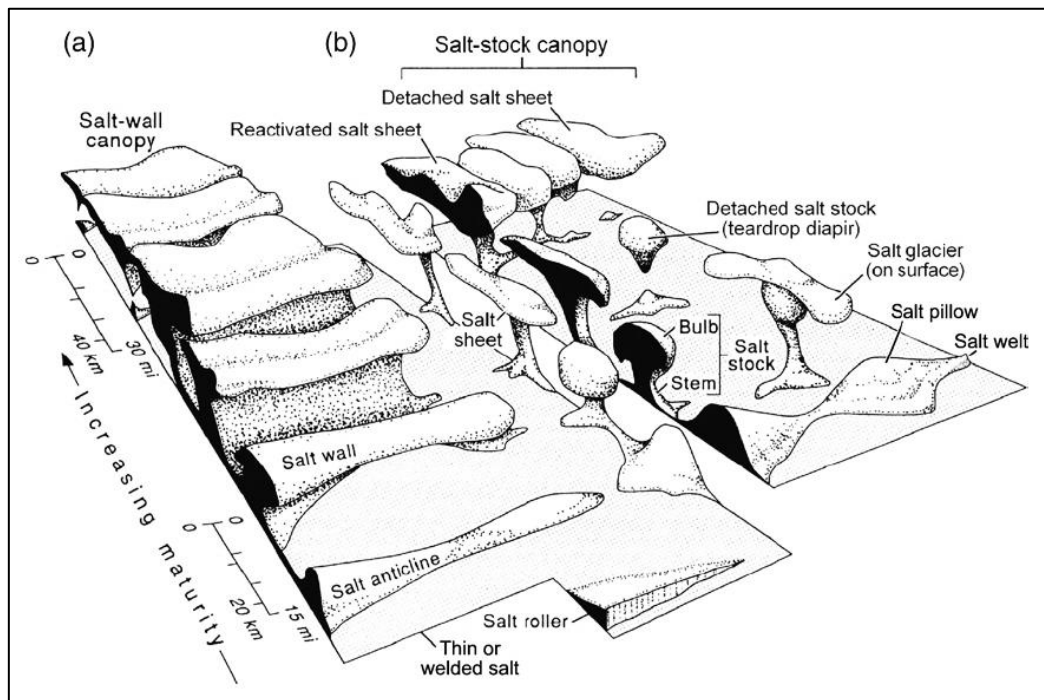


**Figure 16** Salt diapir intrusion which push up overburden (after Hudec and Jackson, 2007).

จุฬาลงกรณ์มหาวิทยาลัย  
CHULALONGKORN UNIVERSITY  
2.1.1 Shape of salt diapirs

Salt diapirs are various shapes that the position and shape depend on how the brittle overburden deforms. The three-dimensional forms of salt bodies reflect different stages in the upward migration of salt. The initiation of simple broad anticlines called domes (plugs and pillows) and they proceed to stacks, walls, columns, bulbs and mushroom shaped forms. The bottom part of the resulting teardrop diapir remains at depth to form a salt pedestal or foot (Figure 17). Strata above and below the source salt layer may contact at a weld in which all salt has exhausted caused to the top and bottom contacts of the salt to merge known as salt weld. Finally, the salt domes amplified fully, then they extrude onto and spread

over the topographic surface to form salt glaciers related to allochthonous salt sheets.

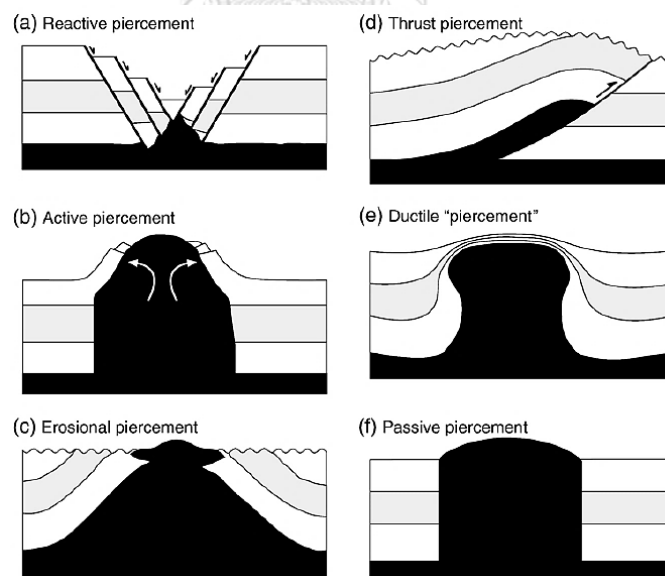


**Figure 17** Diagram showing schematic shapes of salt structures (Hudec and Jackson, 2007).

### 2.1.2 External structure

Salt diapir moves upward in piercing areas through the overlying sediments generally as well as rock which occupies the space because of faulting or uplift of overburden or erosion. These systems effect to create the space of thinning and separation of fault blocks. During process of moving upward, the diapir roof is created. The strata are overlain above the salt body affected by extensional tectonics reflected in arching and thinning of layers and in radial and concentric normal faulting. While flaps of roof rocks may be lifted, rotated and shouldered aside as the diapir amplifies. The surface surrounding salt diapir feature will form “rim syncline” which is the sinking sediments over the area where the salt has migrated due to displacement of subsurface sediments surrounding salt diapir. These features are related to the ADL that it can indicate the stage of evolution of salt dome (Rau and Supajanya, 1985; Vichapan, 1992).

The major mechanisms of allochthons are various processes including recumbent folding, deep intrusion, shallow intrusion and surface extrusion (Schultz-Ela and Jackson, 1996). However, these mechanisms are depended on physics of salt systems such as pressure effects, thermal effects, and flow textures and rates in salt flowing. In particular, pressure effects were explained by Jackson and Vendeville (1994) in three models. First, the sediment thickness is less than the piercement threshold, then, a salt diapir can actively pierce or shoulder aside its overburden. Second, where the floor of an erosional valley in which the trough floor is below the piercement threshold, active piercement can occur once more. Third, active piercement can also occur in situations where the roof is thinned by extension that the rift systems spread actively in a commonplace feature (Figure 18) (M. P. A. Jackson and Vendeville, 1994). Moreover, salt is presented as pressured fluid at rest and the sediment overburden deforms only by frictional sliding of diapir roof along the faults (Vendeville and Jackson, 1992). The salt structures can be formed in both extensional and progradational setting that it will be described later.



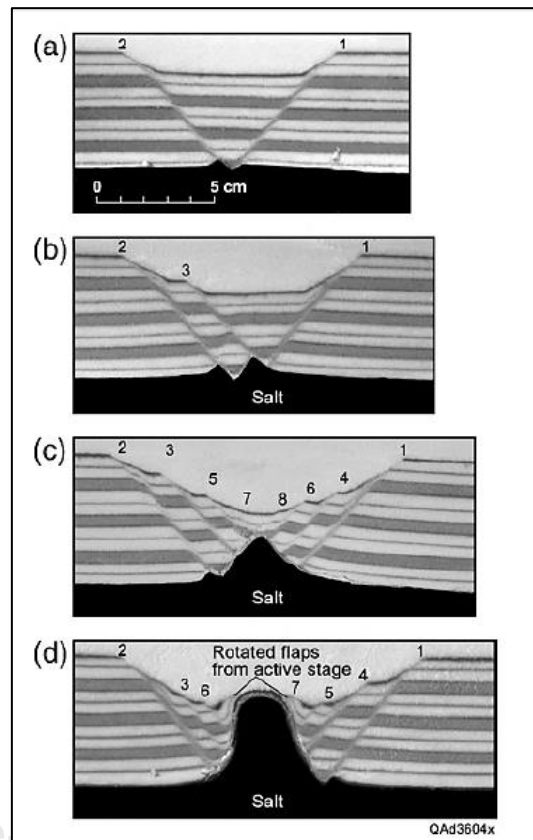
**Figure 18** Modes of diapir piercement shown in schematic cross sections (Hudec and Jackson, 2007).

## 2.2 Evolution of Salt dome

Jackson et al. (1994) divided the evolution of extensional salt diapirs into three stages that will evolve from reactive to active to passive. The first stage is slow reactive piercement, so the local thinning salt moves into overlying grabens and half grabens and floats at its equilibrium level of the top diapir in response to pressure in the salt source layer. The next stage is rapid active diapirism that is largely independent of extensional forces. It can only occur when salt pressure at the crest of the diapir is sufficient to lift its roof. The last stage, the passive stage begins once salt reaches the surface that a passive diapir cannot rise, but it can widen if extension continues. These stages are affected to rates of extension, depletion of source layer and changes in sedimentation rate.

In addition to the extensional diapirism evolution mentioned above, the progradation of thick sedimentary wedges atop a salt bed setting is one of lateral forces aided by gravity sliding and spreading that also drive salt flow. Ge et al. (1997) demonstrate the importance of progradation as a trigger for salt tectonics and formation of allochthonous sheets that they considered two groups for being the models following; 1) the experiments modelled salt with an underlying flat top to the basement, and 2) the modelled salt considered a basement with a stepped top. Both of models are depended on differential loading that it effects to shape of salt diapir or salt sheet in difference (Ge et al., 1997). In conclusion, the salt structure can be divided into two settings including extension salt that is the dominant mechanism for triggering diapirism in deeply buried salt bodies, in contrast, the formation of progradation is commonplace as a driving mechanism whenever salt is near the surface. This can deposit with little or no burial of the salt, or it can occur more once again reached the surface in the form of a passive diapir. Also, it means that diapirs can be later reactivated or overprinted during extensional or compressional regimes (Warren, 1999: 163-166) that in this stage may effect to the growth of rim-syncline around a dome related to radial tilting of truncation in the strata (Jackson et al., 1998), folding and tear faulting over the core of salt anticlines which produced a basin in the salt (Warren, 1999: 178) (Figure 19). Vichapan (1992), in addition, assumed that the rim syncline is associated with the displacement by unconsolidated

sediments surrounding the salt structure. Thus, the syncline is formed as a depression. Finally, the salt structure as a mound was formed along with annular depression. When the water table had been increasingly recharged by precipitation, it dissolved out the salt body by groundwater affecting to cavity features in some region in small scale together with the mound.



**Figure 19** Cross sections from physical models showing stages of reactive piercement in extension that stage (C) may effect to the growth of rim-syncline around a dome. (Hudec and Jackson, 2007).

However, Hite (1982) revealed the evidence of salt diapir in some area of Nong Han Kumphawapi in Sakon Nakorn province, Northeast of Thailand. There is a conspicuous thinning of the Lower Salt in beds adjacent to the anticlines containing thick salt lenses in their axial zones. Significantly, the bedrock surface in Bumnet Narong study was noted that some channels cut into the bedrock surface coincided with anticlinal axes. Therefore, he proposed a theory to account for the formation of salt diapir that the thickening of the salt in the crests of anticlines is not related to a tectonic event or differential loading, but surficial process of paleochannels is the main factor due to resulting in a reduction of compressive stress (Hite, 1982; Rau and Supajanya, 1985).

### **3) Geomorphology of fluvial system**

Fluvial system involves the interaction of surface runoff and groundwater in addition to precipitation from the atmosphere tending to the explanation of hydrological cycle. The hydrological cycle is the recycling movement of water from the oceans through the atmosphere and back to the oceans. This cycle is powered by solar radiation which high quantities of water evaporate from the oceans as the surface waters are heated by solar energy. Indeed, all water entering to atmosphere or about 85% of all water is derived from the oceans while the remaining 15% comes from evaporation of water on land (Wicander and Monroe, 1998: 246-247). For this research, the fluvial system is a part of objectives in case of geomorphologic study, so its basic knowledge is necessary that it includes evolution, features, and types of river system. These are indicators of processes and ecological changes in the area.

#### ***3.1 River system: Analysis in catchment scale***

Geologically, external processes following weathering, erosion, transportation and deposition can be adopted for explanation in the origin of river leading to process and evolution. The river is running water on surface or called “runoff” and “stream flow” that receives water directly from several sources to stream channels. Usually, streams flow downhill from a source area to a lower

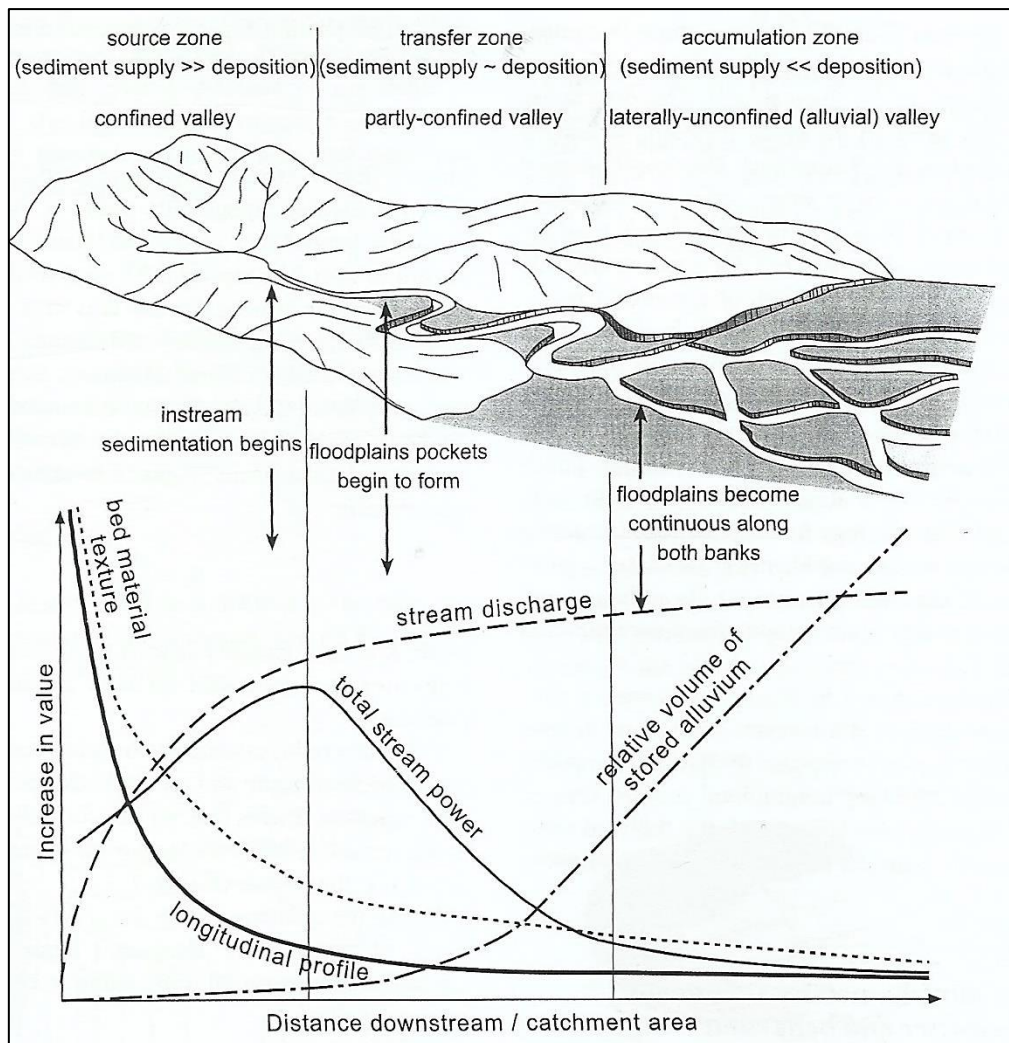
elevation and confine to long trough depressions forming to ephemeral channels or rills.

A single fluvial system that is linked internally by a network of channels is called “catchment”. If we analyze the catchment-scale relationships along longitudinal profiles, the balance of erosion and deposition along river courses is determined the distribution of sediment process zones in catchments and resulting patterns of river morphology. Fryirs and Brierley (2013) divided catchments into three process zones following as below (Figure 20).

- Source zones are dominated by erosion processes, especially vertical downcutting. These zones are net exporters of sediment. Normally, source zones occur in headwater regions of catchments where is the elevated area such as mountain ranges, tableland, and escarpments. This produces steep and narrow valleys called V-shape valley and U-shape valley.

- Transfer zones occur where there is a balance between sediment supply and sediment export. These zones tend to occur in the middle parts of catchments as downstream of the headwater sediment source zones e.g. rounded foothills or piedmont zones. The vertical incision is dominant that creates floodplain pockets in partly confined valley settings.

- Accumulation zones are dominated by depositional processes and associated sediment stores. These zones contrast remarkably to source zones due to being net importers of sediment. Moreover, this zone is marked by alluviation, aggradation and long-term sediment storage that typically occur in lowland regions of catchments such as lowland plains or broad alluvial plains in endorheic basins.



**Figure 20** Relationship between downstream changes in slope and sediments of process zones (Fryirs and Brierley, 2013).

Indeed, the distribution of erosion or deposition in process zones as mentioned above can be interpreted from catchment morphometrics (i.e. catchment shape, relief, drainage density and network extension, and drainage pattern). All these characters are the controllers on character and behavior of river (Fryirs and Brierley, 2013: 34-37). The drainage patterns are selected in this review that they indicate a product of lithology and structure of a region as following: 1) Dendritic drainage patterns being the most common form develop in areas of homogenous terrain where there is no distinctive geologic control. 2) Trellis pattern is related to a strong regional dip and the presence of folded sedimentary strata that the geologic



control is dominant. 3) Parallel pattern is commonly found in terrains with a steep regional dip or regions in which parallel, elongate outcrops of resistant rock that it is similar to 4) Rectangular patterns are concentrated where the rock is weakest that streams join the trunk stream at sharp angles. And 5) Radial and annular drainage patterns develop around a central elevated point that this pattern represents disparate erosion of volcanoes and eroded structural domes.

Moreover, river behavior and character are affected by geologic controls such as lithologic controls reflecting on sediment movement and volume, impacts of tributary networks, and stream order. A measure of the relative size and pattern of channels within a drainage network is called “stream order” that Horton (1945) introduced a theory of development in drainage networks and drainage basin. Strahler (1952) had subsequently introduced the geometric equation applied to analyze fluvial system. It developed to The Horton-Strahler stream order approach that involves the following analysis:

1) Small tributaries that occur in the upstream of drainage networks are assigned order 1.

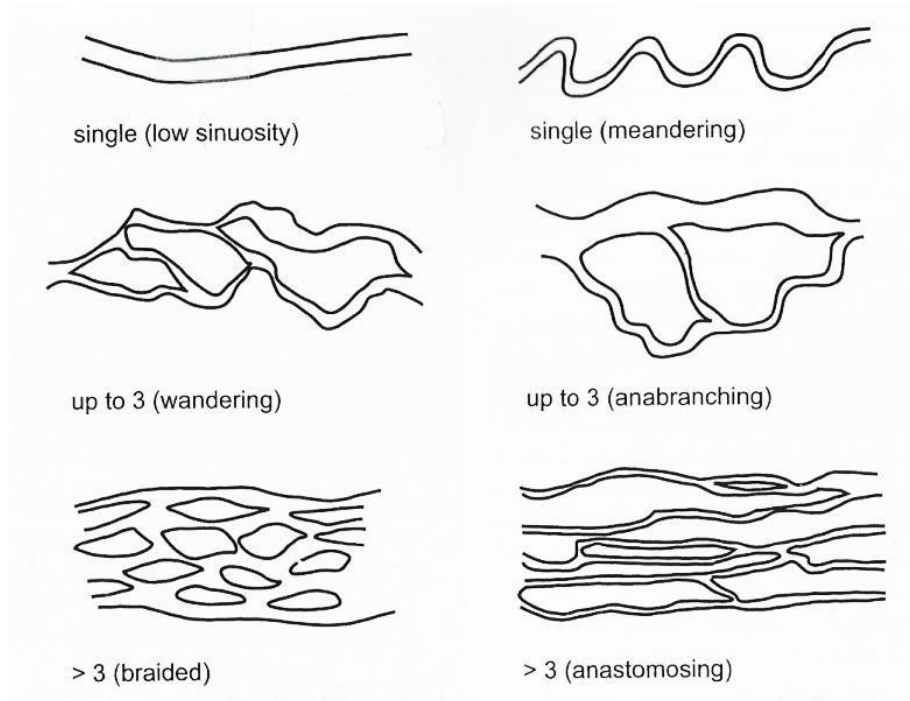
2) The junction of two streams when two first-order streams come together, the segment of channel downstream of the confluence is assigned an order of 2.

3) The junction of two streams when a second-order stream meets a third-order stream, no change in order results and the segment downstream of the confluence remains as a third-order stream.

### ***3.2 Classification of channel types and degree of sinuosity***

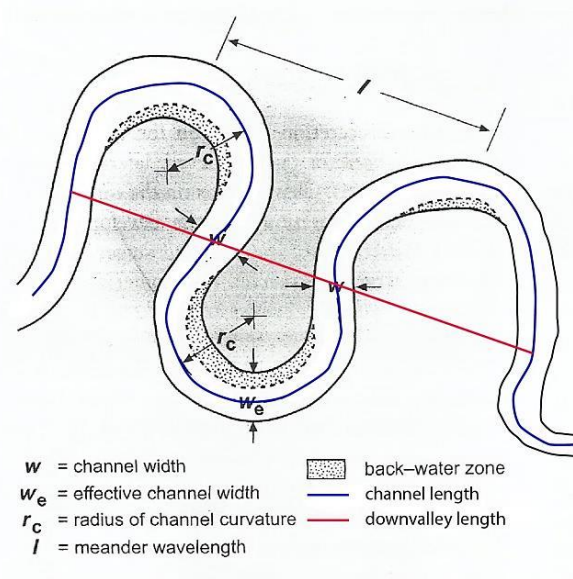
The number of channels can be characterized in descriptive terms such as mainly single channeled with isolated models in which flow divides into two or three channels. In facts, the difference of number of channels is made between single-channeled and up to three channels and more than three channels used in analysis of channel planform following as below. (Figure 21)

- The single channel (in straight) and single channel with meandering
- The channels up to three in wandering or anabranching
- More three channels may be braided or anastomosing



**Figure 21** Classification of channel types (Fryirs and Brierley, 2013).

Furthermore, degree of sinuosity can be used to identify the type of channel. Most channels are meandering rivers that channel sinuosity  $P$  is measured as the ratio of channel length  $\lambda$  to valley length  $Z$  for a representative reach of river. Three classes of sinuosity are used including: straight is 1; sinuous is 1-1.5; and meandering is more 1.5. Elsewhere, the channel may be inactive or passive with little evidence of channel adjustment (e.g. features of cut-offs or ridge and swale topography). The channel may have relatively low sinuosity, but it could also illustrate irregular or tortuous meandering patterns.



$$SI = \frac{\text{Channel length}}{\text{Downvalley length}}$$

**Figure 22** Sinuosity Index Theory (SI) in river morphology (modified from Fryirs and Brierley, 2013).

### 3.3 Mechanic and geomorphic of river in alluvial plain

As mentioned previously, Fryirs and Brierley (2013) divided catchments into three process zones following source zones, transfer zones and accumulation zones. The mechanic of river is necessary for this research in case of erosional and depositional processes reflecting to the difference zone, especially the transfer and accumulation zones. Since the geomorphic works of river exist three possibilities of energy, the process of erosion and deposition is formed following: 1) a river may have more energy to move its water and sediment load; 2) it may have exactly that required or in case it is stable; and 3) it may have an energy shortage which will result in the form of deposition (Fryirs and Brierley, 2013: 65-66) that the stream deposition types is included braided streams, meandering streams, floodplain deposits and deltas. Nonetheless, author reviews only specific detail in braided streams and meandering streams relating to characteristics of river in study area.

### 3.3.1 Braided streams

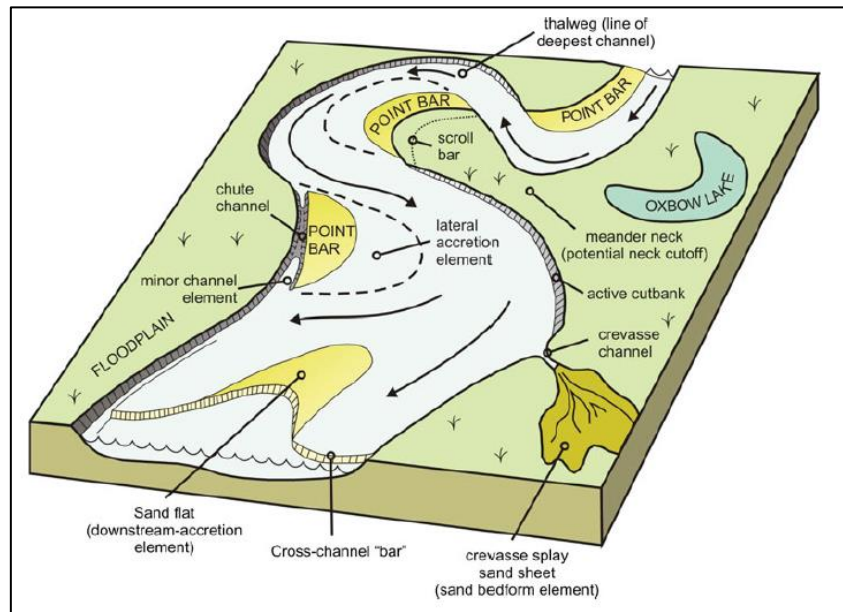
The braided streams represent an intricate network of dividing and rejoining channels that it develops when a stream is supplied and deposited with excessive sediment as sand and gravel bars within its channel respectively. Hence, their deposits are composed of sheets of sand and gravel. Braided streams have broad, shallow channels and are commonly characterized as bed load-transport streams. The most of internal structures is mid-channel bars with sand beds or gravel beds depended on transfer zones. Miall (1985) proposed that this environment is composed of the assemblage of cross-bedding fragments of bar deposits including channels (CH) with lateral accretion (LA) of upstream to downstream accretion that their features are indicated by distributary shifting on alluvial fans or bars (Miall, 1985). This valley may contain three or four distinct topographic levels, with the higher levels covered by sparse to dense vegetation.

### 3.3.2 Meandering streams

The meandering streams represent a single, sinuous channel with meanders which are broadly looping curves. These streams channels are semicircular in cross section along straight reaches, but at meanders they are asymmetric. The deepest of channel is near the outer bank which descends vertically into the channel known as “thalweg” which is the highest energy point of water flow. The outer bank is called the cut bank or erosional bank since flow velocity and turbulence are greatest on this side where it is eroded, in contrast to the depositional bank where flow velocity is a minimum near the inner bank.

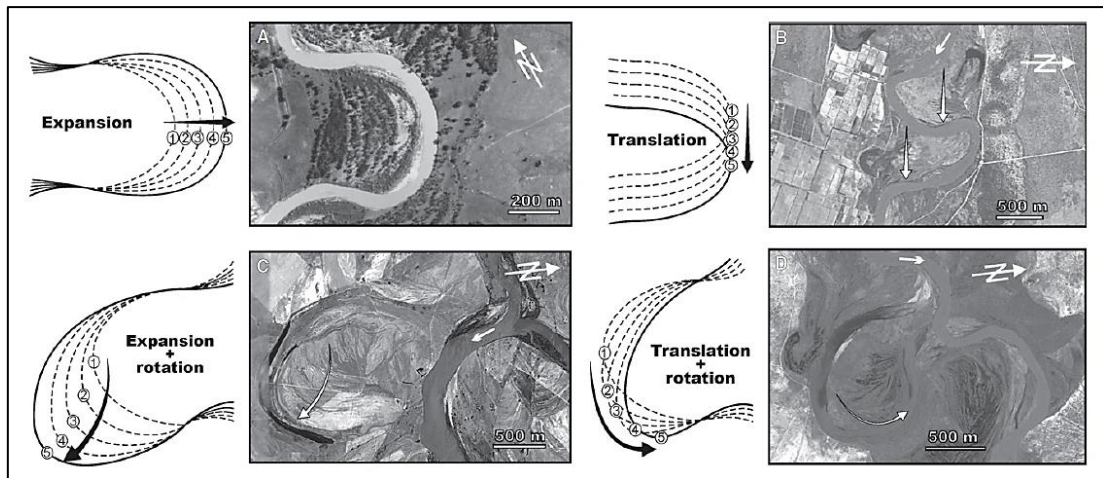
Due to the unequal distribution of flow velocity across meanders, the cut bank is eroded and deposition always takes place along the opposite side of the channel. The deposit formed in this manner is a point bar consisting of cross-bedded sand or gravel that it appears the ridge and depression known as swell (ridge) and swale (depression) topography in geomorphic definition. These appearances of point bars are the most distinctive feature of meandering river deposits, but some bars in braided rivers also show the lateral accretion (Miall, 2016). Afterwards, the channel is more meandering in side of cut bank as a result of the

erosion at thin neck of land separating created to cut-off. It is divided into two types including neck cut-off marked by crescent shape known as oxbow lakes (or called meander scars) and another is chute cut-off cut the swale of point bar directly originating the new channel (Figure 23).



**Figure 23** Morphological features of meandering river (i.e. neck-cutoff, point bar, ridge and swale, natural levee, crevasse splay) (Miall, 2016).

For the reconstruction in meandering channels or migration of meander-belt, the evolution of channel bends can be considered in terms of one or more of transformation modes following expansion, translation and rotation (Ghinassi et al., 2014; Daniel, 1971; Brice, 1974; R. G. Jackson, 1976). These are explained in changes of meandering based on direction. Expansion increases the channel-bend curvature and flow-path length while the bend apex migrates transversely away from the channel-belt axis. Translation maintains the channel sinuosity while the bend apex migrates parallel to the channel-belt axis in a down-valley direction. Finally, rotation develops meander-bend asymmetry through the migration of the bend apex away from or towards the channel-belt axis that these patterns always occur in combination between expansion mode and translation mode (Jackson, 1976) (Figure 24).



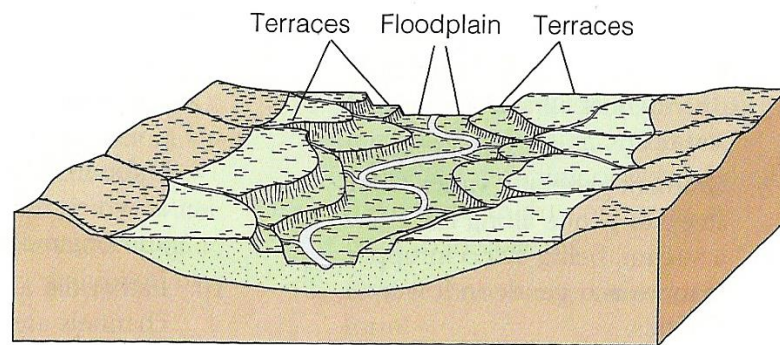
**Figure 24** Transformation modes following expansion, translation and rotation (e.g. Daniel, 1971; Brice, 1974; Jackson, 1976; Fryirs and Brierley, 2013).

When a stream erodes its cut bank and deposits on the opposite bank in more supply, the plain is created that it is called “floodplain” being flat and adjacent to their channels. The bank, in addition, appears the common ridges on both of margins known as natural levee created when a stream overflows, the velocity of the water spilling onto the floodplain decreases rapidly effecting to deposit along the margins of the stream channel.

Lateral accretion and overbank vertical accretion are the primary processes of floodplain formation. The first process occurs when unstable bedload and suspended-load deposits on the convex slope of banks are incorporated into the floodplain as the migration of channel across the valley floor of transfer downstream remaining features with ridge and swale. In another process, vertical process results from overbank deposition of suspended-load materials during floods. This process is remarkable for the rivers that have sufficient accommodation space to allow floodplains to develop. Finally, the abandoned channel fills have occurred and transform into paleochannel. The geomorphological feature zones of these rivers which remain records of meandering are called as avulsion plain or belt.

Theoretically, a stream could erode its entire valley to very near sea level that is called “base level” which have a lower limit, although streams never reach ultimate base level since maintain flow. Changes in base level occur when sea level

rises of falls with respect to the land, so approach of river terrace formation is related to base level. The river terrace is a feature of river evolution that it identifies base level in aggradation which the river had vertical eroded until reach the new base level with lateral eroded establishing a new avulsion plain. The river terrace divided into two types following paired terrace and unpaired terrace.



**Figure 25** Level of terraces originated from vertical erosion of stream again. (Wicander and Monroe, 1998).

As mentioned above, the fluvial deposits are characterized by a variety of bed forms and sedimentary structures such as longitudinal bars, bank-attached, linguoid bars, side bars, point bars and transverse bars, ripples, dunes, sand flats and crevasse splays (Collinson, 1986; Bridge, 2003). In detailed, the braided rivers are typed as bed-load channels which have gradients, high width or depth ratios (>40) and low sinuosity. These channels are coarse-grained and contained little suspended-load material. The total alluvium of bed-load systems composes significantly of channel and channel-flank deposits that the silty and muddy floodplain deposits play a minor role. On the other hand, the mixed-load fluvial systems are indicated to the meandering channels that they preserve a higher percentage of floodplain deposits including silts, muds, and locally back swamp carbonaceous muds and clays. These channels are more stable and lower width or depth ratio than the bed-load system. The sands are mainly filled with minor proportions of silts and clays that they are flanked by levee sands and silts and crevasse splay sands (Figure 26). Moreover, the suspended-load fluvial systems may be typed as the meandering or anastomosing rivers that they are characterized by

high-sinuosity single channels of great stability and low width or depth ratio (<10). Their gradient and power are generally low that the fills are contained of silts and muds influencing to well-development of silty or muddy levee deposits, as well as flood basin deposits (predominantly of overbank fines or back swamp muds) (Figure 27). Miall (1978) introduced the architectural elements of fluvial deposits shown in Table 1 that they are based on lithofacies of the internal structures (Miall, 1978). They are applied to interpret the environment of paleochannels in this study.

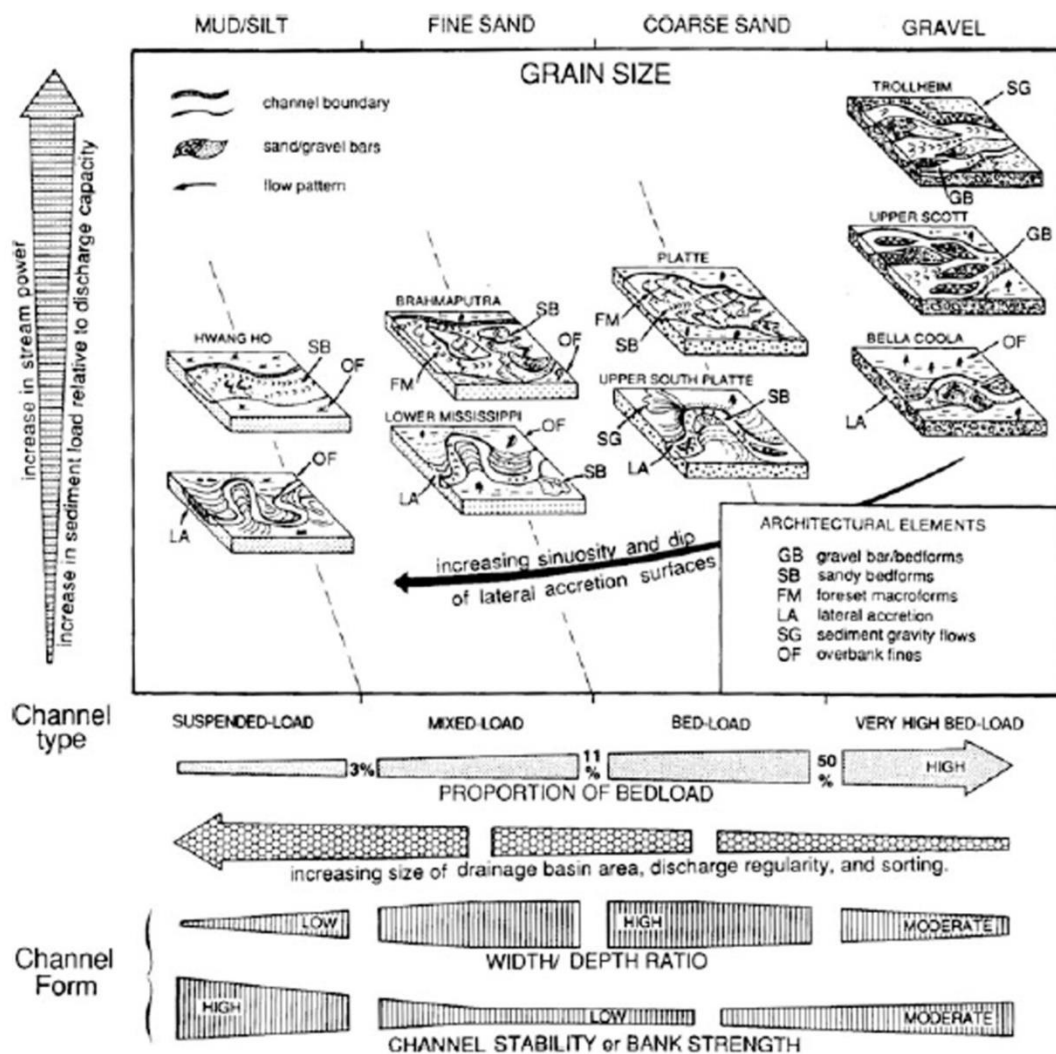
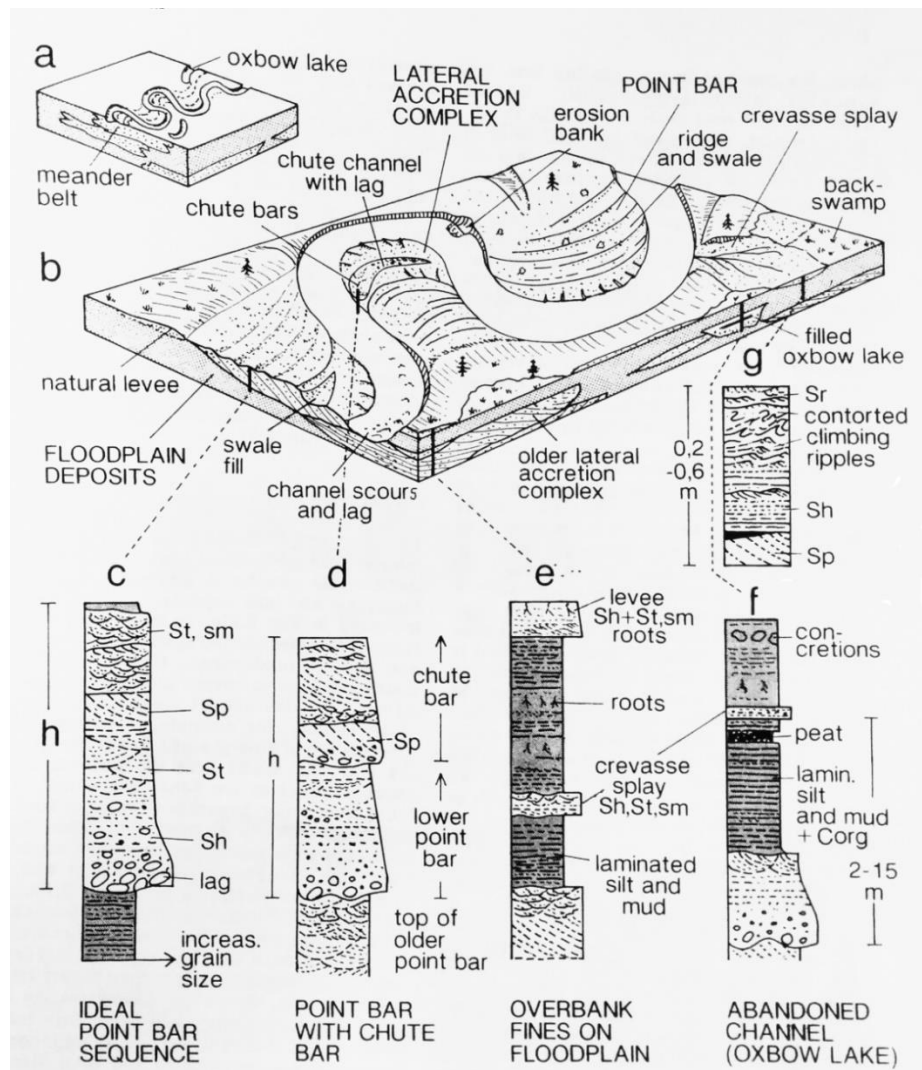
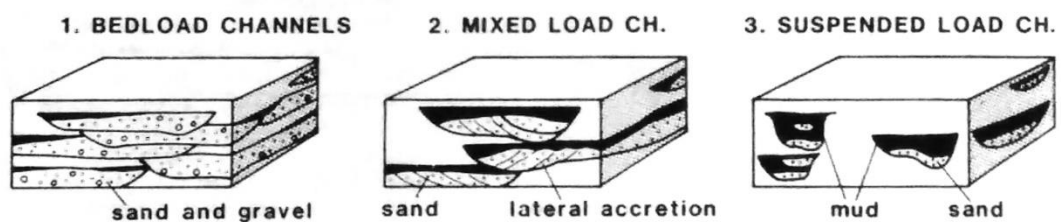


Figure 26 Relationship between grain size and fluvial channel patterns that the architectural elements are those of Miall (1985).





**Figure 27** Meandering river system. a) Formation of sandy meander belt within a flood basin. b) Different sub-environments of meandering channel. c) - g) Characteristic vertical sections of the youngest sediments of the flood basin. h) One fluvial cycle (Einsele, 1992: 47).



**Figure 28** Characteristics of channel fills of bed-load, mixed-load, and suspended-load rivers based on Galloway (1985) (Einsele, 1992: 35).

**Table 1** Lithofacies classification of fluvial deposits, from Miall (1978).

Facies code	Lithofacies	Sedimentary structures	Interpretation
Gms	massive matrix (sand and mud) supported gravel	grading	debris flow deposits
Gm	massive or crudely bedded gravel	horizontal bedding imbrication	longitudinal bars, lag deposits, sieve deposits
Gt	gravel stratified	trough crossbeds	minor channel fills
Gp	gravel stratified	planar crossbeds	linguoid bars or deltaic growth
St	sand, medium to v. coarse, may be pebbly	solitary or trough crossbeds	dunes (lower flow regime)
Sp	sand, medium to v. coarse, may be pebbly	solitary or planar crossbeds	linguoid, transverse bars, sand waves (lower flow regime)
Sr	sand, very fine to coarse	ripple marks of all types	ripples (lower flow regime)
Sh	sand, v. fine to v. coarse	horizontal lamination, streaming lineation	planar bed flow (lower and upper flow regime)
Sl	sand, fine	low angle (<10°) crossbeds	scour fills, crevasse splay, antidunes
Se	erosional scours with interclasts	crude cross-bedding	scour fills
Ss	sand, fine to coarse	broad, shallow scours	scour fills
Fl	sand, silt, mud	fine lamination, very small ripples	overbank or waning flood deposits
Fsc	silt, mud	laminated to massive	backswamp deposits
Fcf	mud	massive, with freshwater molluscs	backswamp pond deposits
Fm	mud, silt	massive, desiccation cracks	overbank or drape deposits
Fr	silt, mud	rootlets	seatearth
C	coal, carbonaceous mud	plants, mud films	swamp deposits

## 2.5 Ground-penetrating radar (techniques and methods)

Ground-penetrating radar (GPR) is an electromagnetic geophysical exploration technique arranged to the modern technique for geomorphologic study in the present day (Schrott et al., 2013). Theoretically, ground-penetrating radar uses high-frequency electromagnetic (EM) waves to acquire information on subsurface composition by transmitting a signal of EM into the ground. The signal is reflected from layers in the subsurface as a sender in which there is a contrast in dielectric properties and returns to the surface where it is recorded as a receiver that this part is used to image subsurface stratigraphy (Bristow, 2013). The wavelength of the radar signal affects to the resolution. The low-frequency signals with a longer wavelength have a greater depth of penetration but less resolution in contrast to higher-frequency signals with a short wavelength have higher resolution but less penetration into the ground (Bristow, 2013: 183-184). Nonetheless, it does not effectively work in the ground being conductive such as areas with saline ground as well as some clay soils, but it works well in soils with a high resistivity such as sand, silt and ice wedges (e.g. Hinkel et al., 2001; Jol and Bristow, 2003; Bristow et al., 2007). Hence, GPR methods are applied to this research of sand splay for assuming and reconstructing the formation of sand shadow dune in the study area.

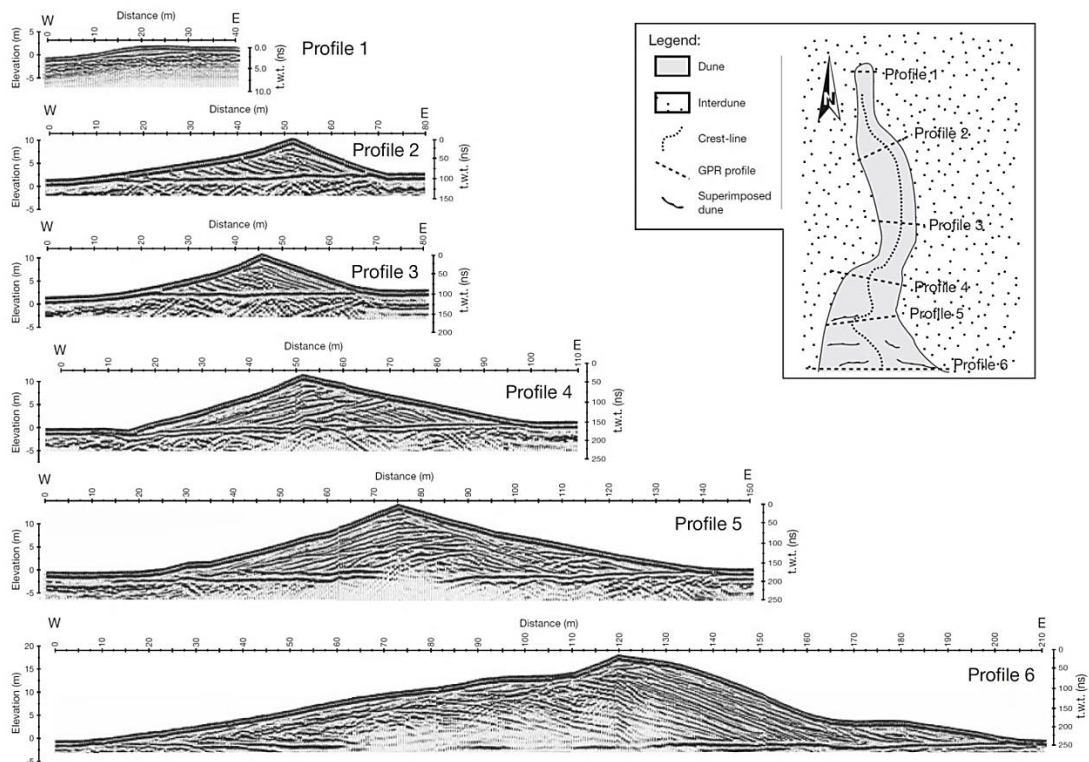
### 2.5.1 GPR methods applied to image the internal structure of sand dune

Using GPR to investigate the formation of sand dune is taken widely. Sand dunes are suitable targets for GPR surveys since they generally have low conductivity and low magnetic permeability allowing good depths of penetration (Bristow, 2009: 274-277). Therefore, wind ripple lamination, air fall lamination and grainflow deposits which have different grainsize and bedding characteristics can be detected by using GPR due to the associated changes in water content which is the most important factor affecting the electromagnetic properties of sediments (van Dam, 2002; Bristow and Pucillo, 2006).

It reveals the internal structure of sand dunes as well as water tables or groundwater tables on image of GPR profile. Harari (1996) had studied "Ground-penetrating radar (GPR) for imaging stratigraphic features and groundwater in sand

dunes” that focused on interpreting the internal bedding related to hydrogeologic features of sand dunes. The results completely showed the internal structures of sand dunes from the eastern province of Saudi Arabia and Moreton Island in Australia with using a 100-MHz antenna and 500-MHz antenna. The lower frequency antenna (100 MHz) was more effective for detecting the groundwater table, but the higher resolution of the 500-MHz antenna was more suitable for delineating the wetting fronts and imaging the cross-strata that represented the erosional and depositional process of dunes as follows; saltation, grainfall and grainflow in cycle respectively (Harari, 1996). In addition, the study of relationship between sand dune and aquifer was taken in 2012 by Rejiba et al. (2012). They used the GPR for imaging the cross-strata of sand dunes in transitional zone along with coring method at niayes ecoregion of Tanma, Senegal. This research revealed that the water table continuity associates with the steep slope of the dune that could be explained by classical surface tension behavior because of pressure gradients (Rejiba et al., 2012: 18-20).

Directly, the study of formation of sand dune by GPR techniques is represented in many papers. Bristow et al. (2000), for example, used GPR methods to reconstruct the sedimentary structure of linear sand dunes in Namib sand sea (Figure 29). These GPR imaging profile shows clear evidence for lateral migration in a linear dune that it is identified by facies of cross-bedding (e.g. wind-ripple laminae, dipping sets, planar tabular, and trough). The results of GPR image indicated the five stages in the evolution of a linear dune that it starts an initial extension of wind-rippled sand and develops the straight-crested transverse element. Next, the dune has grown up, while sinuosity in the dune crest-line develops until super-imposed dunes appear with increasing dune height, width and sinuosity. These characters affect development of slip faces and convex slopes in which winds are diverged along both windward and lee-side dune flanks as well as bi-direction wind (Bristow et al., 2000).



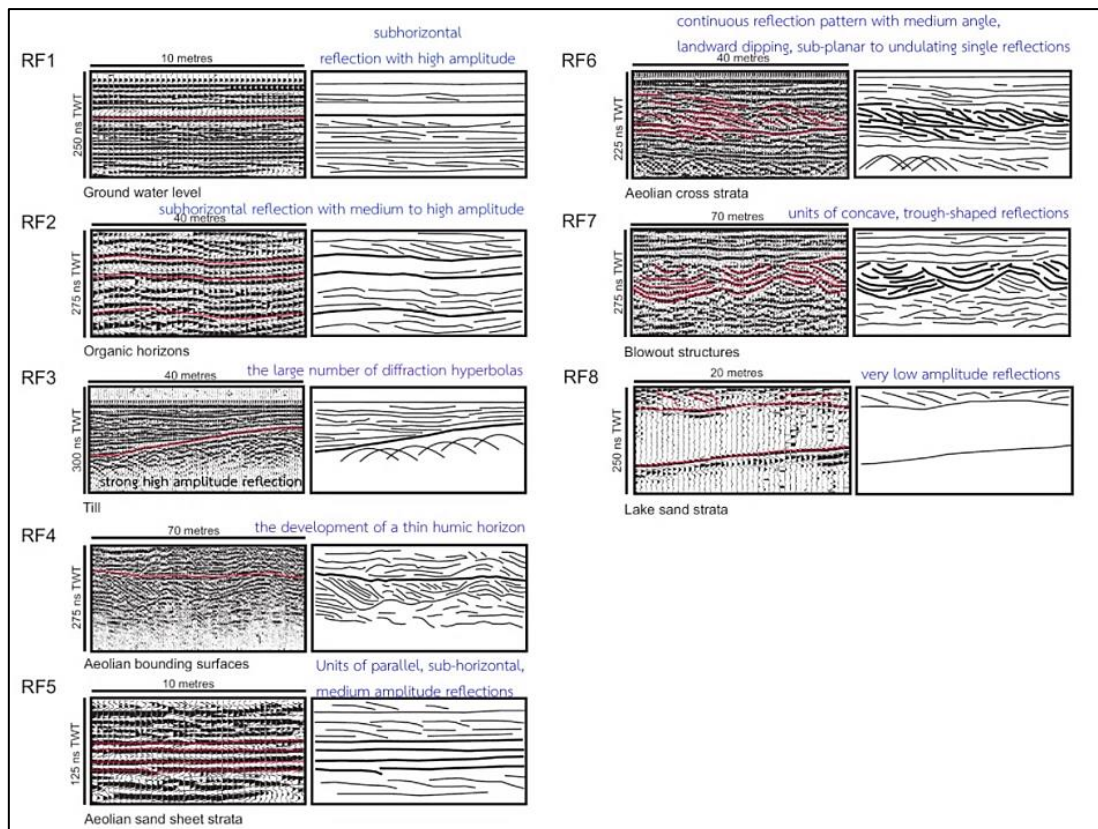
**Figure 29** Dune structures from GPR Profiles of linear sand dunes in Namib sand sea (Bristow et al., 2000).

### 2.5.2 Radar facies and Radar stratigraphy of sand dunes

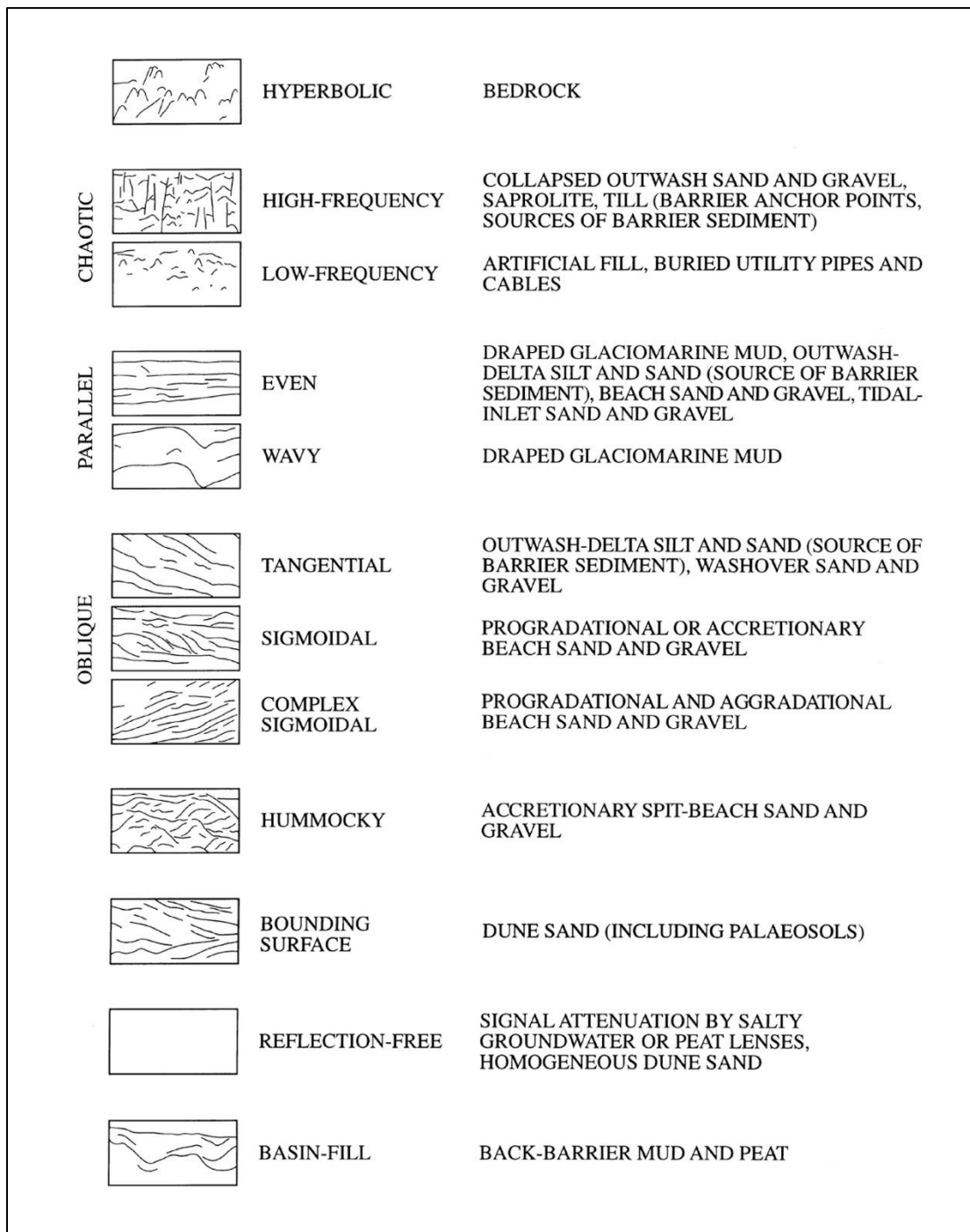
Radar facies are defined as a mappable based on reflection patterns of GPR profiles that it is one method for interpreting GPR profiles (Bristow, 2013: 188-189). Overmeeren (1998) identified a range of radar facies within aeolian dune sand that it is the combinations of inclined, parallel continuous and undulating reflections. The most common is inclined reflections from cross-strata (van Overmeeren, 1998). Pedersen and Clemmensen (2005) indicated five different aeolian radar facies within a parabolic dune: high-angle planar, high-angle oblique tangential, horizontal subparallel and moderate to low-angle convex-up (Figure 30). As the vegetated dunes recognized hummocky discontinuous reflections, trough-shaped reflections and low-angle inclined reflections, Heteren et al. (1998) recognized a so called bounding surface facies (Figure 31). However, radar facies have limitations to this approach since radar facies are not unique to a specific sedimentary structure (Jol and Bristow, 2003), and a 3D object like a set of trough cross-strata can appear as a

different shaped reflection on a GPR profile. Inclined reflections in the dip direction can be trough shaped in the strike direction (Bristow, 1996).

Radar stratigraphy is similar to seismic stratigraphy but it is at a much higher resolution (Bristow, 2013: 188). The concepts of radar stratigraphy were introduced by Beres and Haeni (1991) and Jol and Smith (1991) that it is brought to identify sequences showed on radar stratigraphy and reconstruct a relative chronology following the laws of superposition and cross-cutting relations. It is necessary to identify reflection terminations to identify radar sequence for constructing a relative chronology because reflections are considered as isochronous surfaces and truncations of reflections represent breaks in time called to chronostratigraphic gaps. This interpretation methodology has been applied to radar profiles across dunes in the Namib Sand Sea resulting in a reconstruction of dune migration and evolution (Bristow et al., 2000; 2005). Moreover, the cross-strata of migration dunes includes the internal bounding surfaces which are erosional surfaces found within or between sets of cross-strata. The bounding surfaces are divided into three types following reactivation or redefinition surfaces, superposition surfaces and interdune surfaces that all types relate to identify the chronology of dune.



**Figure 30** Five different aeolian radar facies within a parabolic dune: high-angle planar, high-angle oblique tangential, horizontal subparallel and moderate to low-angle convex-up (modified from Pedersen and Clemmensen, 2005).



**Figure 31** Radar facies on GPR Profiles of paraglacial barrier systems at coastal New England, USA (van Heteren et al., 1998).



## Chapter 3

### Methodology

#### 3.1 Study Plan

This research was carried out by systematic process as shown in Figure 32. It is classified to four major steps as follows: Firstly, concepts, theories and reports or case studies of geomorphology and archaeology are reviewed to prepare the data sources. The data sources are collected to two types including primary data (i.e. aerial photo of WWS project in scale 1:50000, satellite imagery of LANDSAT) and secondary data (e.g. topographic map, geologic map, hydrological map for geomorphological study, in addition to numbers, positions and attributes of archaeological sites). Secondly, the data sources are analyzed by GIS programs; ArcGIS 10.3.1 and ERDAS Imagine 2014 for field survey. The field survey was carried out in April to June 2017. It was operated by ground-penetrating radar (GPR) survey with auger coring for examples of sediment. These examples were progressed in sedimentology laboratory at next step. Moreover, archaeological survey was going on for consideration in the site attributes following landscape, environment, artifacts, and chronology. Thirdly, the examples received from GPR survey and field survey was analyzed in laboratory for results. Fourth, the last step, the data derived from literature review and field survey are integrated to discuss in the relationship between geomorphology and archaeological sites in study area based on results of analysis in laboratory which leads to the conclusion.

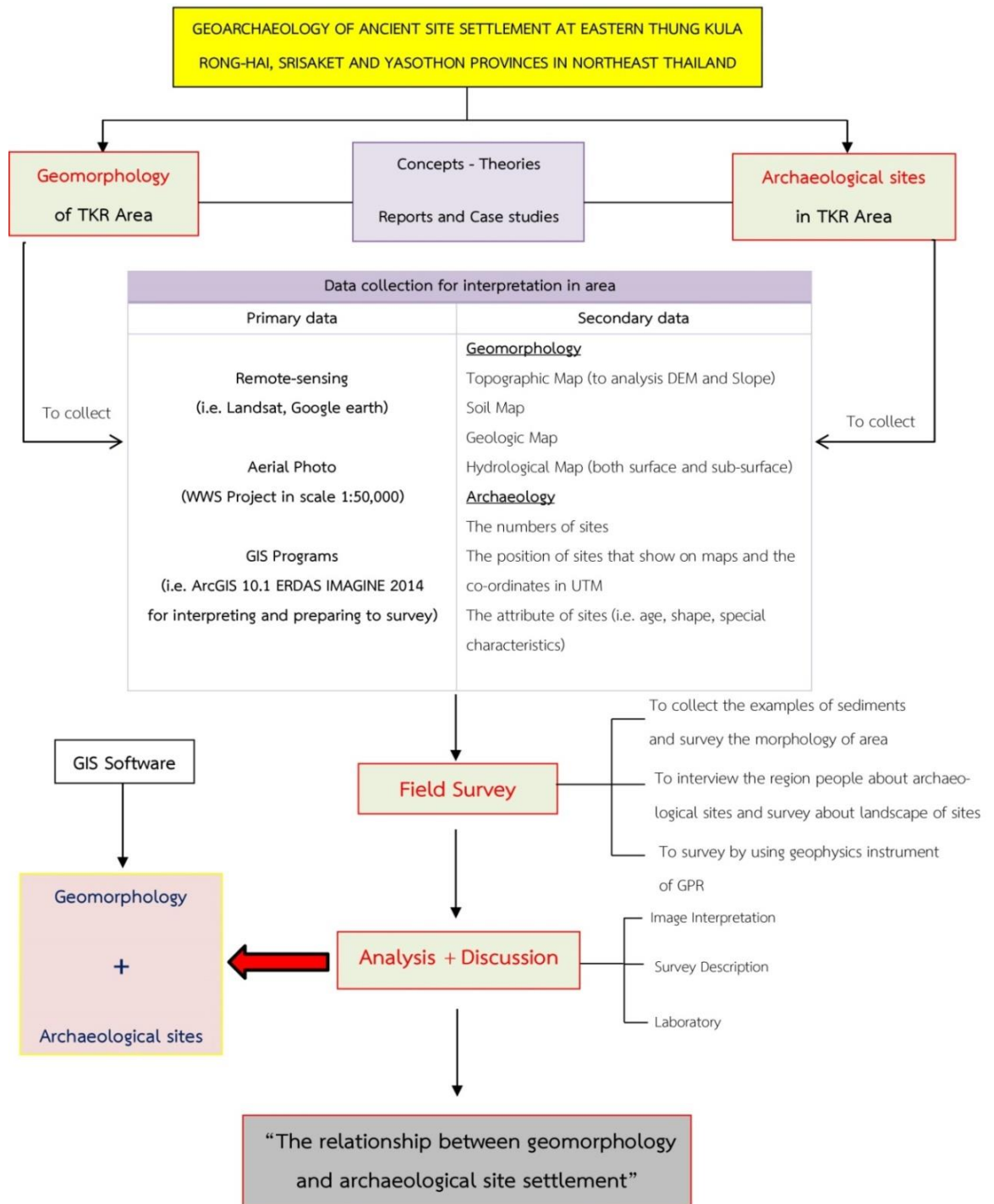


Figure 32 Diagram showing flow chart of methodology in this research.

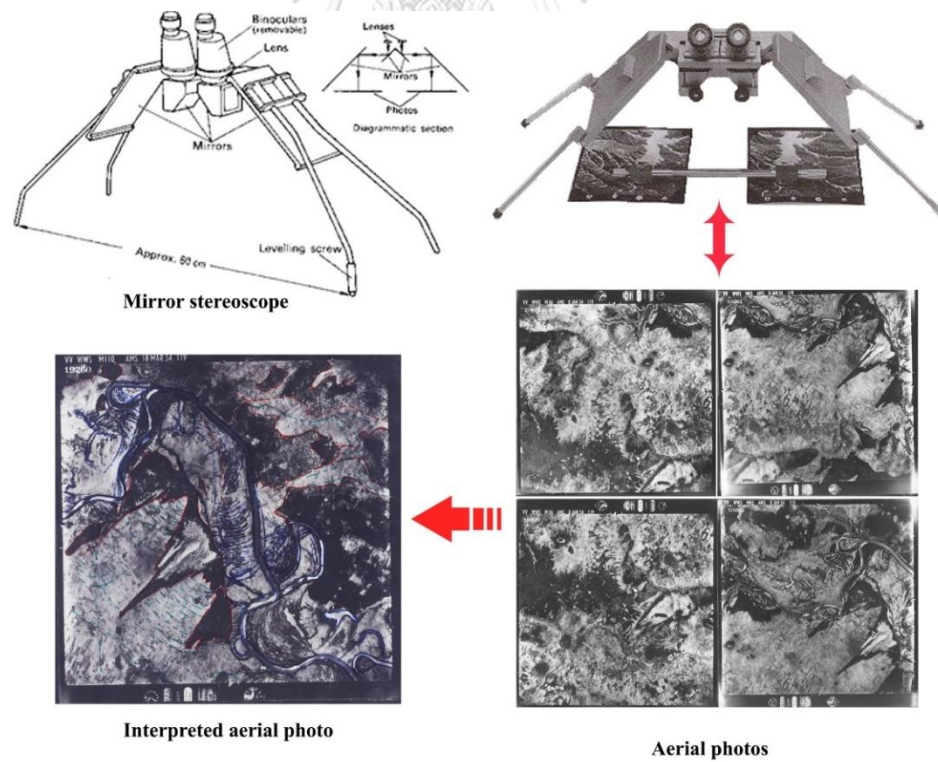
### 3.2 Aerial photograph and satellite imagery interpretation

Both of aerial photograph and satellite imagery were used in this research for interpretation of geomorphology at study area. They are the application of remote-sensing in geomorphological study, especially the aerial photos. The data sources of 85 aerial photos in WWS project in 1952 from Royal Thai Survey Department (RTSD) bordered in study area are derived mainly (Table 2). The interpretation was done under a mirror stereoscope for characterizing the morphology of area (Figure 33), then, they were scanned to digitize on the Geographic Information System (GIS) software and export to the geomorphic map. The principal of aerial photograph interpretation and mapping which contains the classification of characteristics of photographic images to each group under a few headings following color tone, shape, size, pattern, texture and shadow was adopted in this work. It also should separate those of probable ancient human origin from others due to natural causes (Riley, 1987: 60-62).

Moreover, four-sheets of L7018 topographic maps in scale 1:50,000 and six-sheets of L708 in scale 1:50,000 derived from RTSD were used for comparison of landscape changes at study area to digitize the aerial photos accurately. Lastly, satellite imageries of LANDSAT 8 were selected in path 127 row 49 due to locating in study area along with Global Digital Elevation Model (GDEM) (resolution 30 m) received from United States Geological Survey (USGS) (Figure 34). They are applied to analyze together with aerial photo interpretation by using GIS programs (Figures 34-35).

**Table 2** List of 85 aerial photos in WWS projects from RTSD

Roll	Photo number	Total
M65	10190-10199	10
	10253-10263	11
M66	10406-10415	10
	10475-10479	5
M72	11575-11583	9
	11735-11739	5
M73	11743-11750	8
	11825-11832	8
	11892-11894	3
M110	19251-19261	11
M111	19462-19466	5
<b>Total</b>		<b>85</b>



**Figure 33** the process of aerial photo interpretation by the mirror stereoscope.

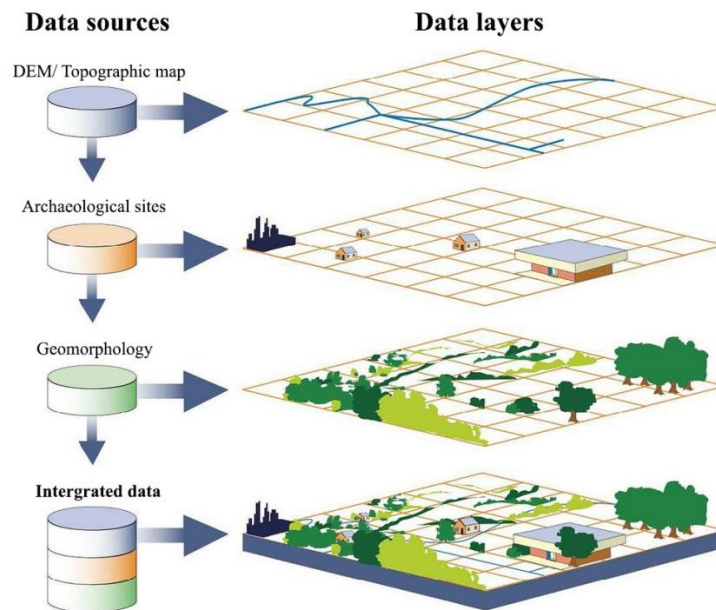


Figure 34 Diagram showing the process of data analysis by GIS software.

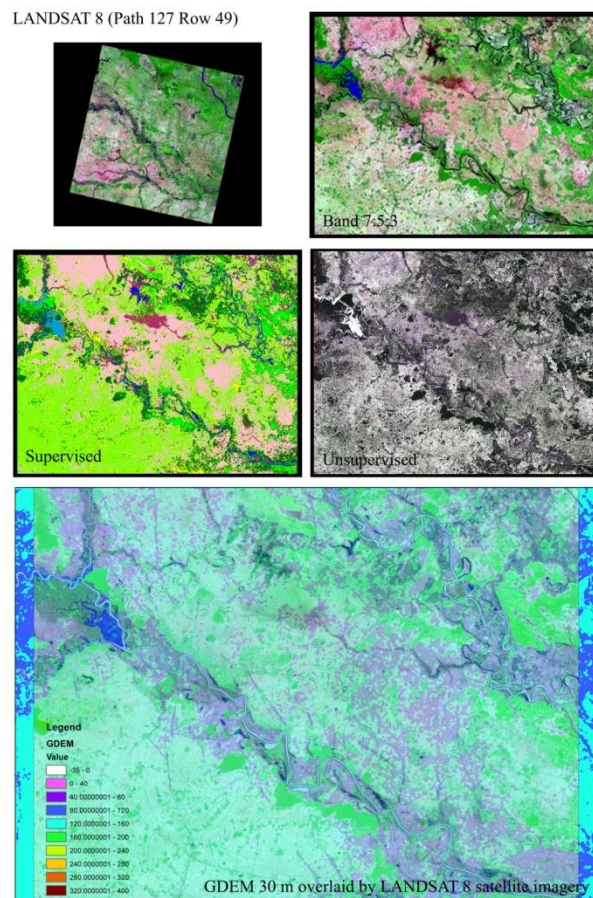


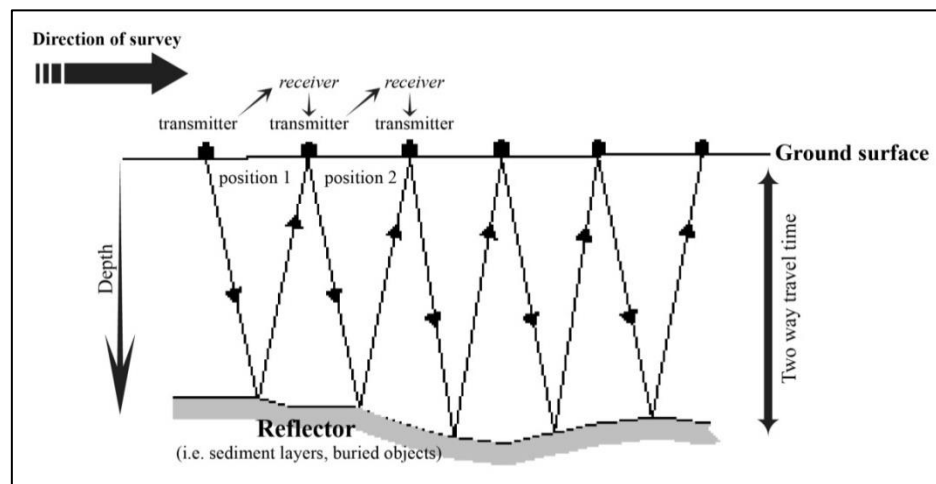
Figure 35 Data sources as satellite imagery of LANDSAT 8 and GDEM 30 m.

### 3.3 Ground Penetrating Radar survey with coring

In the present day, field of geomorphology is studied by two techniques including classic and modern techniques. Ground-penetrating radar (GPR) is arranged to modern technique due to being geophysics instrument. It is not destructive in subsurface survey (Schrott et al., 2013). GPR is an electromagnetic geophysical exploration technique. Theoretically, ground-penetrating radar uses high-frequency electromagnetic (EM) waves to acquire information on subsurface composition by transmitting a signal of EM into the ground. The signal is reflected from layers in the subsurface as a transmitter in which there is a contrast in dielectric properties and returns to the surface where it is recorded as a receiver that this part is used to image subsurface stratigraphy (Bristow, 2013) (Figure 36). The wavelength of the radar signal affects to the resolution. The low-frequency signals with a longer wavelength have a greater depth of penetration but less resolution in contrast to higher-frequency signals with a short wavelength have higher resolution but less penetration into the ground (Bristow, 2013: 183-184). Nonetheless, it does not effectively work in the ground being conductive such as areas with saline ground as well as some clay soils, but it works well in soils with a high resistivity such as sand, silt and ice wedges (e.g. Hinkel et al., 2001; Bristow et al., 2007). For this research, thus, GPR is applied to survey at sand splay landform which is covered by sand layer. The frequency of 200 MHz and 400 MHz as antennae are tracked on study area depending on objectives of study (Figure 37). Moreover, the raw data received from GPR survey in fields should be processed by its software to remove noises or modify resolution of display such as gain adding, background remover, vertical and horizontal scale in elevation, and correct position that SIR-20 system is operated in these processing for this work.

GPR and topography survey data were applied to study the detailed internal structure of sand splays. GPR survey was undertaken for 3 sites that the frequency of 200 MHz was used at Site 1 for viewing the paleochannel feature beneath the sand splay, in addition to Site 2 along longitudinal and transverse transects of sand splay approximately 200 to 300 m distance of GPR lines. The antennae 400 MHz was tracked on Site 3 in two lines of NE-SW and SE-NW for internal structure of sand

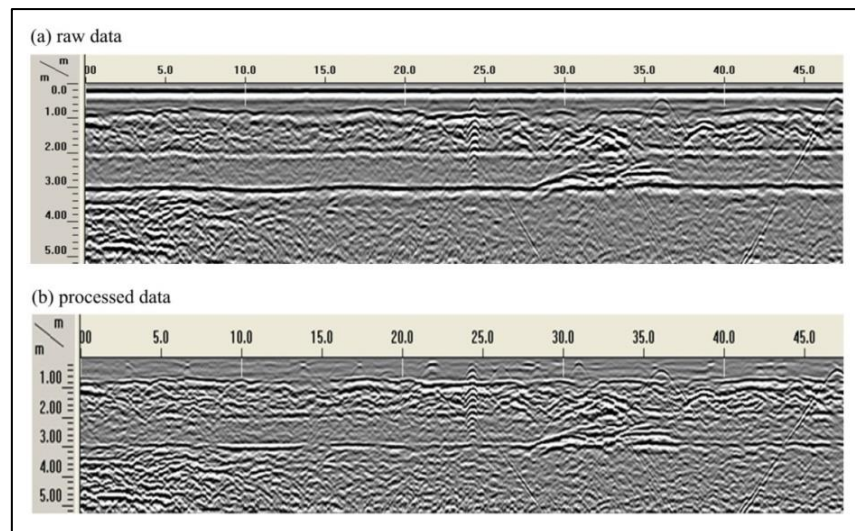
splay (Figure 39). Furthermore, Site 4 which is a moated site or archaeological site was tracked by the antennae 200 MHz for viewing internal structure of mound and buried objects (Figure 40). Raw data were appropriately processed by SIR-20 system before reconstructing to the evolution of process structure of these landforms.



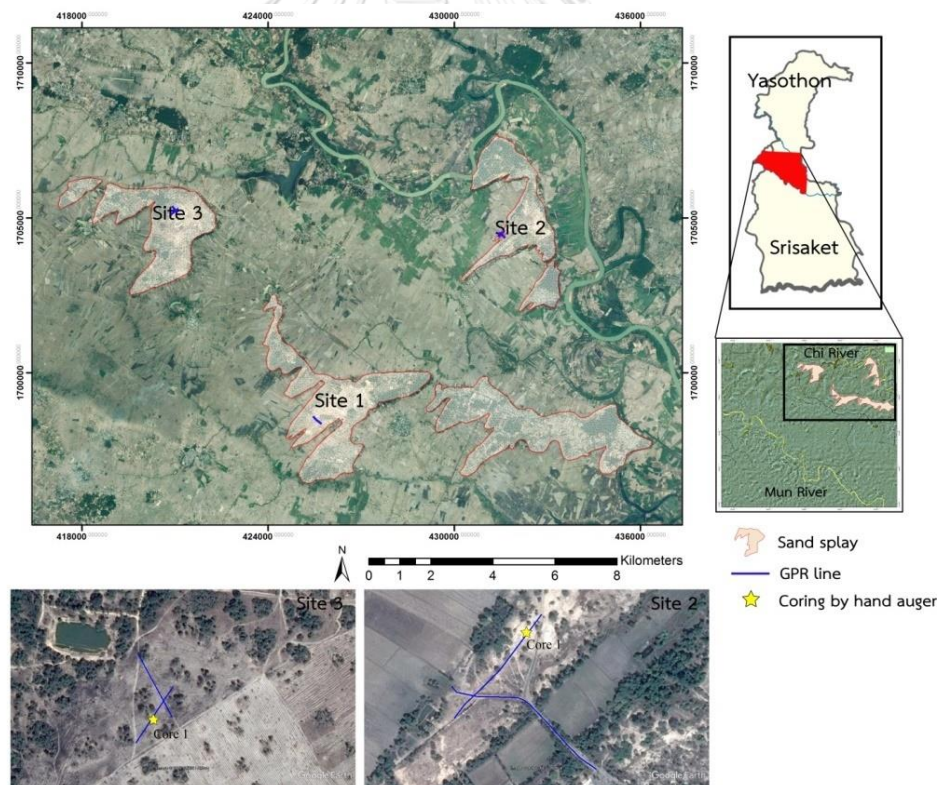
**Figure 36** Block diagram depicting main components of GPR system (modified from Jol and Smith, 1991).



**Figure 37** Instruments of GPR including transmitter/receiver as antenna of 200 MHz and 400 MHz and controller/display as a laptop which is operated by SIR-20.

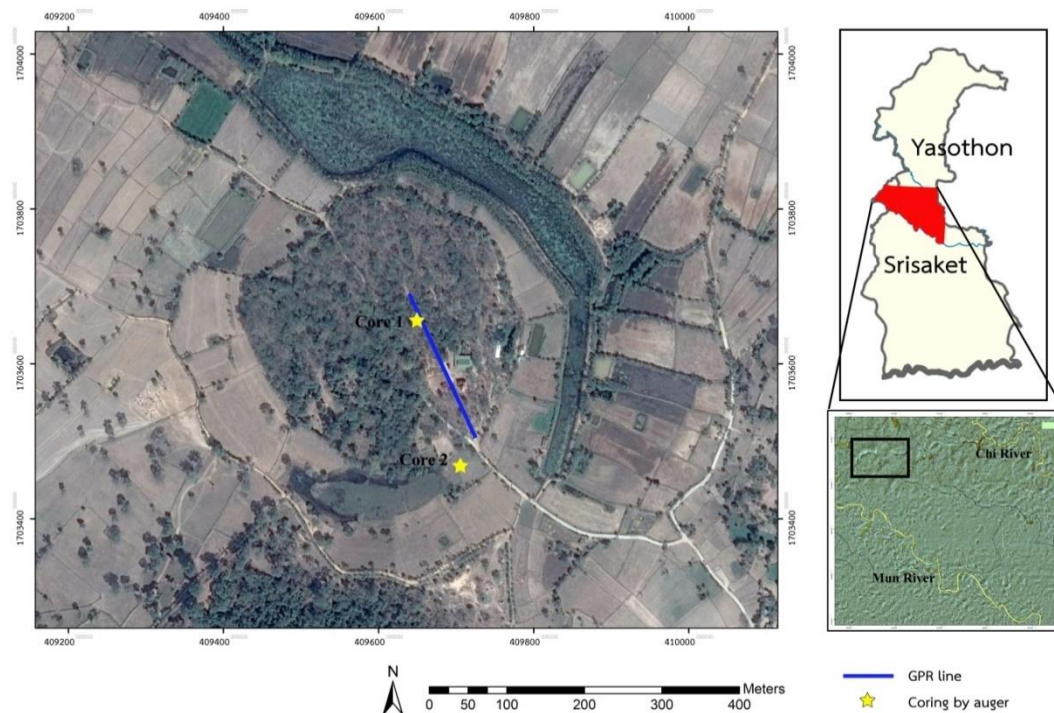


**Figure 38** Examples of GPR data derived from GPR survey as following (a) raw data which composes noises and hyperbolas and (b) processed data which is removed noises absolutely.



**Figure 39** GPR lines tracked on sand splays at 3 sites; Site 1 in SE-NW crossing meander scars, Site 2 in 2 lines NE-SW and NW-SE crossing the floodplain and sand splays and Site 3 same direction as Site 2, in addition to two-coring point at Site 2 and Site 3 on GPR lines.





**Figure 40** A GPR line in blue was tracked on a moated site called as Don Kluea site.

However, the only GPR survey cannot derive data enough in this research because it cannot really see characteristics of sediment such as water table, sediment types or sizes. Therefore, the coring as a classic technique of geomorphological study is used together. The examples derived from coring by hand auger need to analyze by sieving for analysis of sediment types and grain sizes in laboratory, especially sand grain. At Site 2, hand auger was used to core on GPR line 2 at 2.0 m depth which is at 33-34 m distance approximately, as well as GPR line 1 of Site 3 where was cored between 0.0-2.8 m depth and at 46-48 m distance approximately. Both of sites are sand splay landform. The coring is proved for internal structure of aeolian deposits and fluvial deposits found on GPR radar facies interpretation. It can explain the question about stratigraphy of sand splay process in the past. In addition, the moated site of Don Kluea as an archaeological site in study area was cored on GPR line 1 at 23-25 m distance between 0.0-4.0 m in depth for examining the materials as buried objects found on GPR radar facies and the stratigraphy of this moated site along with coring at the east of moats in which was taken due to comparison the characteristic of sediments found at mound and moat.

Grain size is studied for measurement of sediment and sedimentary rock that reflects the mechanisms operative during transportation and deposition as well as the distance of sediment transport (Lindholm, 1987). Classification of grain size based on size grades of J. A. Udden and modified by C. K. Wentworth (1922). It is generally known as the Udden-Wentworth Grade Scale (Wentworth, 1922). Later, Krumbein (1934) proposed that grain size should be expressed as phi ( $\Phi$ ) notation (Fig. 3-10) (Krumbein, 1934). Indeed, sieving is commonly used in determining the grain-size distribution of sand. It is classified to two types including dry sieving and wet sieving. A dry sample is placed in the uppermost sieve in a set of stacked sieves following Mesh no.18, 35, 60, 120 and 230. The stack of sieves are arranged from coarsest sieve at the top with finer ones below, and a pan is arranged at the bottom to catch any sediment that passes through the lowest and finest sieve, is placed on a shaking machine for shaking about ten minutes. After, the sand has collected on each sieve and the pan is removed and weighed respectively (Figure 41).

The 46 samples were collected from coring in every range of 20 cm depth from surface. They need to analyze the grain size distribution by sieving as mentioned above. Moreover, the 7 samples from collection of soil profiles at Site 2 and Site 3 were analyzed together with the 46 samples by sieving, but they also were collected for dating by Optically Stimulated Luminescence (OSL) methods (Figure 42).

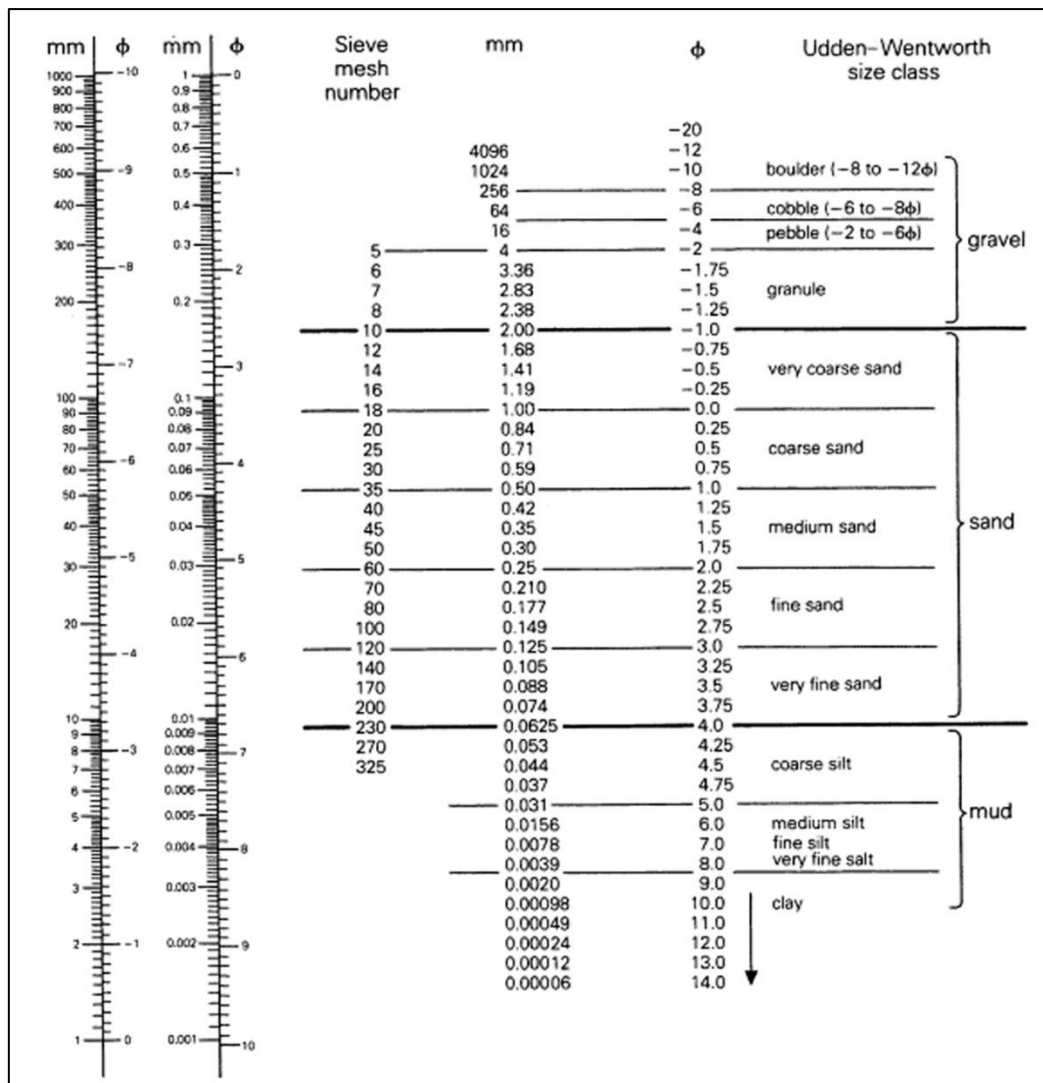
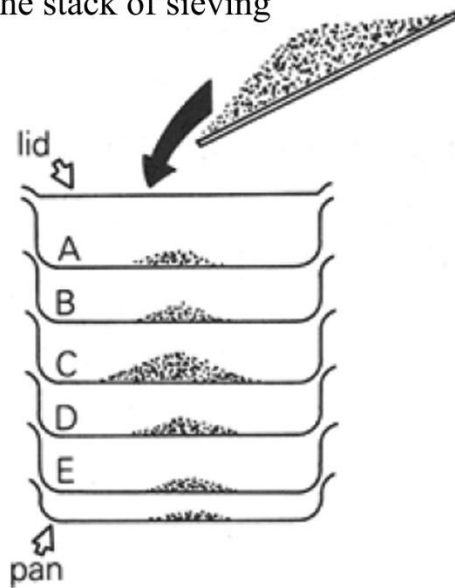
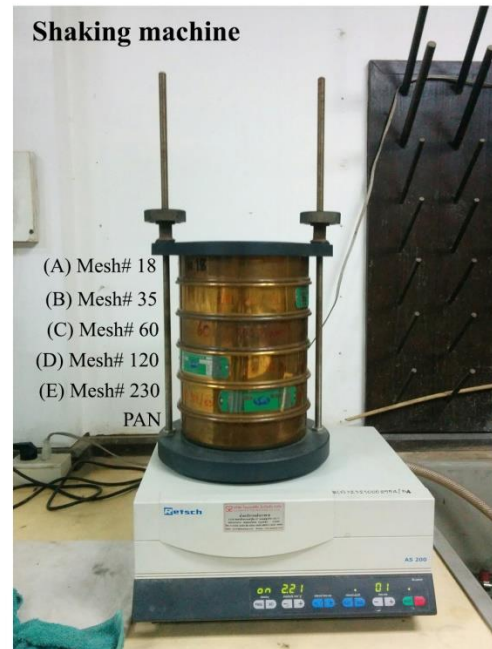


Figure 41 Table of Udden-Wentworth size classes. Nomogram used to convert millimeters to phi ( $\phi$ ) (Modified from Folk, 1980: 23).

The stack of sieving



Shaking machine



- (A) Mesh# 18
- (B) Mesh# 35
- (C) Mesh# 60
- (D) Mesh# 120
- (E) Mesh# 230
- PAN



Grain size after weighing

**Figure 42** Sieving methods that a dry sample is placed in the uppermost sieve in a set of stacked sieves following Mesh no.18, 35, 60, 120 and 230.

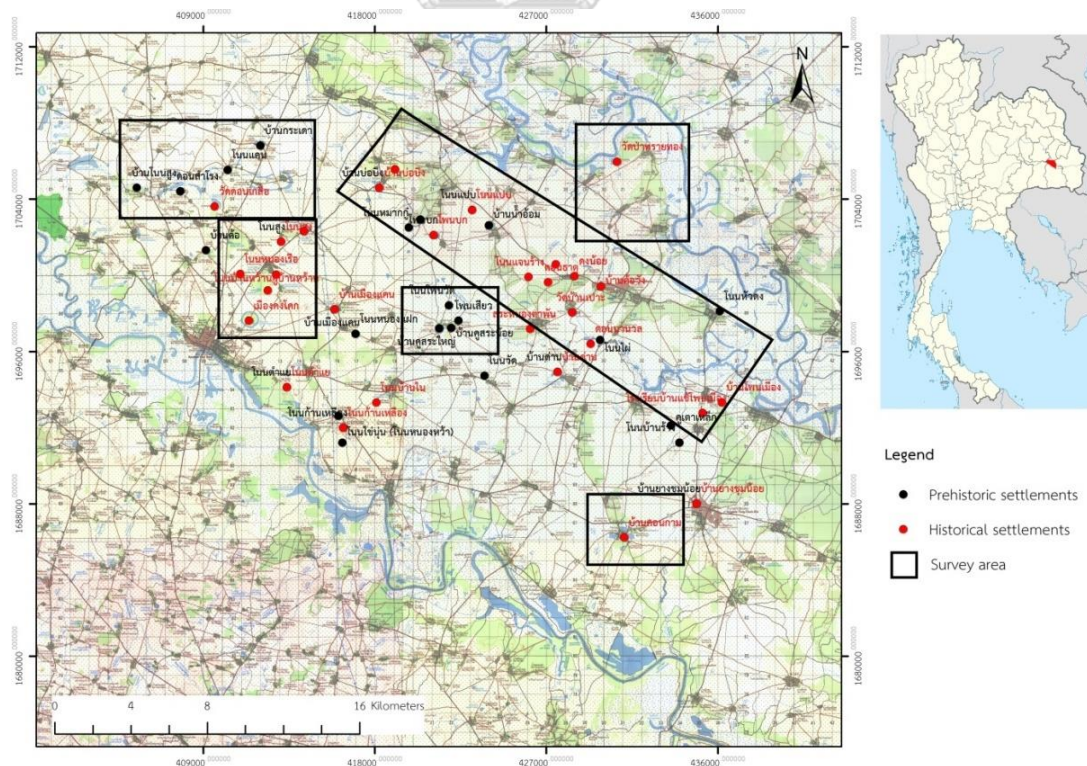
**(a) Coring by hand auger****(b) Collecting data from soil profiles**

**Figure 43** Field pictures showing collecting the data by various methods in this research.

### 3.4 Archaeological Survey

From aerial photograph interpretation, many man-made features and constructions were discovered in study area such as earthworks, moats, and rectangle ponds (known as Baray). The moated sites revealed the settlement pattern of human past at least 2,500 to 1,500 B.P. Thus, they are necessary for archaeological survey for rechecking the site attributes that they were eventually carried out in June 2017.

The aims of the archaeological survey are to find the recording of an archaeological features providing information about the monument's form, construction, function, condition and how it has been affected by subsequent developments and later use (RCHME, 1999: 1). This research applied the survey methods including the collecting of position (by satellite position-GPS), the recording of characteristics (e.g. artifacts, monument forms and decorations, and landscapes) by taking the photos, and the interviewing of local peoples about histories, myths, or discovered archaeological evidences surrounding in villages or sites (Figures 44-45).



**Figure 44** Archaeological survey map, especially the areas within black margins.

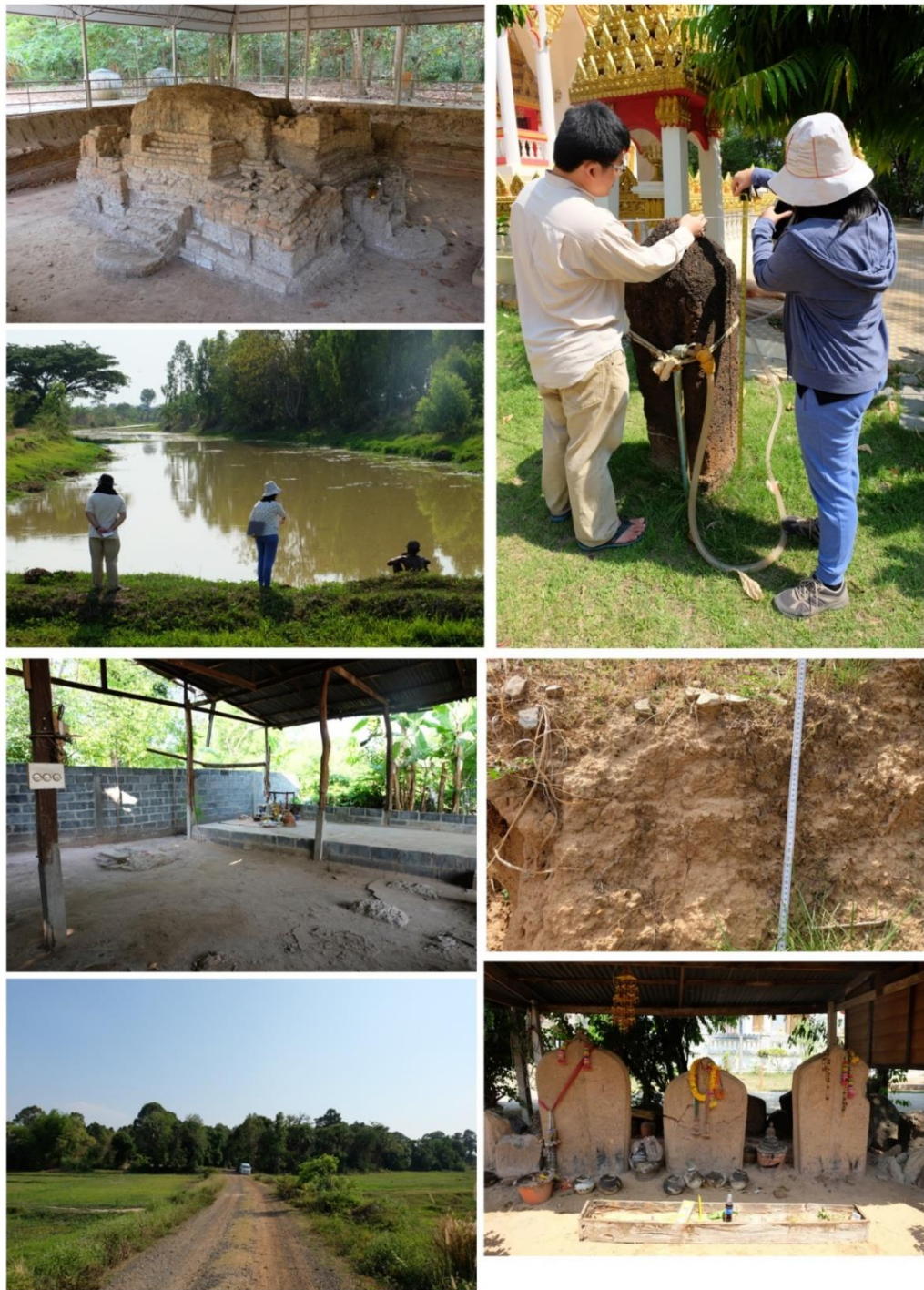


Figure 45 Field pictures showing archaeological survey in study area.

## Chapter 4

### Results

This chapter presents the results from field survey (both of geomorphology and archaeology) and laboratory including aerial photograph interpretation, GPR survey, grain size analysis and OSL dating. These results will be described to four sections as follows; 4.1 Geomorphology from aerial photo interpretation, 4.2 Ground-penetrating radar survey, 4.3 Grain size analysis from coring, and 4.4 OSL dating result of sand splays.

#### 4.1 Geomorphology from aerial photo interpretation

For this work, the results from aerial photograph interpretation reveal interesting landscape and geomorphological features in eastern part of TKR. This area is considered to be the Lower Mun and Chi Rivers locating before joining and flow eastward into Mekong River at Ubon Ratchathani province. Floodplain has developed along both of river sides, especially the south of Mun River where channel width is wider than the north area. The border of this floodplain is visible. These characteristics may be related to some geological structures of this area, in particular, the unusual elevation of the southern part of Mun River.

The terrace can be classified into 2 steps by elevation difference including low terrace and high terrace on both of Mun and Chi River sides. It is characterized by paired terrace. This appearance indicates the evolution of aggradation in both sides of river bank. Especially, the paleochannel features founded on the high terrace illustrating some features, so-called “old-floodplain” of high terrace in the past. Moreover, the other features also support this idea of aggradation can be observed at the eastern TKR margin. Following salt domes (as annular landform depression or ADL) and sand splays (a type of aeolian dune), the specific geomorphologies or landforms founded in study area are discussed. In archaeology, the 54 sites moated sites and man-made features were founded. The positions of these archaeological



sites are related to the landforms, in particular to paleo-channels and ADL (Figure 46).

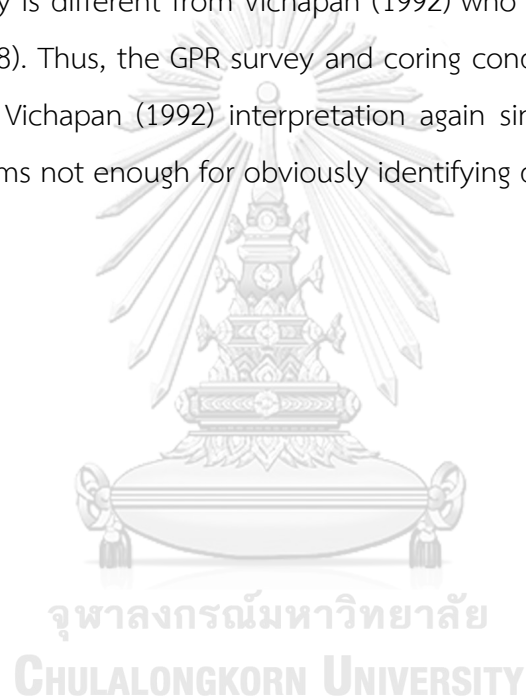
#### 4.1.1 Paleo-channel features

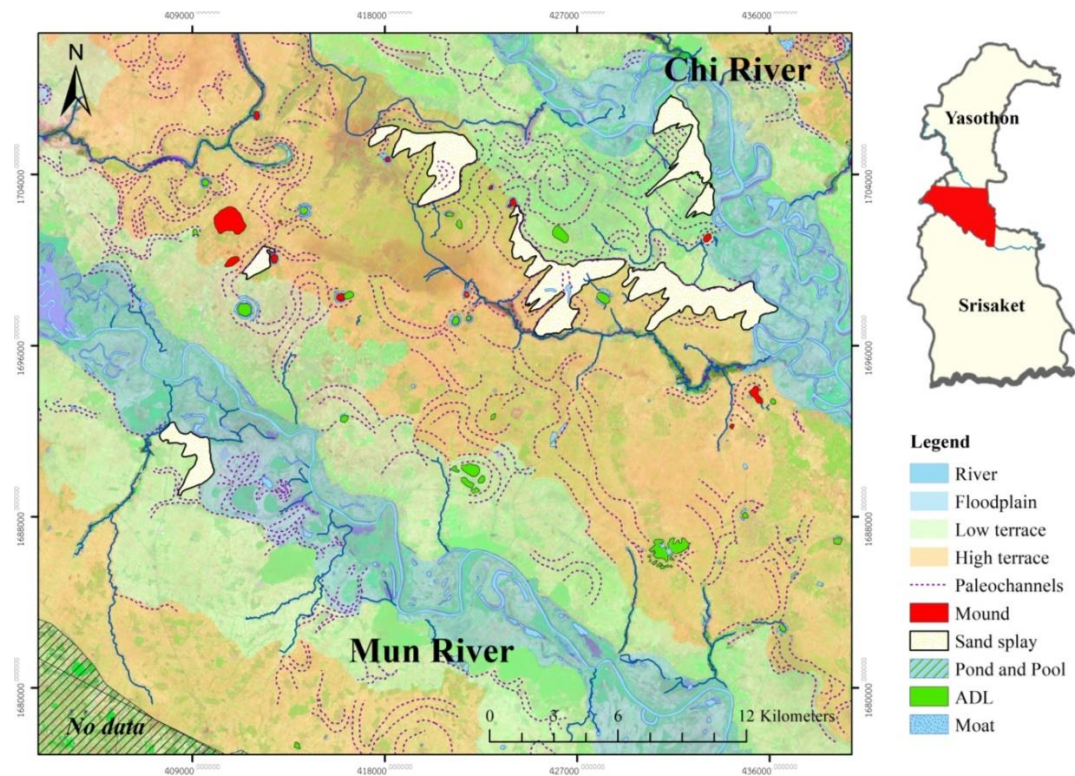
The Lower Mun and Chi Rivers consist of extensive paleo-channels. They can be divided into 3 groups as follows; Group A (Inactive ancient drainage), Group B (Active ancient drainage), and Group C (Recent drainage). Group A is the inactive ancient drainage identified as paleo-Mun and paleo-Chi Rivers. They are interpreted based on the connection between paleochannel features with inactive channels derived from aerial photo interpretation. Remarkably, Group A features are mostly located on high terrace between Mun with Chi Rivers. They flow in NW-SE direction similar to the present. The Paleo-Chi or Mun Rivers may be used as a key criterion to locate terraces on this area, especially the appearance of sand splay margins that they indicate to be a paleo-channel bordered low and high terrace. This relationship will be discussed in Chapter 5. Group B is the active ancient drainage. They are linked to the recent drainage and believed to be younger than Group A. This group connects from Group A and run into recent drainage of Group C. They are founded in low and high terrace. The last, Group C which is the recent drainage, is defined as the Mun and Chi Rivers as well as their branch streams. They are located on floodplain and low terrace (Figure 47).

#### 4.1.2 Annular landform depression (ADL)

Many salt domes as ADL are located in TKR. They are the unique natural landforms of somewhat circular feature including ring shape depression area enclosing mound of higher elevation. It can be identified from aerial photograph and satellite imagery. This landform is related to the structure of TKR basin acting a saucer shaped basin similar to the Khorat Basin in which Maha Sarakham Formation is beneath as bedrock. Significantly, ADL is mostly found in terrace only, not on floodplain. As a result, it may associate with the aggradation of terrace under the condition that there was not enough groundwater flow to erode salt layer on stage of dome-shape or diapir intrusion in bedrock (it will be discussed more in next chapter).

The ADL of lower Mun and Chi Rivers area are classified to be Types 1, 2, 3 and 5 referred to classification of ADL types introduced by Vichapan (1992). This classification is based on number of circular shape and elevation of area. Type 1 is the annular depression of a single level surrounding a mound. Type 2 is the annular depression of different levels surrounding a mound. Type 3 is the annular depression with several minor depressions adjacent to a mound. Type 5 is the annular depression with coalescing mounds (Vichapan, 1992: 54-55). Aerial photograph interpretation reveals 16 ADLs located on terrace of study area. A number of ADL found in this study is different from Vichapan (1992) who discovered the 20 ADLs in this area (Figure 48). Thus, the GPR survey and coring conducted in this research are applied to prove Vichapan (1992) interpretation again since the aerial photograph interpretation seems not enough for obviously identifying due to landscape changes.





**Figure 46** Geomorphic map resulting from aerial photograph interpretation illustrates the specific landforms at eastern Thungkula Ronghai including sand splay in yellow-white, annular landform depression in green and paleochannel in dash-line, in addition to showing the archaeological sites in circular-shaped moats and mounds.

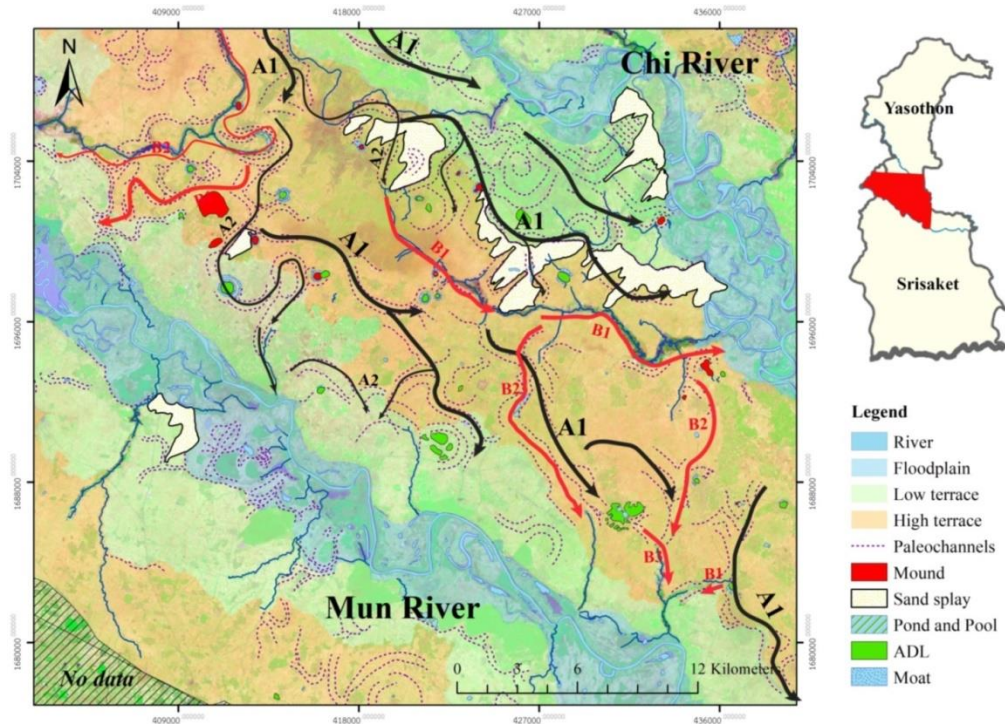


Figure 47 The 3 groups of paleo-drainage founded in the Lower Mun and Chi Rivers of eastern TKR area are based on aerial photography interpretation.

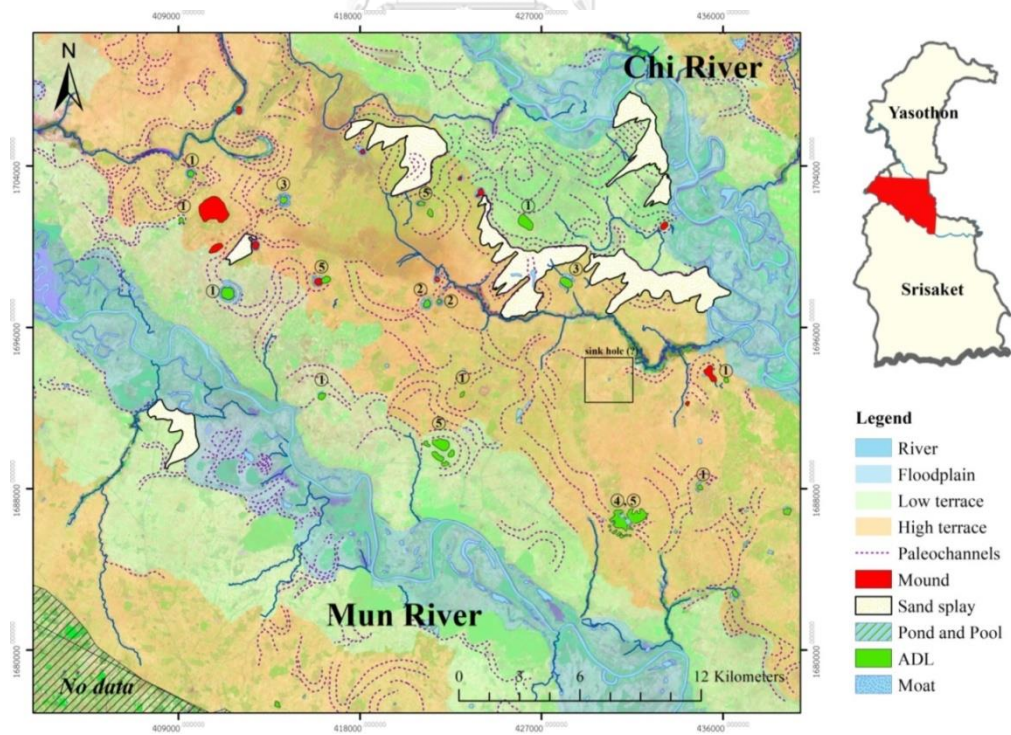
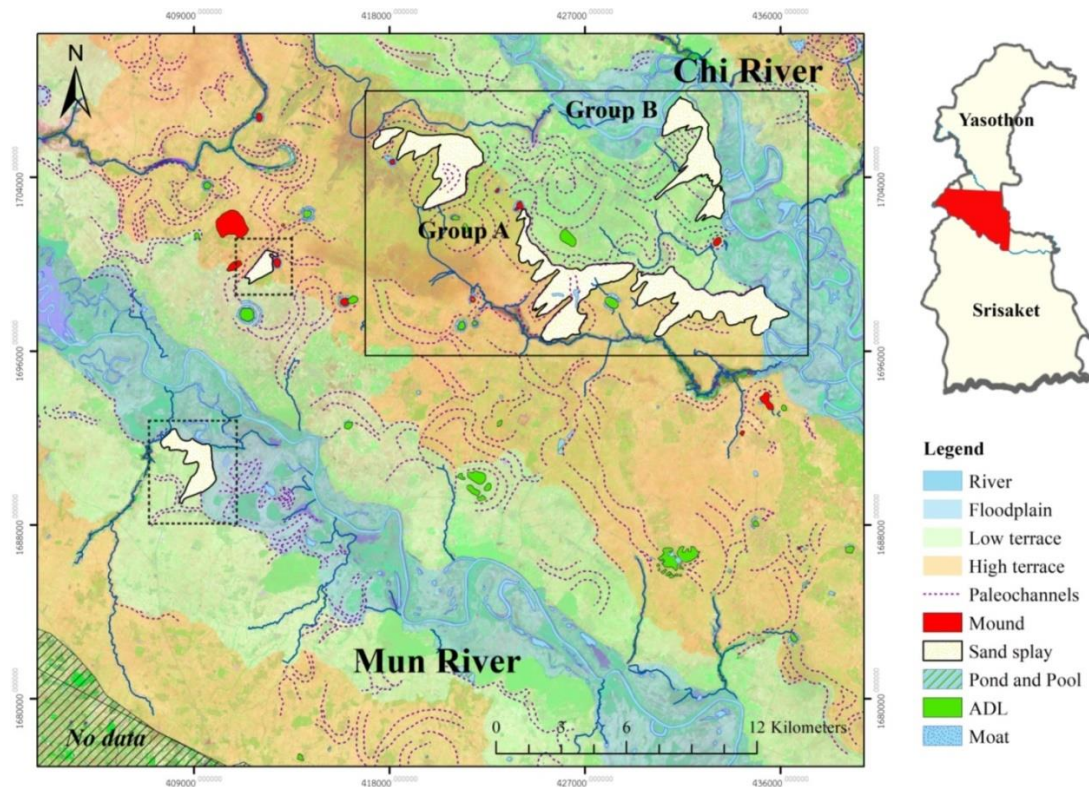


Figure 48 The 16 ADLs with type orders founded on the Lower Mun and Chi Rivers or eastern TKR basin from aerial photo interpretation.

#### 4.1.3 Sand splays or aeolian features

Aeolian features are discovered in study area, in particular, the mounds or ridges of wind-deposited sand that stand a few meters above surrounding paddy field in NE-SW direction and be covered by natural forest. These characteristics are identified as “sand splays” that they are aeolian dune. The sand cover has various thicknesses and overlies on partly weathered regolith of the Maha Sarakham Formation. Sand splays can be commonly founded in Yasothon, Srisaket and some parts of Rot-et, Surin and Ubon Ratchathani provinces. In study area, they were discovered between Mun and Chi Rivers, especially in Khowang district, Yasothon province. They can be divided into 2 groups. Group A is located in high terrace and Group B is situated in low terrace joining to floodplain of Chi River. Group A and Group B may active in the same time (Figure 49).

Based on aerial photograph interpretation, this aeolian sand is classified as shadow dune as the dune influenced by topographic obstacles. The assumption is supported by the recognition of paleo-channel features such as meandered scars, channel belts, and elevation of terrace and floodplain. Remarkably, the northeast margin of sand splays is closed to the edge of terrace. The elevation of terrace acted as obstacle when the prevailing wind is originated from the northeast to form sand splay. Indeed, the paleo-channel features are indicators of material source and paleoenvironment before sand splays originated that this assumption is obviously proved from GPR survey.



**Figure 49** Aeolian sand plays discovered in study area are divided into 2 groups following Group A on the high terrace and Group B on the low terrace.

#### 4.1.4 Moated sites and man-made features as archaeological sites

The interpretation of aerial photographs in the study area revealed man-made features such as the moats in circular-shaped surrounding a mound (called as moated sites), embankments around the moats, and earthworks features in straight-shaped. These features are related to human culture of settlements known as archaeological sites. The 54 archaeological sites located on the Lower Mun and Chi Rivers beneath the influences of TKR culture since at least 2,500-1,500 BP. The site locations are considered to relate with geomorphology dominantly (e.g. paleochannels, salt domes, and aeolian features).

From archaeological survey, the attribute of any sites has changed because of urban development in the present influences to the sites. The construction or invasion closed to sites affects to the decreasing of archaeological evidences in subsurface, as well as being disruption or disturbance. Nevertheless, the most sites are reviewed to remains of archaeological sites. The 37 prehistoric sites

are widely founded on eastern TKR area along 33 historical sites. All sites are classified to be settled from prehistoric to historical periods as shown in Table 3 and Figure 50.



**Table 3** Archaeological sites located in the study area

Site no.	Site	location	Co-ordinate system		Age (BP)	Characteristics	Category
			UTM (47P) E	N			
1	Ban Mak Mai	Ban Mak Mai, Khowang, Khowang, Yasothon	430584.0800	1696873.6300	1,500-1,000 BP to the century 10 <sup>th</sup> AD	Moated site	Village
2	Ban Non Sung	Ban Non Sung, Nong Kae, Rasisai, Srisaket	405500.1751	1704593.4090	2,500-1,500 BP	Mound	Village
3	Ban Kra-Dao	Ban Kra-Dao, Du, Rasisai, Srisaket	411985.2168	1706813.4200	2,500-1,500 BP	Moated site	Village
4	Non Kane	Ban Krang, Gung, Rasisai, Srisaket	410267.2055	1705530.4130	2,500-1,500 BP	Moated site	Village
5	Don Samrong	Wat Don Muang, Du, Rasisai, Srisaket	407785.1894	1704413.4070	2,500-1,500 BP	Mound	Village
6	Ban Kho	Ban Kho, Du, Rasisai, Srisaket	409135.1967	1701313.3870	2,500-1,500 BP	Mound	Village
7	Non Sung	Ban Don Tam, Wan Kam, Rasisai, Srisaket	413075.2217	1701764.3880	2,500-1,500 BP to the century 13 <sup>th</sup> AD	Moated site	Village
8	Nam-Om Noi	Ban Om Noi, Wan Kam, Rasisai, Srisaket	414285.2295	1702313.3910	2,500-1,500 BP to the century 13 <sup>th</sup> AD	Moated site	Village
9	Ban Dan	Ban Dan, Sang Pi, Rasisai, Srisaket	427586.3109	1694922.3400	2,500-1,500 BP to the century 13 <sup>th</sup> AD	Moated site	Village
10	Non Wat	Ban Sra Kaew, Sang Pi, Rasisai, Srisaket	423747.2866	1694729.3400	2,500-1,500 BP	Moated site	Village
11	Ban Yang Chum Noi	Ban Yang Chum Noi, Yang Chum Noi, Yang Chum Noi, Srisaket	434885.3551	1688013.2930	2,500-1,500 BP to the century 13 <sup>th</sup> AD	Moated site	Village, Sanctuary



**Table 3** Continued.

Site no.	Site	location	Co-ordinate system UTM (47P)		Age (BP)	Characteristics	Category
			E	N			
12	Ban Khu Sra Yai	Ban Khu Sra Yai, Phai, Rasisai, Srisaket	421385.2725	1697213.3560	2,500-1,500 BP	Moated site	Village
13	Ban Khu Sra Noi	Ban Khu Sra Noi, Phai, Rasisai, Srisaket	422003.2764	1697234.3560	2,500-1,500 BP	Moated site	Village
14	Non Phon Wat	Ban Khu Sra Yai, Phai, Rasisai, Srisaket	421885.2760	1698413.3640	2,500-1,500 BP	Moated site	Village
15	Phon Siew	Ban Khu Sra Noi, Phai, Rasisai, Srisaket	422385.2789	1697613.3580	2,500-1,500 BP	Mound	Burial
16	Non Tam Yae	Ban Yang, Muang Kaen, Rasisai, Srisaket	413382.2207	1694126.3390	2,500-1,500 BP to the century 13 <sup>th</sup> AD	Mound	Village
17	Non Nong Faek	Ban Saeng, Muang Kaen, Rasisai, Srisaket	416985.2445	1696913.3560	2,500-1,500 BP	Mound	-
18	Ban Muang Kaen	Ban Muang Kaen, Muang Kaen, Rasisai, Srisaket	415885.2381	1698213.3640	2,500-1,500 BP to the century 13 <sup>th</sup> AD	Moated site	Village to Town
19	Ban Bueng Mok Yai	Ban Bueng Mok Yai, Muang Kaen, Rasisai, Srisaket	416085.2373	1692613.3290	2,500-1,500 BP	Moated site	Village
20	Non Karm Laeung	Ban Bueng Mok Noi, Muang Kaen, Rasisai, Srisaket	416335.2386	1691993.3250	2,500-1,500 BP to the century 13 <sup>th</sup> AD	Moated site and embankments in square-shape	Village to Town

Table 3 Continued.

Site no.	Site	location	Co-ordinate system UTM (47P)		Age (BP)	Characteristics	Category
			E	N			
21	Non Nong Wa	Ban Bueng Mok Noi, Muang Kaen, Rasisai, Srisaket	416285.2380	1691213.3200	2,500-1,500 BP	Mound	-
22	Non Ban Rang	Ban Kae, Fa-Huan, Khowang, Yasothon	433985.3504	1691213.3139	2,500-1,500 BP	Moated site	Village
23	Khu Tao Lek	Ban Kae, Fa-Huan, Khowang, Yasothon	433542.3478	1692112.3197	2,500-1,500 BP	Two-Embankments in NW-SE and SE-NE	Road (?)
24	Ban Kae -Phon Muang	Ban Phon Muang, Fa-Huan, Khowang, Yasothon	435205.3585	1692763.3234	3,000-2,500 BP. to the century 12 <sup>th</sup> AD	Moated site	Village
25	Non Hua Dong	Ban Fa-Huan, Fa-Huan, Khowang, Yasothon	436110.3658	1698107.3572	2,500-1,500 BP	Mound	-
26	Wat Ban Po	Ban Por, Khowang, Khowang, Yasothon	428360.0000	1698043.0000	2,500-1,500 BP to the century 9 <sup>th</sup> - 13 <sup>th</sup> AD	Moated site	Village and Sanctuary
27	Non Phai	Ban Ma-mai, Khowang, Khowang, Yasothon	430584.0800	1696873.6300	1,500-1,000 BP	Moated site	-

**Table 3** Continued.

Site no.	Site	location	Co-ordinate system UTM (47P)		Age (BP)	Characteristics	Category
			E	N			
28	Ban Khowang	Ban Khowang, Khowang, Khowang, Yasothon	429872.0000	1699421.0000	1,500-1,000 BP to the century 8 <sup>th</sup> – 13 <sup>th</sup> AD	Mound	Sanctuary
29	Ban Nam Om	Ban Nam Om, Moo 5, Khowang, Khowang, Yasothon	423985.2907	1702613.3895	2,500-1,500 BP	Moated site	Village
30	Non Paep	Ban Bak Noi, Nam Om, Khowang, Yasothon	423101.0000	1703437.0000	1,500-1,000 BP to the century 13 <sup>th</sup> AD	Moated site	Village
31	Phon Bok	Ban Phon Bang, Nam Om, Khowang, Yasothon	421085.2723	1702113.3873	2,000-1,500 BP to the century 13 <sup>th</sup> AD	Moated site	Village
32	Non Mak Gu	Ban Bak Yai, Nam Om, Khowang, Yasothon	419777.0000	1702503.0000	2,500-1,500 BP	Mound	Village
33	Ban Bak Yai	Ban Bak Yai, Nam Om, Khowang, Yasothon	420390.2682	1702918.3926	2,500-1,500 BP	Mound	Village
34	Ban Bo Bueng	Ban Bo Bueng, Song Yang, Maha Chanachai, Yasothon	418237.2552	1704599.4040	2,500-1,500 BP to the century 13 <sup>th</sup> AD	Moated site	Village
35	Wat Pa Don That	Ban Bo Bueng, Song Yang, Maha Chanachai, Yasothon	419061.0000	1705567.0000	2,500-1,500 BP and the century 16 <sup>th</sup> AD	Mound	Burial and Sanctuary

**Table 3** Continued.

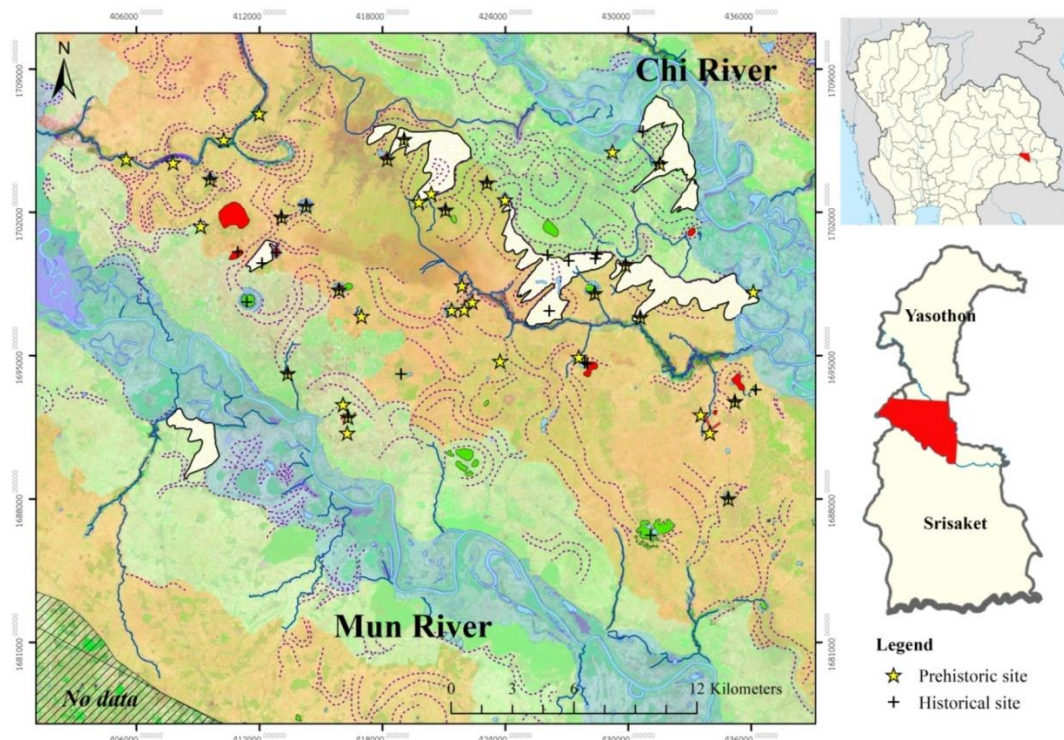
Site no.	Site location	Co-ordinate system		Age (BP)	Characteristics	Category
		UTM (47P) E	N			
36	Pho Kham Chan Ban Kud Nam-sai, Kud Nam-sai, Khowang, Yasothon	431548.4800	1704367.7600	2,500-1,500 BP	Mound	-
37	Don Na Nuan Ban Dan Noi, Sang Pi, Rasisai, Srisaket	427883.7600	1694640.2400	The century of 10 <sup>th</sup> – 13 <sup>th</sup> AD	Mound	-
38	Wat Don Klaeu Ban Du, Du, Rasisai, Srisaket	409585.2004	1703613.4010	2,500-1,500 BP to the century of 13 <sup>th</sup> AD	Moated site	Village and Salt making
39	Non Ban Wan Ban Wan, Wan Kham, Rasisai, Srisaket	412828.0000	1700032.0000	The century of 6 <sup>th</sup> to 13 <sup>th</sup> AD	Moated site	Village
40	Muang Khong Khok Ban Lub Mok, Muang Khong, Rasisai, Srisaket	411385.2094	1697613.3620	The century of 6 <sup>th</sup> to 13 <sup>th</sup> AD	Moated site	Town
41	Non Nong Raeu Ban Bak Raeu, Muang Khong, Rasisai, Srisaket	410935.2075	1700063.3780	The century of 12 <sup>th</sup> - 13 <sup>th</sup> AD	Mound	-
42	Non Ban Nai Ban Kaen Noi, Muang Kaen, Rasisai, Srisaket	418914.6000	1694095.6900	-	Mound	-

Table 3 Continued.

Site no.	Site	location	Co-ordinate system		Age (BP)	Characteristics	Category
			UTM (47P)				
			E	N			
43	Gu Ban Wan	Ban Wan, Wan Kham, Rasisai, Srisaket	412132.0600	1699512.9700	The century of 8 <sup>th</sup> – 10 <sup>th</sup> AD	Mound	Sanctuary
44	Don That	Ban Phi Phuan, Khowang, Khowang, Yasothon	427094.0000	1699632.0000	The century of 16 <sup>th</sup> – 17 <sup>th</sup> AD	Mound	Sanctuary
45	Non Jan Rang	Ban Por, Khowang, Khowang, Yasothon	426065.0000	1699912.0000	The century of 13 <sup>th</sup> – 14 <sup>th</sup> AD to 16 <sup>th</sup> – 17 <sup>th</sup> AD	Mound	Village (?)
46	Sra Nong Ta Phan	Ban Lao Noi, Khowang, Khowang, Yasothon	426150.0000	1697181.0000	The century of 16 <sup>th</sup> – 17 <sup>th</sup> AD	Pond	-
47	Ban Phi Phaun	Ban Phi Phuan, Khowang, Khowang, Yasothon	428400.8600	1699739.7800	The century of 8 <sup>th</sup> – 10 <sup>th</sup> AD	Mound	Sanctuary
48	Dong Noi	Ban Phi Phuan, Khowang, Khowang, Yasothon	428470.3181	1699955.3712	The century of 8 <sup>th</sup> – 10 <sup>th</sup> AD	Mound	Sanctuary
49	Non Lak Sae	Ban Khu Muang, Khu Muang, Maha Chanachai, Yasothon	411797.2195	1717035.4847	The century of 13 <sup>th</sup> – 14 <sup>th</sup> AD	Mound	Sanctuary
50	Non That	Ban Samrong, Khu Muang, Maha Chanachai, Yasothon	410215.2086	1714246.4678	The century of 13 <sup>th</sup> – 14 <sup>th</sup> AD	Mound	Sanctuary

Table 3 Continued.

Site no.	Site location	Co-ordinate system UTM (47P)		Age (BP)	Characteristics	Category
		E	N			
51	Wat Pa Sai Thong Kud Nam Sai, Kud Nam Sai, Khowang, Yasothon	430712.4400	1705959.2700	The century of 10 <sup>th</sup> – 13 <sup>th</sup> AD	Mound	Sanctuary
52	Ban Phon Muang Ban Phon Muang, Fa-Huan, Khowang, Yasothon	436218.5000	1693328.7900	The century of 12 <sup>th</sup> – 13 <sup>th</sup> AD	Moated site	Village
53	Ban Khon-Kham Ban Khon-Kham, Khon-Kham, Yang Chum Noi, Srisaket	431089.0000	1686226.0000	A.D. 984 or the century of 10 <sup>th</sup> AD	Moated site	Town
54	Ban Tum Ban Tum, Kud Nam Sai, Khowang, Yasothon	429227.3700	1704950.2600	2,500-1,500 BP	Mound	Village



**Figure 50** The 54 archaeological sites of prehistory and history located in the study area.

#### 4.2 Sand splay and archaeological site structures from GPR survey

The most of sand splays were surveyed at the distal part. Splay height decreases from proximal to distal area with 10 meters gradually in the longitudinal direction. In transverse direction, the center of wind-blown splays is 2-3 m higher than the two-side margins. The GPR survey was applied at Site 1 where the meandered belt, a fluvial feature, is dominantly located on the center of sand splay from aerial photo interpretation. This area is relatively flat. Grain size of the surface sediments is similar in the whole area. At Site 2, the interdune area is adapted. It locates between floodplain and aeolian dune similar to a linear dune. Finally, Site 3 is relatively flat similar to Site 1 which the grain sizes of the surface sediments are medium to fine sand in the whole area (Figure 51). Furthermore, the archaeological site was applied by GPR survey at Site 4. The site is elevated as a mound in circular-shaped site higher than about 2 meters surrounding with moats. The potsherds are commonly discovered on the surface of mound (Figure 52).



Figure 51 Area of GPR survey run on 3 sites of sand splays.



Figure 52 Area of GPR survey tracked on Site 4 in direction of the west to the east or from the center of mound to the moat.



#### 4.2.1 Radar facies and radar stratigraphy

Facies are characterized by a reflection pattern. In this study, they are produced by a sedimentary sequence or structure of sub-environment under aeolian splays. They reflect various shapes depending on electromagnetic properties of water distribution on surface and in subsurface as well as subsurface sedimentary architecture. Moreover, their depositional environment derived from radar images is defined as radar stratigraphy. To interpret the depositional environments, the characteristics of radar facies can provide the uniform reflector configurations depending on sedimentary structures in subsurface. In this survey, 6 radar facies have been identified (Figure 53).

##### 1) *Facies I: inclined reflections (IA, IB and IC)*

This facies is characterized by a set of dipping reflections at angles between  $19^{\circ}$  and  $30^{\circ}$  up to a maximum of  $40^{\circ}$ . They are mainly presented all sites, especially in longitudinal sections. The dip is parallel relatively to the direction of wind-blown or water flow. Facies of IA and IB commonly appear with sub-horizontal base which exhibit a tangential geometry. In addition, the inclined reflections show occasionally in a len-shaped set in sigmoidal and oblique that it is termed as facies IC (Figure 53-A).

It can be interpreted that these facies represent the migration process of sediments which are interpreted as slipface and lateral migration following scroll bar, point bar and compound bar, as well as the saltation process or inland-migration dunes of aeolian deposits. They are resulted in lateral accretion (e.g. Bristow et al., 2000; Pedersen and Clemmensen, 2005; J. Best et al., 2006; Okazaki et al., 2015).

##### 2) *Facies II: free-discontinuous reflections (IIA and IIB)*

Discontinuous reflections represent a chaotic-shaped to free-reflections in gentle dipping with low angle of  $9^{\circ}$  to  $20^{\circ}$  (Figure 53-IIA). The convex upward reflections are composed of discontinuous facies in distance 5-10 m and 0.7-1.5 m thickness, which is termed as facies IIB. They are generally observed in transverse and longitudinal sections.

It can be interpreted that discontinuous reflections can be indicated to a variety of deposit types. They are interpreted as crudely stratified to massive beds of fluvial or aeolian dune migration. This characteristic is suggested that the reflection-free configuration affects to lithologically undifferentiated sediment (Pedersen and Clemmensen, 2005: 64).

3) *Facies III: set of discontinuous reflections (IIIA and IIIB)*

Set of discontinuous reflections of this facies group represent the Isolated and mound-shaped or random reflections. They are approximately about 2 to 8 m in width and 0.6-5.2 m in thickness. Facies III is occasionally observed in transverse sections. Sometimes, their reflections are high-angle convex-upward (e.g. Figure 53-IIIA).

It can be interpreted that these facies have been interpreted as crudely stratified to deposits related to 3D dunes or small-scale of incipient unit bars in fluvial process and features of adhesion lamination (i.e. adhesion wart) in aeolian sediments, in particular to mound-shaped isolate of IIIB facies. The convex-upward reflections of IIIA facies may be considered as massive deposits or a high density of sources such as buried logs (Hickin et al., 2009).

4) *Facies IV: horizontal to sub-horizontal reflections (IVA and IVB)*

Horizontal reflections are continuous and parallel, rather than undulating. These reflections can be traced for tens of meters, but less than <65 m of IVA facies and <20 m of IVB facies in sub-horizontal reflections. They commonly appear in both of longitudinal and transverse sections, but more than in transverse section. At Site 2, the facies of horizontal and sub-horizontal reflections are observed along the GPR profile of Line 1.

It can be interpreted that the IV facies can be formed as stacks of vertically accreted plane beds on bar surfaces (Hickin et al., 2009; Okazaki et al., 2015). In fluvial process, Lunt et al. (2004) proposed that the subparallel nature of this reflection was tended to be the successive bedload sheets deposition, as well as overbank deposits in vertical accretion (Lunt and Bridge, 2004). Moreover, the occurrence of sub-horizontal stratified sediments in the area identified in all GPR

lines at 2-3 m depth is interpreted as groundwater table (Figures 54 and 55). In aeolian process, Pedersen et al. (2005) suggested that the appearance of horizontal reflections is indicated the changes in sedimentary texture representing aeolian sand-sheet environments. Kocurek and Fielder (1982) proposed the adhesion lamination structure that is may relate to the IV facies, especially the adhesion plane bed which it appears in parallel lamination. Their appearance is obvious on GPR profile of Line 1 at Site 2 (Figures 56-57).

5) *Facies V: facies assemblage with channel-shaped lower boundary*

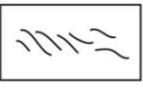
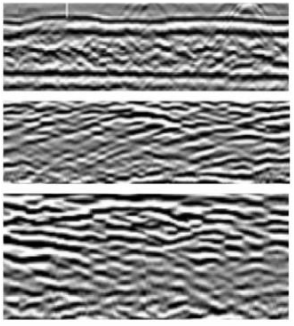


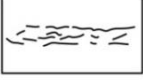
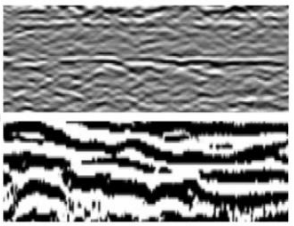


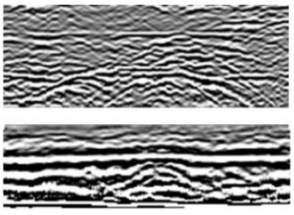

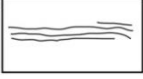
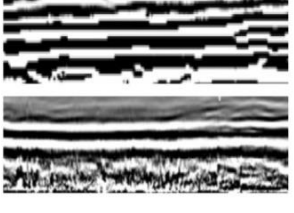




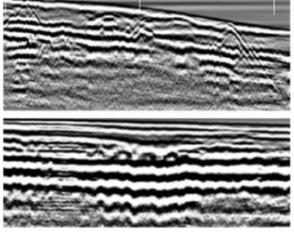
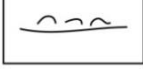
Facies V is interpreted as the small- to large-scale of channel-shaped concave-upward reflections. The basal channel-shaped reflections significantly erodes adjoining reflections of the fills includes facies I, II, III and IV.

It is suggested that this facies is commonly considered to represent channel-fill deposits which are a major architectural element of fluvial systems (e.g. Bristow et al., 1999; Bridge, 2003; J. Best et al., 2006; Hickin et al., 2009; Okazaki et al., 2015). It can be founded in both of longitudinal and transverse sections, in particular to GPR profiles of Line 1 at Site 1 and Line 2 at Site 3 (Figures 54 and 56). Facies V is interpreted as fills of a main channel or a cross-bar channel, as well as a scour fills of overbank process.

6) *Facies VI: diffractions of parabola-shaped reflections (VIA and VIB)*

Facies VI is parabola-shaped steeping convex reflections and multiple small point anomalies in the VIB facies. This radar facies is observed at Site 4 where is a moated site of archaeology and Line 2 of Site 2 discovering the archaeological evidences on surface.

The VI facies are considered to represent discrete items of material culture (Duke et al., 2016). At Site 4, this radar facies is obviously archaeological features due to the distribution of potsherds on surface of GPR line (Figure 57).

Radar facies	Description	Dimension (m)			Interpretation	Example	
		thickness	length	width			
I	A 	Low Inclined in sigmoidal reflections. Their dipping are the angles 19° and 30° up to a maximum of 40°	0.6 - 1.2	-	3.0 - 7.0	Slipface and lateral migration of sediments including scoll bar, unit bar and compound bar	
	B 	Steeply Inclined dipping from top to bottom in tangential reflections	1.2 - 2.0	-	2.0 - 6.0		
	C 	Lens shape, set of inclined in sigmoidal and oblique reflections	1.2 - 2.3	-	3.0 - 5.0		
II	A 	Discontinuous, chaotic-shaped to free reflections	-	-	-	Crudely stratified to massive beds of fluvial or aeolian dune migration (saltation process of aeolian sand).	
	B 	Discontinuous, inclined to low-angled of 9° to 20° and undulating reflections	0.7 - 1.5	5.0 - 10.0	-		
III	A 	Set of discontinuous, convex reflections	3.5 - 5.2	-	3.0 - 8.0	Crudely stratified to massive beds of 3D dunes, adhesion wart, small bars or buried objects.	
	B 	Isolated, mound-shaped reflections	0.6 - 1.2	-	2.0 - 3.0		
IV	A 	Continuous, hummocky; horizontal and parallel reflections	2.0 - 4.0	<65	-	Vertical accretion in overbank deposits and water table in reflector of continuous, horizontal isolated facies. Adhesion lamination of aeolian deposits	
	B 	Discontinuous, horizontal and parallel reflections	1.0 - 2.5	<20	-		
V		Small to large-scale of channel-shaped concave-upward reflection including the assemblage of facies I - IV.	0.6 - 5.0	-	4.0 - 15.0	Channel fills or scour fills deposits	
VI	A 	Diffractions parabola-shaped steeping convex reflections	0.0 - 0.3	-	-	The buried objects as archaeological evidences including potsherds, human remains and other artifacts.	
	B 	Set of small mound-shaped reflections	0.7 - 1.0	-	5.0		

**Figure 53** The characteristics and depositional sub-environments of the key radar facies.

#### 4.2.2 GPR data interpretation based on radar facies and radar stratigraphy

For this study, the radar stratigraphy reveals sub-environments in the past which was divided into two main sequences. The sequences are composed of fluvial deposits and aeolian deposits at Site 1-3 and cultural deposits are revealed in GPR profile of Site 2 and Site 4. Almost GPR data indicates that the aeolian environments are underlain by fluvial environments. They are bordered by remarkable radar stratigraphy and natural break in radar facies.

##### Site 1

Fluvial environments from Site 1 are divided into 2 periods using 200 MHz in order to consider the paleochannel underlain the aeolian sand. This site was tracked across meandered scar of paleo-channel at Line 1. The results indicate that fluvial environment of the first period – Period A (2.0-6.0 m depth) is composed of channel fills with vertical accretion in which it is interpreted as overbank flow of channels. Moreover, the radar facies show continuous small concave-upward lower boundary at between 95-130 m and next to continuous horizontal parallel and gently inclined convex upward reflections which may be considered to erosional surface or mid-channel bar founded generally in meandering channel (e.g., Bristow, 1993; Bridge et al., 1998; J. L. Best et al., 2003). The second period of fluvial deposits – Period B (0.6-2.5 m depth) consists of radar facies similar to Period A. The lateral accretion indicated channel migration is more visible; for example, the facies of inclined tangential reflections at 255-285 m of point bar or side bar deposits of the channel. Next, the uppermost layer is aeolian deposit – Period C recorded at 0.0-0.6 m depth along Line 1. The facies reflection is invisible without internal structure. Thus, it is considered to be “sand splay layers” since the grain size sediments appeared on surface is characterized by fine sand, well sorted and homogeneous, structureless that it is similar to pale yellow color loess (Boonsener, 1991). However, internal structure of sand splay is invisible at Site 1 because GPR line survey is closed to the end of sand splay formation in which downwind is slacken so that dune structure is not formed or unclear structure (Figure 54).

### Site 2

The internal structure of sand splays is clearly visible at Site 2 located on low terrace of the Chi River. The GPR data using 200 MHz was carried out from two lines in order to differentiate aeolian sand and floodplain. Line 1 was tracked in the northwest to southeast direction, in contrast to Line 2 where GPR was assigned in the northeast to southwest. Both lines crossed at 39 m and 162 m distance of Lines 1 and 2, respectively. The characteristics of this splay are similar to the linear dune. It is characterized by their length, relative straightness, parallelism, regular spacing, and low ratio of dune to inter-dune areas (Lancaster, 1982b). Its ridge is parallel to the direction of the prevailing winds that forms in place where the sand supply is limited. The radar stratigraphy shows Period A at the bottom of GPR profile between 2.50-5.00 m depth. It is defined as bedrock. Next, the uppermost layer – Period B is defined as fluvial flood deposit from 5.00 to 2.00 m depth. It is belonged to the IV facies of horizontal and sub-horizontal reflections. They indicated that these characteristics are vertical accretion by flood events. However, the channel fills and lateral migration slightly appeared. They are recorded at 23 to 63 m distance and 2.50-4.00 m depth of Line 1, in contrast to Line 2. The lateral migration of fluvial deposits is obvious in 2.50-4.50 m depth at 30-60 m. The last-upper layer of GPR profile is the aeolian environment at depth 0.00-2.50 m. Radar facies of IA, IIA and IIB are of aeolian process of sand splays. They are identified as saltation process during the sediment was blown along Line 1 and 2, as well as vertical grainfall of sediments after deposition that it might be related to the adhesion structure. At Line 1, the adhesion wart is predominant at 30-40 m distance. This appearance indicates that the strong paleo-wind had frequently shifted direction (Kocurek and Fielder, 1982: 1230-1231). Indeed, the paleo-wind of NE-SW direction is the major influence of appearance and characteristic of sand splays. At distance of 10-65 m, the radar facies of Line 2 is significantly visible of grainflow and grainfall deposit that it is defined the direction from northeast to southwest. In addition, the environment change is revealed at the last distance of Line 2 or 160-195 m distance. It illustrates the VIA facies in parabola-shaped steeping convex reflections that it is defined as cultural deposits that the archaeological evidences are discovered on the surface.

### **Site 3**

Site 3 using 400 MHz was carried out from two lines due to distinctive internal structure of sand splay at the shallow. Line 1 was tracked in the southwest to northeast direction, in contrast to Line 2 in the southeast to northwest. Both lines intersect at 90 m and 30 m distance of Line 1 and 2 respectively. GPR data from each line reveal radar facies of fluvial features similar to Site 1 which is considered to be meandering channel with mid-channel bar. Sand splay layer is also found in the upper layer at 0.0-0.6 m depth without internal structure. It is interesting that the radar reflection at 33-57 m distance of line shows mound-like structure in apparent inclined reflections between 34-44 m and 49-56 m distance, in contrast to 46-49 m distance. However, the signal is lost at depth 1.5-2.5 m, but it becomes obvious in the upper layer at depth 0.6-1.2 m. Signals are composed of gently inclined reflections in two directions. These facies sets are likely to be a channel feature. Therefore, these features are needed to be proved by coring (Figure 59). Radar facies from Line 2 showed meandering channel due to the I and V radar reflections of inclined sets, trough-shaped, and small to large scale of concave-upward lower boundary. As well, the mid-channel bars can be founded in this line. Set of reflections in mound-shaped underlain layer of concave-upward shaped can be interpreted as channel fills; for instance, the feature likes a channel bar in 1.2-2.5 m depth is at 30-50 m of line 2 (e.g., Bridge et al., 1998; Bridge, 2003). Notably, it is composed of sinuous-crested dunes in trough cross strata, ripples in small-scale cross strata and planar strata at upper stage plane beds. Best et al. (2003) described as the migration of large sinuous-crested dunes, but Bridge (2009) suggested that dunes are typically 3 to 4 m high in the deeper parts of the channels, but are 0.5 to 1 m high near bar tops (Bridge, 2009). As a result, the facies of Line 2 as mentioned earlier can be considered to be the bar top of channel bar that filled across-bar channels commonly in the upper-bar deposits (Bristow, 1993). However, the reworking aeolian sand may be related at next period. The channel features of Line 2 at 30-42 m distance are visible which are filled in trough-shaped reflections. This is similar to the blowouts of sand dune that the sand source from fluvial deposits was reworked by aeolian resulted to this character (Figure 59).

#### **Site 4**

Site 4 is a moated site in the study area that GPR survey using 200 MHz was carried out in only line - Line 1 with 200 m distance from the center of mound to the moat in W-E direction for appropriate investigation of GPR in ADL or salt dome in more depth. The radar facies show the noises or lost signals along Line 1 that it illustrates the repeated signal between 1.50-3.00 m depth from surface and loses at the below. These anomalies indicated that the cultural deposits affect to the reflections of signal before showing profile data on receiver. The characteristics of this reflection are similar to GPR data of Ban Non Wat at the Upper Mun Valley where was applied by Duke et al. (2016). As well, the VI facies of parabola-shaped steeping convex interpreted as archaeological materials appear along Line 1, especially at surface level. At distance of 175-180 m, it reveals radar facies of VIB in continuous small circular-shaped mound that this feature may be related to archaeological evidences at depth of 3.50 m (Figure 60). Finally, the obscure stratigraphy of GPR profile was revised by coring.



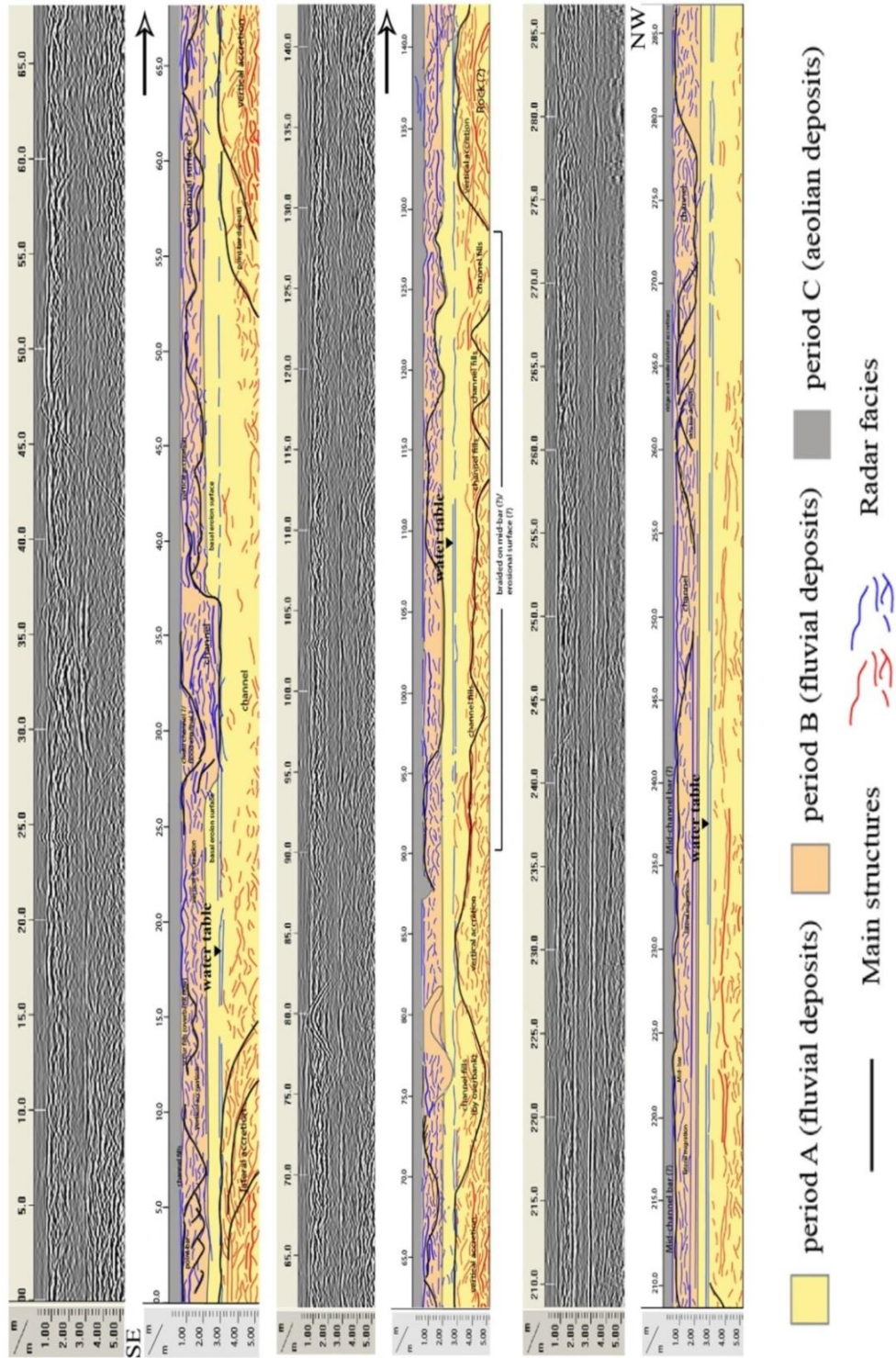


Figure 54 GPR interpretation of Line 1 at Site 1 showing the fluvial stratigraphy in two sequences overlain by aeolian deposit of sand spays.

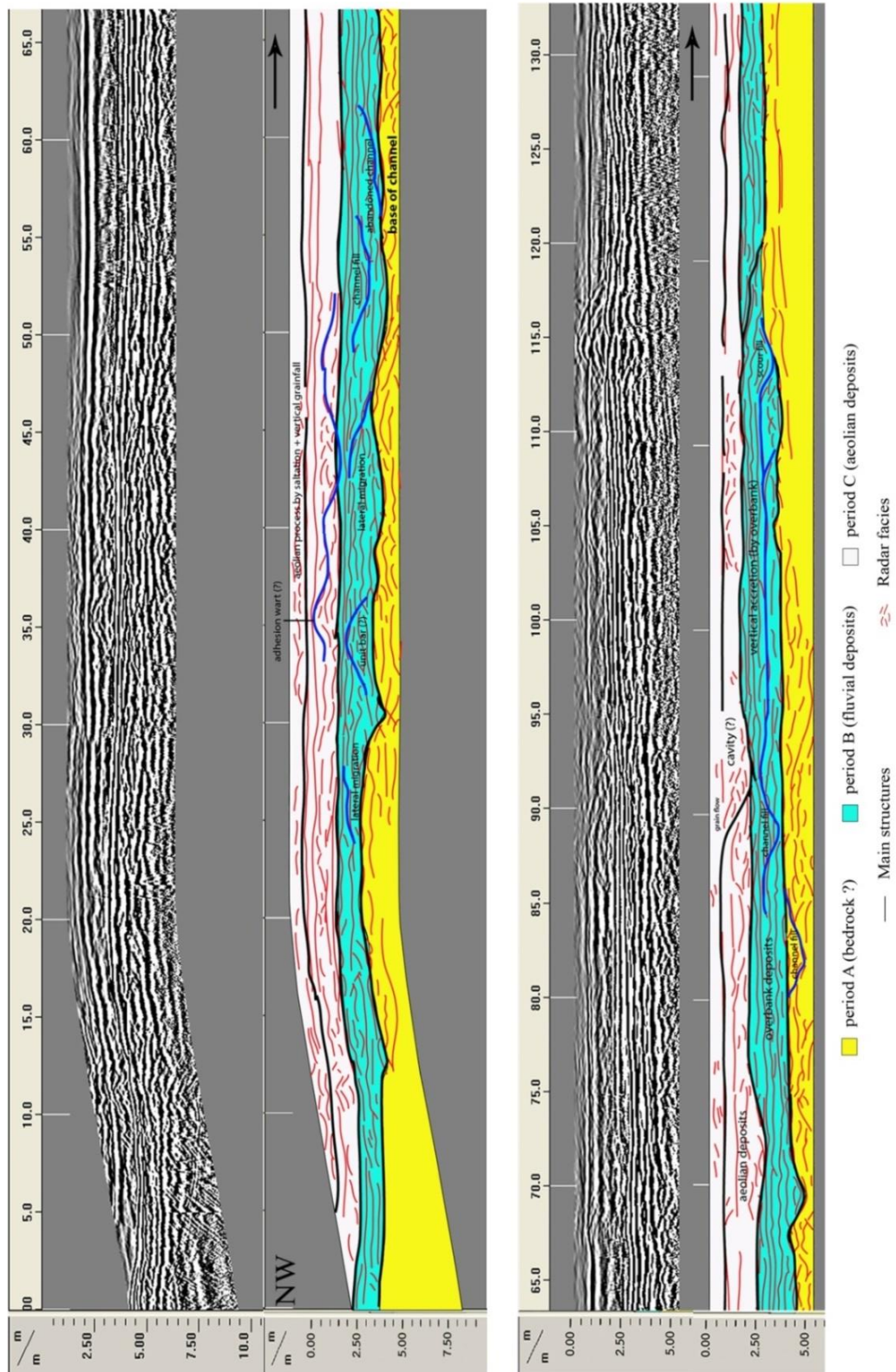
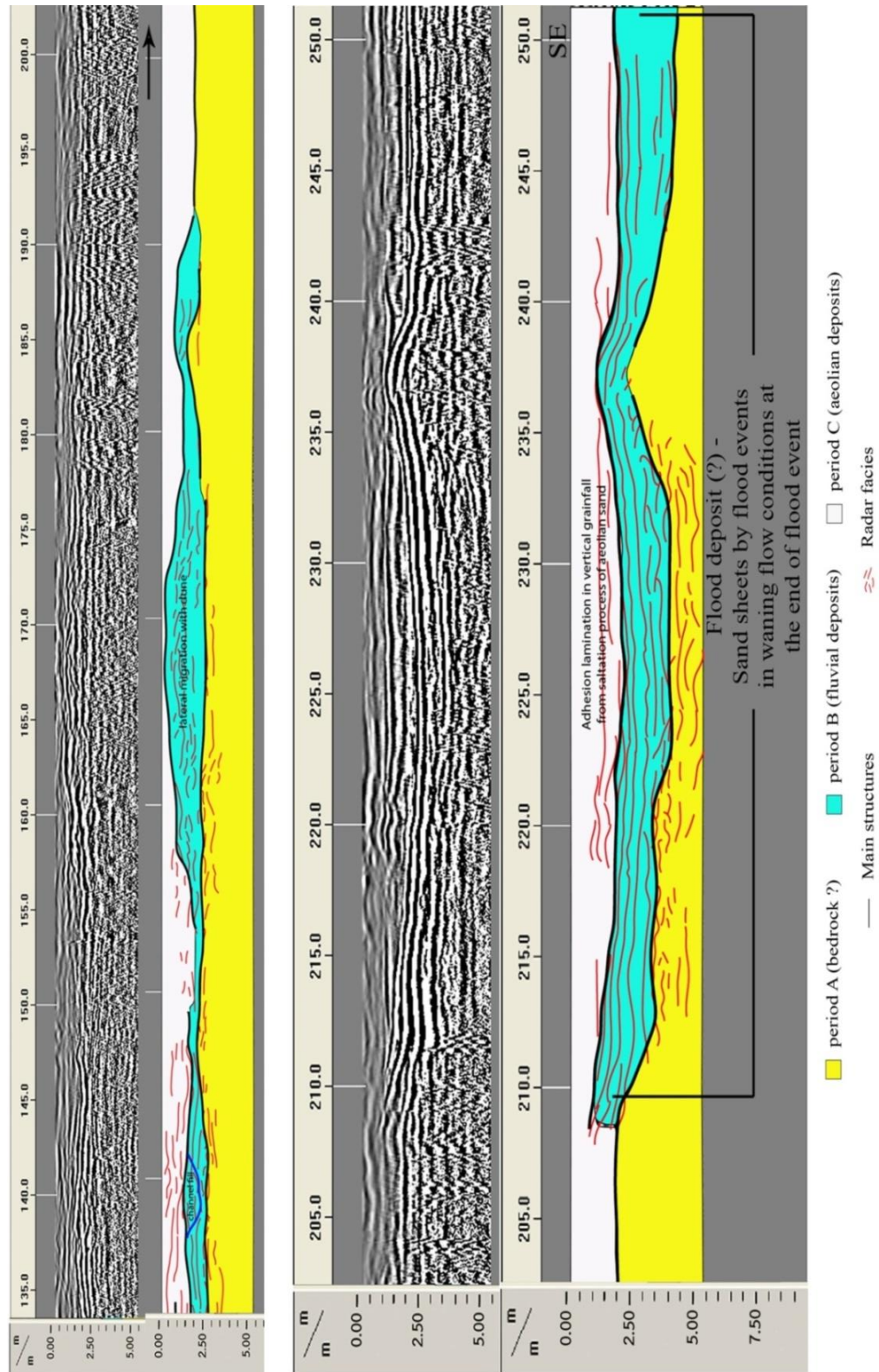
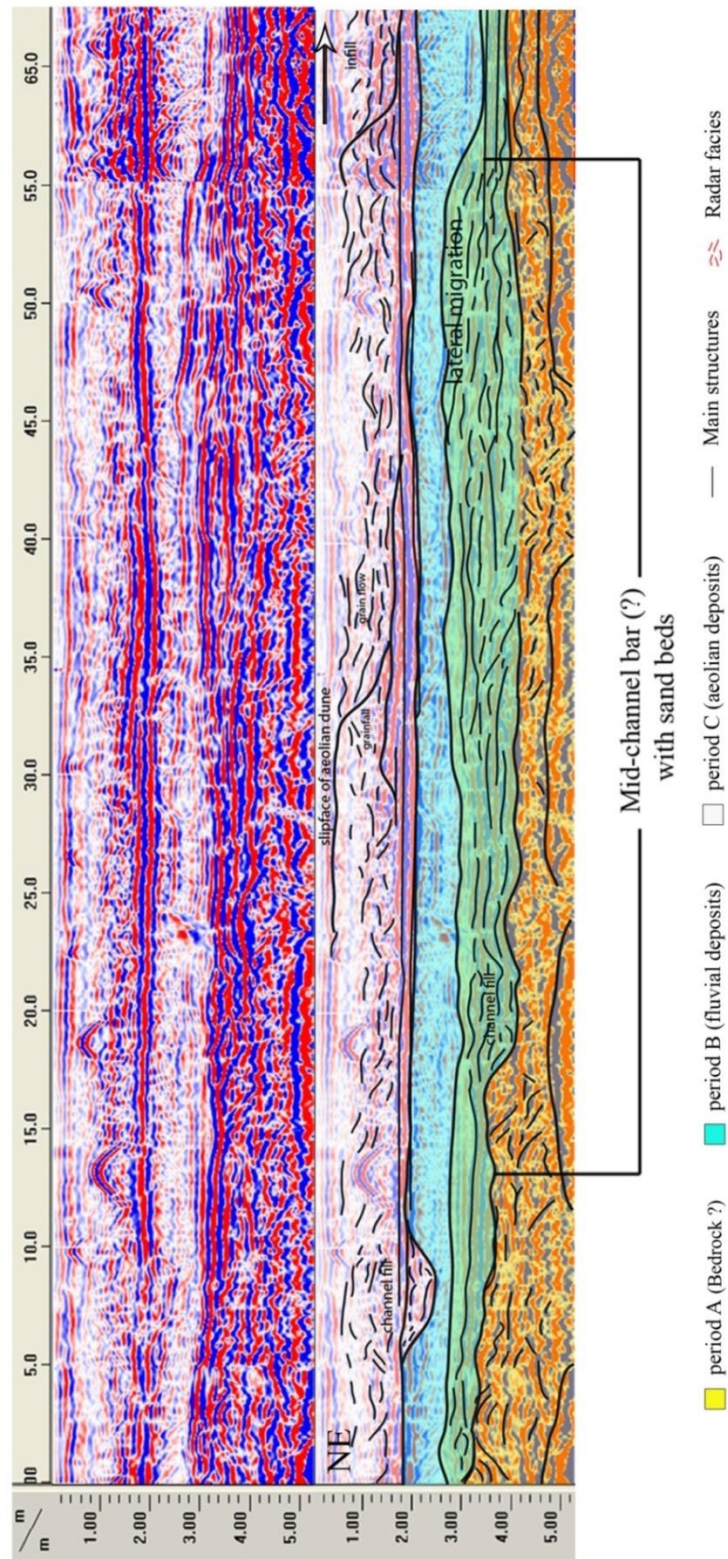


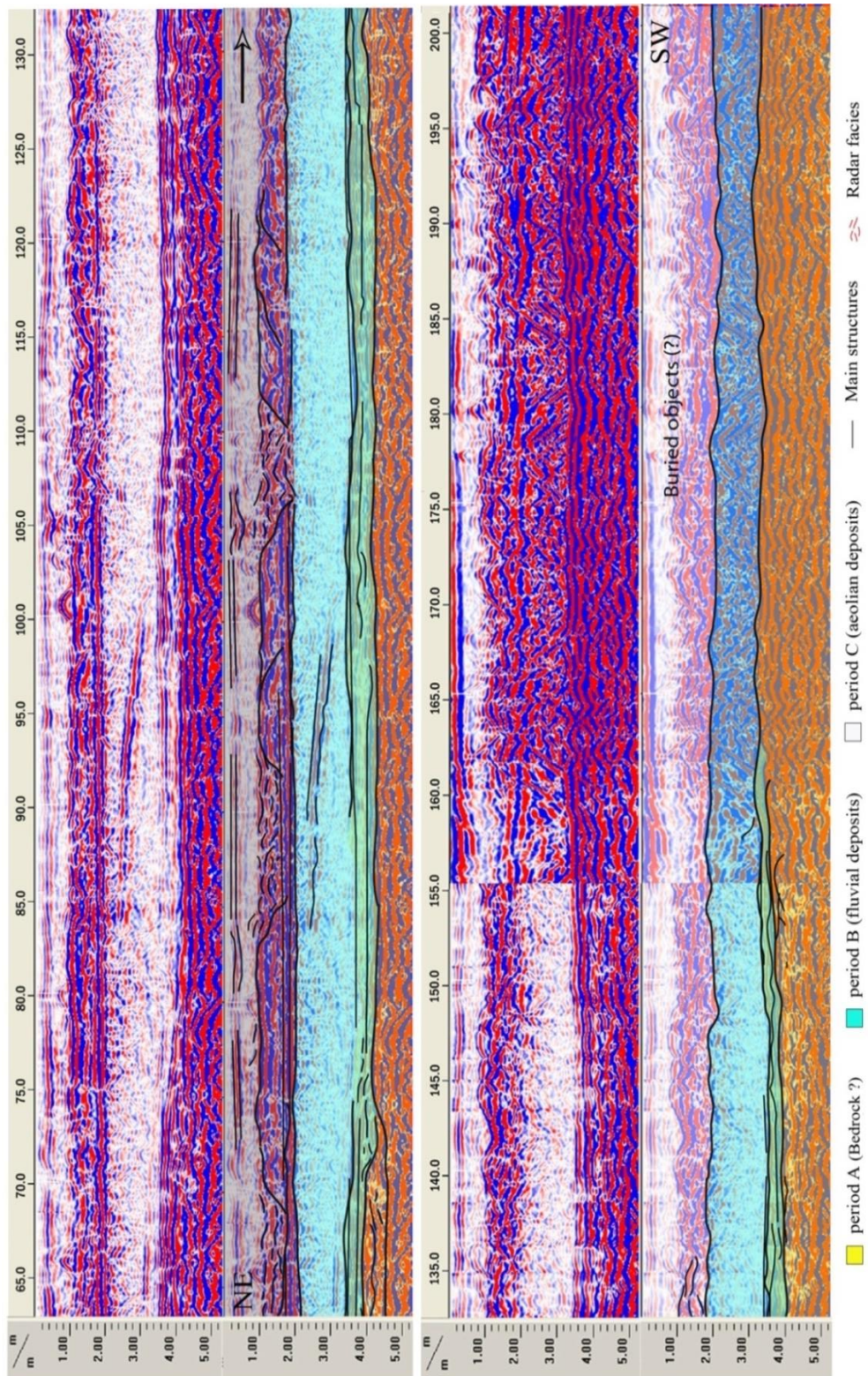
Figure 55 GPR interpretation of Line 1 at Site 2 showing process of sand splays between 0.00-2.50 m depth underlain by flood deposits of fluvial process.



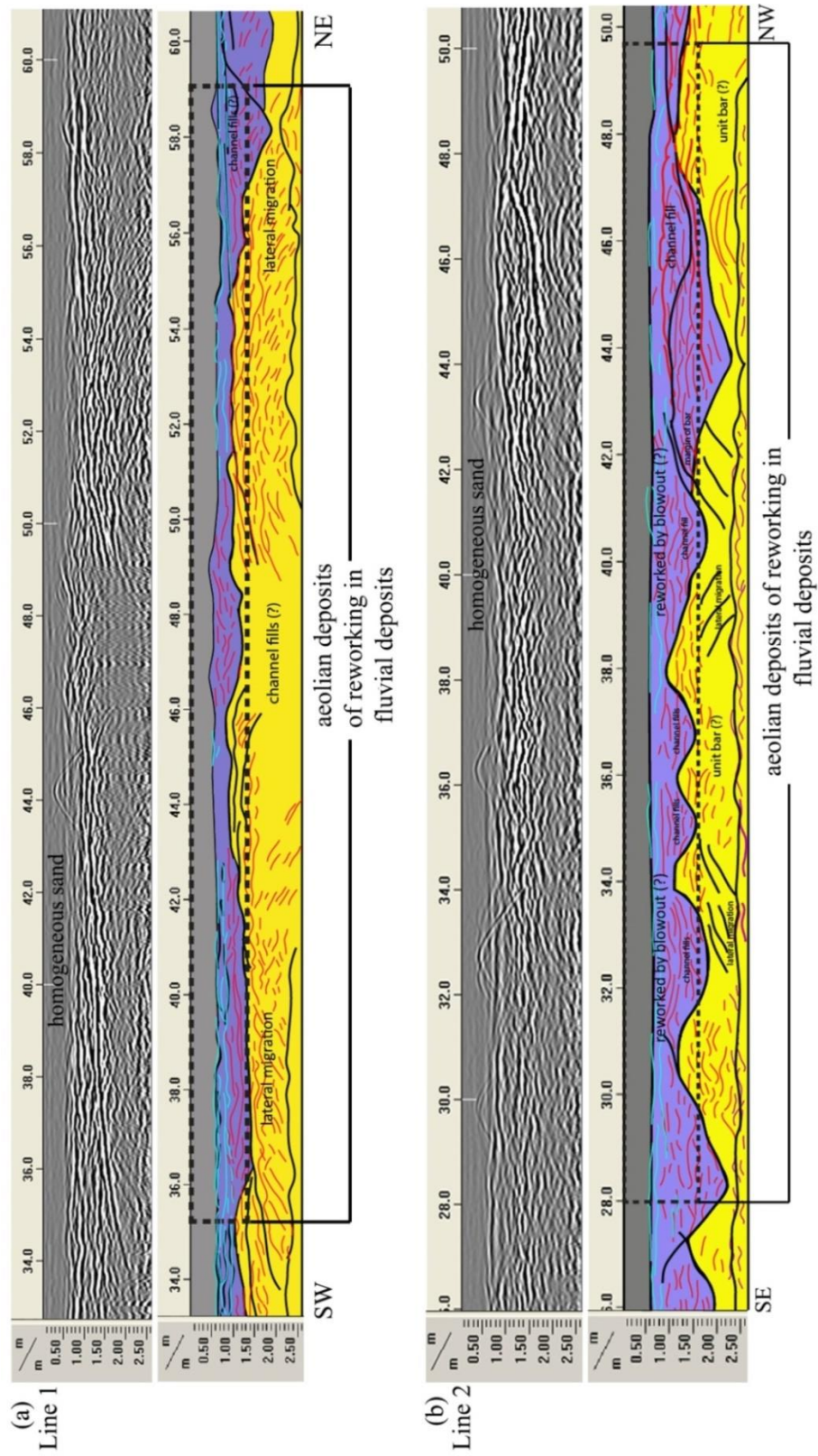
**Figure 56** GPR interpretation of Line 1 at Site 2 showing process of sand splays between 0.00-2.50 m depth underlain by flood deposits of fluvial process.



**Figure 57** GPR interpretation of Line 2 at Site 2 showing process of sand splays between 0.00-2.00 m depth underlain by fluvial process of lateral migration.



**Figure 58** GPR interpretation of Line 2 at Site 2 showing process of sand splays between 0.00-2.00 m depth and cultural deposits at 160-195 m distance in the VIA facies as buried objects.



**Figure 59** GPR interpretation of Line 1 and 2 at Site 3 showing the aeolian reworking of deposited sand in channel fills being a pre-environment in this area.

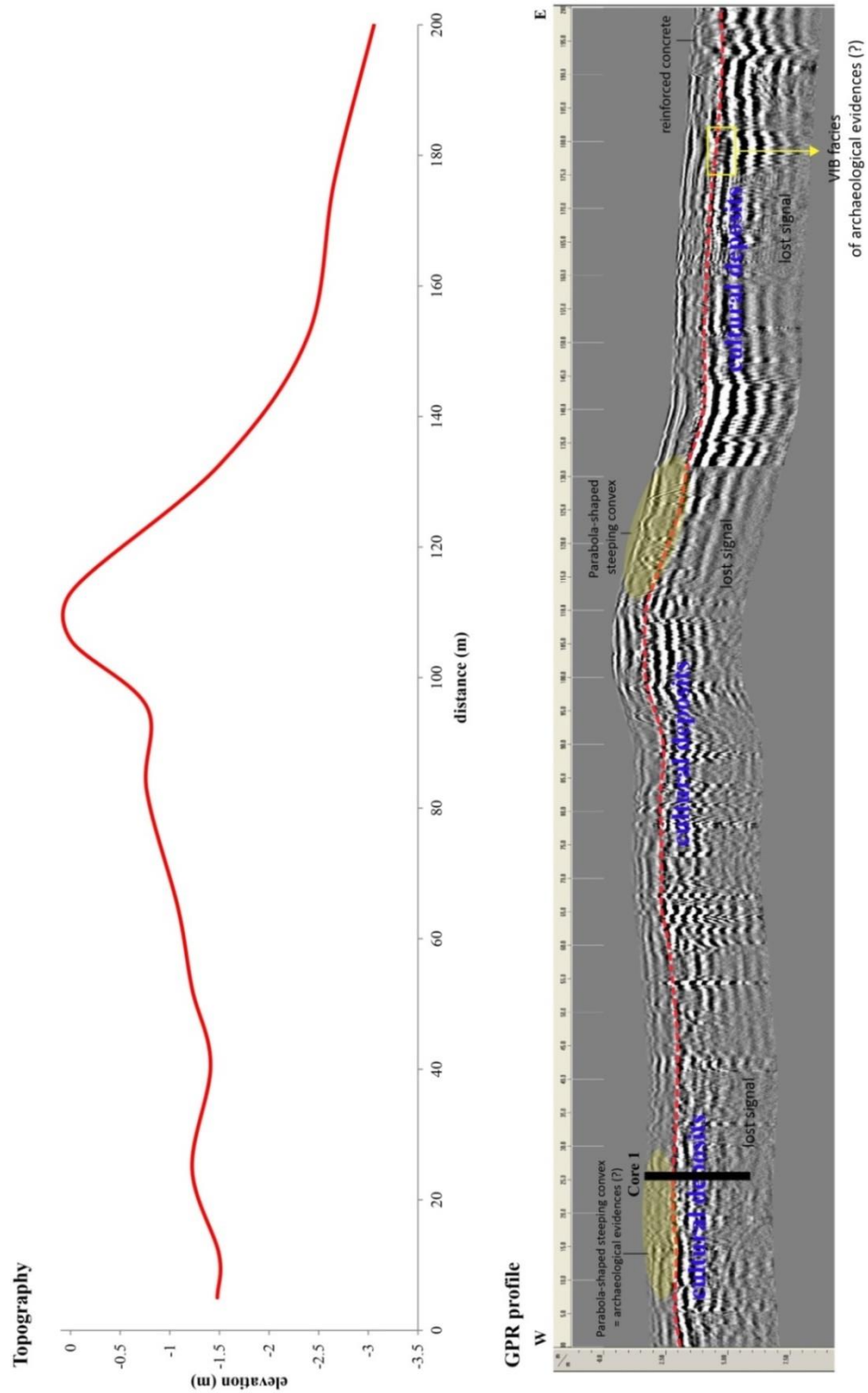


Figure 60 GPR interpretation with elevation of Site 4 indicated that the cultural deposits affect to the reflections of signal.

### 4.3 Grain size analysis from auger coring based on GPR interpretation

#### 4.3.1 Grain size distribution

Results of grain size distribution were obtained from 46 samples collected in every range of 20 cm depth from surface. Based on GPR profiles, they need to be cored and analyzed for explanation of the mechanisms operative during transportation and deposition. The grain size distribution of the sediments from the four sites termed as S2C1, S3C1, S4C1 and S4C2 are shown in Figures 61 and 62. They were calculated with textural parameters such as mean size, standard deviation (sorting), skewness and kurtosis. In addition, the frequency and cumulative plots of grain size distribution in each aeolian environment (S2C1 and S3C1) are shown in Figure 63, as well as S4C1 and S4C2 in floodplain environment (Figure 64) that these calculations were introduced by Udden and Wenworth (1922). They can indicate to the three main sediment transport patterns following suspension, saltation and traction processes (Visher, 1969).

##### 1) Grain-size parameter of sand splays

The mean size of sand splays is obviously homogeneous of fined-grain sands shown in Figures 4-13a, b. The four parameters in the  $\Phi$  (phi) measurement unit following mean size, sorting, skewness and kurtosis, as well as the water content in EC-20 ( $\text{m}^3/\text{m}^3$ ) are illustrated in the plot graphs. They indicate the similarity of lined-shape in each depth range. In S2C1, the ranges of the mean grain size are less varied from 1.90-2.14  $\Phi$  that the mean size increases at 20 cm depth from 1.90 to 2.06 showing the change of medium to fine-grained sand and slightly decreases at 120 cm depth, and again, it raises up at 180 cm depth. Sorting values are around 0.69-0.89  $\Phi$  (moderately sorted) and the skewness values quite change from 1.31 to 0.8 at 120 cm depth and increase to 1.32 at 180 cm, but all values are in the range of very fine-skewed. The kurtosis values tend to continuous decrease and significantly fall at ranges of 120-160 cm. Overall, the mean grain size are identified as fine-grained sand, the sorting values are moderately sorted, the skewness are very fine-skewed and the kurtosis values are indicated to extremely leptokurtic. The



depth of 120-160 cm showed the conditions and components of sediment being different from other layers (Figure 61).

The S3C1 results are similar to S2C1 due to the location on aeolian sand splay environments (Figure 62). However, the mean grain size values are more homogeneous showing between 2.2-2.3 phi (fine-grained sand) and the sorting values are stable. It is identified as moderately sorted. The skewness is in the range of very fine-skewed, but the slightly increase is found at 120-160 cm depth and decrease in straight at 180-260 cm depth. The kurtosis values are lessen from 3.6 to 3.1  $\Phi$  at 0-160 cm depth and raise up to normal values like the upper layer at 180 cm depth. Totally, the sand splay sediments are homogeneous that they are belonged to fine-grained sand, moderately sorted, very fine-skewed and extremely leptokurtic. The water content, moreover, is changed together with the four parameters. It tends to increase along the depth which is dominant at 2.00 m depth (Figure 61-62).

Figures 4 to 14 show the cumulative curves of S2C1 and S3C1 with OSL samples is indicated that the grain-size distributions are modestly differed among the resemble environments. At S2C1, the peak of mean size is in the range of medium sand identified as asymmetry in skewness and leptokurtic in kurtosis, and the cumulative curve reveals dominant size group and similar unimodal profiles representing the same sedimentary components. In contrast, S3C1 shows the peak of mean grain size holding at the range of fine sand and the distribution tends to be negative skewness, but the OSL samples are in the range of medium sand and normal skewness. This cumulative curve is similar to S2C1 indicated to unimodal frequency curve shapes. These curves reveal the transport patterns proposed by Visher (1969) including the traction population in very coarse sand and coarse sand before the medium to fine sand was the most of saltation population at peak. It rarely shows the suspension population in transportation.

## *2) Grain-size parameter of a moated site*

Despite, its GPR survey, a moated site was proved by hand auger in two sites following S4C1 (on the mound) and S4C2 (in the moat). The results in 4.0 m depth of S4C1 indicate that the graph of parameters are resemble in shape along the

depth. Indeed, the distinctive changes are presented at 220-380 cm depth with mottled sandy clay. The mean grain size are  $3.0-3.3\phi$  as very fine-grained sand until it had changed to  $2.7-2.9\phi$  of fine-grained sand at 240-380 cm depth. Sorting values are poorly sorted between  $0.9-1.1\phi$ , but they change to moderately sorted at the bottom layer of 380-400 cm depth. Conversely, the skewness values as very coarse-skewed reverse with mean size and sorting along the depth which the same kurtosis as skewness are shown by inversion with all parameters, except the level of 220-400 cm that it presents the similarity of trendline in mean size and sorting together with the water content values. The most of values are ranged to very to extremely leptokurtic (Figure 64). However, the pottery sherds were also discovered at 110-250 cm depth with silty sand that the graphs reveal the slightly change in sorting and skewness. The S4C2 results of 2.0 m depth illustrate that the S-shaped mean grain size are in the range of very fine to fine-grained sand ( $2.4-3.4\phi$ ) and the sorting (poorly to moderately sorted) was reversely differed at the level of 60-140 cm depth, but it likes the skewness (very coarse-skewed). The kurtosis is distinct obviously which it inverses with all parameters from 0 cm to 180 cm depth. Lastly, the plot graph of water content is strongly indicated that it may relate with the mean and sorting (Fig. 4-15b).

The cumulative curves of S4C1 and S4C2 are shown in Figure 66. The floodplain sediments from the mound (S4C1) indicate no dominant size group and similar bimodal profiles. Most of these cumulative curves transform into a linear shape, in contrast to sediments from the moat (S4C2). Their sediments were shown in S-shaped cumulative curves which appear the truncation points on the profiles such as level of 160-180 cm depth. On the other hand, the frequency probability illustrated to the bimodal profiles is similar to S4C1. These appearances are described that both of the mound and the moat might be processed by natural and human activities in the past reflected by disturbed sediments in sedimentary logs and other charts. Absolutely, this difference will be supported by presentation of scatter plots at next.

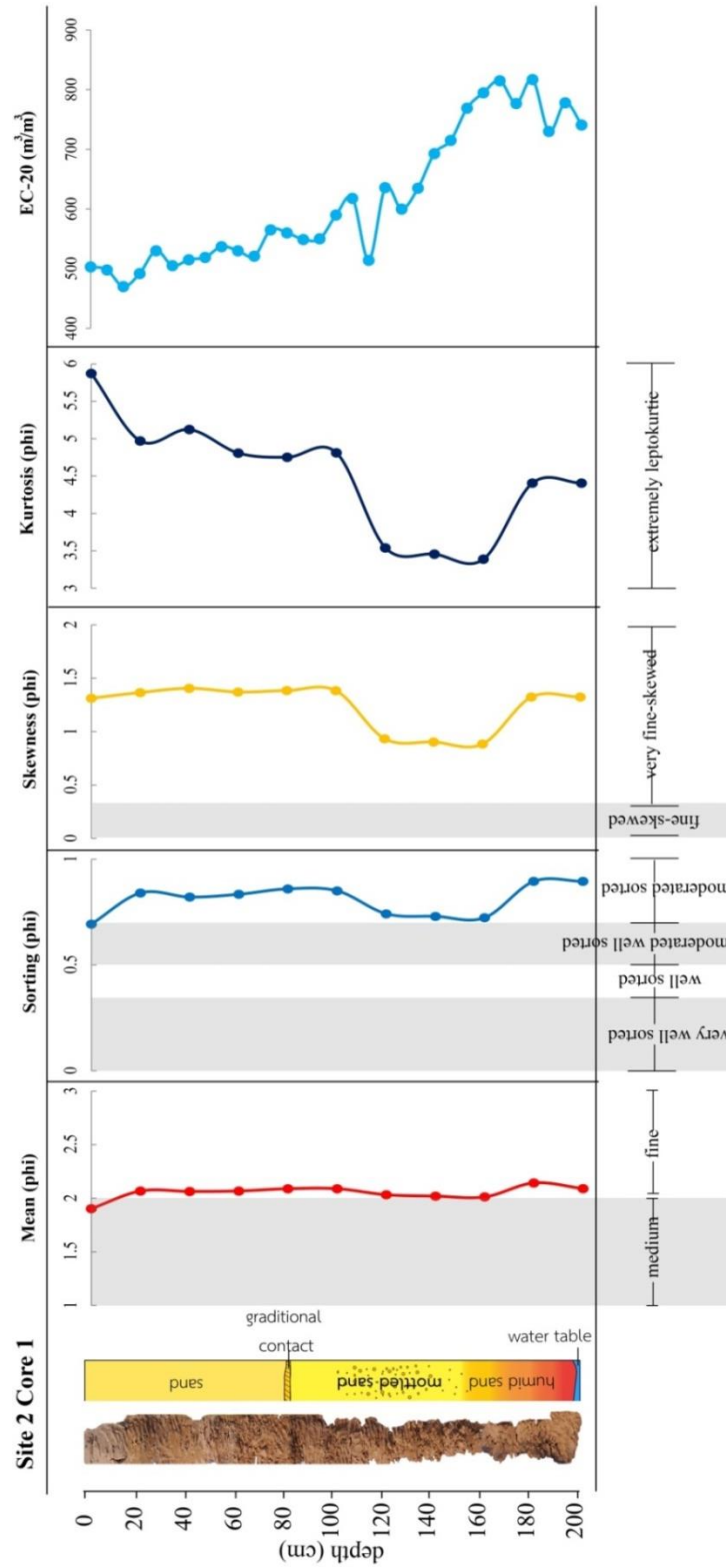
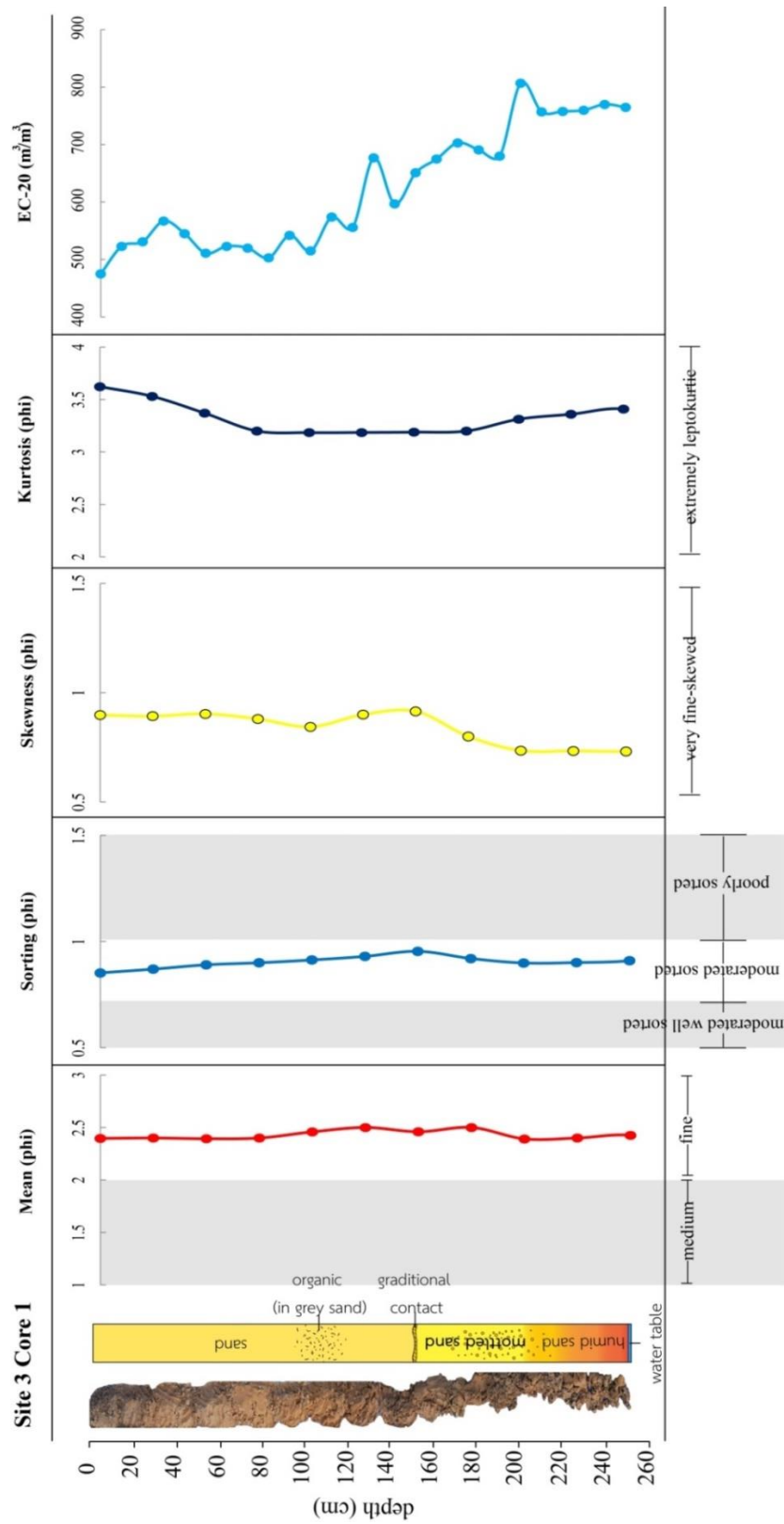
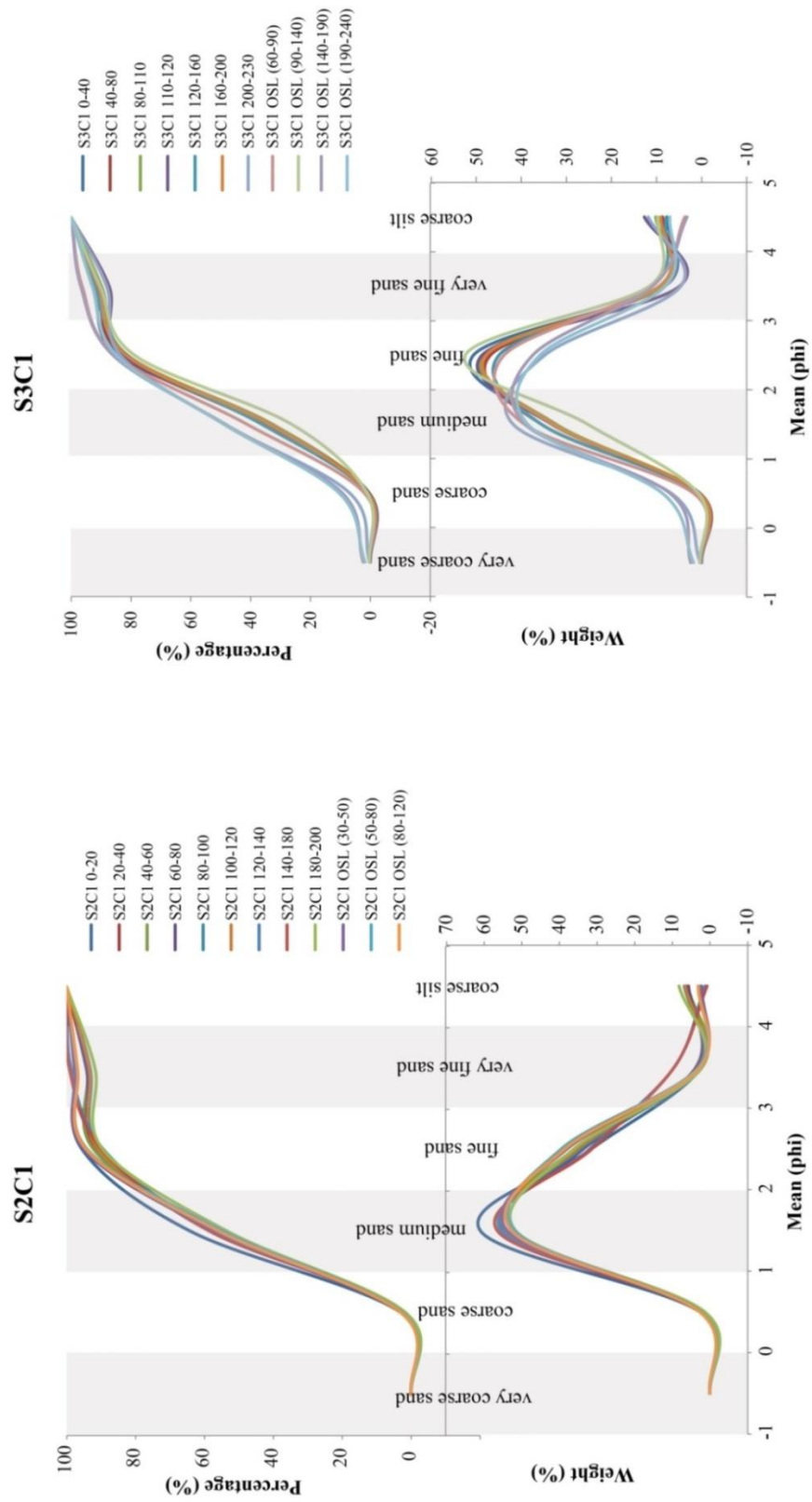


Figure 61 Grain size distribution of S2C1 identified as aeolian sand splays along with the calculated water content.



**Figure 62** Grain size distribution of S3C1 identified as aeolian sand spays along with the calculated water content.



**Figure 63** Cumulative probability and frequency curves of aeolian sediments at S2C1 and S3C1 showed resemble transported and deposited processes.

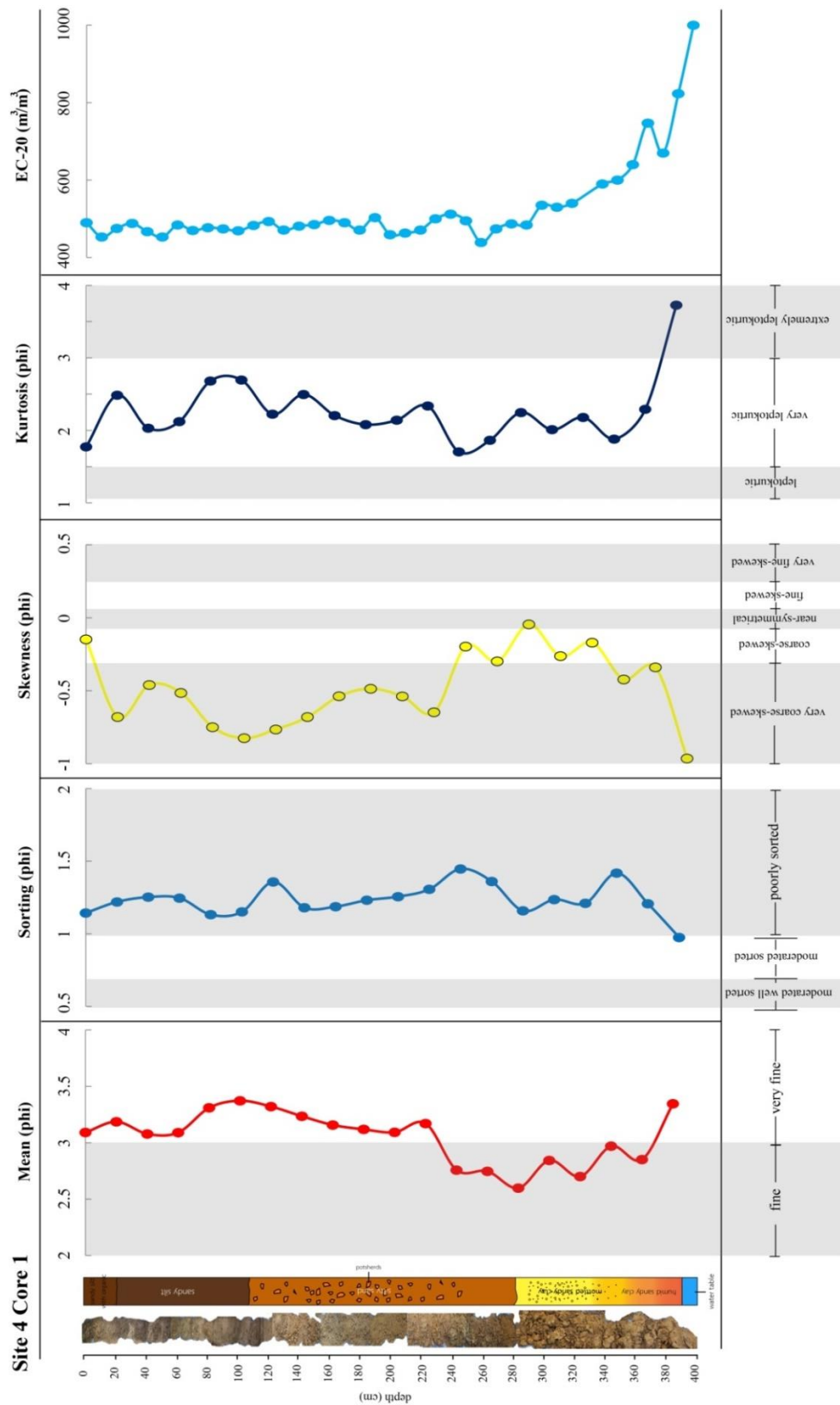


Figure 64 Grain size distribution of S4C1 identified as a mound at floodplain along with the calculated water content.

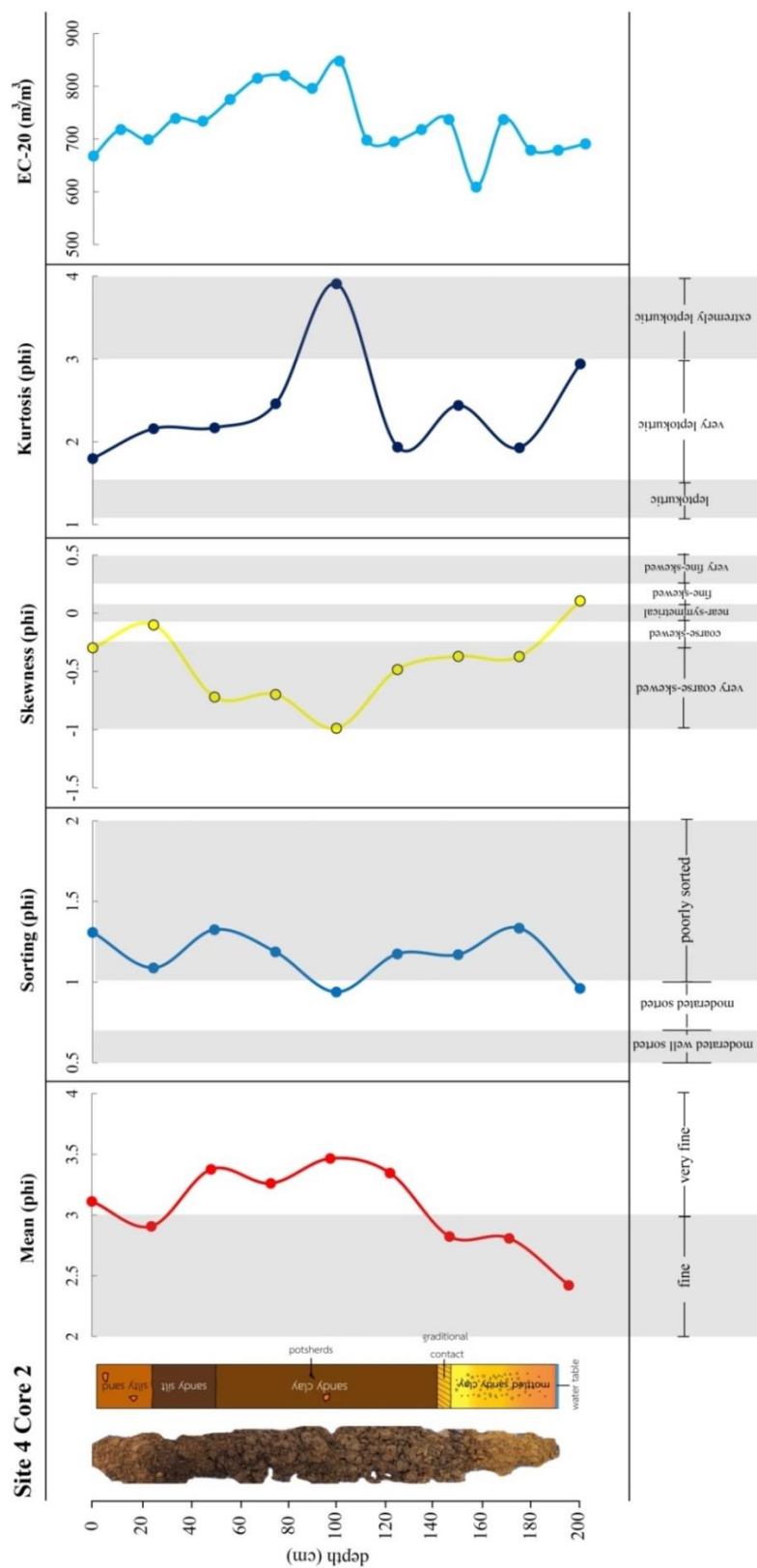
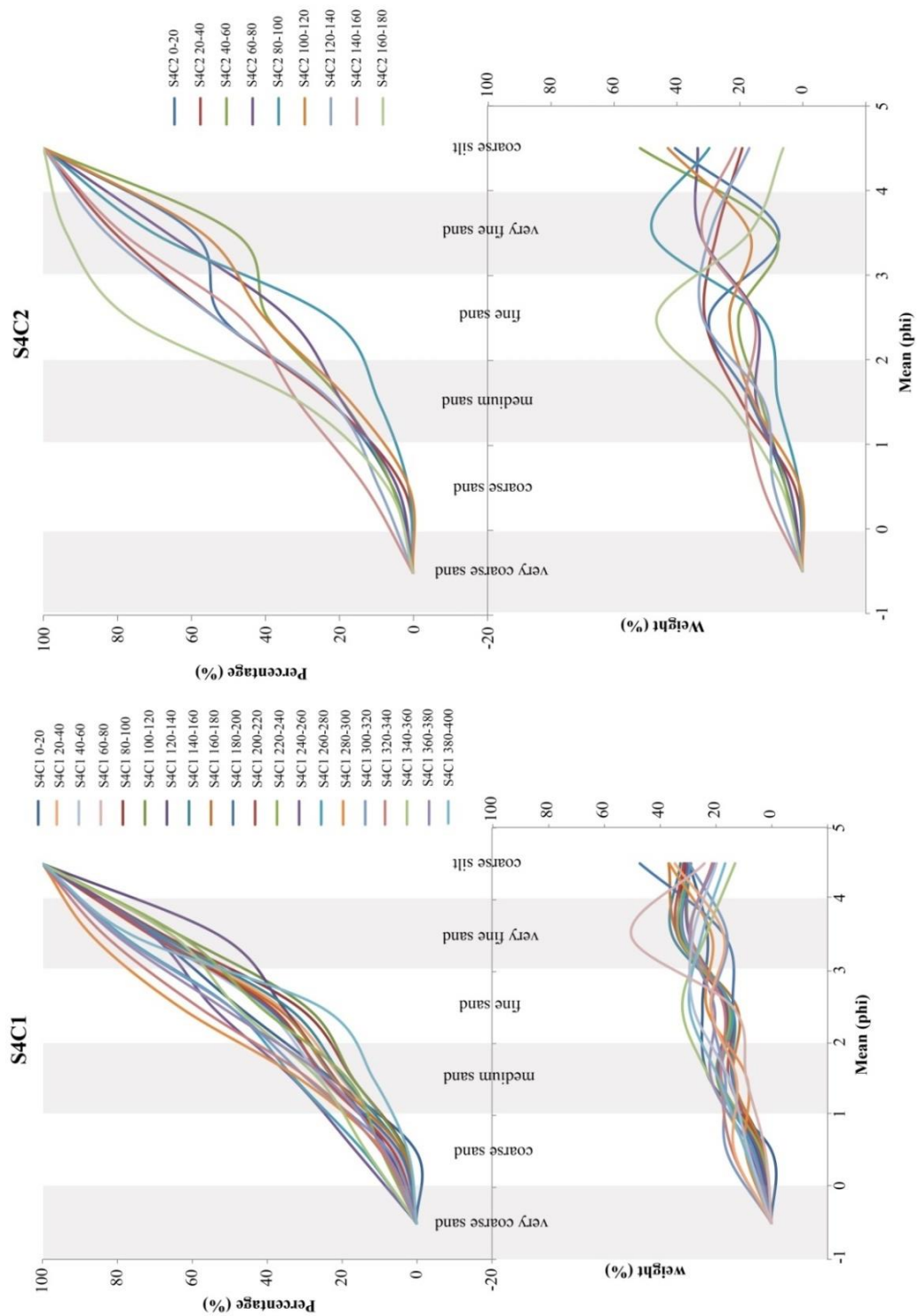


Figure 65 Grain size distribution of S4C2 identified as the moats surrounding a mound along with the calculated water content.



**Figure 66** Cumulative probability and frequency curves of floodplain sediments at S4C1 and S4C2 showed the different process of transportation and deposition in this area being the archaeological site associated with human activities.



#### 4.3.2 Scatter plot of the four statistical grain-size parameters

A scatter plot of the four parameters in the phi measurement unit can be used to indicate the differences in the sedimentary characteristics, in order to distinguish the depositional environments. In this study, the bivariate plots show the relationship between textural parameters for the aeolian sand splay sediments and floodplain sediments. These plots are between mean vs sorting, mean vs skewness and mean vs kurtosis, and other plots such as sorting vs skewness, sorting vs kurtosis and skewness vs kurtosis. The bivariate plot of mean size versus sorting known as Stewart plot (1958) was used to provide significant clues to understand the energy conditions and formation processes at the time of deposition (Stewart, 1958).

The S2C1 with OSL samples in scatter plots are represented that the three groups of sediments might reflect the difference of transportation and deposition processes (Figure 67). As well, the scatter plots of S3C1 with OSL samples show the distinguish sediments in two groups including OSL samples which some condition plots are separated from coring samples. Although, the samples of coring are widely scattered, they can be set to two groups shown in Figure 68.

In floodplain sediments, the scatter plots were applied from the 2 coring of S4C1 and S4C2. They represent the relationship of sedimentary processes between S4C2 with S4C1. Indeed, the S4C2 sediments of 80-100 cm and 160-180 cm depth illustrate that they are worked in the same processes as group III (380-400 cm depth) and group II (240-360 cm depth) of S4C1 respectively (Figure 69).

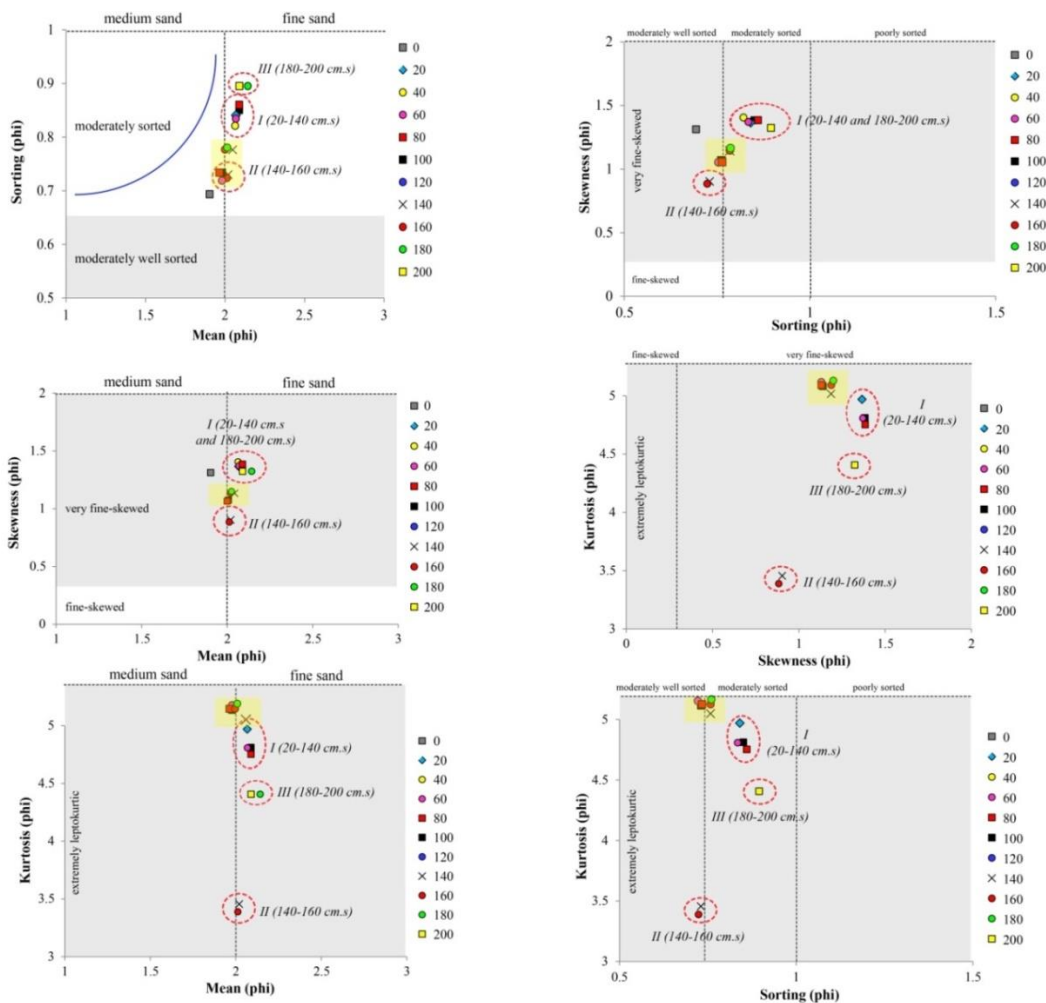


Figure 67 Scatter plots of S2C1 that OSL samples (yellow-background) are separated from coring samples slightly.

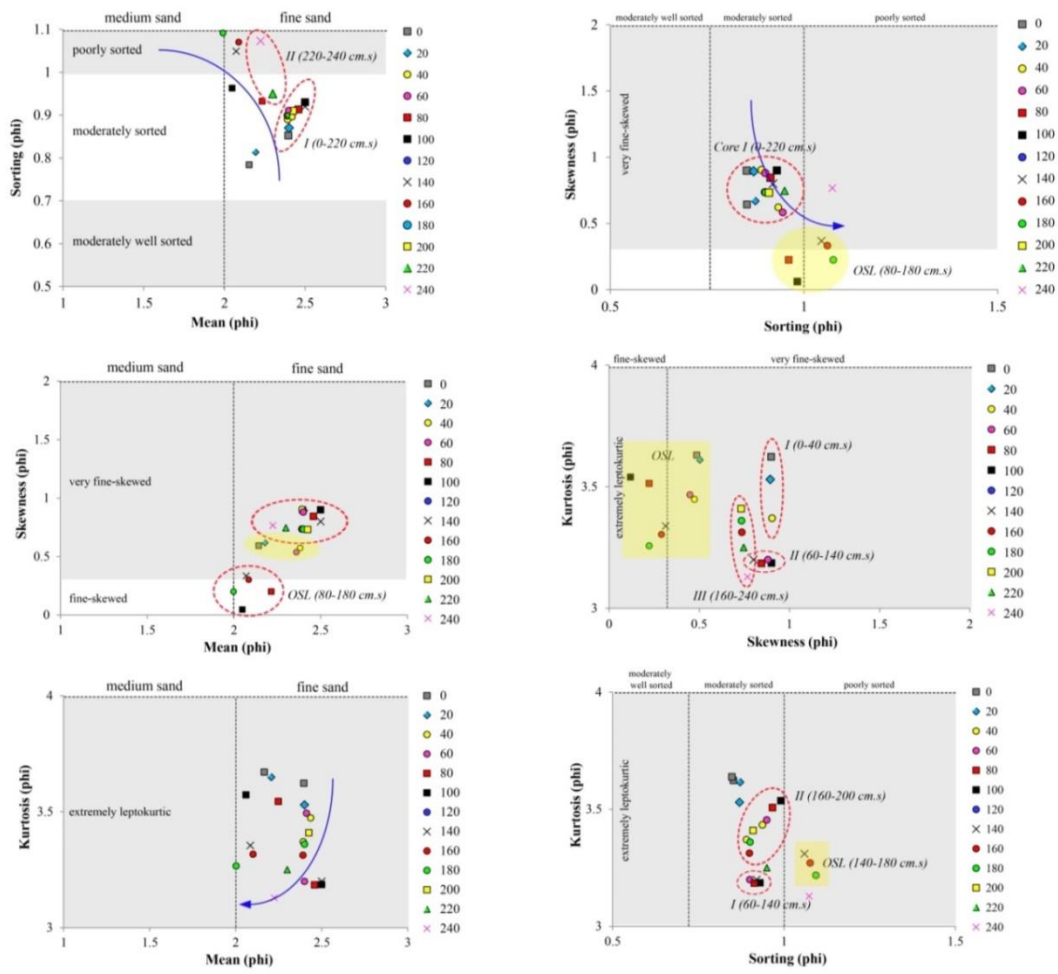


Figure 68 Scatter plots of S3C1 that OSL samples (yellow-background) are distinctively separated from coring samples.

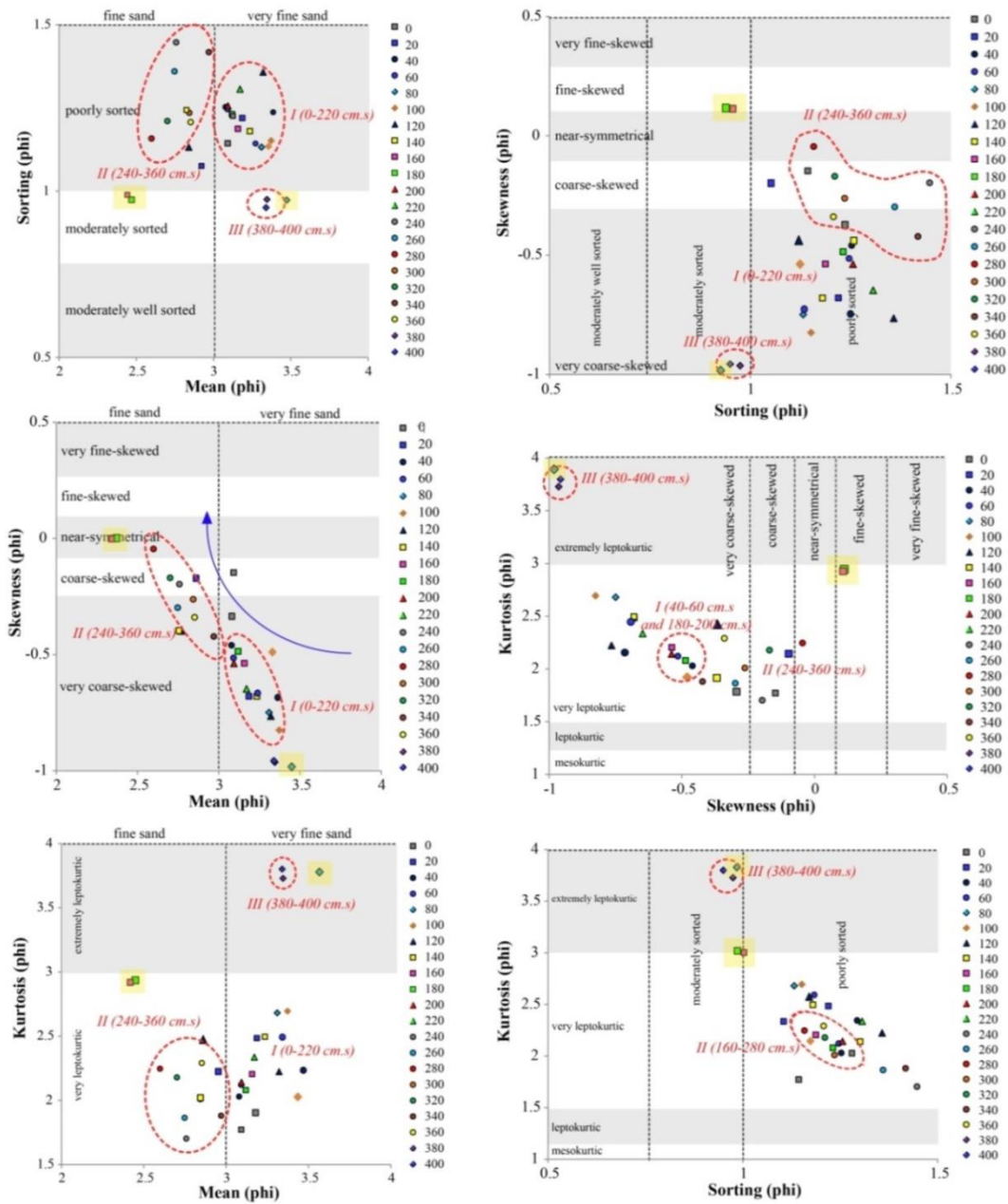


Figure 69 Scatter plots of S4C1 and S4C2 (yellow-background) that some S4C2 sediments are distinctively grouped with some sediments of S4C1.

#### 4.4 Dating of sand splays

The 7 samples were collected from soil profiles based on different characteristics of each sedimentary layer at Site 2 and Site 3 for OSL dating. Results are listed in Table 4, and shown in Figure 70. They reveal the periods of aeolian sand splay along with fluvial activities within the Late Pleistocene to Holocene periods. At Site 2, where is located on the distal part of sand splay, shows the range of  $44.4 \pm 6.5$  ka to  $39.5 \pm 9.0$  ka. The ages of the upper aeolian deposit have a range of  $39.5 \pm 9.0$  ka together with the range of fluvial deposits in 44.4 to 41.0 ka (Figure 71). Generally, the relative dating of this site was assumed that the aeolian activity might be originated after terminated fluvial process, and it should active at the later period of Site 3 based on aerial photograph interpretation. In contrast, the range of  $65.9 \pm 10.0$  to  $4.8 \pm 0.7$  ka was belonged to aeolian sand at Site 3 located on sand splay of high terrace. Significantly, the ages of upper aeolian layer at 20 cm and 50 cm depth are widely ranged following 28.7 ka and jumping to 4.8 ka differed in only 30 cm thick. However, the ages of lower deposits between 80 and 160 cm depth which are show  $81.8 \pm 13.7$  to  $65.9 \pm 10.0$  ka which is older than Site 2. It is possible that the fluvial processes had been active since 80,000 yr BP and supplied sand materials as a source for reworked aeolian at least 60,000-50,000 yr BP until 40,000-30,000 yr BP and 4,800 yr BP of Holocene period. The ages of Site 2 can be assumed that all stratigraphic layers are belonged to aeolian processes due to the facies of GPR profiles and grain size parameters. These ages were younger than Site 3 absolutely that the lower layers show the range of 45,000 – 40,000 yr BP along soil profile from 90 to 200 cm depth. The fluvial process was not founded in this profile (Figure 71), but at the bottom of soil profile is floodplain. Therefore, it can be indicated that the reworking aeolian processes were updated since at least 45,000 to 40,000 yr BP and might be as possible as identified to 4,800 BP like the uppermost layer of Site 3.

Table 4 OSL dating results.

Sample ID	Depth (cm.s)	U (ppm)	Th (ppm)	K (%)	W (%)	AD (Gy/ka)	AD (Error)	ED (Gy)	ED (Error)	Age (Yr)	Error (Yr)
2-1	90	0.42	1.71	0.15	5.54	0.44	0.1	17.33	0.38	39,540	9,060
2-2	135	0.30	2.85	0.23	5.96	0.56	0.1	22.87	0.49	41,080	7,430
2-3	185	0.21	3.61	0.35	5.79	0.69	0.1	30.48	0.66	44,450	6,550
3-1	20	0.41	3.57	0.19	3.21	0.61	0.1	2.97	0.07	4,830	790
3-2	50	0.22	2.87	0.15	1.91	0.49	0.1	14.18	0.31	28,700	5,840
3-3	95	0.17	4.42	0.27	7.19	0.65	0.1	43.16	0.93	65,950	10,170
3-4	140	0.00	4.00	0.35	14.83	0.60	0.1	49.31	1.06	81,890	13,710

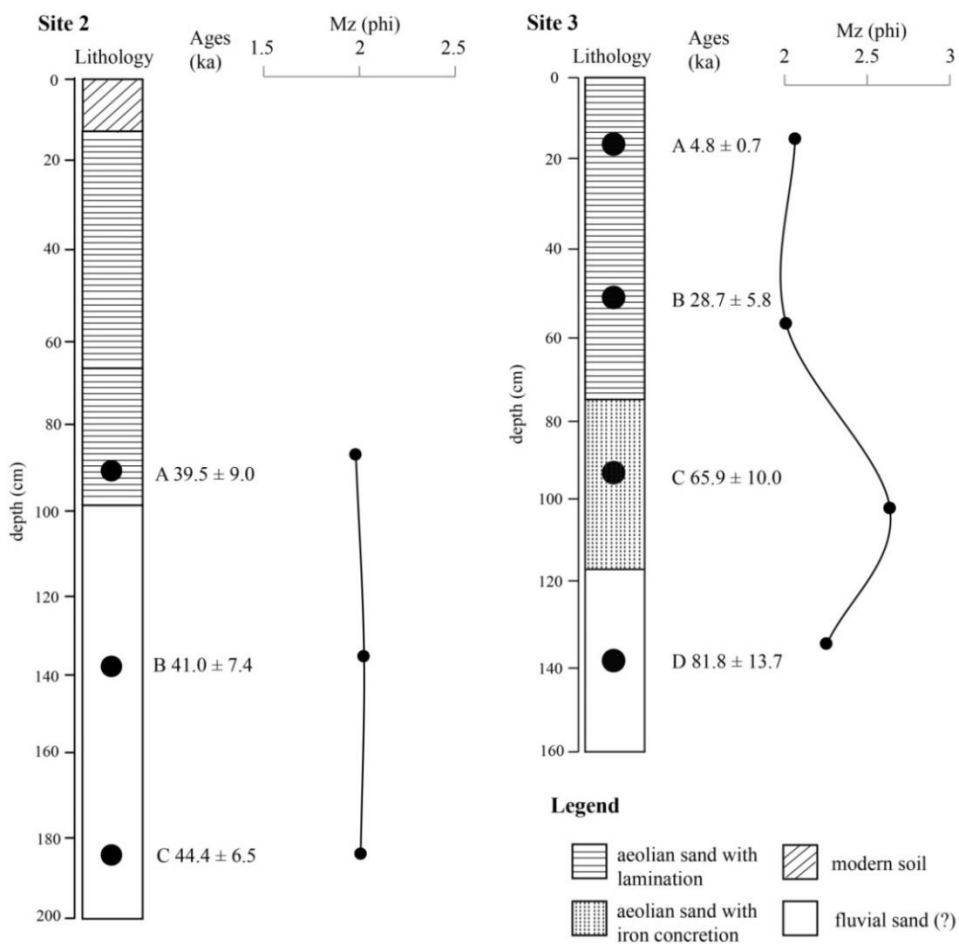
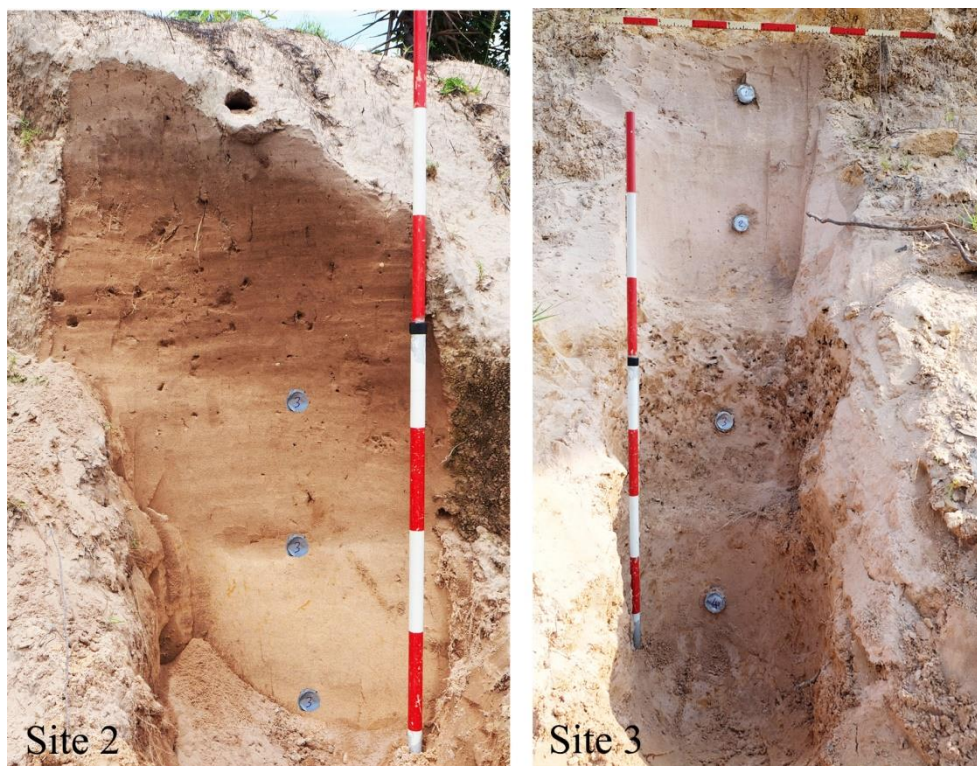


Figure 70 Stratigraphy of the 2 sections in this study along with OSL dating and grain size.



**Figure 71** Soil profiles of Site 2 and Site 3 on the distal part of sand splays showing position of the 7 OSL samples.

## Chapter 5

### Discussion

All results shown in Chapter 4 can be proposed to discuss in the formation and process of sand splays since  $65.9 \pm 10$  kyr BP derived from OSL dating. GPR profiles and grain size distributions revealed the sedimentary significances also linked to the ancient site settlement at sand splay morphology. In addition, the grain size distribution of a moated site seems to indicate the relation with cultural activities of human past. Absolutely, the geomorphological study is a key method to discover human past behavior in adaptation for subsistence tending to social development from small village to urban society in the early state of historical period.

The area is considered to be part of the Lower Mun and Chi Rivers. Floodplain has developed along both river sides, especially the south of Mun Rivers where river width is wider than the northern area. The border of this floodplain is visible. This character might be controlled by some special geological structures leading to the difference in elevation obviously. This causes the river cannot erode down to base level related to river terrace formation (e.g., Wicander and Monroe, 1998; Fryirs and Brierley, 2013). Indeed, the terrace of study area is classified into 2 steps by elevation difference including low and high terraces found at both of Mun and Chi River sides. They show paired terrace. Hence, the terrace had evolved in 2 stages, in particular to the paleo-channel features founded on high terrace. These paleo-channels are classified as “old-floodplain” of high terrace in the past.

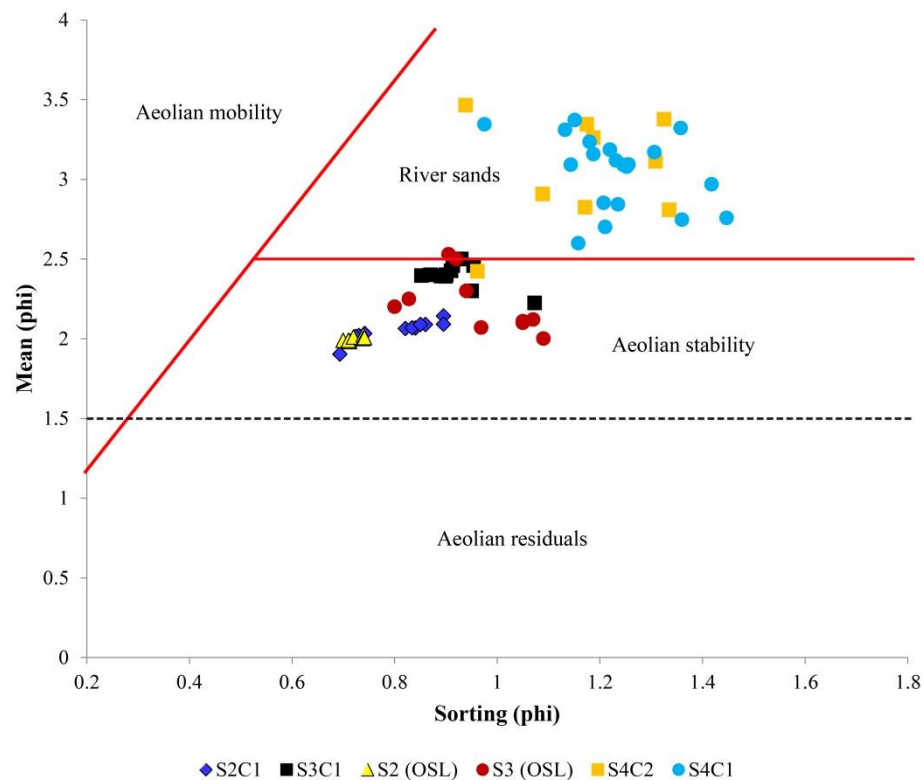
In addition, the other geological features also support the idea of aggradation found at the eastern TKR margin. Salt domes (as ADL) landform is related to the structure of TKR basin acting a saucer shaped basin similar to the Khorat Basin in which Maha Sarakham Formation is beneath as bedrock. Significantly, ADL is specifically found in terrace. Thus, it may associate with the TKR basin where is deeper in Khorat basin. As a result, the ADL can be formed easily since it closed to salt layer in Maha Sarakham Formation. Moreover, the aggradation of terrace not more leaded groundwater flow to erode along salt layer, therefore, the ADL



landform remains in terrace only. It is not founded in floodplain. In addition, sand splays (a type of aeolian dune), the specific geomorphologies or landforms, founded in study area are discussed, as well as the relationship between geomorphology and archaeological site settlement in the study area at the final.

### **5.1 Formation of aeolian sand splays with remarkably archaeological significances from GPR profiles and grain-size distributions**

Sand splays are identified as aeolian sands which is the product of short term aeolian mobilization of fluvial sediments during change in avulsion at the Khorat basin (Hokjaroen, 1989). The features from aerial photographs, GPR profiles, and grain size distributions are explained to two sources of aeolian sand splay formation from fluvial sediments as follows; 1) Overbank crevasse splay deposits and 2) Meandered scar deposits. These river sands were reworked by aeolian process since at least 70,000 yrs BP based on OSL dating with stratigraphy. The Friedman response diagram modified by Besler (1983) identified the S3C1 and S3 OSL sediments as aeolian stability closed to river sands more than S2L1 and S2 OSL sediments. Thus, it was related to source materials from river, especially, sandy bar deposits which were reworked by aeolian at the next time (Figure 72).



**Figure 72** The Friedman response diagram modified by Besler (1983) identified the S3C1 and S3 OSL sediments as aeolian stability closed to river sands more than S2L1 and S2 OSL sediments.

In large scale, the sand splays should be defined as the shadow dunes, the first dune formation developed by topographic obstacle. They are developed under a nearly unidirectional wind regime. The sand accumulation can occur in the lee of gap between two obstacles that sand flow is speeded up and funneled through the gap but fans out and slowed down on the lee side leading to sand deposition. These are important factors for the formation of sand shadow dunes (Bagnold, 1941: 194; H. T. U. Smith, 1954; Howard, 1985). In addition, the sand splays can be compared with the shadow dunes proposed by Xiao et al. (2014). The sand shadow dunes can form in areas where there are strong wind as well as sufficient sand supply and dry climate, especially the suitable obstacles one or both sides of them must have a hill pass effecting to “narrow-pipe effect”. The windward side of the obstacle should have a wide and flat area for providing the spaces for wind flow and transport of material whereas the leeward side must have a sufficiently broad and flat area to

allow the release of transported material. In case of sand splays, the obstacles are crevasse splay sands in hill-shaped which was varied in elevation or relief. When prevailing wind direction had come to these material sands, the sand mound of the proximal part was transported to deposit at the far away distal part depending on topography and wind energy condition at that moment. Due to the different volume and amount of sand supply, splays are disappeared in some areas.

Finally, the development of paleoenvironment and sand splays in the study area can be reconstructed and divided into 3 stages as follows.

#### **5.1.1 Stage I (Pre-formation of aeolian sand splays 95,000 – 75,000 yr BP)**

Remarkably, all sand splays are existed and located close to the margin of terrace. Splays are superimposed on old floodplain where meandered scars were observed. Therefore, sand supply to form splay are of fluvial sands certainly. The predominant locations and GPR profiles revealed the pre-formation of these sands as in case of overbank crevasse splay deposits as Site 2, changes of channel-bend with remaining on mid-channel bars as Site 1 and Site 3. About  $81.8 \pm 13.7$  kyr BP, the braided sand on meandering river had reworked and transported on to floodplain of the Eastern TKR area. Channel fills and mid-channel bar deposits were appeared as the I-V radar facies on GPR profiles of Site 1 and Site 3 (Figures 54 and 59).

Site 1, the first period – Period A (2.0-6.0 m depth) is composed of channel fills with vertical accretion in which it is interpreted as overbank flow of channels. Moreover, the radar facies show continuous small concave-upward lower boundary at between 95-130 m and next to continuous horizontal parallel and gently inclined convex upward reflections. They may be considered as erosional surface or mid-channel bar founded generally in meandering channel (e.g., Bristow, 1993; Bridge et al., 1998; Best et al., 2003). The second period of fluvial deposits – Period B (0.6-2.5 m depth) consists of radar facies similar to Period A. The lateral accretion indicated channel migration is more visible; for example, the facies of inclined tangential reflections at 255-285 m of point bar or side bar deposits of the channel. These characteristics are similar to Site 3.

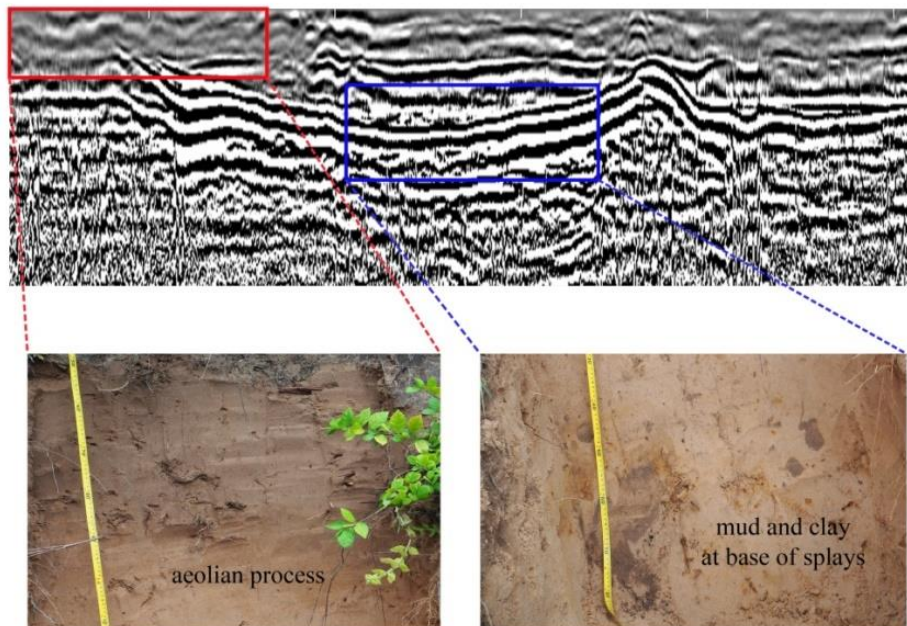
At Site 3, it is interesting that the radar reflection at 33-57 m distance of line shows mound-like structure in apparent inclined reflections between 34-44 m and 49-56 m distance, in contrast to 46-49 m distance. However, the signal is lost at depth 1.5-2.5 m, but it becomes obvious in the upper layer at depth 0.6-1.2 m. Signals are composed of gently inclined reflections in two directions. These facies sets are likely to be a channel fill (Figure 59) that the grain-size distributions derived from sieving can also describe the causes of lost signal. The 120-140 cm depth appeared a pale organic-rich sand layer in blackish-grey color along with high water content might be a cause of lost signal on this GPR profile. Along with water table at 2.20 m depth and homogenous fine-grained sand with moderately sorted from grain size analysis, the channel fills are possible. It can be induced to high-flow stage or overbank flow based on radar facies and the organic matter on sand deposits. Moreover, radar facies from Line 2 showed meandering channel due to the I and V radar reflections of inclined sets, trough-shaped, and small to large scale of concave-upward lower boundary. As well, the mid-channel bars can be founded in this line. Set of reflections in mound-shaped underlain layer of concave-upward shaped can be interpreted as channel fills; for instance, the feature likes a channel bar in 1.2-2.5 m depth is at 30-50 m of line 2 (e.g., Bridge, 1998; 2003). Notably, it is composed of sinuous-crested dunes in trough cross strata, ripples in small-scale cross strata and planar strata at upper stage plane beds. Best et al. (2003) described these structures as formed by the migration of large sinuous-crested dunes, but Bridge (2009) suggested that dunes are typically 3 to 4 m high in the deeper parts of the channels, but are 0.5 to 1 m high near bar tops. As a result, the facies of Line 2 as mentioned earlier can be considered to be the bar top of channel bar that filled across-bar channels commonly in the upper-bar deposits (Bristow, 1993). The grain-size distribution from S3C1 demonstrated to be homogeneous of fine-grained sand with moderately sorted along 2.6 m depth. Mottled zone was founded in both core S3C1 and stratigraphic sections from a pond on sand splays. This layer is indirectly inferred to drier phase due to decreasing in recharge to groundwater table which might be related to low precipitation, thus, the oxygen reacted with iron as oxidation leading to iron concretion. It was dated to  $65.9 \pm 10.1$  kyr BP (Figure 73). Furthermore, the

bivariate plots suggested the different processes between the area on sand splays (S3C1) and at margin of splays (OSL stratigraphy). At level of 80-180 cm depth from surface, sieving OSL sample results were ranged to poorly sorted with ranging from fine to medium-grained sand. Therefore, this group is belonged to fluvial sediments like the 160-220 cm depth of S3C1. It is closed to water table influencing to form the mottle layer at the upper. By the dating, this layer was deposited since  $81.8 \pm 13.7$  to  $65.9 \pm 10.1$  kyr BP that the fluvial system of meandering channels with braided sand were operated broadly.

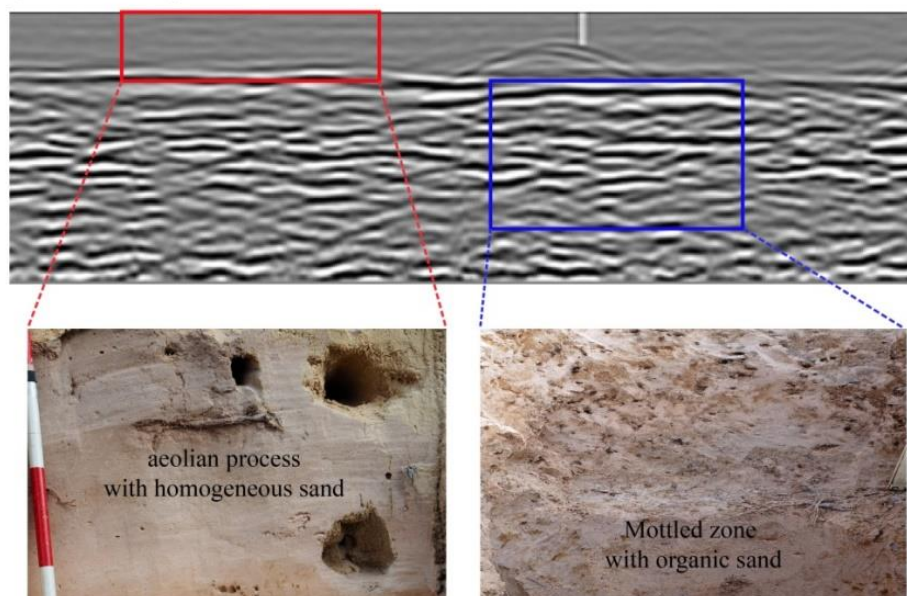
The crevasse splays on flood deposits are significantly shown in GPR profiles of Site 2 (the appearance of dominated laminated sand and overbank fines, less lateral accretion and a few channel fills (Miall, 1985) (Figure 55). They also indicated that the back swamp or wetland environment was compacted beneath aeolian sand deposits. GPR profiles showed on Period B which is fluvial deposit as flood deposit from 5.00 to 2.00 m depth. It is belonged to the IV facies of horizontal and sub-horizontal reflections suggesting that these characteristics are vertical accretion by flood events (Miall, 1985; Bridge et al., 1986; Okazaki et al., 2015). This appearance indicates that sediment input to the system is very high (Einsele, 1992). From aerial photograph and satellite imagery, floodplain on this area was widely worked by meandering channels, as well as many times of change of the avulsion belts tended to form as splay. The initial cause of the formation of splays is the bank breaching by overbank flow resulting from high water-surface, or high velocities characteristic of outer bends (N. D. Smith et al., 1998; Tooth, 2005). the other possible cause is from the constricted flow due to obstructions or channel bed aggradation, leading the formation of splay (Woodyer et al., 1979; Gibling et al., 1998). This phenomenon is described when the splay had rapidly spread to the standing water in poorly drained swamp environment or floodplain, the progradation of overbank sediment developed to establish a well drained swamp by tapping fine-grained sediment from distal sheet floods (Farrell, 1987). Thus, it is possible that the sediments of 2.00 to 4.00 m depth on GPR profiles at Site 2 might be deposited as long as they formed to clay or mud with peat. Clay and mud layer at 2.00 m depth from stratigraphic section was found (Figure 73). Indeed, most of interdune characters

recognized at Site 2 are the wetland deposited when the water table had raised up closed to base of sand dune (Pye and Tsoar, 2009). Thus, the horizontal facies found along Line 1 at 1.00-1.50 m depth may be related to form mottled zone (recognized in sample S2L1) due to fluctuation of groundwater level at 2.00 m depth. However, mud or clay layer was not observed from core sediment, although, it is commonly found in overbank or flood deposits (e.g. Miall, 1985; Florsheim and Mount, 2002; Joeckel et al., 2016). Because the coring point and stratigraphy section are located on the distal part of sand splays, mud or clay received from bank breaching are not found or may be eroded in later. Tooth (2005) stated that the distal part of splays was modified with less frequently and rapidly than the proximal part. The grain size distributions show similar mean size of fine-grained sands that belong to the distal crevasse splay. They are homogenous with medium to fine grained sand (e.g. Florsheim and Mount, 2002). In contrast, values of standard deviation are in ranges of moderately to moderately well-sorted found at 1.2-1.6 m depth of mottled zone. Thus, these observations are inferred to the base of sand splays with higher energy conditions or effects of iron concretion.

a) Site 2 - GPR profile of 200 MHz



b) Site 3 - GPR profile of 400 MHz



**Figure 73** GPR profiles with internal structure from stratigraphic section including a) Site 2 shows mud and clay layer at 2.00 m depth and b) Site 3 shows the homogeneous sand with aeolian facies and the lower layer of mottled zone from the section.

Overall, it is possible that the GPR profiles and stratigraphy of Site 2 between 2.0-5.0 m depth on GPR profiles shown in vertical accretion are belonged to

flood deposits or crevasse splays resulting in the upper flow stage of channel bends to avulsion changes in the paleo-Chi River as final abandonment crevasse splay and channels (Bernal et al., 2013). It should be reworked before by aeolian process recognized in  $44.4 \pm 6.5$  kyr BP. At Sites 1 and 3, on the other hand, the GPR profiles show more lateral and vertical accretions such as side bar deposits, unit bar and channel fills or scour fills (Figures 54 and 59). These are referred to the meandering channels, obviously on aerial photographs, and led to the explanation of aeolian splay formation in 0.0-0.6 to 1.0 m depth. It originated from this river sand of mid-channel bar or side-bar deposits. Splay here had formed about 95,000 yr BP that comparatively equivalent to Marine Isotope Stage 5 (MIS 5) of the Middle to Late Pleistocene period. The period was indicated warm and wet tropical forest conditions from speleothem or pollen data analysis (e.g. van der Kaars and Dam, 1995; Fleitmann et al., 2003).

#### **5.1.2 Stage II (Development stages of aeolian sand structure in the 1<sup>st</sup> at 75,000 – 19,000 yr BP and the 2<sup>nd</sup> at 5,000 - 4,000 yr BP)**

The climate in MIS 4 had changed from wet to dry condition in the 75,000-65,000 yr BP (van der kaars and Dam, 1995; Zheng and Lei, 1999; Fleitmann et al., 2003; Chen et al., 2003) affecting the decrease in flow velocity and left behind the remains of sand bars with shallow channel-fills. Previously, the crevasse splays were splashed into floodplain of paleo-Chi River due to avulsion at natural levee until the drought occupied in Sundaland, as well as the South China Sea within this period. Meanwhile, sands from breaching in levee were rested at the margin of floodplain. Then, they were blown by strong prevailing wind in NE-SW direction to rest of the present area during 40,000-20,000 yr BP or later.

The Friedman response diagram as mentioned above (Figure 72) identified the S3C1 and OSL sediments as aeolian stability closed to river sands more than S2L1 and OSL-S2 sediments. Thus, it can be linked to source materials from river, especially sandy bar deposits on which they were subsequently reworked by aeolian process. In contrast, Site 2 should be identified as aeolian deposits along the depth of 0.0-2.0 m. They were winnowed from original crevasse splays covering on



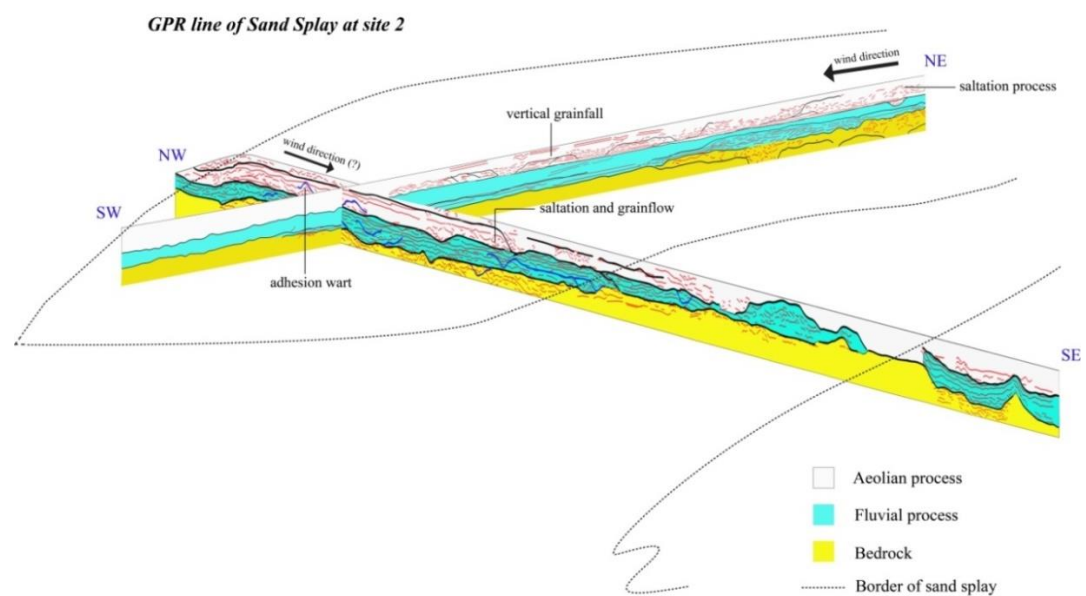
margin of terrace or the paleo-Chi River to finish as aeolian stability on the recent area in case of shadow dune.

For Site 2, in assumption of crevasse splays, GPR profiles of 0.0-2.0 m depth remarkably showed as aeolian deposits. The internal structure of sand splays was homogenous with pale horizontal lamination revealed by soil profiles at the distal part (Figure 73). Moreover, the radar facies of IA, IIA and IIB are among important characteristics of aeolian process of sand splays. They are identified as saltation process during the sediment was blown along Line 1 and 2, in addition to vertical grainfall of sediments after deposition in which might be related to the adhesion structure. The adhesion structures were formed by the adhering of dry sand to a wet or damp surface (Reineck, 1955; Hunter, 1979; Kocurek and Fielder, 1982). The pre-aeolian environment of area was located by floodplain in meandering channels, so that the adhesion structures are possibly formed. The adhesion wart is dominated at 30-40 m distance of Line 1. This appearance indicates that the strong paleo-wind had also frequently shifted from NW to SE directions beneath pre-existing microtopography assumed to a unit bar of fluvial system (Reineck, 1955; Kocurek and Fielder, 1982).

Indeed, the paleo-wind of NE-SW direction is the major influence of appearance and characteristic of sand splays. At distance of 10-65 m, the radar facies of Line 2 is significantly visible of grainflow and grainfall deposit with slipface. It defines the prevailing wind from northeast to southwest (Figure 74). Although, the facies on the upper part of soil profile was unclear and looked likely as ripple features. They might be eroded by saltating sand grains at lower water content closed to the surface. However, the grain size distributions are still distinctive. They indicated sand splays formed as sand dunes because of the dominant of medium to fine grained sand with moderately to well sorted characteristics (Pye and Tsoar, 2009).

At the depth of 120-160 cm from surface, both S2C1 and OSL stratigraphy showed the transition of sorting from moderately to moderately well sorted. This observation can be referred as the base of sand dunes of Site 2. The upper sands were winnowed since at least 37,900-30,000 yr BP which was indicated

drier phase possibly related to a prograding coastal environment and the sea level change between 50,000-34,000 yr BP. It is additional in agreement with the discovery of an extensive buried land surface with coastal swamp and lagoon environments in deep- and shallow-water at peninsular Malaysia and Kalimantan and the Bonapart Gulf (Yokoyama et al., 2001; Hanebuth et al., 2003).



**Figure 74** Model of wind direction at sand splays based on GPR interpretation from Site 2.

GPR profiles at Site 3 showed the characteristic of mid-channel bar deposits with small channel-fills between 1.6-2.2 m depth. They are identified as mottled zone being influenced from groundwater table in S3C1. It is similar to the level of 0.8-1.8 m depth in OSL stratigraphy form a pond at the margin of splays. Thus, the 0.0-0.8 m and 0.0-1.6 m depth is belonged to aeolian deposits in OSL stratigraphy and S3C1 core, respectively.

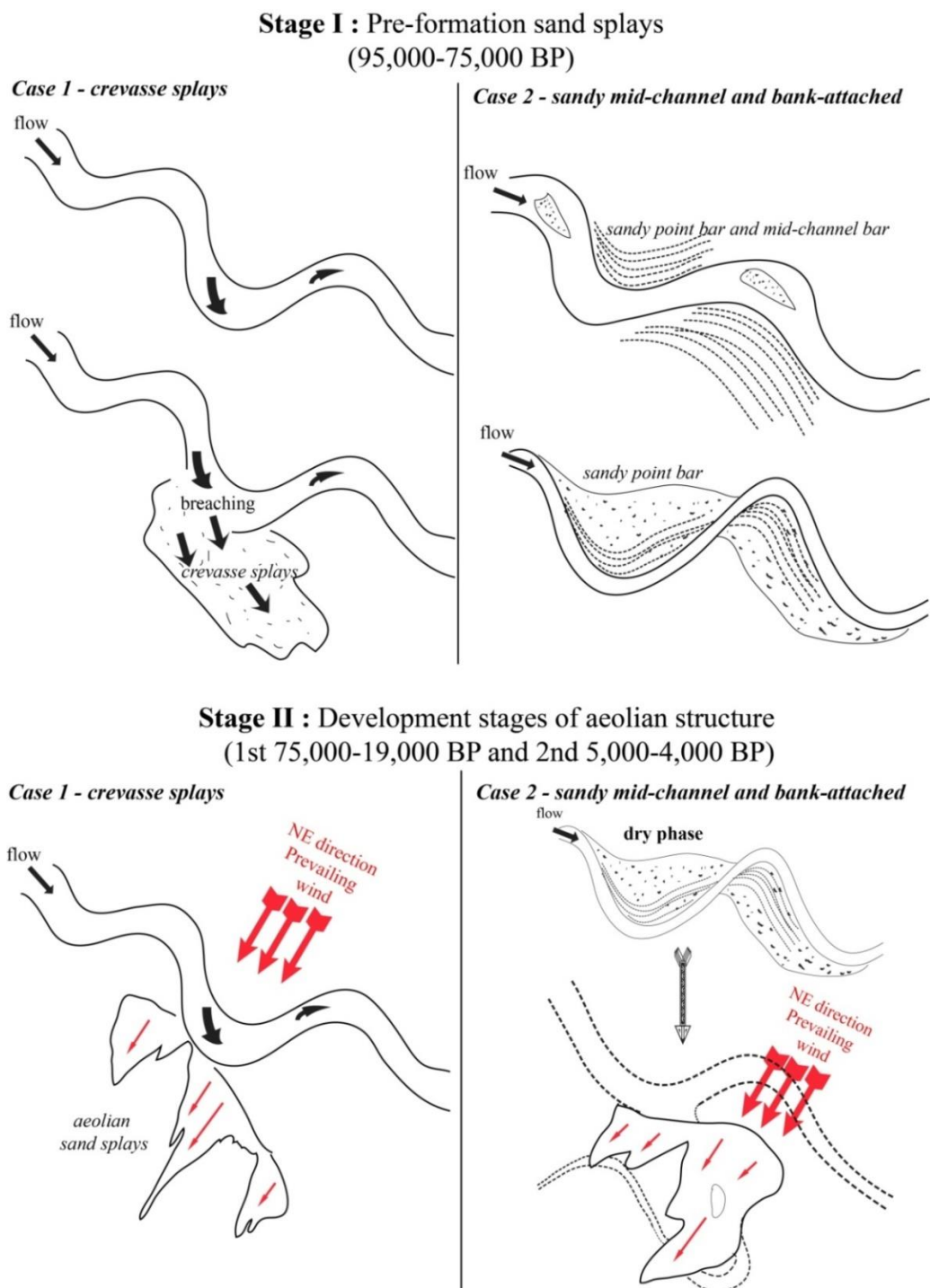
The thickness of splays is different due to topographic relief and sand supply in different transported distances. Considering grain-size distributions, the significant parameters help in indicating the distinct deposition in each level include the bivariate plots of mean size vs. skewness and skewness vs. sorting. The layer in 80-180 cm depth of OSL profile was deposited in different mode with 0.0-0.8 m

depth similar to the 0.0-2.2 m depth of S3C1, as well as the mean size vs. sorting that it can be inferred to energy condition and processes at deposition. The depth of 0.0-2.2 m was derived from higher energy than the lower level.

From GPR profiles, the reworked aeolian sand may be related with channel features of Line 2 at 30-42 m distance. Their range in 0.0-2.0 m depth is visible in trough-shaped reflections. This is assumed that the windblown sand was transported to paleo-channel fills from sand supply of unit bars in old channels. GPR facies is characterized by the horizontal lamination similar to the uppermost layer of Site 2. Thus, it is belonged to aeolian (Figure 73). Nevertheless, these facies were not occurred in distinctive aeolian process. It is inferred to strong wind energy that has not enough power to form as desert dunes. This obscure structure may support the assumption of Penny (2001) who had studied the paleoclimate in LGM at Northeast Thailand. Penny (2001) suggested that temperature and precipitation changes were not severe in northeast Thailand in addition to location of Intertropical Convergence Zone (ITCZ) boundary in the interval 20-19 kyr BP (Chawchai et al., 2013 ; Chabangborn et al., 2014). It is an indicator for slightly change not severe in this area. Initial aeolian process might be occurred after 55 kyr BP at Site 3 and stronger since 20,000 yr BP approximate to the Last Glacial Maximum (LGM). The climate condition during that time was probably cool and dry based on the decreased sea-level change and strong winter monsoon in Pleistocene-Holocene transition (Chen et al., 2003; Penny, 2001; Chabangborn et al., 2014). Previously, the climate was observed to wetter condition with increased summer monsoons in the interval 50,000-40,000 BP or MIS 3 (Chen et al., 2003). Therefore, the mottled zone of this site dated to 55,000 BP might be influenced by fluctuating water table during climate changes before changing to dry phase again.

As well, this research found that the second period of reworked aeolian sand occurred in  $4.8 \pm 0.7$  ka BP (about 5,000-4,000 yr BP) from the uppermost layer of OSL stratigraphic sections at Site 3. These reworked sand are assumed that they might be again processed from previous windblown sands in accordant well with the decreasing in Lake Kumphawapi that the hiatus of transition from wetland to peatland can be inferred from very dry climatic conditions after 5 kyr BP

(Wohlfarth et al., 2012; Chawchai et al., 2013). The climate during that period was appropriate for stopping the development of active sand splays after 4,000 BP, and the beginning of human settlements had developed at next time (Figure 75).



**Figure 75** Stages of sand splays formation at the study area during the Late Pleistocene and Holocene period.

### 5.1.3 Stage III (Development stages of human settlement on aeolian sand splays after 4,000 yr BP)

Based on OSL dating from the uppermost layer of sand splays at Site 3, sand splays were stopped and abandoned their development because of climate changes after 4,000 yr BP. Most of archaeological sites located on this morphology are belonged to the historical periods during the 6<sup>th</sup> – 13<sup>th</sup> century A.D. (or Dvaravati to Angkor periods).

A few moated sites constructed on sand splay morphology were recognized in this area. It confirmed that the distal parts of sand splays are favored for site settlement because there were close to groundwater level and not far from streams. From GPR profiles, the water table can be visible at all 3 sites that illustrates as continuous horizontal reflections following at 2.00 m depth of Site 2 proven at area between floodplain and sand splay deposits and at 3.00 m depth of Site 1 and Site 3 proven at middle to distal part of sand splays. These locations suggest that human past settlement needs to access freshwater resources in dry period. As well, the characters and composition of sand splay are not suitable for rice agriculture which is extremely needed for living and trading at that time. Hence, ancient settlements were likely to place on floodplain more than sand splays.

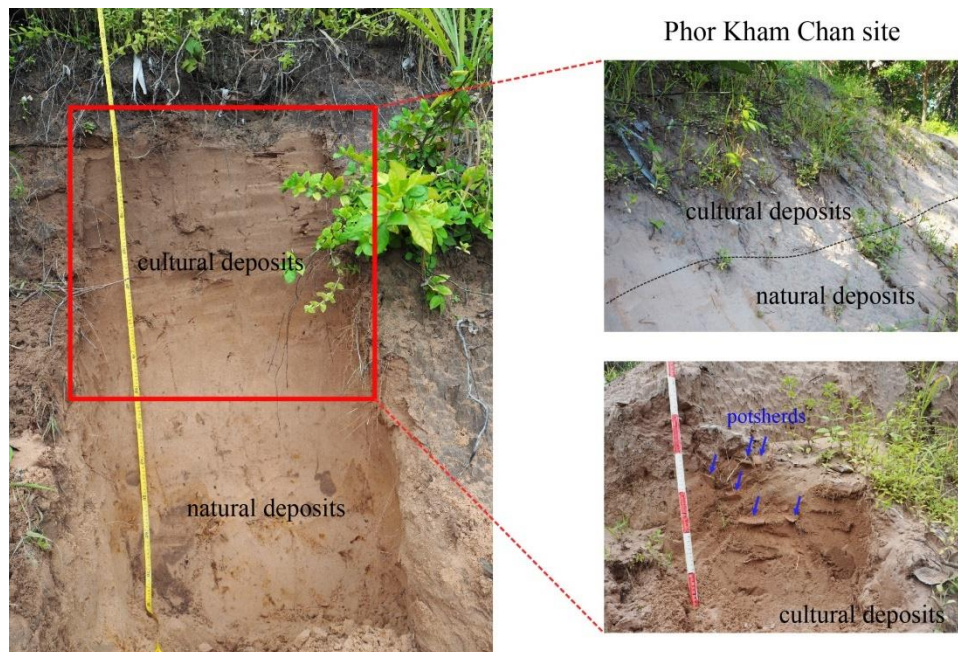
Notably, the GPR profiles of Site 2 revealed the archaeological features at the last distance of Line 2 or 160-195 m distance. It illustrates the VIA facies in parabola-shaped steeping convex reflections. It is defined as cultural deposits where the archaeological evidences are discovered on the surface. The stratigraphic section showed cultural layer with a large amount of pottery sherds in both earthenware and stoneware in 50 cm thickness (50-100 cm depth from surface). This site was dated as 2,500-1,500 BP in the prehistoric period by relative dating based on characteristics of archaeological evidences. It is called as Phor Kham Chan site. However, the discovering on this sand splay is led to question about site-formation processes since the characteristics of these sites tended to locate on a high-relief with broad sand splay such as Ban Bo Bueng and Ban Bak Yai, in contrast to Phor Kham Chan site of flat area with narrow distal part (Figure 76).

Absolutely, the archaeological survey can explain the cultural process occurred here by human past who occupied in this sand splay during 2,500-1,500 BP. The sherds and other evidences were extensively discovered on the splay of Site 2. Most of sherds are in-situ. The grain size distribution showed homogeneous sand with the resemble results of mean size, sorting, skewness and kurtosis along the section. Nonetheless, the uppermost layer containing of archaeological evidences was different in soil color with greyish brown, but the same texture as the lower sand layers which were collected for sieve analysis. The color of upper sands is considered to have formed by organic matter from roots or grasses at the topsoil (Figure 77).

Finally, results of grain size distribution inferred that this location of sand splays was not extremely modified by cultural processes. The natural disasters might no longer affect to site abandonment at next time, but the cultural factors should be more possible due to the homogeneous sand on the stratigraphic sections and grain size analysis. The relationship between archaeological site and sand splays will be discussed in detail at next topic.



**Figure 76** Archaeological evidences were founded in the distal part of sand splays at Phor Kham Chan site.



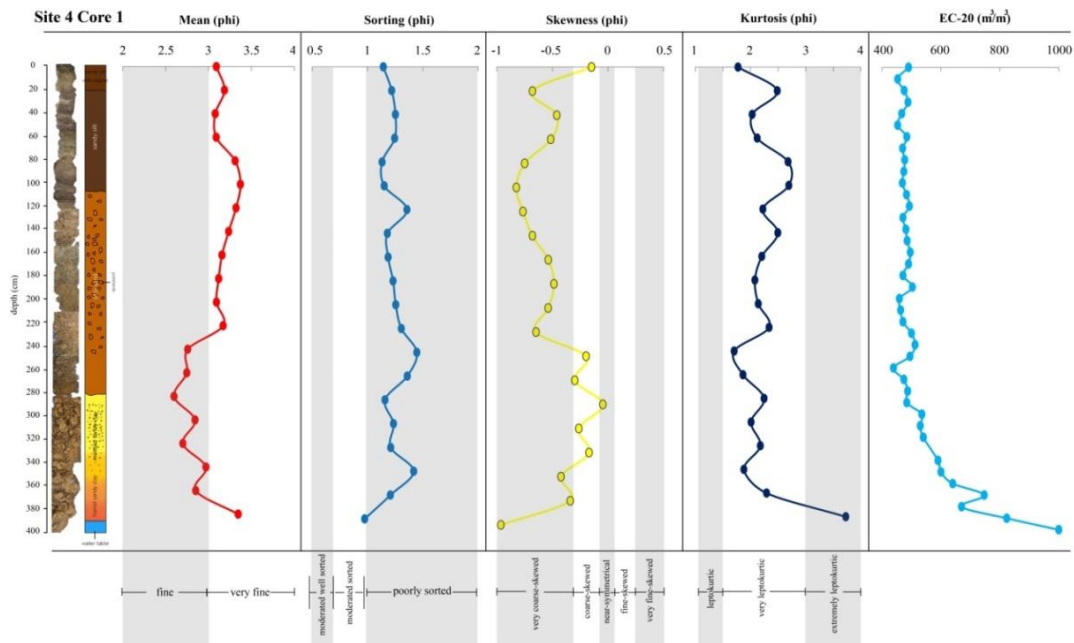
**Figure 77** Stratigraphic sections of Phor Kham Chan site with the characteristics of both soil deposits.

## 5.2 Implication of GPR profile and grain size distribution at Wat Don Kleua as a moated site on ADL

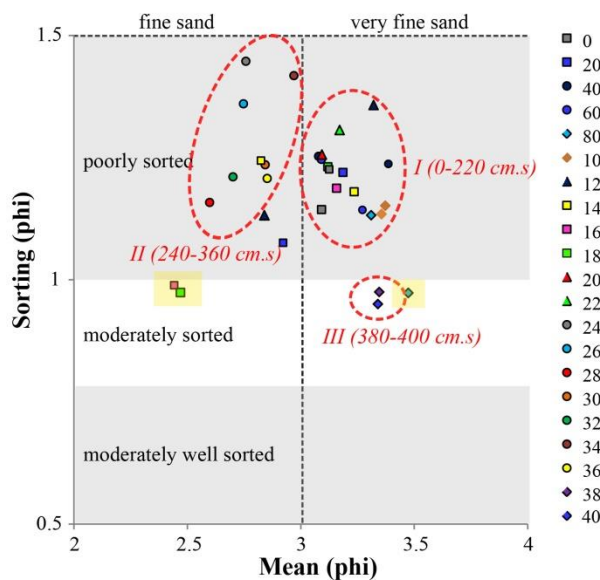
Wat Don Kleua is located on Annular Landform Depression (ADL) defined by Vichapan (1992) based on aerial photograph interpretation. This archaeological site is a moated site where the potsherds were found on surface around the mound. The GPR survey was occurred in only line across the mound together with coring for reconstructing the internal structure. The noises along the GPR line illustrates the repeated signal between 1.50-3.00 m depth from surface and loses at the below (Figure 60). These anomalies were, then, proved by hand auger coring. They were belonged to cultural deposits. The characteristics of this reflection are similar to GPR data of Ban Non Wat at the Upper Mun Valley. This GPR feature has been reported by Duke et al. (2016) on which the repeated signal was founded on the cultural deposits. This strangeness of GPR signal might be caused by compaction of soil with archaeological evidences in range of cultural layers between 1.50 and 2.30 m depth or throughout subsistence period at the site that their activities were extremely taken place and abandoned in remains of various objects until the present day (Figure 78).

Moreover, the grain size distribution implied that the surface of past subsistence might be filled by floodplain deposits. This is evidenced from excavation the moats around the mound and the scatter plots of among mean grain-size and sorting indicated that the sediments of the mound (S4C1) between 0-220 cm depth. They were very fine-grained sand with poorly sorted. The same values as the moat (S4C2) between 0-80 cm were belonged to floodplain sediments (e.g. Friedman, 1961; Valia and Cameron, 1977; Stewart, 1958; Luo et al., 2013; Kanhaiya et al., 2017) (Figure 79). Therefore, some mounded-levels might be a product from sediments of the moats excavated around the mound. The internal structure of this mound was defined as salt dome in ADL (Vichapan, 1992). The cultural deposits in level of 100 to 220 cm depth replied that the deposit was formed in floodplain at the same elevation as surrounding floodplain. It might be extruded to anticline during ADL formation. Mean size at depth of 0-80 cm in the mound was ranged in 3.1-3.4 phi of very fine-grained sand with s-inversed shape. This can be defined as Stage III of cultural process derived from excavation in stage I of the moats due to the inversion of mean size values between 40 cm and 120 cm depth (Figure 80).

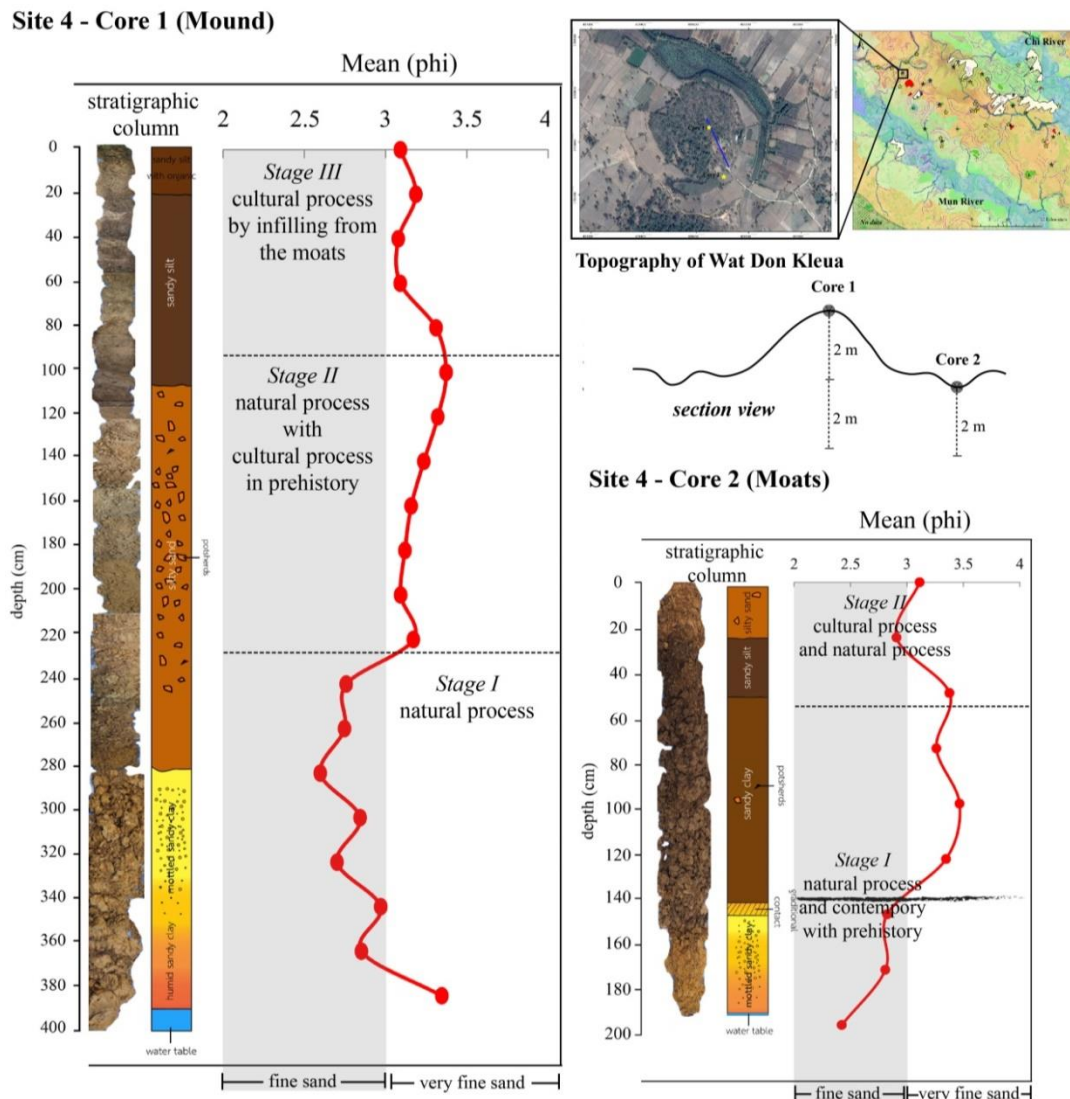




**Figure 78** Grain size distribution with four parameters of S4C1 that the repeated GPR signal between 1.50-3.00 m depth from surface and loses at the below might be caused by compaction of soil with archaeological evidences in range of cultural layers.

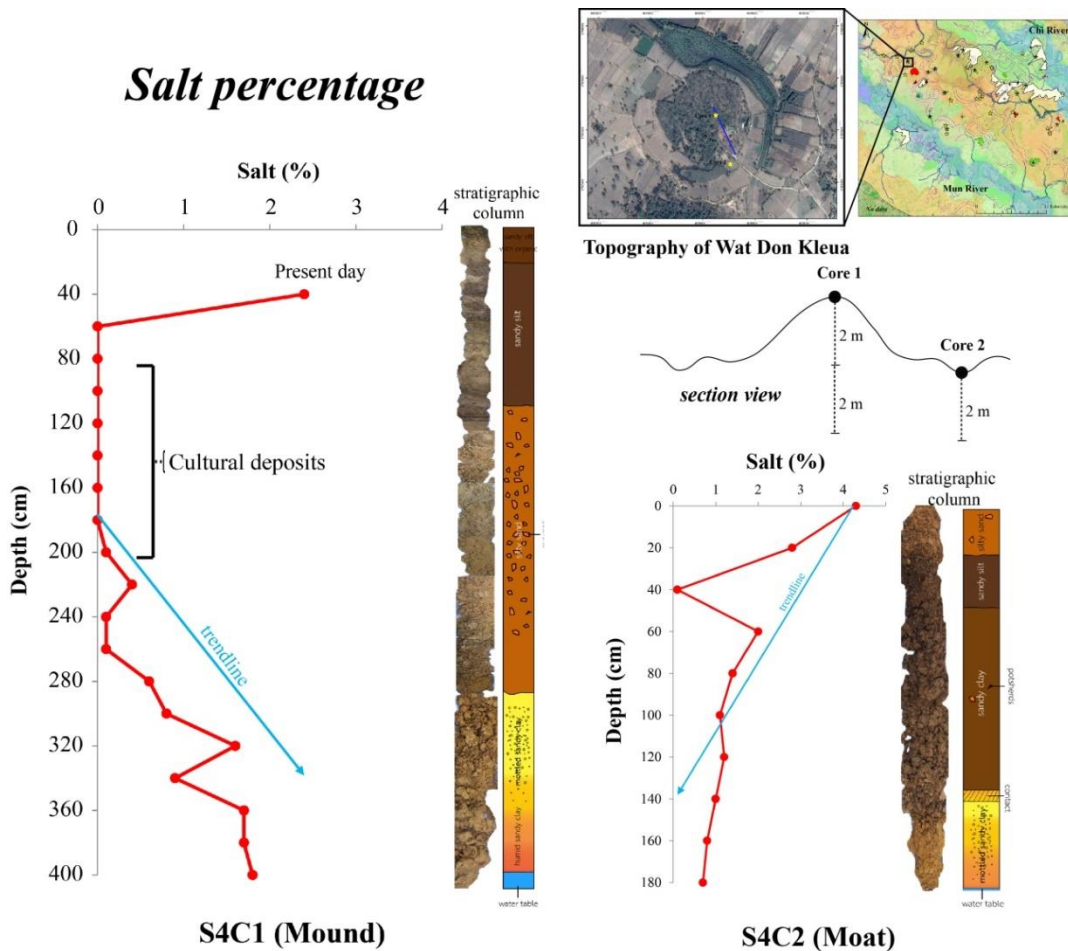


**Figure 79** Bivariate plot between mean size and sorting of S4C1 (mound) and S4C2 (moats) at Site 4 Wat Don Kleau that it showed the 0-220 cm depth of S4C1 as floodplain sediments (poorly sorted) likes the 0-80 cm of S4C2.

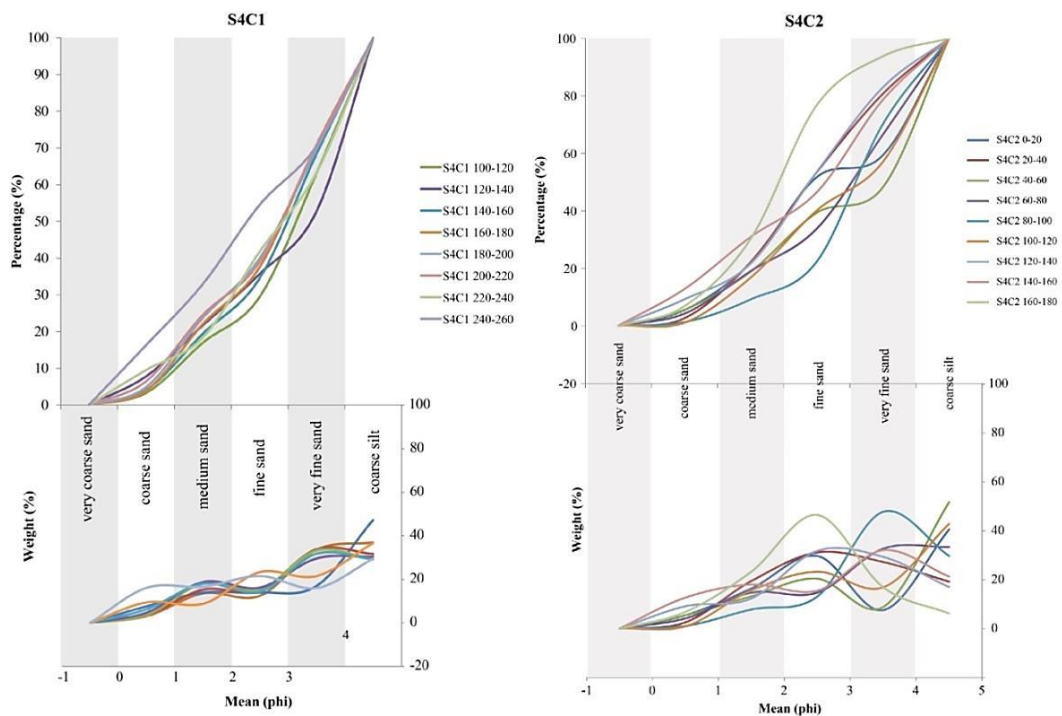


increased at the upper layer 0-60 cm depth. Thus, it is possible that the mound was filled by sediments from the moats afterwards which might be created by human activity or aeolian process. This characteristic is similar to the study of archaeological sediments from Upper Mun Valley at Ban Non Wat (McGrath et al., 2008). Their results suggested that the source of the mound material was from the surrounding floodplain. The mound and floodplain sediments have similar particle-size distributions.

In addition, the electrical conductivity (EC) was analyzed in the sediments related to salt percentage. The same EC trendline of mound as the Wat Don Kleau mound show less values in cultural deposits between 0.0-1.5 m depth with more increasing in lower layer of natural process (Figure 81). Again, the grain size distribution showed frequency curve in bimodal of cultural deposits both in S4C1 and S4C2 which reflected the mixing of grain associated with human activity (Roskin et al., 2017; Zou et al., 2017) in contrast to the homogeneous or unimodal in cumulative curve or frequency in natural process of S2C1 and S3C1 (Figure 82).



**Figure 81** Electrical Conductivity (EC) was analyzed in the sediments related to salt percentage. The same EC trendline of S4C1 as S4C2 was less values in cultural deposits between 0.0-1.5 m depth with more increasing in lower layer of natural process, but the salt was not appeared between 60 cm and 200 cm depth. It gradually increased at below related with ADL structure and groundwater fluctuation.



**Figure 82** The frequency and cumulative curves of S4C1 and S4C2 showing the bimodal in cultural deposits indicated to the activity of human past.

Geologically, the ADL is mostly found in the terrace. Therefore, it may relate to the aggradation of terrace leading groundwater flow to erode salt layer on stage of dome-shape or diapir intrusion in bedrock. Subsequently, the depression was formed around salt dome as rim-syncline feature. Since the rim-syncline feature is characterized by the sinking sediments over the area in which the salt has migrated, the surface water has flowed into this depression and become to lake or pond as a resource of freshwater. Hite (1982) has described a formation of salt diapir theory that the thickening of salt in the crest of anticline is not related to tectonic event or differential loading, but surficial processes of paleochannels are the main impact factor due to resulting in a reduction of compressive (Rau and Supajanya, 1985). Indeed, the moats of Wat Don Kleau became salty because of the water from Huai Nam Khem located at the north of site. In the past, the moats were dug to store the water from surface water or precipitation which created to freshwater. The man thought to bring the freshwater against the saline water with excavation the wide and shallow moats that they were common sight in ancient settlement at Khorat Basin.

For instance, in case of Wat Don Kleau, the channels or moats are about 45 m width and 2 m depth.

As a result, Wat Don Kleau is really located on ADL. It can be defined as naturally moated site since the human past had occupied initially, and, they modified the natural depression of ADL to the circular moats surrounding the mound for storage the freshwater at the next period. The spoils might be created to the banks of moats and some filled on the mound. For this study, furthermore, the GPR survey is an optional way for archaeological survey and confirm as an appropriate method in this kind of typical site. It can reflect and visible the profiles of natural and cultural process in saline soil.

### **5.3 Relationship between ancient site settlement and geomorphology at the eastern TKR**

Based on aerial photograph interpretation, archaeological sites were observed as circular moated sites and sites. A total of 54 archaeological sites found in study area were occupied by human since at least 2,500-1,500 BP or Iron Age. Some sites can be an indicator of the historical period in 6<sup>th</sup>-10<sup>th</sup> century A.D. or Dvaravati and Pre-Angkor to Angkor periods. In fact, archaeological survey and excavation identified various artifacts (e.g. Roi-et ware, metal tool, and Khmer pottery), human remains and ancient monuments were found on surface and subsurface at sites. This research, however, focuses on site settlement and landforms including paleochannel features, ADL and sand splays. Archaeological sites are plotted on aerial photographs along with GPR data and grain size distribution for discussion.

Archaeological sites are almost placed close to paleo-channels. Most are associated with morphology of ADL circular features including ring shape depression area enclosing mound of higher elevation. This landform is effective in human settlement for protecting flood and drought. Since the features of paleo-channel had showed flow direction into ring shape depression of ADL, the freshwater derived from channels was stored in this area. The mound which is identified as dome-shaped of salt layer can be used for activities of human in the past such as living or salt-making due to high elevation and salt source. From salt percentage and grain size

distribution of Wat Don Kleau, it showed that ADL is a natural feature and archaeological moated sites had been built on this landform by human. The human past had occupied on this ADL or naturally moated site initially, and then, they excavated additional moats at next time for obtaining the freshwater as the inner moat closed to the foot slopes of the mounds tended to more saline (Rau and Supajanya, 1985). It is possible that the reason to which human past have chosen this location type is not necessary for the excavation of pond or reservoir because of the ring shape depression around the mound performing in moated features, but some sites, especially the historical site occupied continuously since prehistoric period might be more excavated moats depending on functions of site or the environmental changes. Nonetheless, a few moated sites by man-made are also discovered. They show circle-shaped mound, but not surrounded by rim-shaped depression and smaller size. Most of these moated sites are the mortuary and closed to the residence of moated sites that it indicates the land use functions within the village.

### **5.3.1 Prehistoric settlements of Iron Age (2,500-1,500 BP)**

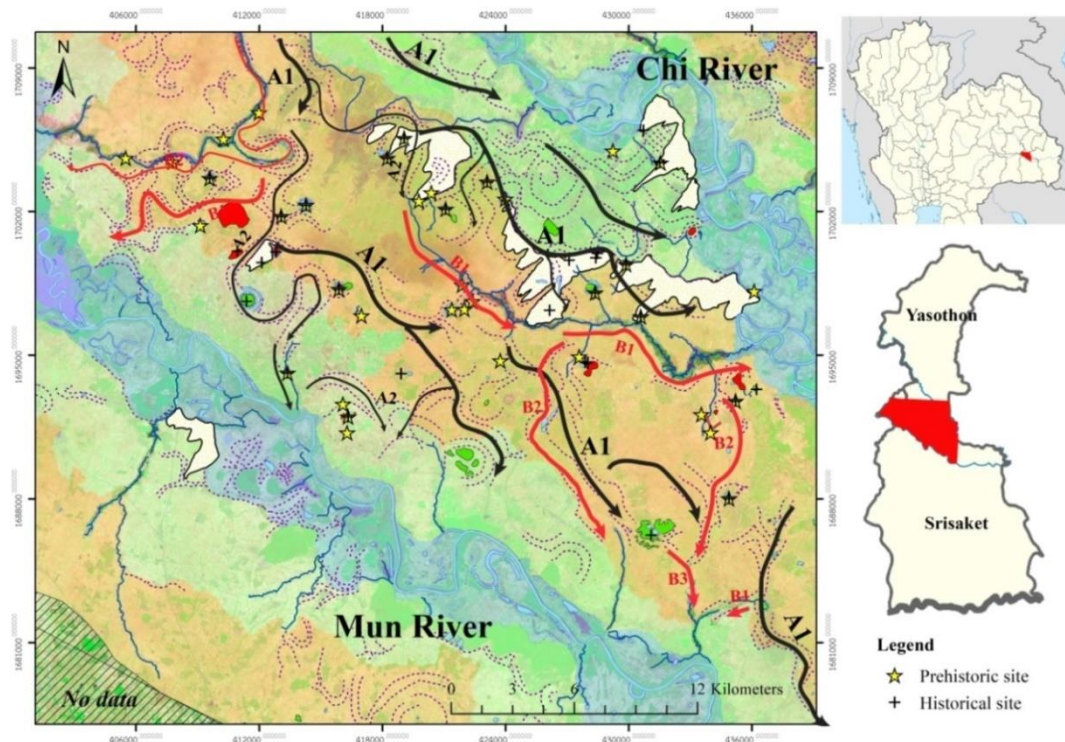
The prehistoric site location on geomorphic map illustrates that the sites were located on the ADL as the first natural choice of settlement linking to paleo-channels. This can be explained that human past in the Iron Age needed high relief location as a mound for living and protecting from disasters. Thus, the ADL was the first place which is predominant in Khorat Basin for appearance of mound. The moated construction was an adaptation for protecting floodwater on the land surface and may have been managed as controlled flow or supply into the constructed moats (Boyd et al., 1999a; 1999b; McGrath et al, 2008). In contrast, Scott et al. (2015) studied the number of moats at a site together with rainfall data. They suggested that sites in the driest areas would have multiple moats to collect much of water as possible. Likewise, Wohlfarth et al. (2016) mentioned that paleo-climate in Iron Age at Northeast Thailand are the relative aridity occurred during Late Iron Age effected to adapt in agricultural revolution and irrigated rice cultivation by water control measures as the moats. However, the appearance of settlement on the

natural ADL or naturally moated sites can be inferred that the saline might also be an essential factor for discussion in excavation the additional moats in prehistoric period of Late Iron Age (1,500-1,000 BP) at TKR.

As mentioned above, the intelligent prehistoric man selected this landform to settle and excavate moats for reservoir which related to water management for agriculture on floodplain. It is predominant in excavation the water route as a small canal from main channels to moats including Ban Nam Om, Muang Khong Khok, Wat Ban Po and etc. (Figure 83). This is represented that the human had begun to control the nature for surviving in Iron Age.

Relatively, the factors of Lower Mun and Chi Rivers ancient site settlement can be linked with flow direction of paleo-channels for controlling the floods and water storage. The later moats might be built when paleoclimate became drier around 1,300 cal. BP and the inner moats became saline. Thus, it needed to excavate additional moats. Eventually, the migration took place at the historical period of Dvaravati and Pre-Angkor in 7<sup>th</sup> – 9<sup>th</sup> century A.D. when the ADL was not suitable for subsistence (e.g. saline waters and soils, cavities, channel changes). Most of archaeological settlements in study area are prehistoric sites of Late Iron Age (1,500-1,000 BP). Some place occurred continuously cultural activity to Dvaravati of historical period. This assumption is supported by the settlement sites closed to aeolian sand splay landform.





**Figure 83** Water routes as a small canal from main paleochannels to moats of prehistoric sites.

### 5.3.2 Historical settlements of Dvaravati and Pre-Angkor to Angkor periods in Thailand (9<sup>th</sup>-12<sup>th</sup> century A.D.)

Significantly, the sand splay landform was predominated for settlement in Dvaravati period about 900 A.D., especially the sanctuary in Buddhism. Most of prehistoric sites were derived from the influence of Dvaravati culture when the religion was a factor for the settlements. The density distribution indicated that the prehistoric people had migrated to the bigger town. They were distinctively related to sand splays. The historical sites of Dvaravati distributed from the ADL moated sites to the sand splays. This phenomenon led to the assumption of salty water, in that, the moated sites in prehistory favored to locate on ADL which is not necessary for the excavation of pond or reservoir as a result of the ring shape depression around the mound performing in moated features. The water in the moats became more saline eventually along with the wetter climate in the proto-history (about 500-600 A.D.) and continuously increasing rainfall in 800-1,000 A.D.

(Wohlfarth et al., 2016; Yamoah et al., 2017) indirectly affecting to increase the recharge of freshwater to surface or channels. Therefore, the people in some towns had to excavate the additional moats for storage while the others had searched for the new settled place for protecting the floods and accessing the freshwater source easily such as sand splays. Nonetheless, the big village of prehistory on ADL had been remained the original status and survived until the Angkor period (1,000-1,200 A.D.).

On one hand, the moated sites which located at the distal part of sand splays were longer occupied than the faraway moated sites on ADL. The GPR profiles of sand splays indicated that the shallow water table of 2-3 m depth and the characteristic of sands were the factors for settling down on sand splays at the distal part due to freshwater reservoir. In addition, the distal sand splay was higher about 2-3 m around the floodplain. It represented as the good mound for settlements because their high relief and the margin closed to floodplain can protect the floods and utilize to the agriculture, in particular to rice cultivation (e.g. Pho Kham Chan, Ban Tum, and Ban Bo Beung).

The obvious Dvaravati Culture group appeared at Muang Khong Khok and Ku Ban Wan of Rasisai district. They were composed of the architecture of Dvaravati Art in 900-1,000 A.D. known as “*Chedi*”. These architectures were discovered in Wat Gu Kheaw Ga Singh for 8 places. They were different plan, shape and decoration, and were placed on the sand splay landform surrounded by the prehistoric moated sites as well as spreading of new settlements closed to sand splays. On the other hand, some sites of Dvaravati Culture located at the top or proximal sand splay where is the location in higher elevation about 4-5 m (e.g. Wat Khowang, Wat Pa Don That, Ban Phi Phoun, Dong Noi). Most of these sites were represented in Buddhist temples of Dvaravati Arts (or about 9<sup>th</sup>-10<sup>th</sup> century A.D.). Especially, the “*Sema*”, significant evidences of Northeast Dvaravati Culture in Thailand, were founded at Dong Noi and Ban Phi Phoun located on proximal of sand splays. This appearance is described under an approach of landscape archaeology in the distinction of spaces and places that the space becomes a meaningful term. The area is created a meaning or a symbol of activities. In contrast to a place, as an

element of space, it is a location or point of activity. By taken the environmental factors and the influences to human behavior into consideration, the high elevation was considered as “space” being appropriate to settlement of temples for being a landmark representing of gods by the monuments built at this space are considered to a place in the space. Tilley (1994) defined this phenomenon as Perceptual space and Architecture space. Thus, the sand splays landform can be termed as sacred space of the Northeast Dvaravati Culture in Thailand.

However, the *Sema* were also founded at Wat Ban Po moated site located on ADL closed to sand splays. This site had been discovered human remains and earthenware that it can be identified as prehistory, thus, the people had occupied at this site during prehistoric to historical period of Dvaravati. From interviews, the region people said that this village known as “Ban Po” derived the freshwater all the years. The freshwater should be precipitation and groundwater table flowing from the upper sand splay at the north to the margin of sand splay in floodplain at the south before recharging to the moats of village. In regard as culture, the human migration might extensively occur during the transition of Dvaravati, or Pre-Angkor to Angkor periods (Reign of the King VII Jayavaraman) because of political power or population growth, so the small village needed adhere to the big city as a central place during 1,000-1,200 A.D.

When the political complex of Angkor had come, some villages might be promoted to be a center depending on the size, location, population growth, historical significance or relationship with their power. For example, the Muang Khon Kham site was in Angkor period or 984 A.D. based on the inscription of Ancient Khmer founded within the site. It was located on the large ADL and appeared the narrow-unshaped moated features which are assumed to natural moats (?). At the southeastern part of the study area, the sites with the earthwork features built in rectangle shape or known as “Baray” were discovered. This earthwork was applied to control flow direction of stream for storage. It might be applied to the Lower Mun and Chi Rivers since 11<sup>th</sup> century A.D. referred to the age of the inscription at Muang Khon Kham, Prasat Srakampang-Yai and Prasat Preah Vihear (Khamtho, 1986; Kashima,

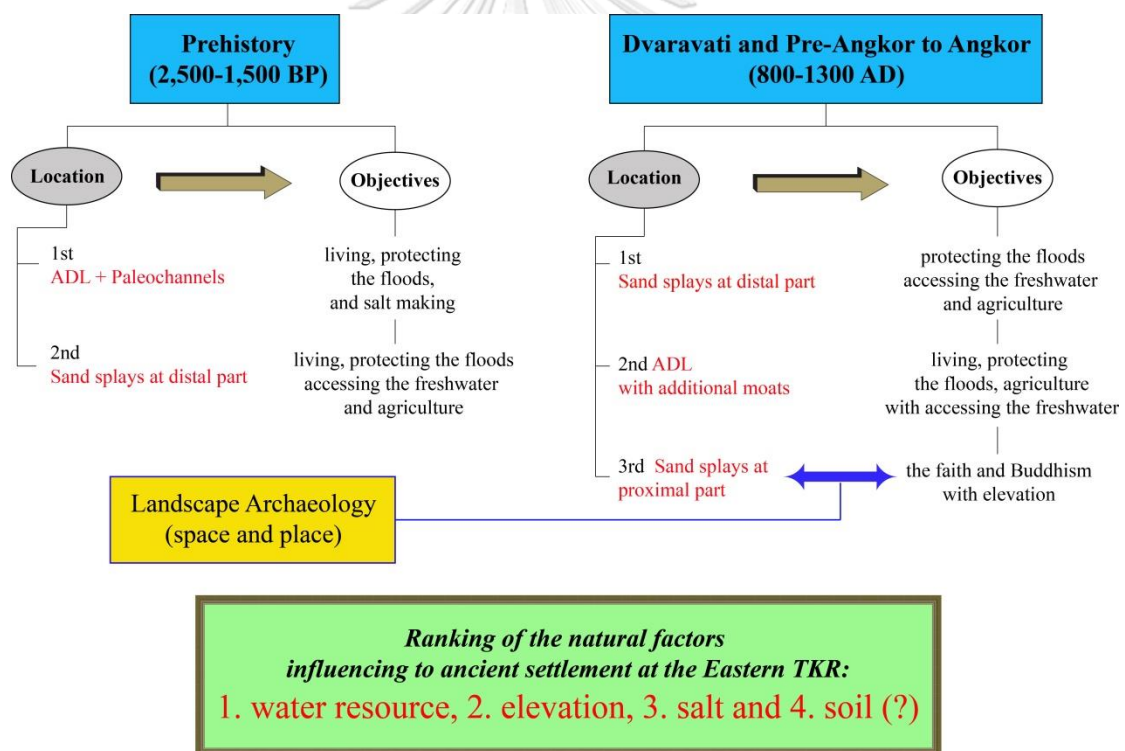
2014). The idea of water management buildings was taken place since prehistoric period in “moated sites”.

Unfortunately, the prehistoric culture was not found at Muang Khon Kham as it has never excavated in archaeology. However, it was found at some surrounding prehistoric sites. Accordingly, it is possible that these prehistoric sites were associated with Muang Khon Kham where it might be defined as an important city in Angkor period of the late 11<sup>th</sup> century A.D. It should be occupied since prehistoric period. Despite discovering of Angkor sites at study area, they were not formed as big city or capital unlike archaeological sites at Upper Mun River such as Phimai, Muang Tam, and Sema in Nakorn Rachasima province or Phanom Rung in Buriram province. In other words, the main towns of Angkor Culture are more discovered at the south of the study area or the south of Mun River that it was a route to Angkor in Cambodia.

Overall, the archaeological sites within the study area were just the small communities under the pathway of culture between Dvaravati and Khmer Cultures. These both cultures owned high power during 900-1,200 A.D. When the power of Dvaravati from Central Plain of Thailand was almost succeeded in the northeast Region, the power of Angkor from Cambodia was more influenced in the southern part of northeastern Thailand in 10<sup>th</sup>-11<sup>th</sup> century A.D. The cities in study area were affected from both of them, in particular, the Dvaravati community carried on prehistoric people during 900-1,000 A.D. these communities were abandoned when the Angkor Culture of the King Jayavaraman VII had powered completely in Northeast Thailand about 13<sup>th</sup> century A.D as the records of the King Jayavaraman VII were not founded in the study area. As a result, some people who had been lived in the north of Mun River or the eastern TKR area migrated to the bigger city under Khmer Empire at the south of Mun River because these cities were adopted in public utilities for better life.

As mentioned previously, the archaeological sites in the study area of the eastern TKR were distributed in random patterns. Both of prehistory and history were relied on the natural morphology following ADL, sand splays, and paleo-channels.

The ADL was the first for the prehistoric settlement in 2,500-1,500 BP. When the Buddhism had influenced from Dvaravati Culture of Central Plain Thailand that it reflected in the appearance of Buddhist fine arts at Ku Ban Wan and Wat Ban Po, the sand splays were a choice for extended settlements in 600-1,000 A.D. due to the wetter climate and population growth, especially the faith. In 1,000-1,200 A.D., Angkor political power spread to the prehistoric site in TKR or the northern Mun River. The some village was promoted to a main city under Angkor such as Muang Khon Kham which might be named as “Indrapura” in the reign of King Jayavaraman V based on the inscription and some village might be abandoned by migration when the bigger city with public utilities from Angkor was established at the south of Mun River.



**Figure 84** Flow chart summarized the influencing factors of ancient settlement during 2,500 BP to 750 BP.

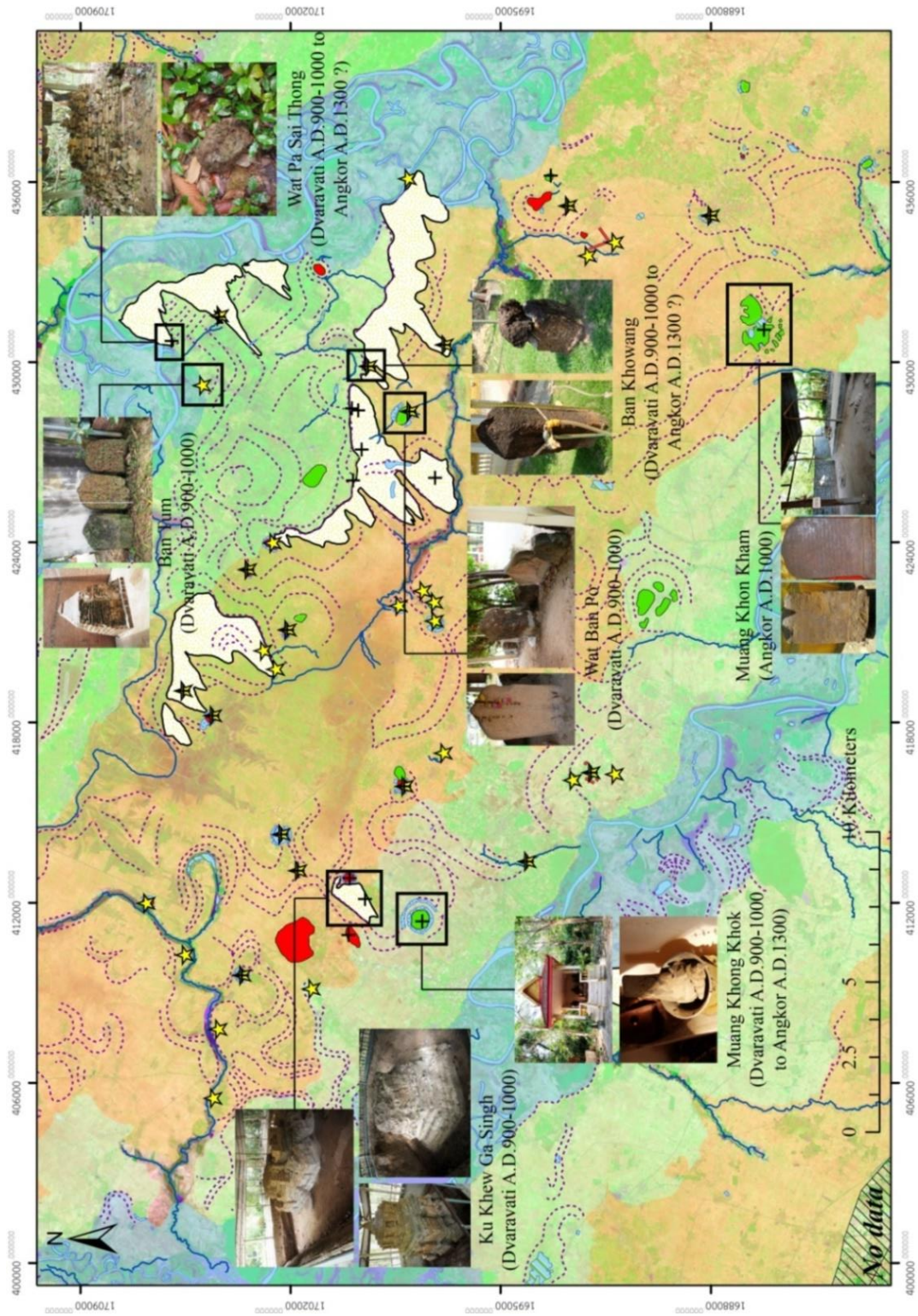
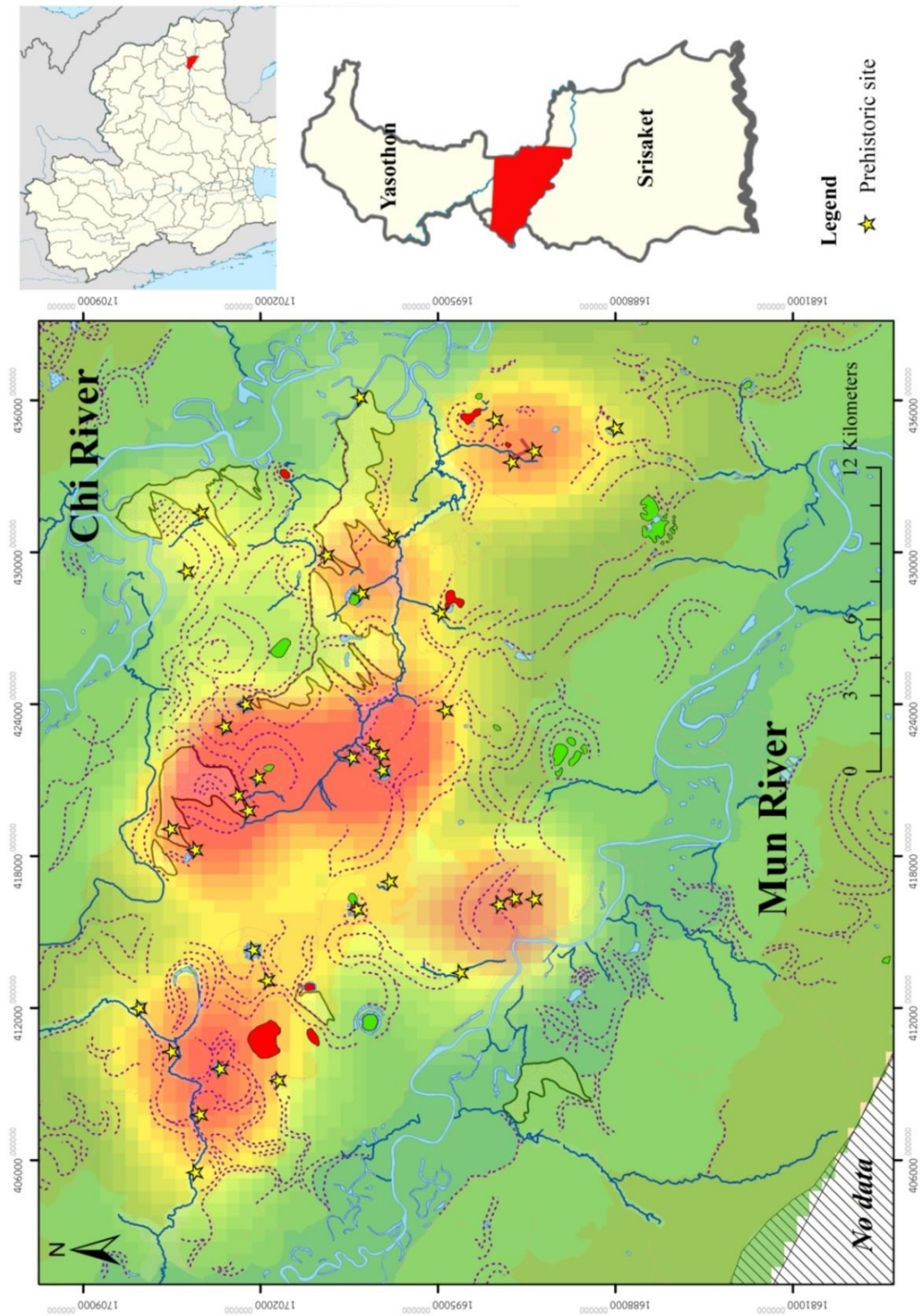
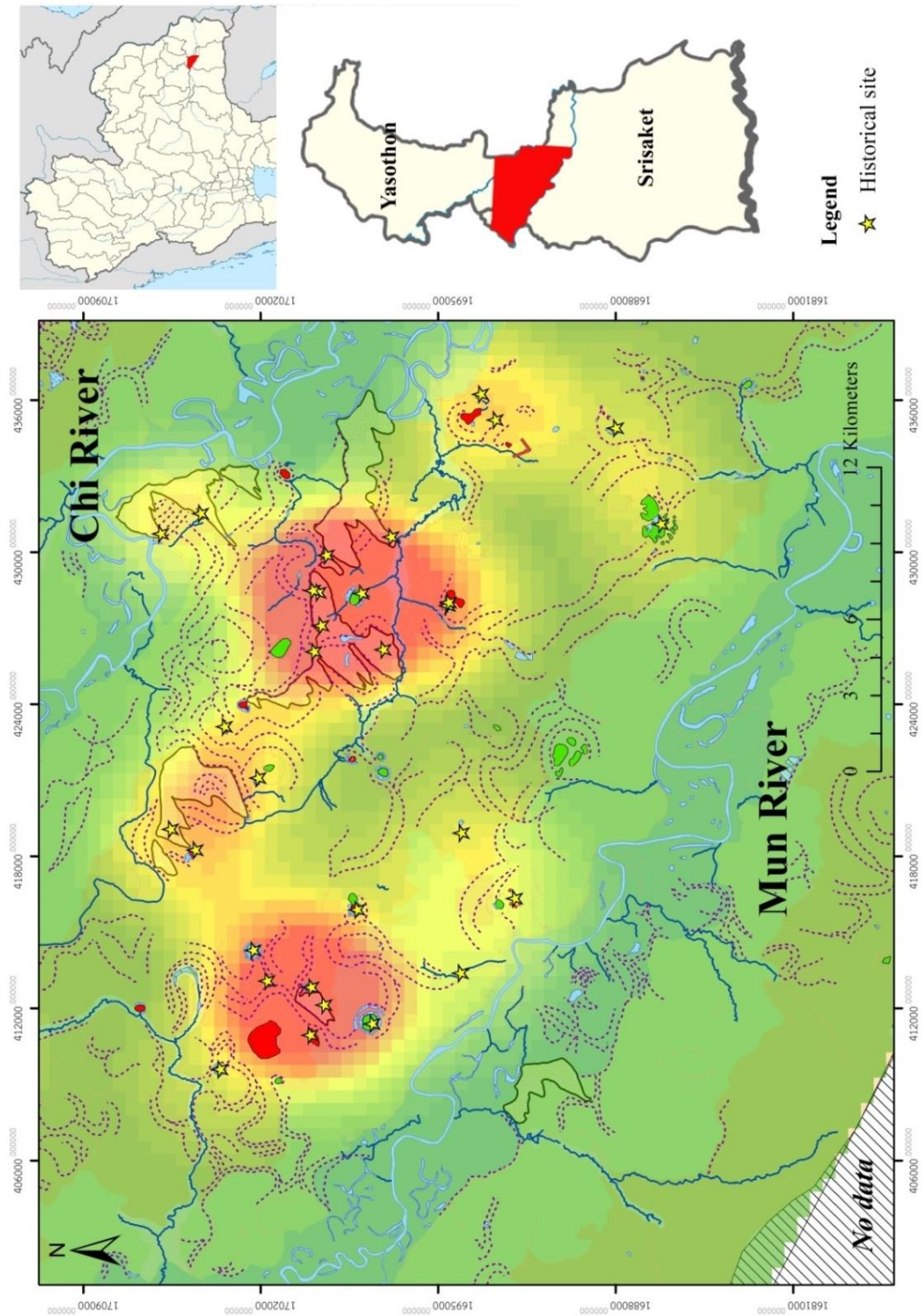


Figure 85 Archaeological evidences founded at historical sites such as Chedi, Sema, and Stone inscription.



**Figure 86** Density of prehistoric sites associated with location of ADL and paleo-channels.



**Figure 87** Density of historical sites associated with ADL and Sand plays for placing the Buddhist temples, especially the Dvaravati period during 900 – 1000 A.D.



## Chapter 6

### Conclusion

The result and discussion derived from integration of remote-sensing (aerial photographs and satellite imagery), GPR survey, and auger coring indicated that TKR was essential habitats of human past since prehistoric period during 2,500-1,500 BP. It had been so plentiful composing of various natural resources such as salts and waters. However, these resources might over exploitation leading to salinity in soils and waters of channels or moats and extreme floods. Thus, human past needed to search for new settlement at each landform. The ADL was a main place and the sand splay was minor. Geologically, the ADL is mostly found in the terrace. Therefore, it may relate to the aggradation of terrace leading groundwater flow to erode salt layer on stage of dome-shape or diapir intrusion in bedrock. Since the rim-syncline feature is the sinking sediments over area in which the salt has migrated, the surface water has flowed into this depression and become to lake or pond as a resource of freshwater linking to surficial processes of paleo-channels which are the main impact factor. This process is appeared in the moats; for example, the moats of Wat Don Kleau which was original rim-syncline feature of salt dome. In the past, the moats were dug to store the water from surface water or precipitation which created to freshwater. As well, the dome or overburden was a mound for habitation that it protected the floods with higher elevation. The ADL is predominant for prehistoric settlements during 2,500-1,500 BP or Late Iron Age.

The sand splay landform being a significant choice for settlement in historical period during 900-1,200 AD was surveyed by GPR instruments with OSL dating. It showed geochronology in the 3 stages as following:

*Stage 1* (Pre-formation of aeolian sand splays 95,000 – 75,000 yr BP) that the locations and GPR profiles revealed to pre-formation of these sands in case of overbank crevasse splay deposits.

*Stage II* (Development stages of aeolian sand structure in the 1<sup>st</sup> at 75,000 – 19,000 yr BP) that the sands from breaching in levee were rested at the margin of floodplain. They, then, were blown by strong prevailing wind in NE-SW direction to rest of the present area during 40,000-20,000 yr BP and the 2<sup>nd</sup> at 5,000 - 4,000 yr BP.

*Stage III* (Development stages of human settlement on aeolian sand splays after 4,000 yr BP) that most of archaeological sites located on this morphology are belonged to the historical periods during the 6<sup>th</sup> – 13<sup>th</sup> century A.D. (or Dvaravati to Angkor periods) and they are favored to locate on distal sand splay due to groundwater level and distance from streams.

In conclusion, the results of aerial photograph interpretation and GPR survey reveal the landscape and geomorphological evolution in eastern part of Thungkula Ronghai or the Lower Mun and Chi Rivers. Geomorphic features include paleochannels, salt dome (as ADL) and aeolian sand splays. These morphologies influence to ancient site settlement since at least 2,500 to 1,000 BP or Late Iron Age in prehistory.

The spatial analysis demonstrates that “water resources” with “higher elevation” are the major factor reflecting the advantage of landforms for considering to be occupied. The moats and earthworks indicated an adaptation of water management for using in live and agricultural activities, especially rice cultivation. Moreover, GPR shows level of shallow water table in the distal portion of sand splays. Thus, they were appropriate to live and develop to be the village or town later. In conclusion, the geoarchaeological approach is a subject regarding the understanding of human past culture under the application of geoscience or earth science techniques and methods. Geomorphology and ancient site settlement at the Lower Mun and Chi Rivers suggest the relationship between advantages of various landforms following paleochannels, ADL, and sand splays and developing the great civilization of human past which arose after the evolution of geomorphology.

## REFERENCES

- Auetrakulvit, P., and Winayalai, C. 2012. Thai-French Paleosurvey Final Report. Retrieved from Faculty of Archaeology, Silpakorn University
- Bagnold, R. A. 1941. The physics of blown sand and desert dunes. London: Methuen
- Baoneod, S. 2010. Archaeology of Thung Kula Rong-Hai. Ubon Ratchathani: FAD 11th Ubon Ratchathani
- Bernal, C. et al. 2013. Crevasse and capture by floodplain drains as a cause of partial avulsion and anastomosis (lower Rio Pastaza, Peru). Journal of South American Earth Sciences, 44: 63-74. doi:10.1016/j.jsames.2012.11.009
- Best, J., Woodward, J., Ashworth, P., Sambrook Smith, G., and Simpson, C. 2006. Bar-top hollows: A new element in the architecture of sandy braided rivers. Sedimentary Geology, 190(1-4): 241-255. doi:10.1016/j.sedgeo.2006.05.022
- Best, J. L., Ashworth, P. J., Bristow, C. S., and Roden, J. 2003. Three-Dimensional Sedimentary Architecture of a Large, Mid-Channel Sand Braid Bar, Jamuna River, Bangladesh. Journal of Sedimentary Research, 73(4): 516-530. doi:10.1306/010603730516
- Boonsener, M. 1977. Engineering Geology of the Town of Khon Kaen, Northeast Thailand. (MSc.), Khon Kean University, Asian Institute of Technology.
- Boonsener, M. 1991. The Quaternary stratigraphy of northeast Thailand. Journal of Thai Sciences, 1: 23-32.
- Boyd, W. E., Higham, C., and McGrath, R. J. 1999. The Geoarchaeology of Iron Age "Moated" Sites of the Upper Mae Nam Mun Valley, N.E. Thailand. I: Palaeodrainage, Site-Landscape Relationships and the Origins of the "Moats". Geoarchaeology, 14(7): 675-716.
- Boyd, W. E., and McGrath, R. J. 2001. The geoarchaeology of the prehistoric ditched sites of the Upper Mae Nam Mun Valley, NE Thailand, III: Late Holocene vegetation history. Palaeogeography, Palaeoclimatology, Palaeoecology, 171: 307-328.

- Boyd, W. E., McGrath, R. J., and Higham, C. 1999. The Geoarchaeology of the prehistoric ditched sites of the Upper Mae Nam Mun Valley N.E. Thailand, II: Stratigraphy and morphological sections of the encircling earthworks. Indo-Pacific Prehistory Association Bulletin, 18(2): 169-179.
- Brice, J. C. 1974. Evolution of Meander Loops. Geological Society of America Bulletin, 85(4): 581-586.
- Bridge, J. S. 2003. Rivers and floodplains: forms, processes, and sedimentary record. Journal of Quaternary Science, 19(6): 617-622.
- Bridge, J. S. 2009. Advances in Fluvial Sedimentology using GPR. In H. M. Jol (Ed.), Ground penetrating radar : theory and applications (pp. 323-359). Oxford, UK: Elsevier Science
- Bridge, J. S., Collier, R., and Alexander, J. 1998. Large-scale structure of Calamus River deposits (Nebraska, USA) revealed using ground-penetrating radar. Sedimentology, 45: 977-986.
- Bristow, C. S. 1993. Sedimentary structures exposed in bar tops in the Brahmaputra River, Bangladesh. Geological Society Special Publication, 75: 277-289.
- Bristow, C. S. 1996. Reconstructing Fluvial Channel Morphology from sedimentary sequences. In Advance in Fluvial Dynamics and Stratigraphy (pp. 351-371). England: John Wiley & Sons
- Bristow, C. S. 2009. Ground penetrating radar in aeolian dune sands. In H. M. Jol (Ed.), Ground penetrating radar: theory and applications. UK: Elsevier Science
- Bristow, C. S. 2013. 14.16 Ground Penetrating Radar. In Treatise on Geomorphology (pp. 183-194)
- Bristow, C. S., Bailey, S. D., and Lancaster, N. 2000. The sedimentary structure of linear sand dunes. Nature, 406(6 July 2000): 56-59.
- Bristow, C. S., Jones, B. G., Nanson, G. C., Hollands, C., Coloman, M., and Price, D. M. 2007. GPR surveys of vegetated linear dune stratigraphy in central Australia: Evidence for linear dune extension with vertical and lateral accretion. In G. S. Baker & H. M. Jol (Eds.), Stratigraphic Analyses using GPR (Vol. 432): Geological Society of America

- Bristow, C. S., and Pucillo, K. 2006. Quantifying rates of coastal progradation from sediment volume using GPR and OSL: the Holocene fill of Guichen Bay, south-east South Australia. Sedimentology, 53(4): 769-788.
- Bristow, C. S., Skelly, R. L., and Ethridge, F. G. 1999. Crevasse splays from the rapidly aggrading, sand-bed, braided Niobrara River, Nebraska: effect of base-level rise. Sedimentology, 46: 1029-1047.
- Bryan, K. 1932. Characteristic forms of dune fields. Geography Reviews, 22: 325-327.
- Bunopas, S., and Vella, P. Tectonic and Geologic Evolution of Thailand. Paper presented at the Workshop on Stratigraphic Correlation of Thailand and Malaysia, Haad Yai, Thailand. (1983)
- Butzer, K. W. 1982. Archaeology of human ecology : method and theory for a contextual approach. Cambridge: Cambridge University Press
- Chabangborn, A., Brandefelt, J., and Wohlfarth, B. 2014. Asian monsoon climate during the Last Glacial Maximum: palaeo-data-model comparisons. Boreas, 43(1): 220-242. doi:10.1111/bor.12032
- Chapman, H. 2006. Landscape archaeology and GIS. Stroud: Tempus
- Chawchai, S. et al. 2013. Lake Kumphawapi – an archive of Holocene palaeoenvironmental and palaeoclimatic changes in northeast Thailand. Quaternary Science Reviews, 68: 59-75. doi:10.1016/j.quascirev.2013.01.030
- Chen, M.-T., Shiau, L.-J., Yu, P.-S., Chiu, T.-C., Chen, Y.-G., and Wei, K.-Y. 2003. 500 000-Year records of carbonate, organic carbon, and foraminiferal sea-surface temperature from the southeastern South China Sea (near Palawan Island). Palaeogeography, Palaeoclimatology, Palaeoecology, 197(1-2): 113-131. doi:10.1016/s0031-0182(03)00389-4
- Collinson, J. D. 1986. Submarine Ramp Facies Model for Delta-Fed, Sand-Rich Hirbidite Systems: Discussion. The American Association of Petroleum Geologists Bulletin, 70(November 1986): 1742-1743.
- Cooke, R. U., and Warren, A. 1973. Geomorphology in Deserts. London: Batsford
- Daniel, J. F. 1971. Channel movement of Meandering of Indiana Streams. Paper presented at the Physiographic and Hydraulic Studies of Rivers, Washington, USA.

- Duke, B. J., Chang, N. J., Moffat, I., and Morris, W. 2016. The invisible moats of the Mun River Valley, NE Thailand: The examination of water management devices at mounded sites through ground-penetrating radar (GPR) Journal of Indo-Pacific Archaeology, 40: 1-11.
- Einsele, G. 1992. Sedimentary basins : evolution, facies, and sediment budget. Berlin: Springer-Verlag
- FAD. 2010. Research of Burial Tradition in Late Prehistory of Thung Kula Rong-Hai Culture. Ubon Ratchathani: The regional 11th of FAD
- Farrell, K. M. 1987. Sedimentology and Facies Architecture of overbank deposits of the Mississippi River, False River Region, Louisiana The Society of Economic Paleontologists and Mineralogists: 111-120.
- Ferring, R. 1994. The role of geoarchaeology in Paleoindian research. In Method and Theory for Investigating the Peopling of the Americas (pp. 57-72). Oregon: Corvallis
- Fleitmann, D. et al. 2003. Holocene Forcing of the Indian Monsoon Recorded in a Stalagmite from Southern Oman. Science, 300(13) (June): 1737-1739.
- Florsheim, J. L., and Mount, J. F. 2002. Restoration of floodplain topography by sand-splay complex formation in response to intentional levee breaches, Lower Cosumnes River, California. Geomorphology, 44: 67-94.
- Folk, R. L. 1980. Petrology of sedimentary rock. Austin, Texas: Hemphill
- Friedman, G. M. 1961. Distinction between dune, beach, and river sands from their textural characteristics. Journal of Sedimentary Petrology, 31(4): 514-529.
- Fryirs, K. A., and Brierley, G. J. 2013. Geomorphic analysis of river systems : an approach to reading the landscape. Chichester, West Sussex, UK: Wiley
- Gaylord, D. R., and Dawson, P. J. 1987. Airflow-terrain interactions through a mountain gap, with an example of eolian activity beneath an atmospheric hydraulic jump. Journal of Geology, 15(9): 789-792.
- Ge, H., Jackson, M. P. A., and Vendeville, B. C. 1997. Kinematics and dynamics of salt tectonics driven by progradation. American Association Petroleum Geologists Bulletin, 81: 1283-1293.

- Ghinassi, M. et al. 2014. Plan-form evolution of ancient meandering rivers reconstructed from longitudinal outcrop sections. Sedimentology, 61(4): 952-977. doi:10.1111/sed.12081
- Gibling, M., Nanson, G. C., and Maroulis, J. C. 1998. Anastomosing river sedimentation in the Channel Country of central Australia. Sedimentology, 45: 595-619.
- Glennie, K. W. 1972. Permian Rotliegendes of Northwest Europe Interpreted in Light of Modern Desert Sedimentation Studies. The American Association of Petroleum Geologists Bulletin, 56(6): 1048-1071.
- Hanebuth, T. J. J., Stattegger, K., Schimanski, A., Lüdmann, T., and Wong, H. K. 2003. Late Pleistocene forced-regressive deposits on the Sunda Shelf (Southeast Asia). Marine Geology, 199(1-2): 139-157. doi:10.1016/s0025-3227(03)00129-4
- Hanna, S. R. 1969. The formation of longitudinal sand dunes by large helical eddies in the atmosphere. Journal of Applied Meteorology, 8: 874-883.
- Harari, Z. 1996. Ground-penetrating radar(GPR) for imaging stratigraphic features and groundwater in sand dunes. Journal of Applied Geophysics, 36: 43-52.
- Hickin, A. S., Kerr, B., Barchyn, T. E., and Paulen, R. C. 2009. Using Ground-Penetrating Radar and Capacitively Coupled Resistivity to Investigate 3-D Fluvial Architecture and Grain-Size Distribution of a Gravel Floodplain in Northeast British Columbia, Canada. Journal of Sedimentary Research, 79(6): 457-477. doi:10.2110/jsr.2009.044
- Higham, C. The Prehistory of the southern Khorat Plateau, NE Thailand, with particular reference to Roi Et Province. Paper presented at the Modern Quaternary Research in South East Asia. (1977)
- Higham, C., and Thosarat, R. 1998. Prehistoric Thailand from Early Settlement to Sukhothai. Bangkok: River Books Co., Ltd.
- Higham, C., and Thosarat, R. 2012. Early Thailand from Prehistory to Sukhothai. Bangkok: River Books Co., Ltd.
- Hinkel, K. M. et al. 2001. Detection of subsurface permafrost features with ground-penetrating radar, Barrow, Alaska. Permafrost and Periglacial Processes, 12(2): 157-231.

- Hite, R. J. 1982. Progress report on the Potash Deposits of the Khorat Plateau, Thailand Retrieved from U.S. Geological Survey
- Hokjaroen, S. 1989. Aeolian sand splays of Northeast Thailand : analysis using Landsat TM imagery. Paper presented at the Remote sensing, soil and water management in Northeast Thailand, Khon Kaen.
- Horowitz, D. H. 1982. Geometry and origin of large-scale deformation structures in some ancient windblown sand deposits. Sedimentology, 29: 155-180.
- Howard, A. D. 1985. Interaction of sand transport with topography and local winds in the Northern Peruvian Coastal Desert In (pp. 511-543). USA: Department of Environmental Sciences, University of Virginia
- Hudec, M. R., and Jackson, M. P. A. 2007. Terra infirma: Understanding salt tectonics. Earth-Science Reviews, 82(1-2): 1-28. doi:10.1016/j.earscirev.2007.01.001
- Hunter, R. E. 1973. Pseudo-crosslamination formed by climbing adhesion ripples. Journal of Sedimentary Petrology, 43(4): 1125-1127.
- Hunter, R. E. 1977. Terminology of cross-stratified sedimentary layers and climbing-ripple structures. Journal of Sedimentary Petrology, 47(2): 697-706.
- Hunter, R. E. 1979. Quasi-Planar Adhesion stratification- An eolian structure formed in wet sand. Journal of Sedimentary Petrology, 50(1): 263-266.
- Hunter, R. E., Richmond, B. M., and Alpha, T. R. 1983. Storm-controlled oblique dunes of the Oregon coast. Geological Society of America Bulletin, 94: 1450-1465.
- Jackson, M. P. A., Schultz-Ela, D. D., Hudec, M. R., Watson, I. A., and Porter, M. L. 1998. Structure and evolution of Upheaval Dome: A pinched-off salt diapir. Geological Society of America Bulletin, 110(12): 1547-1573.
- Jackson, M. P. A., and Vendeville, B. C. 1994. Regional extension as a geologic trigger for diapirism. Geological Society of America Bulletin, 106(1): 57-73.
- Jackson, R. G. 1976. Depositional Model of Point bars in the Lower Wabash River. Journal of Sedimentary Petrology, 46(3): 579-594.
- Joeckel, R. M., Tucker, S. T., and McMullin, J. D. 2016. Morphosedimentary features from a major flood on a small, lower-sinuosity, single-thread river: The unknown quantity of overbank deposition, historical-change context, and



- comparisons with a multichannel river. Sedimentary Geology, 343: 18-37. doi:10.1016/j.sedgeo.2016.07.010
- Jol, H. M., and Bristow, C. S. 2003. GPR in sediments: Advice on data collection, basic processing and interpretation, a good practice guide Geological Society Special Publication, 211: 9-27.
- Jol, H. M., and Smith, D. G. 1991. Ground penetrating radar of northern lacustrine deltas. Canadian Journal of Earth Sciences, 28: 1939-1947.
- Kanhaiya, S., Singh, B. P., Tripathi, M., Sahu, S., and Tiwari, V. 2017. Lithofacies and particle-size characteristics of late Quaternary floodplain deposits along the middle reaches of the Ganga river, central Ganga plain, India. Geomorphology, 284: 220-228. doi:10.1016/j.geomorph.2016.08.030
- Kashima, K. Journal and Comments of Kangvola Khon Kham Inscription (about 1,000 years ago). 2014. Available from [http://kangvol.blogspot.com/2014/11/blog-post\\_74.html](http://kangvol.blogspot.com/2014/11/blog-post_74.html)
- Khamtho, A. 1986. Inscription of Prasat Preah Vihear. Bangkok: FAD
- Kleinbans, M. G. 2005. Grain-size sorting in grainflows at the lee side of deltas. Sedimentology, 52(2): 291-311. doi:10.1111/j.1365-3091.2005.00698.x
- Kocurek, G., and Dott, J. 1981. Distinction and Uses of stratification types in the interpretation of eolian sand Journal of Sedimentary Petrology, 51(2) (June): 579-595.
- Kocurek, G., and Fielder, G. 1982. Adhesion Structures. Sedimentary Petrology, 52(4): 1229-1241.
- Krumbein, W. C. 1934. Size frequency distribution of sediments. Journal of Sedimentary Petrology, 4: 65-77.
- Lindholm, R. C. 1987. A Practical Approach to Sedimentology. New Zealand: Allen & Unwin (New Zealand) Ltd.
- Loffler, E., Thompson, W. P., and Liengsakul, M. 1984. Quaternary geomorphological development of the Lower Mun River Basin, North East Thailand Catena, 11: 321-330.

- Lunt, I. A., and Bridge, J. S. 2004. Evolution and deposits of a gravelly braid bar, Sagavanirktok River, Alaska. Sedimentology, 51(3): 415-432. doi:10.1111/j.1365-3091.2004.00628.x
- Luo, C. et al. 2013. Palaeoenvironmental significance of grain-size distribution of river flood deposits: a study of the archaeological sites of the Apengjiang River Drainage, upper Yangtze region, Chongqing, China. Journal of Archaeological Science, 40(2): 827-840. doi:10.1016/j.jas.2012.09.020
- Lupe, R., and Ahlbrandt, T. S. 1979. Sediments in ancient eolian environments – reservoir inhomogeneity. Retrieved from US:
- McGrath, R. J., Boyd, W. E., and Bush, R. T. 2008. The paleohydrological context of the Iron Age floodplain sites of the Mun River Valley, Northeast Thailand. Geoarchaeology, 23(1): 151-172. doi:10.1002/gea.20210
- McKee, E. D. 1945. Small-scale structures in the Coconino Sandstone of Northern Arizona. Journal of Geology, 53(5 September 1945): 313-325.
- McKee, E. D., Douglass, J. R., and Rittenhouse, S. 1971. Deformation of Lee-Side Laminae in Eolian Dunes. Geological Society of America Bulletin, 82(2): 359-378.
- Melton, F. A. 1940. A Tentative Classification of Sand Dunes Its Application to Dune History in the Southern High Plains. Journal of Geology, 48(2) (February - March, 1940): 113-174.
- Miall, A. D. 1978. Lithofacies types and vertical profile models in braided river deposits: a summary. In A. D. Miall (Ed.), Fluvial sedimentology. Germany: Springer-Verlag Berlin Heidelberg
- Miall, A. D. 1985. Architectural-Element Analysis: A New Method of Facies Analysis Applied to Fluvial Deposits. Earth-Science Reviews, 22: 261-308.
- Miall, A. D. 2016. Facies Models. In Stratigraphy: A Modern Synthesis (pp. 161-214)
- Moore, E. 1988. Notes on two types of moated settlement in Northeast Thailand. Journal of The Siam Society, 76: 275-287.
- O'Reilly, D. J. W., and Scott, G. 2015. Moated sites of the Iron Age in the Mun River Valley, Thailand: New discoveries using Google Earth. Archaeological Research in Asia, 3: 9-18. doi:10.1016/j.ara.2015.06.001

- Okazaki, H., Kwak, Y., and Tamura, T. 2015. Depositional and erosional architectures of gravelly braid bar formed by a flood in the Abe River, central Japan, inferred from a three-dimensional ground-penetrating radar analysis. Sedimentary Geology, 324: 32-46. doi:10.1016/j.sedgeo.2015.04.008
- Pedersen, K., and Clemmensen, L. B. 2005. Unveiling past aeolian landscapes: A ground-penetrating radar survey of a Holocene coastal dunefield system, Thy, Denmark. Sedimentary Geology, 177(1-2): 57-86. doi:10.1016/j.sedgeo.2005.02.001
- Penny, D. 2001. A 40,000 year palynological record from north-east Thailand; implications for biogeography and paleo-environmental reconstruction Palaeogeography, Palaeoclimatology, Palaeoecology, 171: 97-128.
- Piyasin, S. The Hydrocarbon Potential of Khorat Plateau. Paper presented at the Proceedings of the International Conference on Geology, Geotechnology and Mineral Resources of Indochina, Khon Kaen University. (1995)
- Pramojanee, P., Liengsakul, M., and Engkagul, V. Grain size analysis of some sand rises and stream sediments in the northeast of Thailand in order to indicate depositional environment. Paper presented at the Geology and Mineral Resources Development of the Northeast, Thailand, Khon Kean University. (1985)
- Pye, H., and Tsoar, H. 2009. Aeolian Sand and Sand Dunes. Germany: Springer-Verlag Berlin Heidelberg
- Rapp, G., and Hill, C. L. 2006. Geoarchaeology: The Earth-Science Approach to Archaeological Interpretation. London: Yale University
- Rau, J. L., and Supajanya, T. Sinking Cities of Northeast Thailand. Paper presented at the Geology and Mineral Resources Development of the Northeast, Thailand Khon Kean University, Thailand. (1985)
- Reineck, H. E. 1955. Haftrippeln und haftwarzen, ablagerungsformen von flugsand. Senckenbergiana Lethaea, 38: 347-357.
- Rejiba, F., Bobée, C., Maugis, P., and Camerlynck, C. 2012. GPR imaging of a sand dune aquifer: A case study in the niayes ecoregion of Tanma, Senegal. Journal of Applied Geophysics, 81: 16-20. doi:10.1016/j.jappgeo.2011.09.015

- Riley, D. N. 1987. Air photography and archaeology. London: Duckworth
- Roskin, J., Bookman, R., Friesem, D. E., and Vardi, J. 2017. A late Pleistocene linear dune dam record of aeolian-fluvial dynamics at the fringes of the northwestern Negev dunefield. Sedimentary Geology, 353: 76-95. doi:10.1016/j.sedgeo.2017.03.011
- Rubin, D. M., and Hunter, R. E. 1983. Reconstructing bedform assemblages from compound crossbedding. In Eolian sediments and processes. Amsterdam: Elsevier
- Rubin, D. M., and Hunter, R. E. 1985. Why deposits of longitudinal dunes are rarely recognized in the geologic record. Sedimentology, 32: 147-157.
- Schrott, L., Otto, J. C., Götz, J., and Geilhausen, M. 2013. 14.2 Fundamental Classic and Modern Field Techniques in Geomorphology: An Overview. In Treatise on Geomorphology (pp. 6-21)
- Scott, G., and O'Reilly, D. 2015. Rainfall and circular moated sites in north-east Thailand. Antiquity, 89(347): 1125-1138. doi:10.15184/aqy.2015.130
- Smith, H. T. U. 1954. Eolian sand on desert mountains. Geological Society of America Bulletin, 65: 1036-1037.
- Smith, N. D., Slingerland, R. L., Perez-Arluca, M., and Morozova, G. S. 1998. The 1870s avulsion of the Saskatchewan River. Canadian Journal of Earth Sciences, 35: 453-466.
- Stewart, H. B. 1958. Sedimentary reflections of depositional environment in San Miguel Lagoon, Baja California, Mexico Bulletin of the American Association of Petroleum Geologists, 42(11 November 1958): 2567-2618.
- Supajanya, T. 1980. Ancient Cities on the Former Coastline in the Central Plain of Thailand : The Study of Sites and Geographical Correlation. Bangkok: Chulalongkorn University
- Tilley, C. 1994. A phenomenology of landscape : places, paths and monuments. Oxford: Berg
- Tooth, S. 2005. Splay Formation Along the Lower Reaches of Ephemeral Rivers on the Northern Plains of Arid Central Australia. Journal of Sedimentary Research, 75(4): 636-649. doi:10.2110/jsr.2005.052

- Trigger, B. G. 1967. Settlement Archaeology -Its Goals and Promise. American Antiquity, 32(2 April 1967): 149-160.
- Tsoar, H. 1983. Wind tunnel modelling of echo and climbing dunes. In Eolian sediments and processes. Amsterdam: Elsevier
- Tuan, Y.-F. 1977. Space and Place. The Perspective of Experience. London: Arnold
- Tuckson, M., Thompson, W. P., Loffler, E., Hartley, A., and Hunter, G. 1983. Tung Kula Ronghai Salinity Study. Paper presented at the Thai-Australia Tung Kula Ronghai Project.
- Udomchoke, V. Quaternary stratigraphy of the Khorat Plateau area Northeastern Thailand. Paper presented at the Correlation of Quaternary Successions in South, East and Southeast Asia, Bangkok, Thailand. (1988)
- Valia, H. S., and Cameron, B. 1977. Skewness as a paleoenvironmental indicator. Journal of Sedimentary Petrology, 47(2): 784-793.
- Valibhotama, S. 1990. A Northeastern site of civilization : new archaeological evidence to change the face of Thai history. Bangkok: Matichon
- Valibhotama, S. 2003. Thung Kula Rong-Hai Culture. Muang Boran, 29(2) (April - June, 2003): 11-22.
- van Dam, R. L. 2002. Internal structure and development of an aeolian river dune in the Netherlands, using 3-D interpretation of ground-penetrating radar data. Netherlands Journal of Geosciences, 81(1): 27-37.
- van der Kaars, W. A., and Dam, M. A. C. 1995. A 135,000-year record of vegetational and climatic change from the Bandung area, West-Java, Indonesia. Palaeogeography, Palaeoclimatology, Palaeoecology, 117: 55-72.
- van Heteren, S., Fitzgerald, D. M., Mckinlay, P. A., and Buynevich, V. 1998. Radar facies of paraglacial barrier systems: coastal New England, USA. Sedimentology, 45: 181-200.
- van Overmeeran, R. A. 1998. Radar facies of unconsolidated sediments in The Netherlands: A radar stratigraphy interpretation method for hydrogeology. Journal of Applied Geophysics, 40: 1-18.
- Vendeville, B. C., and Jackson, M. P. A. 1992. The rise of diapirs during thin-skinned extension. Marine and Petroleum Geology, 9(4) (August): 331-354.

- Vichapan, K. 1992. Photogeology and gravity survey of the annular depression landform in parts of Changwat Surin and Roi Et. (MSc.), Chulalongkorn University, Bangkok.
- Visher, G. S. 1969. Grain size distributions and depositional processes Journal of Sedimentary Petrology, 39(3): 1074-1106.
- Warren, J. K. 1999. Evaporites. Oxford: Blackwell Science Ltd.
- Wentworth, C. K. 1922. A scale of grade and class terms for clastic sediments. Journal of Geology, 30: 377-392.
- Wicander, R., and Monroe, J. S. 1998. Essentials of geology (Vol. 2). Minneapolis/St. Paul: West Pub. Co.
- Wohlfarth, B., Higham, C., Yamoah, K. A., Chabangborn, A., Chawchai, S., and Smittenberg, R. H. 2016. Human adaptation to mid- to late-Holocene climate change in Northeast Thailand. The Holocene, 26(11): 1875-1886. doi:10.1177/0959683616645947
- Wohlfarth, B. et al. 2012. Holocene environmental changes in northeast Thailand as reconstructed from a tropical wetland. Global and Planetary Change, 92-93: 148-161. doi:10.1016/j.gloplacha.2012.05.008
- Woodyer, K. D., Taylor, G., and Crook, K. A. W. 1979. Depositional processes along a very low-gradient, suspended-load stream: The Barwon River, New South Wales Sedimentary Geology, 22: 97-120.
- Xiao, J., Qu, J., Yao, Z., Pang, Y., and Zhang, K. 2014. Morphology and formation mechanism of sand shadow dunes on the Qinghai-Tibet Plateau. Journal of Arid Land, 7(1): 10-26. doi:10.1007/s40333-014-0074-9
- Yamoah, K. A. et al. 2017. Societal response to monsoonal fluctuations in NE Thailand during the demise of Angkor Civilisation. The Holocene, 27(10): 1455-1464. doi:10.1177/0959683617693900
- Yokoyama, Y., Deckker, P., Lambeck, K., Johnston, P., and Fifield, L. K. 2001. Sea-level at the Last Glacial Maximum: evidence from northwestern Australia to constrain ice volumes for oxygen isotope stage 2. Palaeogeography, Palaeoclimatology, Palaeoecology, 165: 281-297.

- Youngmee, W. 2004. Structure and evolution of Maha Sarakham rock salt formation : results from seismic reflection intretation. Khon Kean: Khon Kean University
- Zou, G.-N.et al. 2017. Geochronology and paleoenvironment of the Taoshan site, northeastern China, and archaeological implications. Quaternary International. doi:10.1016/j.quaint.2017.06.073
- Zulauf, J., Zulauf, G., and Zanella, F. 2016. Formation of dome and basin structures: Results from scaled experiments using non-linear rock analogues. Journal of Structural Geology, 90: 1-14. doi:10.1016/j.jsg.2016.07.001



## VITA

Patcharaporn Ngerkerd was born on November, 12 1991. She graduated Bachelor Degree of Arts (Archaeology) from Department of Archaeology, Silpakorn University in 2013. In 2015, she started a Master Degree of Sciences in Earth Sciences Major at Department of Geology, Faculty of Sciences, Chulalongkorn University and completed in November 2017.

